Fate-mapping neural stem cells in the mouse ventral neural tube by Cre-lox transgenesis

Raquel Taveira-Marques

The Wolfson Institute for Biomedical Research

University College London

A thesis submitted to the University College London in part fulfilment of the degree of Doctor of Philosophy

October 2011

Abstract

Neurons and glia (astrocytes and oligodendrocytes) are the two major cell types that make up the central nervous system (CNS). They are generated from precursor domains within the neuroepithelial germinal zone (ventricular zone, VZ) that surrounds the ventricles of the brain and the central canal of the spinal cord (the embryonic neural tube). In general, neurons are generated before glia. The intra-spinal circuits that control movement and locomotion are made up of different neuronal and glial elements that develop separately but come together to form interconnected functional units. To understand the logic of circuit development and ultimately circuit-driven behaviour, it is necessary to understand where and when each type of cell originates. To identify the products of the most ventral progenitor domain in the developing spinal cord, known as (*Nkx2.2*-expressing p3 domain), I made use of *Cre-loxP* technology. I generated a transgenic mouse line that expresses an inducible form of *Cre* recombinase (*CreER*^{T2}) under *Nkx2.2* transcriptional control and crossed this with a *Cre*-dependant reporter mouse to visualize p3-derived progeny. I confirmed that the p3 domain generates *Sim1*-expressing V3 interneurons, serotonergic interneurons as well as visceral motor neurons of the hindbrain. p3 progenitors also produce two spatially restricted subtypes of astrocytes, a few oligodendrocytes and ventrally-positioned ependymal cells. Unexpectedly, my studies also revealed that pre-ganglionic motor neurons of the sympathetic nervous system (SPNs, visceral motor neurons of the thoracic spinal cord), as well as a population of dorsally-located *Sim1*-expressing interneurons, are produced from *Nkx2.2*-expressing precursors. SPNs have been generally believed to originate from the same progenitor pool as HB9-positive somatic motor neurons (sMNs), defined by expression of *Olig2* (pMN domain, immediately dorsal to p3). Supporting this idea, no spinal sMNs or SPNs are formed in *Olig2*-null mice. However, I found that *Nkx2.2*-expressing p3 precursors do not generate any HB9-positive sMNs, implying that sMNs and SPNs derive from distinct precursors - the latter from the most ventral part of the pMN domain that transiently co-expresses *Nkx2.2* and *Olig2*. Thus, segregation of SPNs and sMNs occurs already in the neuroepithelium before their post-mitotic progenitors migrate away from the VZ into the ventral horns. This is how visceral and somatic MNs are known to develop in the brainstem, so my results provide a unifying theme to MN development at different levels of the neuraxis.

Acknowledgements

I would like to thank several people who made my stay in London possible and this Thesis a reality.

Professor William D. Richardson, my supervisor in this research project deserves a special thanks for having received me in his laboratory and given me the necessary support at the right times. My thanks also go to **Dr Nicoletta Kessaris** duly helped by **Matthew Grist** and **Palma Iannarelli**, for initiating me in laboratory techniques which were new for me.

Thanks to the **many cosmopolitan people at the Wolfson Institute for Biomedical Research**, especially **past and present members of the Richardson's lab** from whom I received fragments of their knowledge and with whom I exchanged ideas and shared great fun moments. I thank our colleagues at UCL (especially **Giti Garthwaite** and **Matteo Rizzi**) for help and advice, **Ulla Dennehy** for transgenic mouse production, and **Mark Turmaine** for electron microscopy. I am also grateful to **Fabienne Alfonsi** for sharing her knowledge and techniques in hindbrain analysis with me. My gratitude to **Stephen Price** (UCL) for advice on retrograde DiI labelling and to all the various investigators who kindly provided valuable reagents for the experiments reported in this Thesis. Many thanks to **Irma K** and **Sonsoles M** for helping me out with statistical analysis and drawings, respectively.

To my fellow friends in research **Marta GDB**, **Bettina R**, **Palma I**, **Lisbeth FG**, **Françoise J**, **Suzanne G**, **Nina C**, **Marisa H**, **Joana PF**, **Ana A**, **Marco P**, **Florian P** thank you for all your friendship, for cheering me up when I was down, and for the unforgettable moments of pure enjoyment outside the lab!

To all my friends from **Ashwell House** and **Newman House**, I heartily thank you for the sense of community you arise in me. It is something to last forever. To **Carmen G** and **Nadia B**, my lunch buddies at the end of my PhD, you deserve my many thanks for keeping me sane and in good spirit thus supporting me throughout the process of writing. **Carmela J-A** (and company), for knowing how to party – you kept me going smiling – thank you! **Auntie Luísa ("Titi")** and **my brother** for their support when I needed them.

Last but not least, I owe an immense debt of gratitude to **my father** for all his unconditional never-ending love and encouragement throughout my life. His guidance on my PhD was impressive, keeping me always stuck to its accomplishment.

Declaration

I, Raquel Taveira-Marques, confirm that the work presented in this thesis is my own. Where information has been derived from other sources, I confirm that this has been indicated in the Thesis.

_____

(Raquel Taveira-Marques)

Preface

This Thesis is not an exhaustive one. To report an orderly relationship between parts of the research work some intermediate and auxiliary tasks were deliberately set aside.

Part of the work in this Thesis has been integrated in Tsai et al. 2011 (unpublished) and substantial technical upgrades were achieved during a fruitful collaboration which resulted in a publication Del Barrio et al. 2007.

The bulk of the data described in this Thesis, complemented with more stringent time-consuming experimental results already very hard pursued but not yet successfully obtained in full, will give rise to a forthcoming research paper. I could, however, assert the main conclusions of this thesis even acknowledging some "riddles with the hope of *complete* solution" remain.

"What has been achieved is but the first step; we still stand in the presence of riddles, but not without hope of solving them. And riddles with the hope of solution - what more can a man of science desire?"
(Hans Spemann, Croonian Lecture 1927)

Raquel Taveira-Marques

Sponsors

FCT Fundação para a Ciência e a Tecnologia

MINISTÉRIO DA CIÊNCIA, TECNOLOGIA E ENSINO SUPERIOR

Ciência.Inovação 2010 Programa Operacional Ciência e Inovação 2010

MINISTÉRIO DA CIÊNCIA, TECNOLOGIA E ENSINO SUPERIOR

European Union — Structural Funds

Government of the Portuguese Republic

Table of Contents

List of Tables and Figures

Abbreviations

5HT	5-hydroxytryptamine (serotonin)
BAC	Bacterial Artificial Chromosome
BHI	Brain heart infusion
BMN or BM neuron	Branchiomotor neuron
BMP	Bone Morphogenetic Protein
bp	Base pairs (of DNA)
BrdU	5-bromo-2-deoxyuridine
bw	body weight
cDNA	complementary DNA
Cm^r	Chloramphenicol resistance
CNS	Central Nervous System
Cre	constitutive Cre recombinase
$CreER^{T2}$	tamoxifen-inducible form of Cre recombinase
DAPI	4',6-Diamidino-2-phenylindole
dATP	2'-deoxyadenosine 5'-triphosphate
dCTP	2'-deoxycytidine 5'-triphosphate
DEPC	Diethylpyrocarbonate
dGTP	2'-deoxyguanosine 5'-triphosphate
DIG	Digoxigenin
DMSO	Dimethylsulphoxide
DNA	Deoxyribonucleic Acid
DNase	Deoxyribonuclease
dNTP	deoxyribonucelotide triphosphate
DSHB	Developmental Studies Hybridoma Bank
DTA	Diphtheria toxin A fragment
dTTP	2'-deoxythymidine 5'-triphosphate
E	Oestrogen
E#	Embryonic Day # (number of days after conception)
EDTA	Ethylenediaminetetracetic acid
EGFP	Enhanced Green Fluorescent Protein
ER	Oestrogen Receptor
ES cells	Embryonic Stem Cells

FCS	Foetal Calf Serum
FGF	Fibroblast Growth Factor
FGFR	Fibroblast Growth Factor Receptor
FITC	Fluorescein isothiocyanate
GABA	Gamma aminobutyric acid
GFAP	Glial Fibrillary Acidic Protein
GFP	Green Fluorescent Protein
HB	Hindbrain
hCG	human chorionic gonadotropin
HD	Homeodomain
IAA	Indole acetic acid
iCre	codon-improved Cre recombinase
INs	Interneurons
IPCs	Intermediate Progenitor Cells
IPTG	Isopropyl-beta-D-thiogalactopyranoside
Kb	Kilobase pairs (of DNA)
LB	Luria-Bertani broth
LBD	Ligand Binding Domain
LMP	Low-melting point (normally applied to agarose)
Mash1	Mouse achaete-scute homolog 1
MBP	Myelin Basic Protein
MN	Motor Neuron
mRNA	messenger Ribonucleic Acid
NEP	neuroepithelial
nls	nuclear localisation signal
NSC	Neural stem cell
NT	Neural tube
O/N	Overnight
OD_{600}	Optical Density at a wavelength of 600nm
OLPs	Oligodendrocyte Precursors
ORF	Open reading frame
P#	Postnatal Day # (number of days after birth)
pA	Poly-adenylation signal
PAC	P1 bacteriophage-derived Artificial Chromosome
PBS	Phosphate Buffered Saline
PCR	Polymerase Chain Reaction
PDGFRα	Platelet-Derived Growth Factor Receptor α

PFA	Paraformaldehyde
PFGE	Pulsed Field Gel Electrophoresis
Phox2b	Paired-like homeodomain protein 2b
PLP	Proteolipid Protein
PNS	Peripheral Nervous System
PR	Progesterone Receptor
r	Rhombomere
RA	Retinoic Acid
RG	Radial Glia
RNase	Ribonuclease
rpm	Revolutions per minute
RT	Room temperature
SDS	Sodium dodecyl sulphate
SEM	Standard Error of the Mean
SHH	Sonic Hedgehog
sMN	Somatic motor neuron
SPN	Sympathetic preganglionic motor neuron
SV40	Simian Virus 40
SVZ	Sub-Ventricular Zone
TE	Tris EDTA solution
TGF-ß	Transforming Growth Factor-ß
TM	Tamoxifen
UCSF	University of California, San Francisco
UTR	Untranslated Region
UV	Ultra-Violet
vMN	Visceral motor neuron [*]
VMN or VM neuron	Visceromotor neuron
WIBR	Wolfson Institute for Biomedical Research
Xgal	5-bromo-4-chloro-3-indolyl-beta-D-galactopyranoside
YFP	Yellow Fluorescent Protein

---

[*] In the hindbrain, visceral motor neurons (vMN) comprise visceromotor (VMN) and branchiomotor (BMN) neurons.

Chapter 1 - Introduction

1.1. Vertebrate Central Nervous System Development

The vertebrate central nervous system (CNS) is a complex, highly organized network of billions of neurons and glial cells (the specialized support cells of neurons). Neurons can be split into hundreds of subtypes, the exact number of which is still unknown. It is also not known how many subtypes of glial cells – astrocytes and oligodendrocytes – there are. The CNS (brain, spinal cord and retina) is responsible for highly complex tasks as diverse as sensory perception, memory, behaviour, motor coordination and homeostasis. The interplay of these multineuronal pathways relies on each distinct class of cells being generated in appropriate numbers during development, at the correct time, in an appropriate location and forming precise connections within each other.

Neurons are generally regarded as the electrically active cells of the CNS. They transmit signals from one location to another in response to stimuli coming from sensory cells and other nerve cells. Before arriving at the end target, a stimulus can pass through several relay neurons where messages can be weakened, strengthened, selected, stored, and integrated into the system. The information conveyed by a chain of neurons runs through the two semi-independent systems that make up the CNS – the somatic and the autonomic systems. The former allows us to act on the external environment and the latter on the body's internal environment. Often those two systems interact with each other in tasks such as swallowing, breathing and heat conservation by interchanging information between specialised neurons from each branch of the nervous system.

It was thought that glial (literally "glue") cells only gave structural and trophic support to the nervous tissue. However, it is now clear that they fulfil a lot of other functions including insulation of axons (myelination), regulation of the blood brain barrier, synapse

formation, neurotransmitter uptake, or regulation of water and ion balance. In the CNS glial cells are divided into macroglia (mainly oligodendrocytes, the myelinating cells, and astrocytes) and microglia, which are the immune surveillance cells of the CNS.

Understanding how the CNS develops is not only interesting in itself but can also provide insights into more general questions of developmental biology as well as neurodevelopment and neurodegenerative diseases.

1.1.1. Neurulation

An essential early step of the development of the vertebrate CNS is the formation of the neural tube, the most primitive form of the CNS and the origin of the PNS, from a group of ectodermal cells on the surface of the embryo at the dorsal midline. The process, referred to as neurulation, is triggered by the migration of mesodermal cells to the region underneath the neural ectoderm during gastrulation. Neurulation occurs mainly in three spatially and temporally overlapping stages: (1) neural plate stage, (2) neural fold stage, and (3) neural tube stage (Gilbert 2000).

Neural plate stage

At the end of gastrulation the vertebrate embryo is arranged into three layers: endoderm (inner layer), mesoderm (middle layer) and ectoderm (outer layer). This three layered form of the gastrula is attained by the movement of cells from the epiblast through the primitive streak and groove, which results first in the formation of the endodermal layer and later the mesodermal layer. During this cell movement, a group of mesodermal cells, called the chordamesoderm, keeps contact with the ectoderm and their migration underneath and along the node (also referred to as the organizer) and the ectoderm directly causes the start of neurulation (Figure 1.1 A). The existence of an "organizer" – a group of cells that can instruct neurulation – was first demonstrated by Spemann and Mangold (Spemann et al. 1924) who concomitantly showed that cell fate can be determined by signals produced by other cells (for an historical review see Sander et al. 2001). The molecular nature of this signal is now partially understood and involves inhibition of bone morphogenic protein (BMP) signalling that prevents surface ectodermal cells from acquiring a neural fate. Among ectodermal cells, a tonic level of BMP is produced, particularly BMP-4, which maintains the ectoderm in an epidermal-like state. As chordamesodermal cells migrate underneath the ectoderm they produce chordin and noggin, two proteins that inhibit BMP-4 and, in turn, allow the process of neurulation to proceed (for review see Munoz-Sanjuan et al. 2002). It now appears that neurulation begins prior the formation of the node and that signalling

molecules like fibroblast growth factors (FGFs) have a role in promoting neurulation too (Streit et al. 2000; reviewed in Stern 2006).

The formation of the neural plate is the first distinguishable change seen in neurulation. In response to the inhibition of BMP signalling, a portion of the ectoderm is specified to become neural ectoderm and its cells elongate and acquire a columnar appearance. This thickened region of ectoderm forms the neural plate. The rest of the ectoderm tissue becomes the epidermal ectoderm (Figure 1.1 B). Meanwhile, the chordamesodermal cells form the so called notochord, a longitudinal structure that is critically involved in patterning the neural tube.

Neural fold stage

A complex series of morphogenic movements follows. The neural plate undergoes apico-basal thickening, mediolateral narrowing and further rostrocaudal lengthening. Once this is reached the neural plate curls up, anchored to the underlying notochord, and the subsequent bending produces an elongated furrow-like shape, the neural fold or groove (Figure 1.1 C).

Neural tube stage

Closure of the neural tube is a continuation of the bending process described above. As the neural folds elevate and fuse in the midline, the epidermal ectoderm from each fold detaches and comes to cover the newly formed neural tube (Figure 1.1 D). The midline cells of the neural plate become the ventral-most cells in the neural tube and are fated to give rise to the floor plate at the ventral midline. The cells at the crest of the folds turn into the dorsal-most cells in the neural tube and later form the roof plate or migrate away as neural crest cells, which eventually generate the Peripheral Nervous System (PNS) and many other cells and structures. Meanwhile, the cells of the newly formed neural tube are destined to form the entire CNS.

Even as the neural tube forms, it begins to differentiate. The allocation of cell fate in the neural tube depends on signalling systems along the rostrocaudal and dorsoventral axes that establish a grid-like set of positional cues. The position of each cell along these axes is thought to influence its fate by defining the identity and concentration of inductive signals to which they are exposed. At the tissue level different functional regions are organised thus dividing the neural tube into four regions (see below, section 1.1.2), while at a cellular level precursor cells begin to differentiate into various subtypes of neurons and glia (discussed in sections 1.2, 1.3 and 1.4).

1.1.2. The Neuroepithelium

The neural tube is initially a monolayer of pseudostratified neural ectodermal cells. This monolayer of cells is called the neuroepithelium and directly lines the fluid-filled central canal. They rapidly proliferate and differentiate into neurons and glia which move laterally to form the mantle layer.

The process of cell diversification from neuroepithelial (NEP) cells is now better understood and involves a succession of intermediate progenitor cell types that are restricted to certain lineages. At the beginning of CNS development, neuroepithelial cells are in contact with both the inner/apical and the outer/basal surface of the neural tube, known as the ventricular and pial surfaces, respectively. These two surfaces define a region designated as ventricular zone (VZ), within which NEP cells undergo so called interkinetic nuclear migration during their cell cycle. Cells going through S-phase form a layer at the apical (outerpial) side of the VZ, while mitotic cell bodies line up along the ventricular surface and cells in G1 and G2 phases are found in the mid region. As NEP cells are not synchronized and at any one time can be found at any given phase of the cell cycle, the epithelium adopts a pseudostratified arrangement. Before neurogenesis, NEP cells increase in number by dividing symmetrically to form two identical progenitors. It is thought that longer periods of symmetrical division occur in regions of the neuroepithelim that later give rise to larger CNS regions. For example, the telecephalon, the forerunner of the forebrain and one of the largest structures of the mammalian brain, has been reported to have the longest period of continuous symmetrical divisions (Rakic 1995). As development proceeds, NEP cells begin to express "glial" markers such as the astrocyte-specific glutamate transporter (GLAST), brain lipid-binding protein (BLBP), while maintaining an apical-basal polarity (for review, see Campbell et al. 2002). They are thus termed radial glia (RG). They also express nestin, vimentin, the RC1 and RC2 epitopes and, in some species (including humans) but not in rodents, the astroglial intermediate filament, glial fibrillary acidic protein (GFAP) (for review see Kriegstein et al. 2009 and also Malatesta et al. 2007).

RG cells were long thought to be precursors only of astrocytes (for an historical perspective see Rakic 2003 and Kriegstein et al. 2009). However, recent data showed that RG self-renew (Misson et al. 1988; Hartfuss et al. 2001) and generate different cell types throughout embryonic development (Gray et al. 1992; Miyata et al. 2001). A spate of other studies contributed to the establishment of RG as the founder cells for most, if not all, lineages in CNS. For instance, Cre/loxP fate mapping experiments based on the expression of the human GFAP promoter (which is expressed in rodent RG; Malatesta et al. 2003) or BLBP promoter (Anthony et al. 2004), resulted in large numbers of neurons as well as glial being labelled. Furthermore, when FACS-isolated RG cells of a mouse transgenic mouse line that

expresses the green fluorescent protein (GFP) from the human GFAP promoter were differentiated in vitro, they could generate clones composed either of neurons or astrocytes (Malatesta et al. 2000). Interestingly, Malatesta et al 2000 also observed that the percentage of mixed neuronal/non-neuronal clones was extremely small, suggesting that RG are a heterogeneous population committed very early on to a neuronal or glial fate. This partial restriction was also observed in NEP cells (Qian et al. 2000; McCarthy et al. 2001).

Nevertheless, during development, many neurons and glial cells are not the direct progeny of RG, but instead originate from transit amplifying or intermediate progenitor cells (IPCs). IPCs are fate-restricted progenitor cells that derive from RG by asymmetric division, whereby one neuron/glial progenitor cell and one new RG are produced. They populate a region adjacent to the VZ, now called the embryonic sub-ventricular zone (SVZ), and undergo symmetrical divisions to produce two differentiated progeny or else two additional IPCs (Noctor et al. 2004; Miyata et al. 2004). Their existence as functionally distinct subtypes of precursors was proven in retrovirally mediated lineage tracing experiments (Grove et al. 1993).

A peculiar property of RG is their transformation into astrocytes around birth. Progressively, RG's morphology changes from bipolar to unipolar as they leave the ventricular surface and go off, and retract towards the pial surface. Eventually they become multipolar and adopt an astrocyte morphology. Both RG and astrocytes express RC1, thus supporting a lineage relationship (Misson et al. 1991). Moreover, when RG cells are labelled in newborn ferrets with a fluorescent dye (DiI), the appearance of DiI-labeled astrocytes coincides with the disappearance of labeled RG (Voigt 1989). More recently, the translocation of RG and transformation to astrocytes has been directly visualized by using retroviral labeling and time-lapse imaging (Noctor et al. 2008).

Later in development, ependymal cells are also known to derive from late RG cells (Spassky et al. 2005) whereas some other RG persist into adult life in some vertebrates and serve as multipotent stem cells (Doetsch et al. 1999; Merkle et al. 2004).

Thus the uniformity of the embryonic neuroepithelium quickly undergoes successive restructurings that transform it from a relatively homogeneous proliferative zone into a complex layered structure. The molecular mechanism underpinning neuroepithelial specification will be discussed in section 1.2.

1.1.3. Rostro-caudal regionalisation of the neural tube

Signalling along the rostrocaudal axis of the neural tube establishes the main subdivisions of the CNS: the forebrain, midbrain, hindbrain and the spinal cord. The rostral or caudal character of the neural cells emerges soon after neural induction but before and independently of fate restriction along the dorsoventral axis (see section 1.2). Many classes of secreted factors have been implicated and all are proposed to function in different locations or developmental windows. In general, these signalling molecules assign cell fate by transcriptional control of gene expression. Many of these factors or "morphogens" belong to one of the following signalling factor families: retinoids, fibroblast growth factors (FGFs), hedgehogs, and Wnts (for a review see Lumsden et al. 1996).

The term 'morphogen' was first coined by Turing in his reaction-diffusion model of pattern formation. In this model, a diffusible substance is responsible to set a gradient of concentrations (a non-homogeneous environment) which determines patterns of gene expression on cells exposed to different concentrations (Turing A.M. 1952). This idea of pattern formation by a simple physical process arising from homogeneity was then widely used to support the French Flag model which describes space-dependent distribution of morphogens to induce positional specification in the embryo (Wolpert 1969; Figure 1.2). Morphogens are key regulators of development and they seem to be the trigger for cells to acquire a positional value in the embryo, although we know now that additional or alternative mechanisms are also crucial for positional information (Kerszberg et al. 2007; also see section 1.2.1).

During neurulation the signals produced from the mesoderm (chordin, follistatin, noggin) initiate neural development by imposing an anterior character on the entire neural tube. Subsequently, this anterior neural tissue is converted into more caudal regions by exposure to posteriorizing signals. Hence, in the absence of porteriorizing factors the whole neural tube develops as forebrain tissue (Lamb et al. 1995). A posterior character is imposed on the anterior neural tissue by the signalling molecules Wnts, FGF and retinoic acid (RA), which are produced by the newly generated mesoderm after gastrulation.

Wnts have a direct and graded effect on anterior neural cells that induce their differentiation into progressively more caudal regions: caudal forebrain, midbrain, and rostral hindbrain (Kiecker et al. 2001; Nordstrom et al. 2002). For example, inactivation of Wnt8 function leads to the expansion of forebrain markers and abrogates formation of posterior regions of the neuraxis (Glinka et al. 1997; Erter et al. 2001). Conversely, Wnt antagonists (e.g. DKK1) are released by anterior neural tissue and are responsible for its specification (Hashimoto et al. 2000).

FGFs and RA work in synergy for posterior tissue regionalisation (Diez del et al. 2004). While FGF signalling induces continuous generation of new caudal tissue by maintaining a stem cell character (Lobjois et al. 2004), RA signalling provided by the adjacent somites is required for the induction of neural differentiation by antagonizing FGF activity (Diez del et al. 2002; Diez del et al. 2003; Novitch et al. 2003). Subsequently, the progenitors become responsive to D-V patterning molecules such as sonic hedgehog (Shh) and differentiate into neurons and glia. In the developing spinal cord, for example, FGF and RA signalling impose an anterior-posterior identity on developing motor neurons (MNs) through the regulation of Hox genes. Whereas graded FGF signals cause the expression of specific Hox-c proteins at defined rostro-caudal levels of the branchial and thoracic spinal cord (Pownall et al. 1996; Liu et al. 2001; Bel-Vialar et al. 2002; Dasen et al. 2003), RA from the flanking paraxial mesoderm induces cervical Hox genes by acting in a paracrine fashion (Sockanathan et al. 1998; Novitch et al. 2003; Sockanathan et al. 2003).

Combinatorial and reiterated actions of the above-mentioned signalling molecules are proposed to be integrated locally to pattern further the hindbrain (Hernandez et al. 2004), the midbrain-hindbrain boundary (McMahon et al. 1992), the anterior neural ridge (Hebert 2005) to name a few examples (for reviews see Martinez 2001; Ciani et al. 2005; Mason 2007).

Another signalling molecule involved during neural tube regionalisation is Shh. Loss and gain of function experiments have recently been shown that the establishment of the different midbrain territories (or arcs) depends on Shh, derived from the underlying notochord (Britto et al. 2002), in a concentration- dependent manner (Agarwala et al. 2001; Agarwala et al. 2002). Shh also plays a well-defined role in the specification of neuronal cell type in the ventral spinal cord (see below, section 1.2).

1.2. Spatial patterning along the dorsoventral axis of the SC

Due to its anatomical simplicity the spinal cord has become a good model for addressing problems related to cell diversification in the CNS and has allowed the identification of molecular mechanisms that control cell fate in the CNS. In the following two subsections I review spinal cord development; however, as substantial progress has been made in the field of spatial patterning and cell specification in the brain, I also highlight the numerous similarities between the spinal cord and brain specification, which are extensively reviewed

elsewhere (Chandrasekhar 2004; Lupo et al. 2006; Guthrie 2007; Guillemot 2007a; Hebert et al. 2008; Sousa et al. 2010).

Dorsoventral patterning has a prominent role in establishing cell type diversity within each of the rostrocaudal subdivisions. This further level of organisation along the dorsal-ventral axis is not surprising and reflects the regionally-restricted distribution of the different types of neurons in the spinal cord. Two functional systems are segregated anatomically in the spinal cord: motor circuits, concentrated ventrally, that participate in motor output and body movements, and neurons that process and relay sensory input from the body to higher order brain centres, largely located in the dorsal half of the spinal cord (Brown 1981).

1.2.1. Extrinsic signals involved in dorsoventral patterning

There are two local organising centres that initially generate dorsoventral pattern in the developing embryonic neural tube: the signal from the notochord underneath the midline ventralises the neural tube and, simultaneously, signals from the epidermal ectoderm adjacent to the lateral edge of the tube dorsalise the neural tube.

The main signal from the notochord is the secreted protein Sonic hedgehog (Shh), a glycoprotein, discovered in 1993 (Echelard et al. 1993; Krauss et al. 1993), which is synthesised by the notochord at the time of floor plate induction, thus causing floor plate differentiation. The floor plate itself then begins to produce Shh, setting up a gradient of Shh concentration along the dorsoventral axis of the ventral spinal cord over long distances, which is interpreted by neighbouring cells in a quantitative fashion thus directing distinct cell fates at different concentration thresholds (Roelink et al. 1995; Chiang et al. 1996; Briscoe et al. 2000; Wijgerde et al. 2002). Signals like Shh that act in a concentration-dependent manner are know as morphogens (Vincent et al. 2001). Furthermore, the role of Shh in ventral spinal cord patterning is both necessary (Chiang et al. 1996; Ericson et al. 1996) and sufficient (Marti et al. 1995; Roelink et al. 1995), inasmuch as increasing concentrations of Shh induces a progressively more ventral character (Ericson et al. 1997a; Ericson et al. 1997b). Two main studies implicate Shh as a morphogen that acts directly to specify ventral spinal cord fates: 1) cell-autonomous activation of the Shh signalling cascade induces ventral patterning (Hynes et al. 2000) and 2) mutations in components of the Shh signalling pathway cause dorsalization of the ventral cord (Briscoe et al. 2001a; Wijgerde et al. 2002).

While Shh patterns the ventral spinal cord, the generation of certain cell populations in the dorsal-most region of the ventral neural tube does not depend exclusively on Shh signalling.

These cell populations can be induced by a parallel signalling pathway that is mediated by retinoids, derived from the paraxial mesoderm and, probably, from neural plate cells too (Pierani et al. 1999; Pierani et al. 2001; and see section 1.2.2.). Moreover, two other signalling pathways – Nodal and Fibroblast growth factor (FGF) – have been shown to be required for correct ventral neural patterning too. Whereas Nodal proteins, members of the Transforming Growth Factor β (TGF-β) superfamily, play a role in floor plate specification and regulation of Shh expression, FGF signals can modulate ventral patterning in the SC, specifically generation of MNs , in collaboration with RA and Shh (Novitch et al. 2003 and recently reviewed in Lupo et al. 2006).

Dorsal patterning is less well studied than Shh-mediated ventral patterning. Although we know that BMP signalling is implicated in suppressing neurulation in ectoderm (see section 1.1.1) it also likely mediates dorsalising activity within the spinal cord. After neural induction ceases, BMP activity starts to induce the dorsal-most cells of the neural tube to form the roof plate, which in turn secrete their own BMPs (Liem, Jr. et al. 1995; Liem, Jr. et al. 1997; Lee et al. 2000). Together with BMP antagonists noggin, chordin and follistatin, produced in the notochord and the paraxial mesoderm surrounding the ventrolateral neural tube, BMP proteins diffuse to create a dorsal to ventral gradient of BMP activity, with higher levels of activity existing in the more dorsal regions of the neural tube. It is then expected that this gradient has influence over cell fate decisions. Supporting this model, increasing or decreasing BMP signalling causing the enhancement of dorsal fates or reduced specification of dorsal cell types, respectively (Caspary et al. 2003 and references therein).

While there is not convincing evidence that Shh plays a role in dorsal patterning of the spinal cord (Chiang et al. 1996; Wijgerde et al. 2002), it is now known that Shh and BMP signalling pathways intersect in a way that BMPs act to limit the ventralizing activity of Shh (Liem, Jr. et al. 2000), possibly by sustaining Gli3 expression, a transcription factor along the Shh signalling cascade (Meyer et al. 2003; and see below). Several other key observations implicate BMPs in patterning ventral regions of the neural tube. McMahon and collegues reported that mice lacking noggin, a BMP antagonist, have reduced floorplate and extensive depletion of ventral neurons in the caudal spinal cord, despite normal level of Shh in the floor plate and notochord (McMahon et al. 1998). Moreover, gain-and-loss of function have shown that overexpression of chordin or follistatin, two other BMP antagonist, in chick SC leads to the expansion of ventral domains at the expense of dorsal ones reflecting a stronger ventralising effect when compared to Shh induction alone (Liem, Jr. et al. 2000; Patten et al. 2002). Conversely, overexpression of constitutively active forms of BMP receptors suppresses specification of ventral fates while enhancing dorsal ones (Timmer et al. 2002). These results suggest that both expression of Shh and repression of BMP signalling

are required for correct ventral specification. Futhermore, evidence at the molecular levels indicate that Shh and BMP pathways cross-talk (Liem, Jr. et al. 2000) and the components of their pathways can be physically associated with each other (Liu et al. 1998). In contrast, conditional deletion of BMP signalling hampers specification of the most dorsal SC progenitors without affecting ventral fates. This result has many possible interpretations, but an obvious one would be that another signalling molecule can compensate for the loss of BMP – Wnt/β-catenin signalling has been proposed in this context (recent evidence has raised increasing interest in this signalling pathway due to its demonstrated role in D-V patterning and this is extensively reviewed in Ulloa et al. 2010).

The diversity of neuronal cell types generated during embryonic development cannot be understood by only taking into account the actions of long-range secreted signals. Signals transmitted locally between cells are required to achieve the full repertoire of cell subtypes. Notch signalling is an example. In a seminal paper, Henrique et al (1995), show that, also in vertebrates, nascent neurons can laterally inhibit their neighbours by activating Notch signalling pathways in order to preserve a balance between precursors and differentiated cells, so that different cell subtypes can be generated in timely fashion and in appropriate numbers (Henrique et al. 1995). Additionally, recent data suggest that Notch does not always simply maintain cells in an undifferentiated state, but can also positively promote non-neuronal (see section 1.4.2) and neuronal cell fates (carefully reviewed in Pierfelice et al. 2011).

As development proceeds, the neural tube becomes increasingly compartmentalised; the position (and therefore the environment) experienced by a cell population at a specific time of development determines its fate. This process can be summarised in the following unifying principles of cell patterning: 1) in the early neural tube a signalling grid is set up by secreted extracellular signalling molecules (such as Shh, BMPs, Wnt, FGFs among others) that spread over variable distances across the neural tissue, thus accounting for the regionalisation of the CNS; 2) the combined activities of these signalling molecules are spatiotemporally integrated to determine the specific combination of transcription factors, typically bHLH and HD transcription factors, that is expressed by cell populations at distinct AP and DV locations, thus dividing the neural tube into particular progenitor domains; 3) these unique transcription factor expression profiles will then determine which cell type(s) a particular domain of the neuroepithelium gives rise to; 4) even subtler aspects of cell development, like the timing of differentiation, the rate of proliferation or the targeting of axonal connections, are all tighly dependent on the position at which each proginitor cell population occupies along the AP and DV axes at a specific time of development (Wolpert 1969; Jessell 2000; Dessaud et al. 2008).

1.2.2. The establishment of ventral progenitor domains

How do ventral progenitor cells interpret and respond to a graded Shh signal? The readout of the Shh signaling is an intricate one (Chen et al. 2007; Dessaud et al. 2008). Concentration gradients of Shh throughout the neural tube depend on the tight regulation of Shh secretion, diffusion, retention and degradation by the combined action of multiple mechanisms. Briefly, two transmembrane proteins mediate the intracellular transmission of the Shh signal: Patched1 (Ptc1), which is the Shh physical receptor, and Smoothened (Smo), which initiates intracellular signalling. In the absence of Shh ligand, Ptc1 blocks Smo activity. The binding of Shh to Ptc1 releases Smo inhibition, allowing intracellular signal transduction. It has been shown that graded activation of Smo is sufficient to explain the graded response of neural cells to Shh (Hynes et al. 2000; Dessaud et al. 2007), and its activity is necessary for normal formation of most ventral progenitor domains (Zhang et al. 2001; Wijgerde et al. 2002). Ultimately, Smo activity regulates the activity of zinc finger transcription factors Gli1-3, which act as repressors (GliR) of transcription of Shh signalling target genes in the absence of Shh signal; however, activation of Smo by Shh inhibits the proteolytic processing of Gli proteins, converting them into transcriptional activators (GliA) (Jacob et al. 2003; Vokes et al. 2007; Vokes et al. 2008). In other words, Shh signalling specifies ventral progenitor domains by removing the repression imposed by GliR activity (Litingtung et al. 2000; Wijgerde et al. 2002).

A three-step model for progenitor specification by Shh in the ventral neural tube has been proposed. 1) graded Shh signalling initially establishes five distinct domains of progenitor (p) cells, known as p3, pMN, p2, p1 and p0 (ventral to dorsal), by controlling the expression of a group of transcription factors at different Shh concentration thresholds. 2) the subsequent sharpening and maintenance of domain boundaries depends on cross-regulatory interactions between class I and class II proteins (for definition see below). 3) the combinatorial activities of class I and class II proteins within each domain determines distinct profiles of progenitor gene expression that ultimately specify which neuronal subtypes the cells within a specific domain will give rise to (e.g. the pMN domain is specified by the combined activity of Nkx6.1/Pax6/Olig2). In this model, which is based mainly on loss-of-function and gain-of-function studies, the Shh-regulated transcription factors are divided into two classes: Class I proteins, which are repressed at distinct concentrations of Shh so that their ventral boundaries of expression delineate progenitor domains, comprise homeodomain transcription factors Pax6, Pax7, Dbx1, Dbx2 and Irx3. Class II proteins, which are activated by Shh signalling so that their dorsal limits of expression define progenitor domains, include homeodomain transcription factors Nkx6.1, Nkx6.2, Nkx2.2, Nkx2.9 as well as the basic helix-loop-helix (bHLH) protein Olig2 (Novitch et

al. 2001) (Jessell 2000 and references therein; see also Figure 1.3, panel A). Analysis of mouse mutants that lack one or more of these TFs of different progenitor proteins has reinforced the idea that the activity of individual Class I and Class II proteins is required to establish progenitor domains and to direct ventral neuronal fates (Ericson et al. 1997b; Mansouri et al. 1998; Briscoe et al. 1999; Sander et al. 2000; Pierani et al. 2001; Vallstedt et al. 2001; Zhou et al. 2002; Lek et al. 2010).

One example of cross-repressive interaction leading to progenitor domain formation is the case of *Pax6* and *Nkx2.2* (depicted in Figure 1.3, panel B). Low concentrations of *Pax6* repress *Nkx2.2* expression, excluding it from the pMN domain and restricting it to the p3 domain. In chick, ectopic expression of *Pax6* in the normal *Nkx2.2* expression domain (p3) suppresses *Nkx2.2* expression in p3 (Briscoe et al. 2000). Conversely, ectopic expression of *Nkx2.2* in more dorsal domains downregulates *Pax6* (Briscoe et al. 2000). Accordingly, in the *Small eye* (*Sey*) mutant, which lacks Pax6 function, *Nkx2.2* is derepressed and expands dorsally into the pMN domain (Ericson et al. 1997b); however, expansion of Nkx2.2 does not inhibit the expression of *Pax6* transcript (Genethliou et al. 2009). Also unexpected is the observation that Pax6 does not expand into the prospective p3 domain of *Nkx2.2* null spinal cords (Genethliou et al. 2009; Holz et al. 2010), suggesting that a more complex gene regulatory network is involved in defining the p3 domain. *Nkx2.9* has also been reported to define the p3 domain, since forced expression of Nkx2.9 downregulates cell-autonomously Pax6 (Briscoe et al. 2000). But once again Pax6 expression was reported not to change in *Nkx2.9* knock-out mice even in the absence of *Nkx2.2* (Holz et al. 2010), presumably because others factors are required to specify the p3 domain. These factors remain unknown thus far.

The conventional model of morphogen action proposed to interpret the role of Shh in progenitor fate specification, which relies solely on the concentration of Shh perceived by cells at specific positions in the Shh gradient (see Figure 1.3, Panel A), has been questioned in the light of fresh evidence. It has recently been shown that in addition to the concentration of Shh, the duration of Shh signalling also contributes to the establishment of progenitor identity (Dessaud et al. 2008; Ribes et al. 2009). In an unexpected twist, lineage tracing data in mouse indicate that cells from the p3 domain had previously expressed *Olig2* (Dessaud et al. 2007), a transcription factor known to be upregulated only in the pMN domain at a specific Shh concentration determined by the positional information hold by their progenitor cells. Histological studies further confirm that Olig2 is first expressed in the most ventral neural progenitors and then gradually expands dorsally (Jeong et al. 2005; Stamataki et al. 2005). As it does so, ventral progenitors that once expressed Olig2 activate Nkx2.2 expression and downregulate Olig2. In turn, Nkx2.2 expression also expands dorsally, repressing Olig2 expression as it goes (Novitch et al. 2001; Jeong et al. 2005;

Stamataki et al. 2005; Dessaud et al. 2007). Eventually, two adjacent but spatially non-overlapping progenitor domains are formed. *Olig2* and *Nkx2.2* genes are also activated sequentially when chick spinal cord explants are exposed to a fixed concentration of Shh (Dessaud et al. 2007). This has been explained by proposing that cells are able to integrate Shh signalling over time (Dessaud et al. 2008; Ribes et al. 2009; Dessaud et al. 2010). This, however, requires a gradual desensitization of cells to ongoing Shh exposure so as to assure an accurate graded readout of Shh signalling over time. Such a "negative feedback" mechanism was found to be mediated by the SHH-dependent upregulation of Ptc1, performing its role as a ligand-binding inhibitor of SHH signalling (Chen et al. 1996). Concomitantly, a gradient of Gli transcriptional activity emulates the graded Shh signalling and those activities together become ultimately integrated to orchestrate patterning of ventral neural tube (Stamataki et al. 2005). This temporal adaptation mechanism prompts the suggestion of a dynamic model for progenitor fate specification whereby progenitor domains can be specified in a step-wise fashion (Nishi et al. 2009). Thus, p3 would transiently pass through a "pMN-like" state, before *Nkx2.2* expression established the ultimate p3 domain. Neverthless, this model presents difficulties since prospective p3 progenitors cannot take on the full characteristics of their pMN conterparts, as they lack a history of *Pax6* expression (Jeong et al. 2005; Ribes 2010).

In the developing spinal cord, progenitor cells begin to leave the cell cycle and migrate away to form neurons and glia in the mantle layer, or intermediate zone. The neuroepithelial layer (also known as the ventricular zone, VZ) remains adjacent to the lumen. Neurons send out axons from the intermediate zone towards targets either in the brain or in more rostral and caudal spinal cord, generating the cell pool marginal zone. In the marginal zone, axons are later covered with myelin-sheaths thus becoming white matter. The ventricular and intermediate zones, rich in neuronal cell bodies, later become the grey matter.

1.3. Establishment of neuronal identity

1.3.1. Further development: from progenitors to neurons

Distinct progenitor domains positioned along the dorsal-ventral axis of the spinal cord and hindbrain give rise to specific classes of neurons. Thus, the 5 progenitor domains p3, pMN, p2, p1, and p0 generate, respectively, ventral (V)3 interneurons, motor neurons (MN), V2 interneurons, V1 interneurons and V0 interneurons (Briscoe et al. 2000; see also Figure 1.3 Panel A, Table 1.1 and Table 1.2). In the spinal cord, Nkx2.2$^+$ progenitors within the p3 domain give rise to V3 INs and their generation is dependent on the selective expression on Nkx2.2 (Briscoe et al. 1999) , whereas, in the pMN domain, production of somatic motor neurons (sMNs) requires combined activity of Nkx6.1, Olig2 and Pax6 (Ericson et al. 1997b; Sander et al. 2000; Lu et al. 2002; Zhou et al. 2002). While its expression spans the three most ventral domains (p3, pMN and p2), Nkx6.1 activity is only eminent in the pMN domain, where its loss results in a reduction of sMN number and ectopic expression of Nkx6.1 induces sMNs (Briscoe et al. 2000; Sander et al. 2000). In the p3 domain, expression of Nkx2.2 overrides the activity of Nkx6.1 and leads to the production of V3 INs, whereas in the p2 domain, the combining activity of Nkx6.1 and Irx3 promotes the generation of V2 INs instead of sMNs (Briscoe et al. 2000). Nevertheless, Nkx6.1 is required for the correct generation of the V2 domain, besides MNs, as indicated by the reduction in number of V2 INs and MNs in Nkx6.1 mutant mice (Sander et al. 2000). Nkx6.2-expressing progenitors of the p1 domain generate V1 INs and their proper production is dependent on the selective expression of Nkx6.2 (Vallstedt et al. 2001). Finally, p0 progenitors that express Dbx1 give rise to V0 INs, which are also dependent on Dbx1 expression for their generation (Pierani et al. 2001).

1.3.1.1. The derepression model

Through what mechanism do progenitor domain proteins steer production of specific neuronal subtypes? The antagonistic interaction between specific Class I and Class II transcription factors raises the possibility of acting as transcriptional repressors. In fact, most Class I and Class II proteins function as transcriptional repressors through the recruitment of members of the Groucho/TLE co-repressor complex (Muhr et al. 2001). Although not directly binding to DNA, Groucho/TLE proteins are a family of co-repressors that are recruited to target gene promoters via direct interaction with sequence-specific DNA binding proteins, the transcription factors (Fisher et al. 1998). The observation that Class I and Class II proteins act as transcriptional repressors of cell fates suggest that specification of neuronal subtype within a given neuroepithelial domain results from the repression of all other possible fates in that domain. The suggested model comprises two

sequential steps of repression: 1) operating at the level of the VZ to establish progenitor domains, and 2) acting on neuronal subtype determinants to regulate downstream events in neuronal subtype specification such as cell migration, axon projection, morphology and neurotransmitter phenotype (Muhr et al. 2001; Briscoe et al. 2001b). Based on this model, the pattern of neuronal generation in the ventral neural tube is set by the spatially restricted repression of transcriptional repressors, that is, a "derepression strategy" of neuronal specification.

Various experimental results support such a model. In Olig2 mutants, Irx3 is derepressed and expands ventrally into the pMN domain, where it represses MNs leading to ectopic V2 IN generation in the pMN domain (Mizuguchi et al. 2001; Novitch et al. 2001; Lu et al. 2002; Zhou et al. 2002; see also Figure 1.3 Panel C). This happens because Irx3 is known to promote V2 IN production by suppressing homeodomain protein HB9, a motor neuron subtype determinant required to suppress the expression of V2 IN subtype genes in somatic MN. By repressing HB9 activity, Irx3 disrupts the consolidation of MN identity (Arber et al. 1999; Novitch et al. 2001; Lee et al. 2004). In wild type mice, Olig2 therefore induces MN specification in the pMN domain by repressing a repressor of MN fate. The loss of Olig2 also leads to the dorsal expansion of Nkx2.2 (Briscoe 2011), however at a smaller scale (two-cell thick), due to the repressive activity of Pax6 on Nkx2.2 (Briscoe et al. 2000). This evidence supports the idea of a cross-repression interaction between Olig2 and Nkx2.2, Olig2 being a weaker repressor than Nkx2.2.

Additional support for a derepression strategy of neuronal fate determination comes from studies using Nkx2.2 null mice. In the spinal cord of Nkx2.2 mutants, the expression of Olig2 expands ventrally into the p3 domain which no longer is able to produce V3 INs due to the loss of Nkx2.2 activity (Briscoe et al. 1999; Holz et al. 2010; also see Figure 1.3 Panel B). Moreover, Nkx6.1 expression within the p3 domain allows the bHLH protein Olig2 to be expressed (Novitch et al. 2001) which, in turn, is able to promote the expression of downstream somatic MN determinants (e.g. Lim3/Lhx3 and MNR2/Hb9) and of the proneural bHLH protein Ngn2 (Mizuguchi et al. 2001; Novitch et al. 2001). Thus, in wild type mice, Nkx2.2 induces V3 IN specification in the p3 domain by suppressing MN production via repression of Olig2. The ectopic production of somatic MNs seems, however, restricted to the medial motor column (MMC) only (Agalliu et al. 2009) suggesting an early divergence in motor neuron subtype identity in the spinal cord. Such an early divergence in MN subtyte is not novel in the developemt of the CNS since it is known that visceral and somatic MNs derive from distinct progenitors of the hindbrain (Osumi et al. 1997; Ericson et al. 1997b).

In the *Small eye* (*Sey*) mouse mutant, which lacks Pax6 function, cross-regulatory inhibition of *Nkx2.2* by *Pax6* is relieved resulting in the dorsal expansion of *Nkx2.2* into the pMN domain. There, Nkx2.2 promotes the generation of V3 interneurons at the expense of somatic MNs (Ericson et al. 1997b).   However, somatic MNs are recovered later in development (Sun et al. 1998), suggesting that suppression of Olig2 by Nkx2.2 might not be complete or lasting. In fact that is the case as Olig2^{+} scattered cells can be detected within the pMN domain of the Sey eye mutants spinal cords (Genethliou et al. 2009). Albeit at an inappropriate time of MN developemnt, the few Olig2-expressing cells are able to produce normal numbers of somatic motor neurons, possibly because other factors, apart from Shh, might be involved. Recent studies have linked retinoid signalling and the activator funtions of retinoid receptors to several phases of MN specification in the SC (Novitch et al. 2003; Sockanathan et al. 2003).

Table 1.1 - Characteristics of post-mitotic motor-neurons in the ventral spinal cord.
(not a likely exhaustive summary but at least a compilation of the most generally accepted facts about the different post-mitotic motor neuron populations in the spinal cord) (For clues of the undermentioned abbreviations, please look through the beginning of this thesis in the Abbreviations page) (below).

Table 1.2 - Characteristics of post-mitotic interneuron populations in the ventral spinal cord.
(once again, not a likely exhaustive summary but at least a compilation of the most generally accepted facts about the different post-mitotic interneuron populations in the spinal cord; adapted from Lewis 2006 and updated based on Goulding 2009) (below).

Table 1.1 - Characteristics of post-mitotic motor-neurons in the ventral spinal cord.

Progenitor domain	Post-mitotic neuronal population	Neuronal subtype determinants	Final position of cell body	Axonal projections	Neurotransmitter phenotypes	Functional properties	Key references
pMN	Median Motor Neurons – medial subdivision	Isl1 (Islet1), Isl2 (Islet2), Lhx3 (Lim3), Lhx4 (Lim4) , Hb9 (MNR2)	Located in the ventral horn, medial position (lamina IX) at all level of the spinal cord	Axons project ventrally to axial muscles that differentiate near the vertebral column	Choline Acetyltransferase	Synapse directly onto muscle cells	Tsuchida et al. 1994; Sharma et al. 1998; Tanabe et al. 1998; Arber et al. 1999; Kania et al. 2000; Sharma et al. 2000; Dasen et al. 2003; Kania et al. 2003; Dasen et al. 2008; Rousso et al. 2008
	Median Motor Neurons – lateral subdivision	Isl1 (Islet1), Isl2 (Islet2) , Hb9 (MNR2)	Located in the ventral horn, lateral position (lamina IX) between T1 and T12 level of spinal cord	Axons project ventrally to body wall muscles that differentiate within the ventral lateral plate mesenchymal			
	Lateral Motor Neurons – medial subdivision	Isl1 (Islet1), Isl2 (Islet2) , Hb9 (MNR2), Hoxc6 (for neurons located at branchial levels), Hoxc10 (for neurons located at lumbar levels), FoxP1	Located in the lateral horn, medial position (lamina IX) between C5 - C8, and L1 – L6 level of spinal cord	Axons project ventrally to limb muscles – ventral muscle mass			
	Lateral Motor Neurons – lateral subdivision	Isl2 (Islet2), Lhx1 (Lim1), Hb9 (MNR2), Hoxc6 (for neurons located at branchial levels), Hoxc10 (for neurons located at lumbar levels), FoxP1	Located in the lateral horn, dorsal to lateral MN medial subdivision (lamina IX) between C5 - C8, and L1 – L6 level of spinal cord	Axons project ventrally to limb muscles – dorsal muscle mass			
	Sympathetic Preganglionic Neurons (also known as pre-ganglionic motor neurons or column of Terni, in chick)	Isl1 (Islet1), nNOS, Hb9 (MNR2; late appearance), Hoxc9, FoxP1, pSmad	Clustered at two major sites in the intermediate grey matter, near the lateral white matter (intermediolateral nucleous, IML), and besides the central canal (central autonomic nucleous, CAN)	Axons project ventrally to visceral targets indirectly via relay neurons in the sympathetic ganglia, with the exception of those axons which project ventrally and directly to the adrenal gland	Choline Acetyltransferase, (a subset of these also express NADPH Diaphorase)	Involved in homeostatic maintenance of widespread functions of the Sympathetic NS	Cabot 1990; Markham et al. 1991; Wetts et al. 1994; Arber et al. 1999; Dasen et al. 2003; Dasen et al. 2008; Rousso et al. 2008
	Parasympathetic Motor Neurons	Isl1 (Islet1) (?), nNOS (?), Hb9 (late) (?)	Located in the sacral spinal cord	Axons project ventrally to visceral targets indirectly via relay neurons in the parasympathetic ganglia	Choline Acetyltransferase	Regulate visceral functions of the Parasympathetic NS	Loewy 1990
p3	Spinal Acessory Neurons	Isl1 (Islet1), Phox2b, Tbx20	Located dorso-laterally between C1 and C4 level of spinal cord	Axons project dorsally via the spinal accessory (XIth cranial) nerve	Choline Acetyltransferase		Loewy 1990; Ericson et al. 1997b; Pattyn et al. 2000; Song et al. 2006

Table 1.2 - Characteristics of post-mitotic interneuron populations in the ventral spinal cord.

Progenitor domain	Post-mitotic neuronal population	Neuronal subtype determinants	Final position of cell body	Axonal projections	Neuro-transmitter phenotypes	Functional properties	Key references
p0	V0 ventral	Evx1/2 (a subset of these also express Pax2)	Migrate ventro-medially and settle in the ventral horn medial to MNs & close to FP (lamina VIII).	Contralateral axons that extend rostrally (commissural neurons). Descend to FP, cross midline & extend 1-4 segments. At least most of the cells contact MNs.	Glutamate	70% of V0 neurons are inhibitory and 30% are excitatory. V0 inhibitory commissural neurons are critical in controlling left-right alternation during motor activity, like walking or swimming. V0 neurons are possibly disynaptic crossed commissural INs during adulthood; neurons that give rise to C neurons might derive from V0 cells, but they could also come from V1 cells and dorsal progenitors.	Briscoe et al. 2000; Moran-Rivard et al. 2001; Pierani et al. 2001; Lanuza et al. 2004; Miles et al. 2007
	V0 dorsal	Evx1 negative but Evx2 positive			GABA/Glycine		
p1	V1	En1, Pax2, Foxd3	Migrate laterally & settle in the ventral horn immediately dorsal to MN cell bodies in lamina VI, VII & ventral lamina IX.	Ipsilateral ascending axons. Axons project ventrally & then extend rostrally for 1-2 segments. Renshaw cells extend both rostrally & caudally.	GABA/Glycine	Renshaw cells all derive from V1 cells—but they are only 10% of them. V1 cells also give rise to Ia inhibitory interneurons and together with Renshaw cells they comprise only 25% V1-derived adult population; Ib inhibitory interneurons probably also derive from V1 cells. All of these interneurons fine-tune motor behaviours	Ericson et al. 1997b; Saueressig et al. 1999; Briscoe et al. 2000; Pierani et al. 2001; Goulding et al. 2002; Higashijima et al. 2004; Sapir et al. 2004; Al-Mosawie et al. 2007
p2	V2 a	Lhx3 (Lim3), Chox10, Dll4	Ventral horn, dorsomedial to MN cell bodies but ventral to V1 interneurons; in particular Gata2/3$^+$ V2b INs are interspersed with V1 neurons in lamina VII; V1-derived neurons can also be found in lamina IX	Ipsilateral axons that project for greater than 3-5 segments caudally & rostrally?	glutamate	Excitatory; V2a neurons are ipsilateral components of a commissural pathway that controls left-right alternation	Ericson et al. 1997b; Sharma et al. 1998; Tanabe et al. 1998; Saueressig et al. 1999; Briscoe et al. 2000; Karunaratne et al. 2002; Smith et al. 2002; Al-Mosawie et al. 2007; Del Barrio et al. 2007; Lundfald et al. 2007; Peng et al. 2007; Crone et al. 2008; Joshi et al. 2009; Panayi et al. 2010
	V2 b	Gata2/3, medial V2b also express Tal1 (SCL),, Notch1, LMO4			GABA/Glycine	Inhibitory; function not determined yet.	
	V2 c	Sox1			?	?	
p3	V3 ventral	Sim1	Ventral horn (occupy medial laminae VII and VIII)	Mixed commissural/ipsilateral axons that project for greater than 2 segments; excitatory INs	Glutamate	Excitatory; V3 ventral neurons play an important role in the establishment of a stable and balanced locomotor rhythm, but are largely dispensable for left-right alternation.	Ericson et al. 1997b; Briscoe et al. 1999; Geiman et al. 2006; Zhang et al. 2008
	V3 dorsal (unpublished data)	Sim1	Dorsal horn			Excitatory; function not determined yet.	

1.4. Glia generation

1.4.1. Neurogenic - to - gliogenic switch

A fundamental question in developmental biology is how remarkably different cell types arise from a seemingly homogeneous germinal zone of the embryonic neural tube during development of an organism. Neurons, astrocytes and oligodendrocytes are all specified from the same pool of proliferating progenitor cells which, through dynamic and intricate mechanisms, produce various subtypes of neurons and glial cells. Neurons are produced prior to glia, thereby assuring first the establishment of a neuronal circuitry before glial numbers and positions are matched to each circuit (Rowitch 2004). The mechanisms that underlie the development of glia, similarly to neurogenesis, require precise interplay between regionally-restricted extrinsic signals and cell intrinsic factors; however the developmental stages of glia generation unfold differently from those of their neuronal counterparts - the main phases of glia proliferation and differentiation seem to occur long after the commitment of a relatively small, proliferative precursor pool to the glia lineage thereby obscuring the timing of glia specification and hindering its study. Nevertheless, we now know that the neuron-to-glia switch is governed by multiple mechanisms, which involve transcription factors, extrinsic signals and modifications of histones and DNA (review in Kessaris et al. 2001; Rowitch 2004; Miller et al. 2007; Guillemot 2007b).

At the transcriptional level, two transcription factors Sox9 and NFIA have been proposed to trigger the fate switch of neural progenitors to gliogenesis along the spinal cord by promoting gliogenesis (Stolt et al. 2003; Deneen et al. 2006). Stolt et al (2003) observed that, in the mouse, loss of Sox9 led to a reduction in the number of oligodendrocytes and astrocytes and a concomitant increase in the numbers of somatic motor neurons and V2 interneurons whereas Deneen et al (2006) demonstrated that by silencing *Nfia* gene in the chick SC one can prevent the generation of both oligodendrocyte precursors (OLPs) and astrocyte precursors (APs) with simultaneous premature differentiation of neuronal lineages. These findings also support the concept of a proglial transcription programme (Hosoya et al. 1995; Jones et al. 1995) - that is, a programme independent of neurogenesis and specifically activated during the gliogenic phase. This runs against the prevailing idea that glial differentiation is a "default fate" following downregulation of proneural activity. Deneen et al (2006) went further to realise that NFIA is required for the maintenance of Notch effector expression during the gliogenic phase and that it is the Notch effectors that are responsible for inhibiting neurogenesis. Moreover, Delta-Notch signalling has also been shown to maintain a subset of progenitors in an undifferentiated state so they could be used as a cellular substrate during gliogenesis (Itoh et al. 2003; Park et al. 2003).

From the foregoing discussion one can realise that it is more a combinatorial framework of transcription factors that it is able to instruct progenitor cells to generate multiple fates at a given location and time.   The best studied example to describe such a combinatorial transcription factor code is that operating in the pMN domain in the ventral spinal cord, a progenitor domain where production of oligodendrocytes is preceded by generation of motor neurons (Richardson et al. 1997).   It has been observed in this domain that the onset of gliogenesis is led by the downregulation of proneural genes Neurogenin 1 (Ngn1) and Neurogenin 2 (Ngn2) (Mizuguchi et al. 2001; Novitch et al. 2001; Zhou et al. 2001), two bHLH transcription factors that promote neuronal differentiation (Scardigli et al. 2001; Sun et al. 2001b).   But how is the switch from neurogenic to gliogenic phase made knowing that Ngns are not sufficient to start gliogenesis all by themselves? A key element in this process is the gene Olig2, a bHLH transcription factor that not only was identified in connection with OL development (Lu et al. 2000; Takebayashi et al. 2000; Zhou et al. 2000) , but also has been implicated in promoting MN fate specification (Mizuguchi et al. 2001; Novitch et al. 2001).   While having a dual function in MN and OL specification, Olig2 by itself (i. e. at ectopic locations) is insufficient to induce the switch from MN to OL specification (Zhou et al. 2001).   Instead, Zhou et al (2001) demonstrated that Olig2 is able to induce formation of OLPs when it is ectopically coexpressed with either Nkx2.2 (another transcription factor involved in OL development [Qi et al. 2001; Sun et al. 2001a]) or with constitutively active components of the Notch signalling pathway and with concurrent downregulation of Ngn1 and Ngn2 (Zhou et al. 2001).   On top of this, domains of Nkx2.2 expression and Olig2 expression switch from mutually exclusive to overlapping at late stages of embryonic development (from ~E12 - onwards) (Zhou et al. 2001; Sun et al. 2001a).   Is this change of Nkx2.2 expression responsible for the downregulation of Ngns? This is unlikely to be the case as the disappearance of Ngns expression in the pMN domain precedes the dorsal expansion of Nk2.2.

Meanwhile, recent data suggest that Ngn2 downregulation is more a knock-on effect of a mechanism that triggers the switch than that mechanism's trigger.   Li et al (2011) observed that phosphorilation of residue Serine 147 (S147) of OLIG2 protein would only happen during MN production, but not at or after the onset of gliogenesis (Li et al. 2011).   They further realised that S147 dephosphorylation causes OLIG2 to exchange cofactors, preferring to dimerise with NGN2 than forming Olig2-Olig2 homodimers.   Being sequestered by OLIG2,

NGN2 no longer can play a role in MN production[†] thus shutting down other MN lineage genes such as Hb9, Isl1/2 and Lhx3 (see section 1.3.1 and 1.3.3). Concurrently, remaining undimerised OLIG2 proteins couple with other cofactors to promote OL development (for more details see section 1.4.2.3), hence reinforcing the neuron-to-glial switch.

But the mystery stands, how does the temporal change of Nkx2.2 expression take place and how to explain it? Orentas et al. (1999) already showed that Shh is required during a prolonged period of spinal cord development for specifying motor neurons and OLs (Orentas et al. 1999). Zhou et al. (2001) has recently suggested that the expansion of Nkx2.2 expression into the MN domain and the concomitant retraction of Pax6 expression to more dorsal levels might be controlled by a marked increase in the level of Shh activity secreted by the floor plate (Zhou et al. 2001). The mechanism by which the repression of Olig2 by Nkx2.2 in the pMN domain is relieved and the mechanism by which the ability of Olig2 to trigger Ngn2 expression is suppressed by coexpression of Nkx2.2 still remain to be elucidated.

All in all, mounting evidence focused on pMN domain has highlighted the complex regulatory code that mediates the neuron-glial switch. This involves: downregulation of Ngn2 expression, ongoing activity of Olig2 and Shh, Notch signalling to assure a reservoir of progenitors for the gliogenic phase, and activation of a gliogenic phase-specific transcriptional programme. The mechanism that regulates the interaction of all these components is not fully understood yet.

1.4.2. Oligodendrocyte development

1.4.2.1. The oligodendrocyte lineage and its role in the CNS

Oligodendrocytes are, literally, cells with a few branches/processes, which wrap themselves around developing axons and produce a specialised membrane structure known as the myelin sheath. The unique composition of the myelin sheaths (whose richness in lipids and low water content allow the electrical insulation of axons) and its unique segmental

---

[†] NGN2 has been shown to form heterodimers with Olig2 to control MN differentiation (Lee et al. 2005).
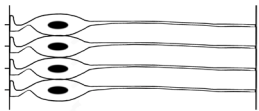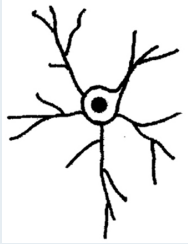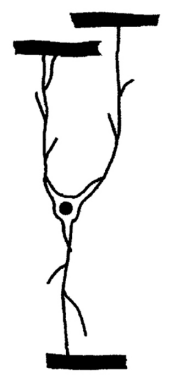
structure (responsible for the salutatory conduction of nerve impulses) assure the adequate conduction of nerve impulses. Each oligodendrocyte can myelinate multiple axonal segments and the unmyelinated junctions between any two of those segments are called nodes of Ranvier. Oligodendrocytes also allow substantial space saving by allowing reduced axonal calibre[‡] (Baumann et al. 2001). Additionally, a population of oligodendrocyte precursor cells, OLPs (NG2^{+} cells), which persists into adulthood, has the capacity to extend processes to synapses (Ong et al. 1999; Bergles et al. 2000) and nodes of Ranvier (Butt et al. 1999), as well as being able to respond to synaptic inputs from neurons (Lin et al. 2004; Lin et al. 2005). Although a matter of speculation at present, OLPs, which have been shown to divide and differentiate into mature oligodendrocytes throughout adulthood (Rivers et al. 2008; Psachoulia et al. 2009; Kang et al. 2010), are thought to act as a reservoir of new myelinating oligodendrocytes upon stimulation by surrounding neurons to meet the requirements of neural circuitry.

In principle, oligodendrocyte development is likely to be a continuous process of morphological transitions. In practice, however, we can only see the oligodendrocyte development as sequential distinct phenotypic stages, characterized by distinct proliferative capacities, migratory abilities, antigenic phenotypes or dramatic changes in morphology (summarised in Table 1.3).

Table 1.3 - Developmental stages of cells of the oligodendrocyte lineage.
Summary of markers identified during the progression from precursor cells to myelinating mature oligodendrocytes in rodents. The timing of appearance of the specific markers varies from region to region of the CNS and markers in this table are grossly according to the time of events in the spinal cord (data compilation based on Baumann et al. 2001; Woodruff et al. 2001; Miller 2002; Rowitch 2004) (below).

[‡] In invertebrate nervous system, due to the non-existence of myelin sheaths, rapid conduction is accompanied by increased axonal calibres (Baumann et al. 2001).

Stage of Maturation	Stage-specific Markers [*]	Stage of Development		Morphology
Neuroepithelial precursors	Nkx2.2 [1]; Nkx6.1; Olig1; Olig2; PDGFRα; Sox9 [2]; Sox10	E12.5	Proliferation	
Oligodendrocytes progenitors	NG2; Nkx2.2 [1]; Olig1; Olig2; PDGFRα; Sox9 [2]; Sox10	E13.5		
Late progenitors/pro-oligodendrocytes	CNPase; DM-20; NG2; O4; Olig1; Olig2; PDGFRα; Sox9 [2]; Sox10	E14.5	Differentiation	
Pre-myelinating oligodendrocytes	CNPase; DM-20; GALC; NG2; O4; Olig1; Olig2; PDGFRα; PLP; Sox9 [2]; Sox10; TCF4 [3]	E16.5	Survival	
Myelinating Oligodendrocytes	APC/CC1; CNPase; DM-20; GALC; MBP; NG2; Nkx2.2 [1]; Nkx6.2 [4]; O4; Olig1; Olig2; PDGFRα; PLP; Sox9 [2]; Sox10; TCF4 [3]	E18.5 ↓ P14 ⋯ Adult	Myelination	

[*] See clue to undermentioned abbreviations at the beginning of this thesis in the Abbreviations page. [1] Reference: Fu et al. 2002; [2] Reference: Cai et al. 2010; [3] Reference: Fu et al. 2009; [4] Reference: Wegner et al. 2005.

1.4.2.2. Specification of oligodendrocytes and their origins

Oligodendrogenesis begins in earnest after the neuron to glial fate switch has ceased. Oligodendrocyte precursors arise from multiple sources across the ventral-to-dorsal axis of the neural tube. While the earliest evidence supported a ventral origin of OLPs, more recently it has become clear that some OLPs also develop from dorsal neuroepithelium (Richardson et al. 2006). The current view is that the ventrally-derived precursors of the spinal cord, which develop earlier during development, compete with and suppress their dorsal counterparts arising later. By contrast, in the forebrain the ventral-most lineages are replaced by dorsal precursors that populate the same regions later on (Kessaris et al. 2006; Richardson et al. 2006 and references therein).

It is generally accepted that the majority of spinal cord oligodendrocytes are generated from a restricted domain in the ventral spinal cord that first give rise to somatic motor neurons – the pMN domain. OLPs, defined by expression of PDGFRα (Pringle et al. 1993; Hall et al. 1996) and Sox10 (Kuhlbrodt et al. 1998), are first detected at around E12.5 in the mouse spinal cord demarcating roughly the region (pMN) that previously generated MNs (Jessell 2000). Moreover, Shh is both sufficient and necessary for oligodendrocyte specification (Poncet et al. 1996; Pringle et al. 1996; Orentas et al. 1999) and together with evolutionary arguments linking MNs and OLs (Richardson et al. 2000), it further supports a developmental connection between somatic MNs and Ols. At last, unequivocal evidence reinforcing the idea of a lineal relationship between MNs and OLs came from *Olig1/2* null mice, two basic helix-loop-helix proteins required for the establishment of the pMN domain (Lu et al. 2000; Takebayashi et al. 2000; Zhou et al. 2000). In *Olig2* and *Olig1/2* mutant mice, the expression of p2 domain protein Irx3 expands ventrally to occupy the pMN domain, resulting in an ectopic generation of V2 interneurons at the expense of MNs and subsquent loss of OLPs, which are replaced by ectopic production of astrocytes (Lu et al. 2002; Takebayashi et al. 2002; Zhou et al. 2002). pMN-derived migratory OLPs disperse laterally and dorsally, occasionally over long distances, to occupy the entire developing CNS before differentiating into myelin-forming oligodendrocytes (Jessen et al. 2001; Takebayashi et al. 2002). But there remains some controversy as to whether other regions of the ventral neuroepithelium ever give rise to oligodendrocytes. For instance, PDGFRα/O4-positive precursors have been shown to arise entirely within the Nkx2.2-expressing neuroepithelium domain in birds (Xu et al. 2000; Soula et al. 2001), somewhat unexpected as *Nkx2.2* gene is known to demarcate the p3 domain (Jessell 2000). It turns out that the domains of expression of Olig2, which defines the pMN domain, and of Nkx2.2 in the neuroepithelium switch from being mutually exclusive to overlapping (Zhou et al. 2001) during later embryogenesis. This has been further confirmed in mice where different OLPs are suggested to be originated from two distinct locations: one population of OLPs coexpresses

Olig2 and Nkx2.2, and which emigrates from the zone of overlap between these two factors, while the other population expresses Nkx2.2 but not Olig2 and emigrates more ventrally possibly aquiring Olig2 expression later on (Fu et al. 2002). The latter source of OLs has been recently confirmed in chick spinal cord by retrovirus experiments (Gotoh et al. 2011). It will be of interest to determine wether or not the same finding is extended to rodents.

Various past studies tentatively put forward the idea of a dorsal source of oligodendrocyte. While Spassky and colleagues support a multiple source of OLPs based on their studies with a proteolipid protein (*Plp*)-*lacZ* reporter line (Spassky et al. 1998; Spassky et al. 2000), Rao and his co-workers suggested a dorsal, as well as ventral, source of OLPs based on the fact that they were able to isolate OPCs from different parts of the spinal cord neuroepithelium and culture them in vitro (Rao et al. 1998; Liu et al. 2003). Moreover, there were also controversial results from chick-quail chimeras that raised the possibility of dorsal OLP sources in birds (Cameron-Curry et al. 1995; Pringle et al. 1998; Richardson et al. 2006). But the idea of dorsal-derived OLPs faded away for some time because of convincing data. Recently, however, it was shown conclusively that a second and later-derived source of oligodendrocytes develops from the dorsal cord of the spinal cord, but these constitute a minor population compared to the pMN-derived oligodendrocytes. These findings were concurrently spotted by three laboratories (Cai et al. 2005; Fogarty et al. 2005; Vallstedt et al. 2005). Cai *et al*. and Vallsted *et al*. examined *Nkx6.1* and *Nkx6.2* double mutants (*Nkx6* null) in which Olig2 expression is lost[§], thus resulting in the concomitant arrest of both MNs and pMN-derived OLs production. They found that PDGFRα^+/Olig2$^+$ expressing cells continue to be generated in the dorsal spinal cord of *Nkx6* mutants and that they co-express paired box gene 7 (*Pax7*), confirming their dorsal origin. These dorsal-derived OLPs could also be found in wild type spinal cord at around E15, a few days later than ventral ones (E12). Fogarty and co-workers confirmed these conclusions by Cre-*lox* fate-mapping experiments in transgenic mice (Fogarty et al. 2005). They generated a *Dbx1*- iCre transgenic line whereby iCre recombinase was placed under control of the *Dbx1* homeobox gene and its expression restricted to the neuroepithelial precursor domains p1, p0, dP6 and dP5. *Dbx1*-derived oligodendrocytes were mainly located in the lateral white matter radially opposite their site of origin in the VZ and made up to 3% of the total population of oligodendrocytes in the spinal cord. Further fate-mapping studies using *Msx3*-iCre transgenic mice, in which iCre expression is restricted to the entire dorsal cord, go as far as suggesting that 20% of OLs

---

[§] *Olig2* gene is primarily responsible for OLP specification and its expression is under tight control of *Nkx6* activity (Novitch et al. 2001; Vallstedt et al. 2001).

originate in the dorsal spinal cord, hence still representing a minor contribution to the total OL population in the SC (Fogarty 2006). Dorsal-derived OLP specification *in vitro* is dependent on FGF signalling but independent of Shh and it requires downregulation of BMP activity (Fogarty et al. 2005; Vallstedt et al. 2005). Unlikely their pMN-derived counterparts, which first appear as a rapidly proliferating group of cells near the VZ, *Dbx*-domain derived OLPs appear to be formed by direct interconversion from radial glial at the time when down-regulation of radial markers begins (E15.5) (Fogarty et al. 2005).

1.4.2.3. Further development: from progenitors to mature oligodendrocytes

After specification, OLPs start to proliferate and migrate widely to populate the entire CNS (Miller et al. 1997). Because they express PDGFRα, OLPs are able to respond to the mitogenic and survival factor PDGF (Pringle et al. 1992; Pringle et al. 1993), and PDGF depletion limits OLP proliferation in vivo (Calver et al. 1998; Fruttiger et al. 1999; van Heyningen et al. 2001). Interestingly, however, continuous stimulation of OLP proliferation by over-expressing PDGF does not yield a proportional increase in the final numbers of myelinating oligodendrocytes, consistent with the idea that the final number of oligodendrocytes is set by axon-derived survival factors, independently of the number of OLPs (Calver et al. 1998).

OLPs settle along fibre tracts of the future white matter, going through several developmental stages, before maturing during late embryonic and early postnatal stages of development. When they convert into pre-oligodendrocytes, they still proliferate but no longer migrate. Pre-OLs become multiprocessed and change their antigenic profile, losing PDGFRα and, in rodents, expressing sulphated glycolipids recognised by the O4 monoclonal antibody. Before their final maturation, involving myelin formation, oligodendrocytes go through a few more stages of development. During this development, about 50% of newly formed oligodendrocytes rapidly die because of competition among those OLPs for limited amounts of axon-derived survival factors (Barres et al. 1992a; Barres et al. 1992b). The presence of unmyelinated axons seems to play a role on OL cell survival rate inasmuch as an increasing number of unmyelinated axons directly boosts OL production (Burne et al. 1996). Fully differentiated mature OLs, now post-mitotic, express the major myelin components such as myelin basic protein (MBP) and proteolipid protein (PLP), which are correlated with the late stages of maturation of the oligodendrocyte lineage, and myelin formation.

1.4.3. Astrogenesis

1.4.3.1. Astrocyte definition and classification

Astrocytes were first visualised over a century ago (Andriezen 1893). Their name derives from the Greek root word "astro", which means "star", referring to their star-like morphology in Golgi stained samples. Today, astrocytes are recognized to be a more diverse cell population than they appear based on morphology alone (reviewed in Hewett 2009 and Zhang et al. 2010). They carry out multiple roles essential for normal neurological function, including maintenance of the blood-brain barrier, trophic support for neurons and modulation of synaptic activity (Christopherson et al. 2005). The most abundant glial population in the CNS, astrocytes paradoxically are one of the least understood cell types that make up the CNS.

Astrocytes are broadly divided into two classes – "fibrous" and "protoplasmic" – on the basis of their morphology, location and expression of glial filaments. In general, fibrous astrocytes populate the white matter, express high levels of the Glial Fibrillary Acidic Protein (GFAP, an intermediate filament protein) (Eng et al. 1971) and are associated with neuronal axons at nodes of Ranvier. Protoplasmic astrocytes are located in grey matter and express little or no GFAP (Nolte et al. 2001). Protoplasmic astrocytes, which are highly ramified, are intimately associated with neuronal cell bodies, ensheath synapses and can be found in contact with blood vessels. The CNS also contains other specialized glial cells that share many common features with astrocytes. These include Bergmann glia in the cerebellum and Müller cells in the retina. These have small cell bodies surrounded by many, branching processes and are closely associated with synapses (Reichenbach et al. 2010). Another cell population expressing GFAP are sub-ependymal astrocytes in the subventricular zone (SVZ) of the lateral ventricles and the subgranular zone (SGZ) of the dentate gyrus in the adult brain. It is something of a misnomer, however, to consider sub-ependymal astrocytes (subsequently renamed type B cells; further discussed in section 1.5) as a sub-population of astrocytes, as they possess distinct characteristics not present in mature astrocytes.

1.4.3.2. Development of astrocytes

Astrocytes are ubiquitously distributed throughout the CNS. Each astrocyte occupies its own microdomain, the extent of which depends on astrocyte-astrocyte interactions (Livet et al. 2007; Imura et al. 2008).

Astrocytes are produced by neuroepithelial cells via direct differentiation from radial glia (Schmechel et al. 1979; Voigt 1989; Goldman 2001). After neurogenesis is over, radial glia cells translocate their cell bodies to the pial surface and differentiate into GFAP expressing astrocytes. Radial glia can also produce intermediate progenitors that expand in number before generating astrocytes (as discussed in sections 1.4.2.2. and 1.1.2). Possibly, fibrous astrocytes, which settle along the pial surface, might originate by direct transdifferentiation of RG whereas protoplasmic astrocytes, which are scattered in the grey matter, develop from proliferative intermediate progenitors. This is rather speculative, however. After migrating to their final positions astrocytes begin the process of terminal differentiation and are generally thought to be quiescent during normal life, becoming "reactive" and proliferative after injury (Buffo et al. 2008).

Recent fate-mapping studies have started to uncover the origins of specific astrocyte populations in the spinal cord. Making use of Cre-loxP technology, Fogarty and colleagues showed that both protoplasmic and fibrous astrocytes collectively can come from dP5, dP6, p0 and/or p1 progenitor domains (Fogarty et al. 2005; Fogarty 2006). *Dbx*-derived astrocytes, unlike oligodendrocytes, tend to settle radially opposite their site of origin in the VZ, and do not migrate tangentially. Fittingly, in Msx3-iCre fate-mapping experiments, where progenitor domains of the dorsal cord are exclusively marked, astrocytes are found occupying almost only dorsal territories (Fogarty 2006).

1.4.3.3.   Molecular determinants of astrocytes development

In spite of stronger appreciation of the functional heterogeneity in astrocytes, it has been generally accepted that they develop by a uniform genetic mechanism. The findings that astrocyte generation is induced in the absence of proneural basic (bHLH) function (Nieto et al. 2001) or by helix-loop-helix (HLH) proteins that inhibit transcriptional activity of neurogenic bHLH transcription factors (Nakashima et al. 2001) have led to the proposal that astrocytes develop "by default", in the absence of signals specifying alternative fates (Ross et al. 2003). However, this view has been recently questioned. In Drosophila different astrocyte-like cells are found to arise from distinct precursors, some of which develop under the action of the transcription factor glial cell missing (gmc) while others do not (Awasaki et al. 2008; Doherty et al. 2009). Likewise, work in vertebrates has suggested that, at least in the ventral spinal cord, astrocyte sub-type specification operates through region-restricted expression of transcription factors in different progenitor domains. For example, glial sub-type generation in the pMN and p2 neuroepithelial progenitor domains is regulated by cross-repressive interactions between the bHLH proteins Olig2 and SCL to produce

oligodendrocytes versus astrocytes progenitor cells, respectively (Muroyama et al. 2005). Moreover, generation of particular fibrous white matter astrocytes, which are molecularly and positionally distinguishable, is dependent on region-specific specification of their respective progenitors by homeodomain transcription factors Nkx6.1 and Pax6 (Hochstim et al. 2008). These studies suggest that the origins of some astrocyte subtypes can be mapped to progenitors in the neuroepithelium with region-specific molecular phenotypes and open additional questions. It has been shown that interneuron specification at all dorsal-ventral levels of the spinal cord is regulated at birth by a segregated transcription code operating in distinct neuroepithelial domains; is also astrocyte identity coupled to neuroepithelial pattern formation along the neural tube?; Is this segmental division of molecularly specific astrocytes linked to their function in the mature CNS, hence mirroring the development of functionally different interneurons of the spinal cord? These and other questions are scope for further studies.

1.5. The role and origin of ependymal cells in the CNS

Ependymal cells are cells with motile cilia at the interface between the brain or spinal cord parenchyma and the ventricular or lumen cavities, respectively, and collectively they comprise the ependymal layer. In the ependymal layer of both brain and spinal cord resides a morphologically heterogeneous population of ependymal cells. In the brain, most of them are multiciliated (containing at least 50 long motile cilia), have large apical surfaces and a cuboid phenotype. However, a novel type of ependymal cells (E2 cells) seem to contain only two long cilia (Mirzadeh et al. 2008). Brain ependymal cells can be stained for S100β, CD24, vimentin, Nestin (Lendahl et al. 1990; Frisen et al. 1995; Carlen et al. 2006) and FoxJ1 (HFH4; Lim et al. 1997) but they are negative for proliferative markers and do not incorporate BrdU in normal conditions. At the ventricular surface, they lay out in a pinwheel pattern with type B cells (the neural stem cells) at the centre surrounded by the two types of ependymal cells (Mirzadeh et al. 2008). On the other hand, ependymal cells of the spinal cord express Sox9 (Pompolo et al. 2001), and also vimentin, Nestin and FoxJ1 like their brain counterparts. They possess a lesser number of cilia, one to three, and display three different morphological phenotypes: cuboidal ependymal cells, the tanycytes and the radial ependymal cells (Meletis et al. 2008). Cells with intermediate phenotypes can be also observed. The classification of ependymal cells, both in the brain and spinal cord, is based purely on morphological criteria (since they show a homogeneous molecular profile) and does not have implied functional heterogeneity thus far.

Ependymal cells play an essential role in the propulsion of Cerebral-Spinal Fluid (CSF) along the ventricular system and their malfunction leads to disturbances of the CSF current and ultimately to hydrocephaly (Brody et al. 2000). Other functions have been attributed to them as diverse as filtration of brain molecules or insulation from damaging substances in the CSF or even dispersion of neural messengers (Bruni 1998).

Cells in the ependymal layer of the adult spinal cord have a low level of mitotic activity (Johansson et al. 1999); around 20% of ependymal cells are labelled after continuous administration of BrdU during one month in the drinking water and they constitute 4-5% of all BrdU-labelled cells in a cross-section of an adult spinal cord (Meletis et al. 2008; Barnabe-Heider et al. 2010). During normal life, this level of proliferation seems sufficient to maintain the ependymal layer, replacing cells that die through normal wear-and-tear. In response to injury, ependymal cells of the adult spinal cord show multi-lineage potential, producing scar-forming astrocytes and very few remyelinating oligodendrocytes, as well as self-renewing (Barnabe-Heider et al. 2010). Ependymal cells of the spinal cord do not contribute to adult neurogenesis, neither in normal nor injury conditions.

A contrasting situation is observed in the brain. Ependymal cells lining the adult lateral ventricle wall do not divide, judging by the lack of incorporation of Ki67 and BrdU markers in uninjured animals (Spassky et al. 2005; Carlen et al. 2009). Neither do they generate neurons in normal conditions as suggested previously (Johansson et al. 1999). However, ependymal cells in the brain are able to generate neuroblasts and astrocytes in response to injury (Carlen et al. 2009). This process involves ependymal cells regaining radial glial cell features (Gregg et al. 2003; Taylor et al. 2005; Zhang et al. 2007) in particular the capacity to re-enter the cell cycle through the suppression of canonical Notch signalling. When forced Notch signalling was maintained, ependymal cells failed to produce functional neurons and astrocytes (Carlen et al. 2009). Hence, Notch signalling normally maintains the quiescent state of ependymal cells. However, although they have multi-lineage potential, ependymal cells in the brain are depleted by stroke and so do not fulfil the defining criteria of a true stem cell, serving instead as a reservoir of primary cells that are used up during injury (Carlen et al. 2009).

A series of recent studies has begun to unveil the origins of the ependymal cells of the spinal cord, albeit little advancement has been done on studies on their brain counterparts. Spassky and colleagues have shown that ependymal cells originate from RG before birth but their committed RG progenitors remain quiescent and only acquire the typical feature of ependymal cells after birth (Spassky et al. 2005). It has also been observed that ependymal cells express the ventral transcription factor Nkx6.1, but not dorsal markers such as Pax7, strongly suggesting that they are derived from Nkx6.1-expressing neuroepithelium (Fu et al.

2003). Fittingly, Fogarty and co-workers show, by means of Cre-fate mapping techniques, that progenitor domains more dorsal than the Nkx6.1-expressing domain do not contribute to the ependymal layer of the postnatal spinal cord (Fogarty et al. 2005; Fogarty 2006). Moreover, it has been reported that Olig2-positive progenitors in the embryonic spinal cord give rise to a subset of ependymal cells of the postnatal spinal cord (Masahira et al. 2006). Taken together, the various studies point to ependymal cells as formed from p3, pMN and p2 domains of the embryonic ventral spinal cord (Richardson et al. 2006). It is not known, however, whether this restricts their regenerative potential to ventral cell types in the adult cord after injury.

It is still unknown how ependymal cells arise from their radial glia progenitors during development.   A deeper understanding of the molecular mechanisms underpinning ependymal cell specification during embryogenesis and adulthood might aid the development of therapeutic approaches where these cells could be modulated in situ to produce required progeny in response to injury, as a substitution for cell transplantation.

1.6. Fate-mapping with Cre and PAC technologies in mice

1.6.1. Brief introduction: a historical perspective

Fate-mapping involves tracking a cell and all of its progeny in order to discover the lineage tree of the different cell types that constitute an organism.

Fate-mapping all cells of an organism constitutes one of the earliest aspirations of developmental biologists and, on account of pioneering work of early experimental embryologists, we know now, at least in a rudimentary form, the main lineages in vertebrates (for a chronology of events see Table 1.4).

The first fate maps date back to the 1900s and, relied on studies using transparent invertebrate organisms combined with Nomarski interference microscopy and video recording to follow cell behaviours. However, only a few organisms are amenable to direct observation. Further improvements on fate-mapping techniques came only some decades later with the use of vital dyes and radioactive markers used to mark individual or groups of cells (Table 1.1). While allowing tracing cell behaviours in higher organisms, fate-maps relying on vital dyes and radioactivity markers were confused by the tendency of the

staining to diffuse and dilute (over cell-division), thus greatly hampering the resolution of the method and its use for long term lineage analysis

In 1969, a milestone was reached with the use of chick-quail chimeras (Table 1.1). Because quail cells can be distinguished from chick cells by their different antigenic profile and interphase nuclei, chick-quail grafts provide a natural way of enabling permanent cell labelling. Nevertheless, chick-quail chimeras offer a few challenges, mainly the fact they are technically demanding, and they confine lineage studies to bird development. Also, they do not allow individual cell lineages to be followed but only the fates of relatively large tissue blocks.

In the late 1980s, fate-mapping studies were revolutionised with the advent of molecular biology, allowing cells to be marked genetically. Since then powerful techniques have evolved enabling permanent labelling by genetically modifying organisms using virus vectors or transgenes to drive expression of marker molecules in a targeted way. And now, thanks to the development of new microscopes and markers, investigators can map single cells in real time in living organisms and combine lineage analysis with genetic ablation of cells and genes.

Table 1.4 - Fate-mapping technologies adopted throughout the years.
For a detailed timescale of events see Clarke et al. 1999.

Year	Milestone	Reference
1905	Edwin Conklin and co-workers make use of the transparent properties of the sea squirt *Styela partita* to generate a remarkable collection of ascidian fate maps.	Conklin EG 1905
1978	Uwe Deppe and colleagues used the transparent invertebrate organism, *Caenorhabditis elegans*, combined with Nomarski interference microscopy and video recording, to follow the cell behaviour of the first 182 cells of the developing worm.	Deppe et al. 1978
1929	Vogt optimised a technique of marking areas of the newt egg using vital dyes and followed the fates of different group of cells on the surface of the developing embryo during gastrulation.	Vogt W 1929
1969	Nicole Le Douarin discovered that quail and chick cells are distinguishable for their specific and different interphase properties which can be revealed after carrying out a simple DNA staining technique.	Le Douarin 1969

Table 1.4 (cont.)

Year	Milestone	Reference
1969-1975	Nicole Le Douarin pioneered the application of chick-quail chimaeras for lineage studies. Her studies are outstanding for their precision and elegance. She greatly contributed for our understanding of neural-crest migration, epithelial-mesenchymal interactions and neural-plate formation.	Le Douarin et al. 1969; Le Douarin et al. 1975
1981	Study describing the tracing of proliferative cells of the ventricular zone to the hippocampus of *Rhesus monkey* performed with the radiolabelled dye thymidine.	Nowakowski et al. 1981
1988	This study reports the use of bright fluorescent dyes in combination with radioactive thymidine, injected into single cells, to follow cell behaviours.	McConnell 1988
1986-1990	These studies report the use of retrovirus for cell lineage analysis; while providing with an indelible, heritable, and accurate labelling, the retroviral approach has no intrinsic marker of clonality and so each clone of cells stain similarly; moreover, cells within a population cannot be distinguished using this technique.	Price et al. 1987; Turner et al. 1987; Leber et al. 1990
1996/1997	These works use an intricate but long-term marking strategy of single cells and their descendants, which can be visualised after LacZ recombination.	Nicolas et al. 1996; Mathis et al. 1997
2006	This study makes extensive use of Cre excision-conditional transgenesis applied to label cell lineages via permanent activation of a reporter gene in combination with cell ablation studies.	Kessaris et al. 2006

1.6.2. Lineage tracing with PAC transgenesis and Cre reporter mice

Genetic marking of cells in transgenic mice can be achieved typically in two distinct ways: 1) by targeted insertion of exogenous DNA into a specific locus in the mouse genome - the so called "knock-in" approach; and 2) by random insertion transgenesis, where a fragment of exogenous DNA is randomly inserted into the genome. Both techniques have their own pros and cons.

In the "knock-in" approach the expression of the exogenous DNA is under the control of the same regulatory elements as the endogenous gene of interest. While assuring that the exogenous DNA mimics the expression of the endogenous gene, this technique is limited to genes that show no phenotypic abnormalities after disruption of one of its alleles (Nutt et al. 1999) or to genes that can be combined with the exogenous DNA to produce a functional bicistronic construct. Furthermore, this technique is based on homologous recombination in ES cells which makes it time-consuming and costly.

In the second approach, the making of transgenic mice relies on exogenous DNA being placed under the control of specific regulatory element sequences, which are not always known for a given gene of interest. The resulting DNA construct, conventionally not longer than 10-20kb, is then inserted into the genome randomly without, one hopes, disrupting any essential coding sequences. This is regarded as a quick-and-easy technique; however, expression of exogenous DNA in conventional transgenic mice is often subject to position (integration site) effects which can result in misexpression or silencing of the transgene.

A new approach to mouse transgenesis has recently been developed based on the manipulation of P1 bacteriophage-derived or bacterial artificial chromosomes (PACs or BACs). These are circular DNA plasmid vectors that hold large fragments of genomic DNA that are likely to contain all the regulatory elements of a gene of interest (Ioannou et al. 1994). Moreover, given their large size, PACs/BACs are unlikely to be silenced, i.e. less likely to be subject to positional effects, and their use avoids problems of haplo-insufficiency. PACs are also simple to manipulate compared with homologous recombination in ES cells and recombinant PAC/BAC DNA can be produced in bacteria and easily purified. The powerful advantages inherent to PAC/BAC transgenesis streamlines the production of transgenic mice and greatly increases our ability to manipulate gene expression in mice.

Another genetic tool that has revolutionised mouse genetics and the science of fate-mapping is Cre recombinase. Cre was isolated from bacteriophage P1 and belongs to the integrase family of site-specific recombinases. In vivo, the function of Cre recombinase is to circularize the P1 bacteriophage genome during infection assuring the maintenance of the genome in a monomeric state during the phage's life cycle. The enzyme efficiently catalyzes recombination between two of its consensus 34bp DNA recognition sites, known as loxP sites, in any cellular environment and on any kind of DNA. If two co-linear loxP sites are orientated in the same direction then Cre-mediated recombination causes the excision of the DNA sequence flanked by the loxP sequences. If the loxP sites have opposing sequence directions then any intervening DNA will be inverted.

Due to the unique characteristics of the Cre/LoxP system, numerous genetic engineering applications of Cre excision-conditional transgenesis surfaced (Nagy 2000). For instance, Cre-mediated recombination has enabled us to direct mutagenesis in a temporarily controlled manner. For this, a mouse Cre line that expresses Cre in a desired pattern, is crossed with another mouse line that carries the gene of interest flanked by loxP sites ("floxed"). When Cre starts to be expressed, it mediates excision of the floxed gene. Furthermore, Cre-mediated excision can be applied to label cell lineages via permanent activation of a fluorescent or chromogenic reporter gene. Temporally-controlled fate map studies can also be achieved when a ligand binding domain is fused with Cre recombinase producing a fusion protein Cre-ER^{T2} (see Figure 1.4 and Figure 1.5, and also see text-box below for more details). This recombinant inducible-Cre recombinase is only able to mediate recombination in the presence of its ligand – the estrogen analogue tamoxifen. In this way tracing cell behaviours both spatially and temporally becomes possible.

Text-box - Cre-ER^{T2} recombinase

Cre-ER^{T2} is a ligand-dependent chimeric Cre recombinase in which a mutated form of the human estrogen receptor (ER) ligand binding domain (LBD) is fused to Cre recombinase (Feil et al. 1997; Indra et al. 1999). In the absence of the ligand, the LBD hinders translocation of the enzyme into the nucleus, thus preventing its function. This is because LBD causes the receptor to bind to a cytoplasmic protein complex containing Heat-shock protein 90 (Hsp90) when no ligand is present, sequestering the protein in the cytoplasm (Picard 1994). Once available, the ligand binds to the LBD releasing the chimeric protein (Cre-ER^{T2}) from Hsp90 allowing nuclear translocation. One problem of these chimeric recombinases is that they can be activated by natural ligands that can be present in the host. In the chosen mutant *Cre-ER^{T2}* the mutation is such that *Cre-ER^{T2}* can be activated by the synthetic ligands OHT (oestrogen 4-hydroxytamoxifen), ICI (ICI 182.780) or tamoxifen (TM), but remains insensitive to E2 (17β-oestradiol), which is endogenously present in mice.

Like Cre recombinase, Cre-ER^{T2} is a site-specific recombinase that recognises and binds to specific sites called loxP (Nagy 2000). Two loxP sites recombine in the presence of Cre, allowing the DNA cloned between two such sites to be removed by Cre-mediated recombination after TM treatment. In the example shown in Figure 1.4 the DNA fragment to be removed is a "Stop" fragment that blocks the expression of the reporter gene (e.g. the *lacZ* gene, the *eGFF* gene or *YFP* gene). The mechanism by which this process occurs is schematically represented in Figure 1.4.

Overall, PAC transgenesis in combination with Cre-mediated reporter gene activation provides us with the possibility of fate-mapping the mouse at a galloping pace compared to previous methods. I have used the Cre-lox approach in my Thesis work to examine cell fate choices in the ventral neural tube. My studies have provided evidence that motor neurons of the autonomic CNS are generated in the ventral-most neuroepithelium domain abutting the floor plate. This contradicts current theories, which place the origin of autonomic motor neurons more dorsally than this, in the same progenitor domain (pMN) that generates somatic motor neurons.

1.7. The aims of the thesis

The study of cell generation in space and over time is an important aspect of developmental neuroscience and a spate of recent studies has brought significant insights to the field. Today, the origin of many neurons and glia has been traced back to specific neuroepithelial domains. In the spinal cord, progenitor cells in the most ventral region of the neuroepithelium expressing *Nkx2.2* have been shown to give rise to V3 interneurons. Generation of visceral motor neurons, serotonergic interneurons, and oligodendrocytes have also been linked to the equivalent *Nkx2.2*-expressing neuroepithelial domain in the hindbrain. While much research has been devoted to the brain, little or only weak evidence is available on the progeny of $Nkx2.2^+$ domain of the spinal cord, mainly concerning its glial progeny. The purpose of this thesis is to clarify and/or identify the differentiated progeny of $Nkx2.2^+$ neuroepithelial progenitor cells in the spinal cord and hindbrain to illuminate their lineage and migration patterns. To do this, *Cre/loxP* technology and PAC transgenesis were used to express an inducible Cre recombinase under *Nkx2.2* transcriptional control (see Chapter 2). Chapter 3 describes the generation of an $Nkx2.2\text{-}CreER^{T2}$ mouse line and its characterisation. Chapter 4 reports the results of my fate-mapping studies. Chapter 5 summarises the findings of the Thesis and discusses their implications for the field of spatial patterning and cell specification in the ventral spinal cord.
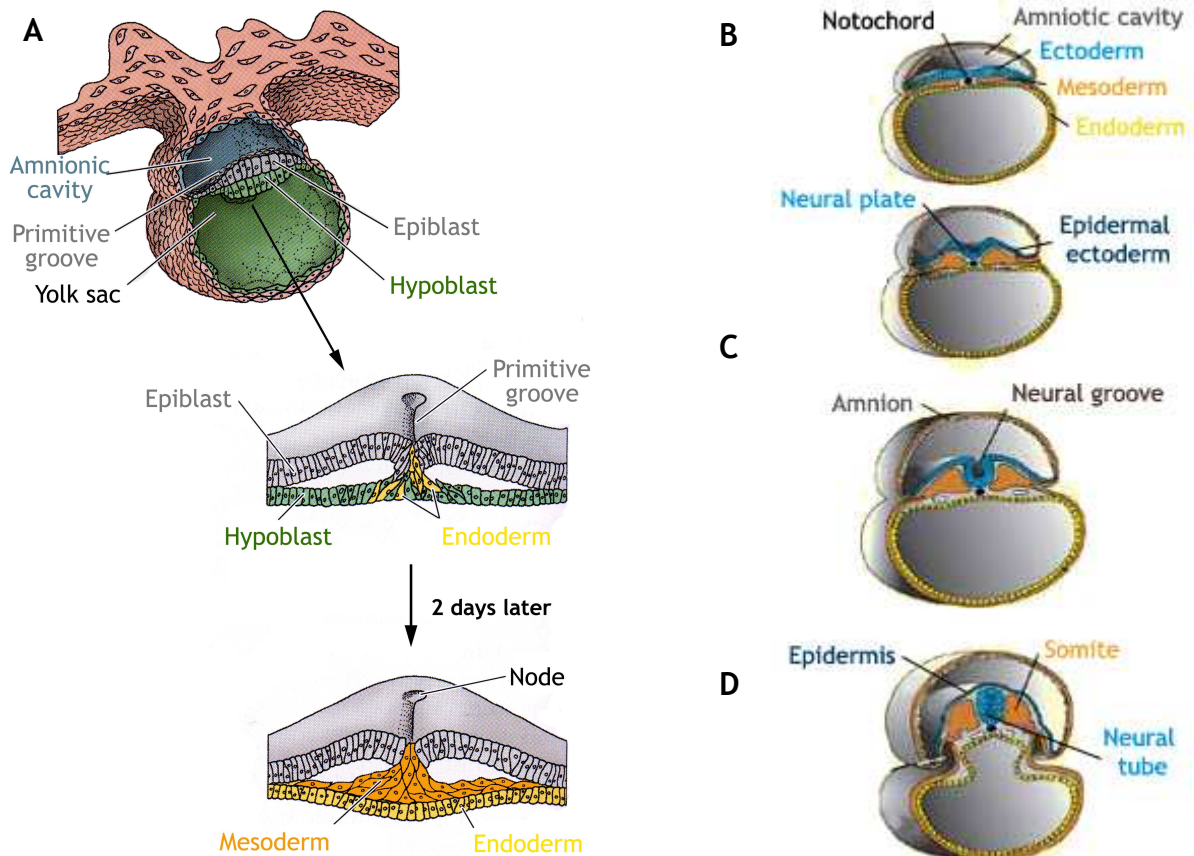
Figure 1.1 - Neurulation. At the start of neurulation it is the ingression of epiblast cells that transform the one layered epiblast to the three layered gastrula **(A and B)**. Signals released by the underlying mesoderm trigger the process of neurulation. The neural plate goes through various morphological changes **(C)** which results ultimately in the formation of the neural tube **(D)**. (adapted from Gilbert 2000 and http://thebrain.mcgill.ca/flash/a/a_09/a_09_cr/a_09_cr_dev/a_09_cr_dev.html).
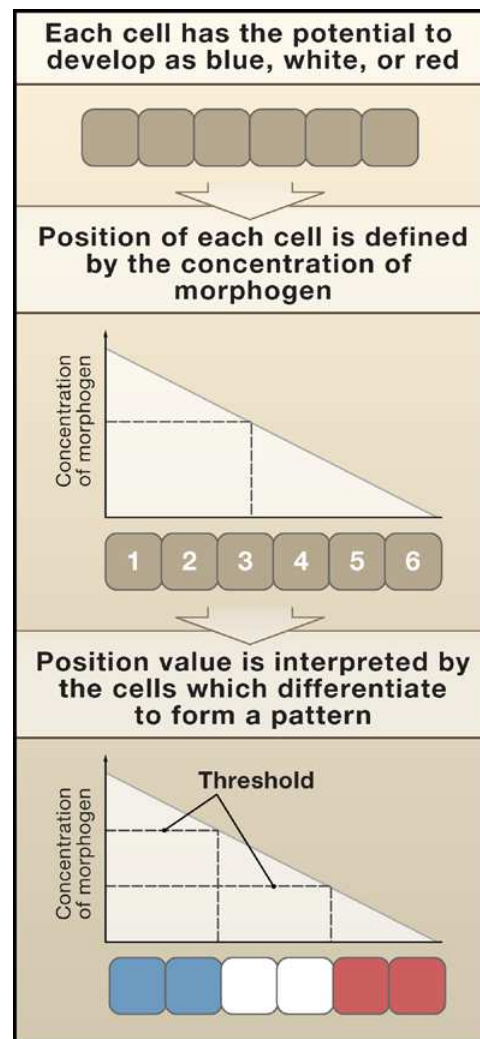
Figure 1.2 - The The French Flag Model for positional specification in the embryo. This model describes pattern formation in a tissue that is originally homogeneous. At first, a spatial distribution of an exogenous factor (the morphogen) is established in the embryonic tissue; for instance, let us consider a morphogen source locating on the left-hand side, and a sink (where the morphogen is degraded) on the right. As the morphogen diffuses, the distribution of it eventually creates a differential but stable gradient of concentrations. This model assumes that each and every cell is then able to read this morphogen concentration and compare it with a given intrinsic threshold concentration spectrum which will determine their genetic program of differentiation. Hence, cells occupying different positions in relation to the source of morphogen acquire distinct identities or positional values which ultimately lead to pattern formation in the embryonic tissue. (Adapted from Wolpert et al. 2006)
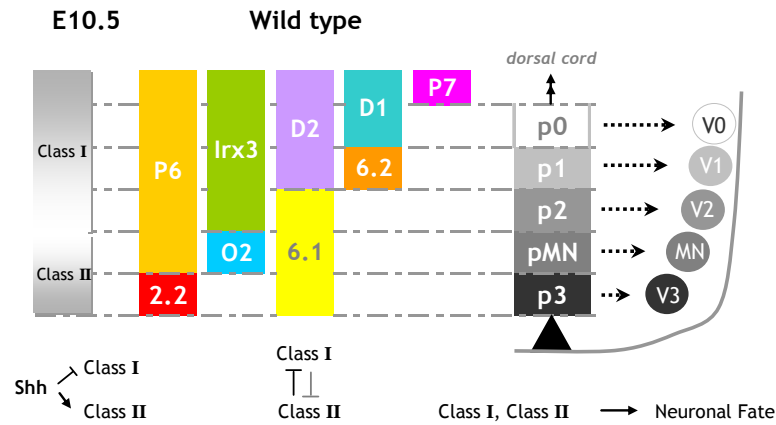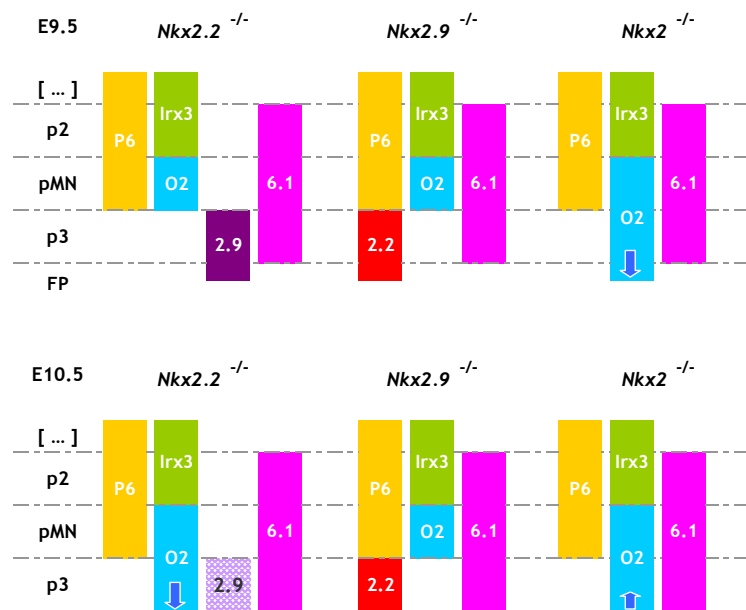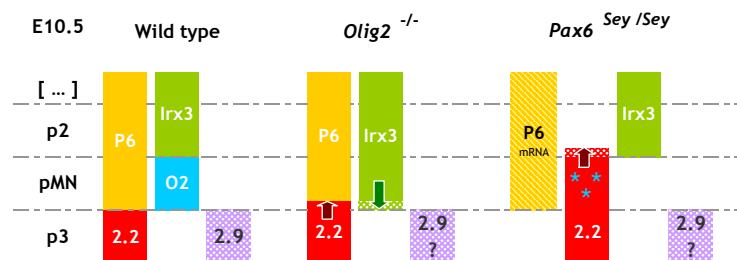
Figure 1.3 - Transcription factor dynamics during patterning of ventral spinal cord. (see text of sections 1.2.2, 1.3.1 and 3.1 for more details) panel A) each progenitor (p) domain is colored using a grey scale, in which the gradation in colour mimics the decreasing Shh concentration along dorsoventral axis, with the maximum concentration at the floor plate (black triangle);   panel B and C) pattern indicates weak or practically absent expression of *Nkx2.9*; panel C) blue stars represent scattered *Olig2*^{+} cells). Arrows indicate that at the specified age the boundary is moving in that direction.   *Note:* Despite not being schematically shown in this diagram, expression of Nkx2.2 and Nkx2.9 in the floor plate of wild type embryos at or before E9.5 has also been referenced (Pabst et al. 2003; Strahle et al. 2004; Jeong et al. 2005; Placzek et al. 2005; Holz et al. 2010).
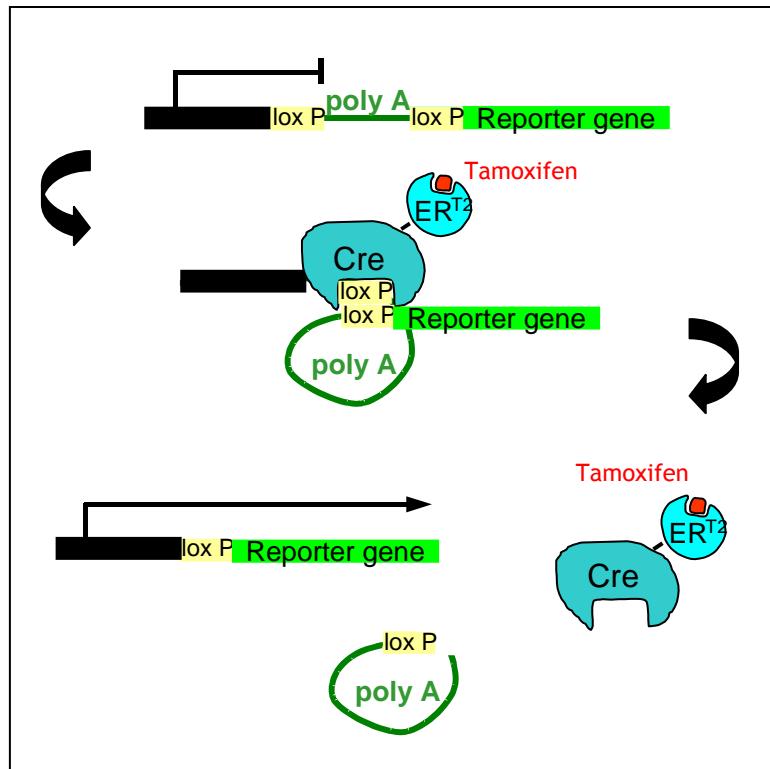
Figure 1.4 - *Cre-ER^{T2}/loxP* **system**. Cre is a site specific recombinase isolated from P1 bacteriophage. It recognises a 34 bp sequence − loxP site. If 2 loxP sites are present in the same fragment of DNA, in the same orientation, Cre catalyses the excision of the DNA sequence flanked by the 2 loxP sites. As exemplified in the figure, upon the presence of tamoxifen Cre recombination event allows the transcription of a reporter gene (bright green) to occur, which expression would otherwise be silenced by the existence of a spacer DNA (such as a poly A sequence) (see text for further details).
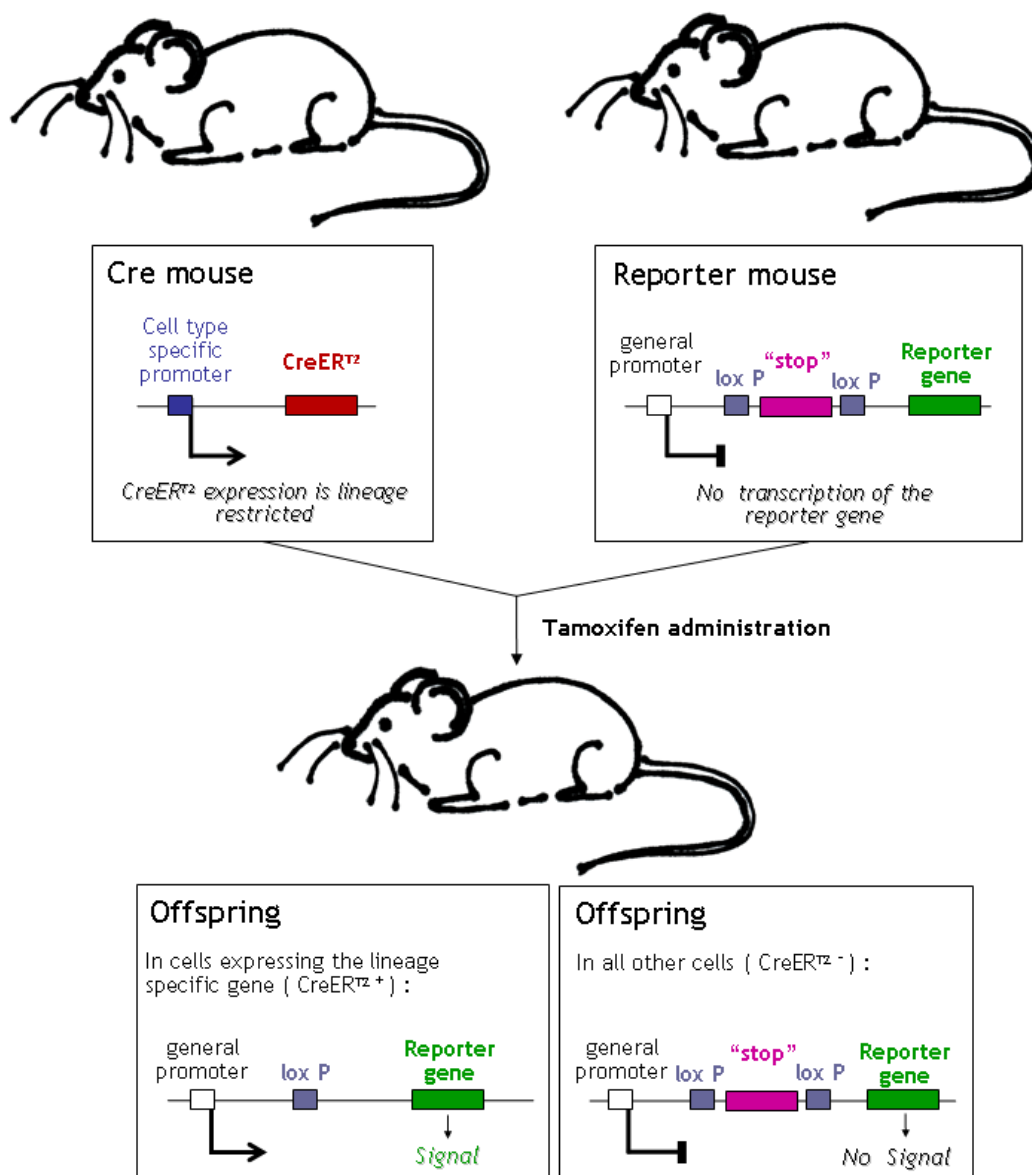
Figure 1.5 - Breeding strategy for a site- and time- specific gene targeting of a cell type specific gene. The technique involves the use of two transgenic mice: a reporter mouse, containing an inactive reporter gene that is constitutively activated by Cre-mediated recombination, and a Cre mouse, in which CreER[T2] recombinase (an inducible form of Cre recombinase only functionally active in the presence of its ligand, tamoxifen) is placed under the control of the regulatory elements of a cell type specific gene. The two mice lines are then crossed to generate double-transgenic offspring. Upon tamoxifen administration, expression of the reporter gene is activated only in cells of these offspring that express Cre-recombinase. Thereafter, reporter gene expression permanently stays activated since its expression is under transcriptional control of a constitutively active promoter in the mouse. This breeding strategy allows to permanently label progenitor cells and all their progeny in a spatio-temporally controlled manner.

Chapter 2 -   Materials and Methods

General chemicals and reagents were purchased from Sigma-Aldrich Co Ltd, unless otherwise stated, and, when available, all of them were of a Molecular Biology grade.

2.1. Bacterial strains, growth and storage

All plasmids were maintained in Escherichia coli (E. coil) strain XL1-Blue (recA1, endA1, gyrA96, thi-1, hsdR17, supE44, relA1, lac [F' proAB, laclqZΔM15, Tn10 {TetR}]). Bacteria grew at 37°C in Luria Broth (LB; per litre: 10g bacto-tryptone, 5g yeast extract, 1Og NaCI) or on LB-agar plates containing LB and 15g/l bacto-agar. Whenever an ampicilin selection was needed, ampicilin was added to the LB or molten LB-agar (after cooling to 55°C) at a final concentration of 1OOg/ml (100mg/ml stock in water, 0.20μm filter-sterilised and stored in aliquots at -20°C). Liquid cultures were continually agitated in a rotating environmental shaker (InnovaTM 4330 from New Brunswick Scientific) at 250rpm. For long-term storage of bacterial strains and clones glycerol was added to overnight (O/N) cultures at a final concentration of 15% (v/v), having these stocks been stored in 1ml aliquots at -80°C.
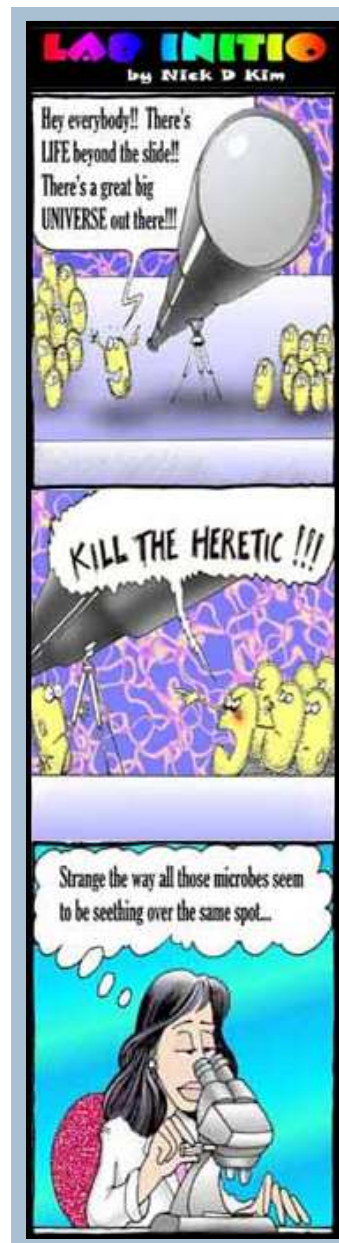
2.1.1. Preparation of Electrocompetent Bacterial Cells

The XL1-Blue E. coli bacterial strain was used for electroporating plasmid DNA while the EL250 strain was used for electroporating PAC DNA (for method see section 2.6). Electrocompetent cells were prepared using the following method Dower et al. 1988. An overnight culture of cells was set up in 10ml of SOC medium (with tetracycline selection at 35 μg/ml in the case of XL1-Blue). 2 x 400ml of SOC were then inoculated with 4 ml of the overnight cultures and grown until the OD600 reached 0.6 – 0.8 (3 – 4 hours). 16 x 50ml centrifuge tubes were pre-cooled on ice and the cultures then decanted into these and cooled for 15 minutes. They were then spun for at 4°C for 15 minutes at 1,500g. In a cold room, the supernatants were discarded and the pellets gently resuspended in 25 ml of cold ultraclean water. The suspensions were then pooled into 8 x 50ml tubes. These were centrifuged again as before, and the pellets once more resuspended in 25ml of ultraclean water and then pooled, this time into 4 x 50ml tubes. The tubes were spun a third time and the pellets resuspended in 10 ml of ultraclean water and pooled into one 50ml tube. After a final spin the pellets were resuspended in 250μl of cold 10% glycerol. These were then aliquoted into 1.5ml screw-cap cryo-tubes and snap frozen in liquid nitrogen. They were stored at -80°C until required.

2.2. Plasmid DNA isolation

2.2.1. Extraction of DNA with phenol/chloroform

An equal volume of 1:1 (v/v) phenol/chloroform was added to the samples to be extracted. The sample was vortexed and centrifuged at high speed (16,3 $\times 10^3$ g) for 5 min. The upper aqueous phase was collected and re-extracted with an equal volume of chloroform, centrifuged at high speed (16,3 $\times 10^3$ g) for 5 min and collected as we have above referred.

2.2.2. Precipitation of DNA with ethanol

2x volumes of 100% ethanol, 0.1x volume of 3M Sodium acetate pH5.3 and 1μl glycogen (Sigma) were added to the sample to be precipitated. The mixture was vortexed, incubated on dry ice for 15 - 30min and then centrifuged at high speed (16,3 $\times 10^3$ g). The pellet was

then washed in 70% ethanol, air dried and resuspended in an appropriate volume of TE buffer (5mM Tris, pH 7.5, 0.5mM EDTA, pH 8.0) or water.

2.2.3. Small scale preparation of plasmid DNA by alkaline lysis (mini-prep)

This preparation was performed according to Sambrook et al. 2001. 3ml of LB containing the appropriate antibiotic was inoculated with a single bacterial colony and was incubated in a 37°C shaking incubator overnight (ON) (12-18hr). 1.5ml of O/N culture was transferred to a Microfuge tube and centrifuged for 1min at high speed (16,3 x10^3 g) in a microcentrifuge (Biofuge pico from Heraeus). 100μl of solution I (50mM glucose, 25mM Tris-HCI pH8.0 and 10mM EDTA pH8.0) was used to resuspend the pellet, followed by 200μl of solution II (1% w/v Sodium Dodecyl Sulphate and 0.2M Sodium Hydroxide). This was gently mixed by inversion. 150μl of solution III (3M Potassium acetate and 8.7% v/v Acetic acid) was added, gently mixed and left on ice for 10 min. After spinning for 10min at high speed (16,3 x10^3 g), the supernatant was carefully removed, avoiding the floating material, and transferred to another tube. The plasmid DNA was precipitated with 2x volume ethanol at -20°C for 10 min. This was spun down at high speed (16,3 x10^3 g) for 10min and the pellet was washed in 70% ethanol, air dried and resuspended in 4Oμl TE buffer pH 7.6. This preparation resulted in 1 - 2μg plasmid DNA.

2.2.4. Large scale preparation of plasmid DNA (maxi-prep)

This method is a scaled-up version of the small scale plasmid isolation method described above with several additional plasmid purification steps. The protocol started with a 50ml stationary O/N bacterial culture grown in Terrific broth (per litre: solution A [per 900ml: 12g bacto-tryptone, 24g bacto-yeast extract, 4ml glycerol, in distilled water] was added to solution B [per lOOml: 2.31g KH_2PO_4, 12.54g K_2HPO_4, in distilled water] after both were heat sterilised and cooled) containing the appropriate antibiotic. The culture was spun down in two 50ml Falcon tubes at 3,800g for 10min. The pellet was resuspended in 4ml of solution I and was left on ice for 5min. 8ml of solution II was then added, mixed well and left on ice for 5min. 6ml of solution III was added to precipitate the chromosomal DNA and the mixture was left on ice for 10min. After centrifugation at 3,800g for 15min at 4°C, the supernatant was transferred to another tube, through a sheet of autoclaved muslin to avoid floating material, and 17ml of isopropanol was added to the filtered supernatant. The plasmid DNA

was allowed to precipitate on ice for 15min. This was centrifuged at 3,800g for 15min at 4°C and the pellet was resuspended in 2ml TE pH7.5. 2.5ml of 4.4M Lithium Chloride was added to precipitate the RNA on ice for one hour. The precipitated RNA was pelleted (3,800g for 15min at 4°C) and the supernatant was transferred to a clean tube. 9ml of 100% ethanol was added to precipitate the plasmid DNA and the solution was left at room temperature for 10 - 15min. The DNA was spun down for 15min at 4°C, washed in 70% ethanol and air dried. Then it was resuspended in 400μl TE and transferred to an Microfuge tube. To remove contaminating RNA, 10μl of RNase A (O.5μg/μl) was added and the mixture was incubated for 15min at 37°C. 2Oμl of 10% SDS was then added and the mixture was heated to 70°C for 10 min to destroy the RNase A. One phenol/chloroform extraction and one chloroform extraction were performed. The DNA was precipitated with 2x volumes of 100% ethanol, 0,lx volume of 3M Sodium acetate pH5.3 at room temperature for 10- 15min. This was spun down at high speed (16,3 $\times 10^3$ g) for 10min and the pellet was washed in 70% ethanol, air dried and resuspended in 2O0μl TE buffer pH 7.6. This method typically resulted in 0.5- 1mg of 10Kb plasmid from a 50ml culture.

2.3. Analysis of Plasmid DNA

2.3.1. Restriction enzyme digestion and agarose gel electrophoresis

Restriction enzymes were supplied by New England Biolabs and Promega. Digestions were carried out using the appropriate buffer systems supplied with the enzyme and following the enzyme manufacturer's protocols. Genomic DNA (maximum 25μg) was digested at 37°C 0/N in a 5Oμl volume containing 0.2 - 0.4U/μl of the relevant enzyme.

Conventional electrophoresis was performed in Life Technologies gel apparatus. Multipurpose agarose (Bioline) was used for all agarose gel electrophoresis at 0.6-4% (w/v), this specific percentage depending on the molecular weight of the DNA of interest. The agarose was dissolved in the appropriate volume of 1x TAE (0.04M Tris, 0.001M EDTA) by boiling in a microwave oven, cooled below 60°C, and ethidium bromide was added to a final concentration of 0.5.μg/ml. The gel was poured into the electrophoresis system and let to solidify. Loading buffer was added to the DNA samples (1Ox stock: 50% glycerol (v/v), 1mM EDTA pH8, 0.25% (w/v) bromophenol blue, 0.25% (w/v) xylene cyanol, destilled water treated with DEPC) and the gel was loaded. Electrophoresis was carried out in 1x TAE buffer. The DNA was visualised in a lightproof cabinet containing an ultraviolet

transilluminator at 302nm, a CCD camera and a thermal printer to record the image (Alpha Innotech Corporation). Alternatively, in the case of gels containing genomic DNA, no ethidium bromide was added to the gel before running it. Instead, the gel was post-stained in ethidium bromide diluted in distilled in deionized water for 15 min and then photographed.

2.3.2. Southern analysis

2.3.2.1. Southern Blotting

The DNA to be analysed was run on an agarose gel as described in section 2.3.1. This was then washed for half-hour periods at room temperature in 3 solutions with thorough rinsing in destilled water in between: O.5M HCl solution to de-purinate de DNA; denaturing solution (0.4M NaOH, 1.5M NaCl) to denature the fragments on the gel; and neutralising solution (1M Tris HCl pH 7.5, 1.5M NaCl, 1mM EDTA) to neutralise the denaturing solution.

Following treatment of the DNA in the gel, an 0/N capillary blot in 10x SSC was set up as described in Sambrook et al. 2001. For this, HybondTM-XL membrane (Amershem Pharmacia Biotech UK limited) was cut to size and rinsed in 1OX SSC prior to use in the capillary blot.

Following transfer to the membrane, the DNA was then cross-linked to the membrane by irradiating with UV light (UV Strata Linker 1800 from Strata Gene; Auto Cross Link program).

2.3.2.2. Pre-hybridizaton

Hybridization of Hybond^{TM}-XL membrane was carried out according to the manufacturer's instructions. In brief: the membrane was placed on a piece of nylon mesh and rolled up into a tight roll in 2X SSC. This was placed in a hybridisation bottle which contained 2X SSC. 2X SSC was replaced with 10-20ml of pre-hybridization solution (MIB solution [0.225 M NaCl, 15 mM NaH$_2$PO$_4$, 1.5 mM EDTA, 10% PEG 8000, 7% SDS] with 0.01% salmon sperm DNA previously denaturated at 95°C for 5min followed by 5min on ice).

Pre-hybridization was carried out for at least 1 hour at 65°C rotating in a hybridisation oven (Hybaid).

2.3.2.3. Hybridization to a labelled DNA probe

The DNA fragment to be used as a probe was prepared by purification from an agarose gel slice using the electroelution method described in the section 2.4.1. This was radioactively labelled using rediprime[TM] II random prime labelling kit (from Amersham Pharmacia Biotech UK Limited) with Redivue[TM] alpha-^{32}P dCTP (from Amersham Pharmacia Biotech UK Limited) according to the manufacturer's instructions. In brief: 25ng of DNA was denatured at 95°C for 5min in a total volume of 45μl and was quenched on ice. The denatured DNA was added to the reaction tube containing the appropriate enzyme DNA polymerase, random primers and three nucleotides (dATP, dGTP, and dTTP). To the above mixture was added 5μl of alpha-^{32}P dCTP. The labelling reaction was typically incubated at 37°C for 1 hour.

^{32}P labelled probes were purified away from unincorporated nucleotides by spun- column chromatography using Micro BioSpin® P-30 Tris chromatography columns from BioRad Laboratories and according to the manufacturer's instructions. In brief: the probe was loaded onto the column and the eluate was collected in an microfuge tube after spinning (16,3 x 10^3 g). The success of the labelling reaction was estimated using a Geiger counter, to count the relative amounts of radioactivity in the column and in the microfuge tube. The procedure was continued only when the amount of radioactivity in the eppendof tube was higher than in the column.

Before use, the purified ^{32}P labelled probe was denatured at 95°C for 5min and was quenched on ice for 5min. This was added to the pre-hybridization solution and incubated at 65°C O/N.

2.3.2.4. Washing of membranes

Following hybridisation, the membranes were washed in two solutions of increasing stringency: 1) 2X SSC, 0.1% SDS, at 65°C, with a slow constant rotation, during 10 min; 2) 0.1X SSC. 0.1% SDS, at 65°C, for as long as needed until no more radioactivity was being removed.

2.3.2.5. Developing of membranes

Excess liquid was blotted off the radioactive membranes, which were then wrapped in Saranwrap and exposed to Hyperfilm[TM] MP (from Amersham Pharmacia Biotech UK Limited)

in a light-sealed cassette with 2 intensifier screens at -80˚C. Exposure time varied according to the intensity of the signal.

2.3.3. DNA sequencing

DNA sequencing was carried by the Wolfson Institute for Biomedical Research automated sequency service using a Beckman Coulter CEQ2000XL Sequencer. The double stranded plasmid DNA templates to be sequenced were prepared according to the instructions specified by the service.

2.3.4. Quantification of DNA

The concentration of DNA was assayed by submitting an aliquot of the DNA to agarose gel electrophoresis. The brightness of the band was then compared to the ladder (Hyper Ladder I from Bioline) to have an estimate of the amount of DNA present. Alternatively, the concentration of DNA was determined using NanoDrop 1000 V3.6.0 spectrophotometer.

2.4. Cloning techniques

2.4.1. Isolation of DNA fragments for cloning

DNA fragments for cloning were usually purified from agarose gels on which they had been run following plasmid digests or PCR amplification. Bands were visualised on the agarose gel using a UV light and then excised from the gel with a scalpel, taking care to remove as much agarose as possible while minimising the time of exposure of the DNA to the UV light. The following steps were carried out:

Dialysis tubing of appropriate size was rinsed with distilled water, sealed at one end using a dialysis clip and filled with 1x TAE buffer. The agarose slice containing the DNA band was placed in it. Most of the fluid was removed leaving enough to keep the gel in constant contact with the buffer. The other end was sealed using another clip avoiding trapping of air bubbles. This was subjected to electrophoresis in 1 X TAE for ~30min at 130V. The buffer solution from the dialysis tube was recovered. The suspension was taken through one

phenol/chloroform and one chloroform extraction and the DNA was precipitated on dry ice for 30mim with 2X volume of absolute ethanol, 0.1X of 3M sodium acetate, pH5.3 and µg glycogen (Sigma). The resulting solution was spun down and the pellet washed in 70% ethanol and air dried. Afterwards, it was dissolved in an appropriate volume of milli Q H_2O. This method resulted in an almost 100% DNA recovery. Alternatively, and more recently, the isolation of DNA fragments was done using the illustra^{TM} GFX PCR DNA and Gel Band Purification kit from GE Healthcare (cat. #28-9034-70). See user manual for details.

2.4.2. Ligation of DNA fragments

Ligations referred in this research report involved DNA fragments digested with restriction enzymes that generated overhanging ends and PCR products. The latter were performed using TOPO TA cloning® (from Invitrogen, Cat no. K4600-01) and according to the manufacturers instructions. TOPO TA cloning® containing pCR®II-TOPO® uses a topoisomerase enzyme to rapidly clone any PCR fragment into its covalently bound vector. The former were performed using 1x ligase buffer supplied with the enzyme, assuming a vector:insert molar ratio of 1:3 and using the T4 DNA ligase from Roche. The reaction was allowed to proceed overnight at 16˚C.

2.4.3. Transformation of electrocompetent cells

2µl of the ligation reaction was usually used to transform electrocompetent bacterial cells (E. coil strain XL1-Blue; stock from the lab, see section 2.1.1). Alternatively, the total volume of the ligation reaction was ethanol precipitated and ressuspended in a small volume of water (~5µl) and used in the transformation. Electrocompetent cells were thawed on ice and 40 µl used immediately for transformation. This was done using Micro Pulser (from Bio-Rad Laboratories Ltd). The cells were mixed gently with the DNA and transferred to a chilled disposable 0.2cm electroporation cuvette (from Bio-Rad Laboratories Ltd). Transformation was carried out at 2.5kV. A time constant between 5-6 seconds was produced. The pulsed bacteria were added to 500ml of LB at 37˚C and decanted into a warm 1.5ml microfuge tube. These were then incubated at 37˚C for 30min before plating on LB agar plates supplemented with suitable antibiotic, afterwards incubated at 37˚C incubator 0/N. Whenever possible, blue/white selection was used to distinguish recombinant plasmids from non-recombinant ones. This was dependent on the insert ligating into the lacZ gene of a cloning vector to cause the gene disruption. Using IPTG (0.1M; 1M stock in water, O.2Oµm filter-sterilised and stored in aliquots at -20˚C) and X-Gal (8mg/ml;

40mg/ml stock in N,N-dimethyl formamide (DMF) and stored in aliquots at - 20°C) as lacZ gene substrates we could distinguish the plasmids which contain inserts (white colonies).

2.5. Polymerase chain reaction

PCR was used at various stages of the project to amplify pieces of plasmid DNA (e.g. for cloning or for use as probes) or to amplify pieces of PAC DNA (e.g. for cloning).

The PCR conditions and the cycling programmes are specified in the relevant sections of Results. The primers used in PCR reactions are listed in the Table 2.1. The PCR machines used were Master Cycler Gradient from Microfuge, Primus 96 plus from MWG-Biotech, Multigene from Labnet, and 96 Universal from peQSTAR.

Table 2.1 - List of primers used for PCR amplification and DNA sequencing.
The names of the primers, their sequence (in a 5' to 3' orientation) and the template from which they were designed are shown.

Name	Primer Sequence (5' → 3')	Template used
T7	GTA ATA CGA CTC ACT ATA GGG C	pNkx2.2
M13-20	GTA AAA CGA CGG CCA GT	-ditto-
M13-reverse	GGA AAC AGC TAT GAC CAT G	-ditto-
MNkx2.2F2	GAA ACT GGC TGA GCC CTG GGT GAC C	Nkx2.2 PAC clones
MNkx2.2R2	CCG AGC CCT GGT GGC AGG AGT TCC	-ditto-
PAC4 5' For1	ACA GTT CTG ACT TTT ACG AC	-ditto-
PAC4 5' Rev1	TTG ACT AGT GGG TAG GCC TG	-ditto-
PAC4 5' For2	TAT TAC ACG CCA TGA TAT GC	-ditto-
PAC4 5' Rev2	TGA GTC GCT CCT CCT GCC AG	-ditto-
PAC4 3' For1	CGA CTC ACT ATA GGG AGA GG	-ditto-
PAC4 3' Rev1	GGC ATG ACT ATT GGC GCG CC	-ditto-
PAC4 3' For2	CGA GCT TGA CAT TGT AGG AC	-ditto-

(cont.)

Name	Primer Sequence (5' → 3')	Template used
PAC4 3' Rev2	CCT TGA GAG CCT TCA ACC CA	Nkx2.2 PAC clones
CreERT2BstAPIF1	GCA TAA ATT GCG GGG TCC GGA ACC ATG TCC AAT TTA CTG ACC GTA CAC C	pCre-ER^{T2}
CreBamR1	CGT TTT CTT TTC GGA TCC GCC GC	-ditto-
Nkx2.23'NotF1	ATA AGC GGC CGC AAG TAG CGA AAC TTG GCC GCA ACG	Nkx2.2 PAC clones (ID: 1 and 2)
Nkx2.2 3' NotF2	ATA AGC GGC CGC CAC CGA GGG CCT CCA ATA CTC CCG	-ditto-
Nkx2.2 3' NotF3	ATA AGC GGC CGC ACA CTC GCT GGC TGG CCA GCA CC	-ditto-
Nkx2.25'AscF1	TTG GCG CGC CCG GAG CCG GAG CTG ACG GCA CC	-ditto-
Nkx2.25'NcoR1	GCG CCC CAT GGT TCC GGA CCC CGC AAT TTA TGC C	Nkx2.2 PAC clones (ID: 1 and 2)
Nkx2.45'PacF1	GGG TTA ATT AAG CCC TAC AAT GGC AGA GGA CGG	Nkx2.2 PAC clones (ID: 1)
Nkx2.45'MluR1	TCA CGC GTT AGT CCA GTG CCA GGT TTA CGA C	-ditto-
Nkx2.43'HindF1	TCA AGC TTG CCT GCG ACT CGC AGG ATC CGC C	-ditto-
Nkx2.43'AscR1	TTG GCG CGC CAT GAG CTG CAT CTT GGG TTG GGG	-ditto-

2.6. PAC techniques

2.6.1. Screening a mouse PAC library

Mouse PAC (RPCI21) library (from UK HGMP Resource Centre) was stored at 4°C and no special treatment of the filters was performed prior to screening by the Southern blot analysis protocol (section 2.3.2) with the following changes: pre-hybridization was carried out for at least 2 hours at 65°C in a rotating hybridization oven; followed by hybridization 0/N. After Hybridazation; filters were washed in two solutions of increasing stringency: 1) 2X SSC, 0.1% SDS, at room temperature, with a slow constant rotation, for 10 min, once; 2) 0.1X SSC, 0.1% SDS, for 15 min, with a slow constant rotation at 65°C; this process being

repeated, with a slow constant rotation, at room temperature, until no more radioactivity was being removed from the membrane.

2.6.2. PAC DNA isolation

Each PAC clone was streaked onto BHI-agar-Kanamycin plates (kanamycin was added to molten brain heart infusion (BHI)-agar [per litre: 37g/l BHI (from Sigma), 15g/l bacto-agar (from Difco), in deionised water; heat sterilized; stored at room temperature] at a final concentration of 12.5µg/ml (10mg/ml stock; from Sigma) in such a way as to obtain single colonies. A single colour was re streaked and incubated, colonies were then incubated at 32°C incubator 0/N.

2.6.2.1. Small scale PAC DNA isolation (mini-prep)

This was performed as described in section 2.2.3. with the following changes: 5Oml of BHI containing an appropriate amount of kanamycin (12.5µg/ml) was inoculated with a single colony and was incubated at 32°C incubator 0/N. Whenever needed the PAC DNA was sampled using wide bore pipette tips.

2.6.2.2. Large scale PAC DNA isolation (maxi-prep)

This was performed according to Low copy PAC purification protocol of the NucleoBond® Nucleic Acid Purification kit (from Clontech). The kit uses NucleoBond® AX resin columns — anion exchange columns, that allow the purification of PACs as well as other nucleic acid species. In brief: the protocol started with a 500ml stationary overnight bacterial culture grown in LB broth containing the appropriate amount of kanamycin (12.5µg/ml) at 32°C. After centrifuging cells, the pellet was lysed and then centrifuged briefly to clear the lysate. The resulting lysate was filtered and allowed to enter the resin of NucleoBond® AX resin columns by gravity flow. The column was washed and the PAC DNA was eluted and then precipitated with isopropanol. For technical reasons, the next step of centrifugation was carried out at 10,000xg for 45min at 4°C (Avanti^{TM} J-20 I centrifuge from Beckman Coulter). The pellet was washed with 70% ice-cold ethanol and then centrifuged at 10,000xg for 10min at 4°C. The pellet was ressuspended in 15Oµl of milliQ water and stored at 4°C. Whenever needed the PAC DNA was sampled using wide bore pipette tips.

2.6.3. PAC analysis by pulse field gel electrophoresis

Pulsed-field gel electrophoresis (PFGE), was performed in a contour-clamped homogeneous electric field apparatus (Bio-Rad). PFGE was carried out in 0.5X TBE buffer pH 8.0 (per litre: 108g Tris base, 55g boric acid, 40ml 0.5M EDTA, in distilled water, at pH 8.0) at 4°C, with fluid recirculation. PAC DNA, to which was added loading buffer, was run in 1% agarose gel in 0.5X TBE at 5.8V/cm, initial switch 2.1 sec, final switch 10 sec, for 12.5hr. The gel was then stained in ethidium bromide diluted in water for 30min. DNA was visualised by UV light and its size estimated by comparing to the Pulse marker™ from Sigma.

2.6.4. Homologous recombination in bacteria

Homologous recombination was performed according to Yang et al. 1997. Electrocompetent EL250 bacteria cells [modified DH10B strain (Gibco) containing defective lambda prophage Yu et al. 2000 and arabinose-inducible *flpe* gene Lee et al. 2001] were transformed with PAC DNA by electroporation. This was carried out as described in section 2.4.3, with the following changes: 2μl of PAC DNA was used to transform the electrocompetent bacterial cells, instead of 2μl of ligation reaction. Transformation was carried out at 1.8kV, instead at 2.5kV, and 0.1cm electroporation cuvettes were used instead of 0.2cm cuvettes. Transformed bacterial cells were allowed to recover in warm LB broth at 32°C for 2hr, then plated on LB-agar plates supplemented with suitable antibiotic (kanamycin; 12.5μl/ml) and incubated at 32°C, O/N. 5ml of LB broth containing the appropriate amount of kanamycin (12.5μl/ml) was inoculated with a single transformed bacterial colony and was incubated in a 32°C shaking incubator O/N. 4ml of the O/N culture was inoculated into 50ml of fresh LB broth (without kanamycin) in a 500ml flask and was incubated at 32°C with shaking until OD_{600}=0.5-0.8. Induction was performed by transferring 10ml of the growing culture into 125ml flask and placing the flask in a water-bath at 42°C. The flask was shaken by hand for 15min, then immediately placed into ice slurry and shaken by hand to cool down the cells quickly, during 5min. A non-induced culture was kept at 32°C and it was also placed into the ice slurry and used as a negative control for the recombination - in between this step and the transformation step of the process should take no longer than 40min and the culture once induced should never rise above 0°C. 10ml of culture (induced and non-induced culture) was transferred to a conical Falcon tube (one for each culture) and it was spun down for 8min at 1,100g at 4°C in a GS-6KR centrifuge from Beckman Coulter. The pellet was ressuspended in 1ml ice cold sterile water and it was then transferred into an 1.5ml microfuge tube. This was spun down using maximum speed (16,3 $\times 10^3$ g) for 20sec. The cell pellet was washed three times using 1ml ice cold sterile water. Between washes, the pellet

was spun down at high speed for 20 sec. After the final wash the cell pellet was ressuspended in 100μl of ice cold sterile water for use in electroporation. Electroporation was performed at 1.8KV. Immediately prior to electroporation, 100-300ng of donor DNA was mixed with 50μl of the competent cells (from induced and non-induced culture) and the mixture was pipetted into an electroporation cuvette (0.1cm). To the pulsed bacteria cells were added 500ml of LB at 32°C and these were incubated at 32°C for 1.5hr with shaking before plating on appropriate selective agar media (LB agar plates supplemented with 20μl/ml of ampicilin) and nonselective agar media (LB agar plates supplemented with 12.5μl/ml of kanamycin). Incubation was carried out in a 32°C incubator 0/N.

2.6.5. Screening for recombinant PACs

Culture obtained following homologous recombination event was, whenever required, titrated prior to screening to obtain an appropriate titre so as to obtain individual isolated colonies.

Two rounds of screens were carried out to isolate single recombinant PAC clones. For this, screening was performed by plating onto 15cm round bacterial plates, containing appropriate selective media (LB agar plates supplemented with 15μl/ml of chloramphenicol) and the recombinant PAC culture. Incubation was carried out in a 32°C incubator 2 x 0/N. Colonies were transferred from agar plates onto Hybond^TM-XL filters as follow: the plates were cooled at 4°C for 30 mins to ensure that the top agarose sticks to the bottom agar; the Hybond^TMXL round filters was then placed on the top agarose for 1min; using a sterile needle, holes were made on the filters thought to the agar to mark the position of the membrane on the plate; the filter was lifted carefully using forceps and was placed on a piece of 3MM paper saturated with 10% SDS solution for 3min, with the colonies side up; this was followed by a treatment in denaturing solution (0.4N NaOH, 1.5M NaCl) for 2min and two rounds of neutralising solution (1.5M NaCl, 1M Tris-HCl, pH7.5) for 3min; the filter was transferred briefly on a piece of 3MM paper to remove excess denaturing solution between steps. Finally, the filters were washed vigorously in 2xSSC for few minutes at room temperature. The DNA was fixed to the membrane by uncrosslinking.

To search for positive clones, filters were placed in between nylon mesh membranes, to ensure an even distribution of the probes on the filters, and washed in 2xSSC for 45 min at 65°C. This was followed by a pre-hybridisation step (pre-hybridisation solution as described in 2.3.2) for again 45min at 65°C. Hybridisation, washing of filters and autoradiography was carried out as described in section 2.3.2 of this chapter. Finally positive clones were then picked from each screen and were either subjected to another round of screen or were

grown to prepare PAC DNA. PAC DNA could then be further analysed by carrying out Southern analysis to determine if recombination had occurred in the desired way.

2.6.6. Arabinose inducible "FLIPE"

The chloramphenicol resistance cassette, flanked by FRT sites, was removed with an arabinose inducible *flpe* gene present in EL250 bacteria. For this 300µl of EL250 bacteria cells containing the recombinant PAC was used to inoculate 15ml of fresh LB and grown at 32°C to O.D.$_{600}$=0.5-0.8 with shaking. Sterile L-arabinose (1% stock) was added to a final concentration of 0.2% (w/v) and grown at 32°C for 1 hour. 1ml of this culture was then taken to inoculate 10ml of fresh LB and incubated for 2 hours at 32°C with shaking before plating on appropriate selective agar media (LB agar plates supplemented with 20µl/ml of ampicilin; 1ul, 10µl and 80µl) and nonselective agar media (LB agar plates supplemented with 15µl/ml of chloramphenicol; 10µl) using a 1 in 100 dilution. Incubation was carried out in a 32°C incubator 0/N. Checking for proper recombination was done by Southern blotting using part of the targeting construct as a probe and recombinant PAC DNA prior to recombination as a negative control. Removal of the chloramphenicol resistance cassette should result in a decrease of about 1.3 kb in fragment size.

2.6.7. Preparing Linear PAC DNA for microinjection

PAC DNA was extracted from an 0/N culture as described above followed by restriction digest with Mlu I enzyme for not less than 4 hours. Digests were run on PFGE as described above, however in this case, 90% of the digested PAC DNA was run in a central wide lane on the gel, while two small 'marker' lanes on each side of the wide lane were loaded with 5% of the digest each. After the gel was run, the 'marker' lanes were cut off and stained in dH$_2$O containing 0.5g/ml ethidium bromide for 10min with gentle agitation. A photo was taken to the gel with a ruler in order to localise the position of the PAC DNA band and PAC Vector band (used as a control) in the unstained gel using the ruler, and excise these bands. PAC DNA band was put in the middle on a mini gel tray with PAC vector on the left side. Set an asymmetric order to identify the PAC band position in the gel easily. A 4 % L.M.P. agarose was poured around the bands in the minitray. The gel was run at 50 volts for approximately 9hr in the cold room (at 50 volts the gel runs 1cm in 3 hours). After the gel has run, the PAC vector lane was cut off and stained in dH$_2$O containing 0.5µg/ml ethidium bromide for 10min with gentle agitation. A photo was taken using a ruler and was checked if the entire DNA had run out of the 1% gel. The position of the PAC DNA was localised in the 4% LMP agarose

gel using the ruler and 0.5- 0.8 cm block was excised. The block was equilibrated on a rotator (in a 15ml Falcon) in 12.5ml of TENPA buffer (1M Tris-HCl pH7.5, 0.5M EDTA pH8, 5M NaCl) with 30µM Spermine and 70µM Spermidine for at least 1.5 hours. Gel slice was dried with a clean tissue by just touching the liquid, transferred to a 1.5 ml microfuge tube, melt for 3min at 68°C, centrifuged the tube for 10sec to bring down the molten agarose and incubated it for additional 5min at 68°C. The microfuge tube was quickly transferred to a 42°C water bath and left for 5min. Working in the 42°C bath, 2 units of ß-Agarase (NEB, stock 1 unit per µl) was added per 100 µl of molten gel slice. Volume of agarose was checked against Microfuge standards. The ß-Agarase was mixed using the p20 pipette and wide bore tips (scooshed ~4 times slowly). Incubation was carried out at 42°C for 3 hr. In a small Petri dish 3 dialysis membranes (Millipore, pore size 0.025µm) were placed floating on microinjection buffer (1M Tris-HCl pH7.5, 0.5M EDTA pH8, 5M NaCl) containing fresh 30µM spermine and 10µM spermidine. 50µl of the PAC DNA solution was put on each dialysis membrane and left at room temperature for 1hr. The PAC DNA solution was recovered carefully from the top of the dialysis membrane and stored at 4°C. DNA concentration and integrity was checked by running 1µl, 3µl, and 5µl of the dialysed, purified, PAC DNA on a Pulse Field Gel for 12hrs (as above) against a known PAC DNA standard. The appropriate dilution was then prepared in micro-injection buffer containing 30µM spermine and 10µM spermidine for injection.

2.7. Genomic DNA isolation

2.7.1. Extraction of genomic DNA from mouse tissue (salt/chloroform extraction procedure)

Genomic DNA was extracted from mouse tissues using a modified version of the salt/chloroform protocol described by Mullenbach et al. 1989. Mouse tissues were isolated and snap frozen in liquid nitrogen where they were stored until required (for DNA extraction). In the case of extraction of genomic DNA from already frozen tissue, care was taken not to thaw samples when taken from liquid nitrogen tank. Samples were then placed in liquid nitrogen until required at the bench. The frozen tissue was homogenized in liquid nitrogen using a pestle and mortar and was transferred to a 50 ml Falcon tube by scraping the frozen tissue from the mortar with a spatula. The pestle and mortar were previously

cleaned with H_2O and then with 70% Ethanol and cooled in liquid nitrogen before being used. The frozen tissue was mixed with 3 - 7.5 ml of proteinase K extraction buffer (10mM TrisHcl pH 8, 0.1M EDTA pH 8, 0.5% SDS) with proteinase K added at a final concentration of 0.3mg/ml. The mixture was vortexed and incubated at 55 - 56°C 0/N. The amount of extraction buffer used was dependent on the size of the tissue. Typically, for one adult mouse kidney, 3 ml of extraction buffer was used. 4 ml of pre-warmed [extraction buffer: 5M NaCl] (at a ratio of 3:1) was added for each 1ml of proteinase K - treated sample and mixed (vortexed). This was followed by one phenol/chloroform extraction and then by one chloroform extraction. For that an equal volume of phenol/chloroform was added, vortexed and centrifuged at 3,000rpm for 10min. The top aqueous phase was transferred to a clean 50ml Falcon and an equal volume of chloroform was added, vortexed and centrifuged at 3,000rpm for 10 min. The top aqueous layer was transferred to a clean 50 ml Falcon tube and the genomic DNA was precipitated with an equal volume of isopropanol. The tube was inverted up and down 8 times. This was kept on ice for 10 minutes. Sometimes, the DNA was visible, in which case it was taken out using a clean pipette tip and transferred to a microfuge tube containing 70% ethanol. In cases where the DNA was not visible by eye, the mixture was centrifuged at 3,700rpm for 10 minutes in a cold rotor. The pellet was washed in 70% ethanol on a rotator at room temperature 0/N. Samples were then centrifuged at 3,700rpm for 5 min. This was just enough to bring down the DNA without compacting it at the bottom of the tube, which would make it more difficult to resuspend. The supernatant was poured off and tubes were allowed to dry (up side down) in fumehood for 10min. The genomic DNA was resuspended in a suitable volume of TE (500µl - 1ml) and incubated at 55°C for 30 - 60 min to dissolve it better. Samples were stored at 4°C.

2.7.2. Extraction of genomic DNA from mouse tails or ear clips

Mouse progenies were genotyped by PCR and Southern blot analysis using DNA extracted from tail samples. Tails were taken from 10-30 day old mice which were toe clipped as a means of identification. Up to 0.5 cm was taken from the tip of the tail and was lysed in 500µl of proteinase K lysis buffer (100mM Tris-HCl pH8.5, 5mM EDTA pH8.0, 0.2% SDS, 200mM NaCl) containing proteinase K at a final concentration of 0.48 mg/ml. This was incubated at 55°C 0/N.

To reduce the coprecipitation of unwanted contaminants (e.g., oligosaccharides) with genomic DNA, 200ul of 6M ammonium acetate was added to the samples, vortexed and left on ice for 15min. Tail debris were separated by centrifugation at 13,200rpm for 20min and the supernatant was transferred to a clean microfuge tube.

The DNA was precipitated by adding equal volume of isopropanol and then centrifuged at 13,200rpm for 3min at room temperature. The DNA pellet was washed with 70% ethanol, air dried and resuspended in 100 μl /50μl of TE or milliQ water.

Through the years, tail biopsy and toe clip were replaced by ear clip as a mean of tissue biopsy and identification. In this case, only 250μl of proteinase K lysis buffer containing proteinase K at a final concentration of 0.48 mg/ml was used and quantities used in the above protocol were adjusted accordingly. Genomic DNA was resuspended in 50μl of milliQ water.

2.8. Transgenic mice procedures

2.8.1. Inducing superovulation

Superovulated females were used for the production of fertilized eggs since the number of female mice maintained for the isolation of eggs is minimized by the use of superovulation. Six 3-4-week-old (B6 x CBA)F1 female mice were injected with 5 i.u. follicle-stimulating hormone (Folligon, Intervet) between 4 and 5pm (assuming a light period of 6 p.m. to 7 a.m., twilight for the first and last hours) and with 5 i.u. human chorionic gonadotropin, hCG (Chorulon, Intervet) 44-45 hours later. Both hormones were diluted in 0.9% sodium chloride (NaCl Injection B.P., Antigen Pharmaceuticals). After the administration of hCG, females were mated with (B6 x CBA)F1 fertile males. Typically, 4-6 female mated yielding a total of 100-200 fertilized eggs. Mice were purchased from the commercial breeding farm Charles River Laboratories (UK).

2.8.2. Pronuclei injection

The gene transfer method used was the microinjection of DNA directly into the pronuclei of fertilized mouse eggs. The microinjection service was carried out by U. Dennehy and P. Iannarelli (Richardson's laboratory, WIBR).

Briefly, linear ~1ng of linear PAC DNA in suspension in microinjection buffer (see section 2.6.7) was injected into the fertilised mouse ova. On average, 18-22 embryos (two-cell stage) were reimplanted into the oviducts of a pseudopregnant foster mother.

Pseudopregnant mice were prepared by mating 6 weeks - 4 months old (B6 x CBA)F1 females in natural oestrus with vasectomised males the day before implantation.

2.8.3. PCR Genotyping

Genomic DNA was extracted from tissue biopsy and used as template DNA for PCR amplification as described above. Primers and PCR conditions for genotyping are listed in table 2.2.

Table 2.2 - List of primers used to genotype the transgenic lines created and also the program required in the PCR reaction.

Reactions were carried out in 0.2ml PCR tubes, each reaction containing 10% of 10X PCR buffer (Promega), 6% of 25 mM magnesium chloride (Promega), 1% of DNA polymerisation mix (containing 20mM each of dATP, dCTP, dGTP and dTTP, Amersham Biosciences), 0.8% of forward and reverse primers at 100 µM/µl (from MWG or TAGN), template DNA (varying concentrations depending on the PCR reaction) and 1unit Taq DNA Polymerase (Promega or home-made). Reaction mix was filled up to 25µl with water.

Transgenic Line	Forward Primer (5' → 3')	Reverse Primer (5' → 3')	Program	Product size
Nkx2.2-CreER[T2] (heterozygous)	Nkx2.2 CreER F2 (ACG CCC ACC GCC TAC ATG)	Nkx2.2 3' R1 (GGG CAT ACT AAG CAA ATG)	94˚C for 4min Cycle (x38): 94˚C for 30 sec 57˚C for 45 sec 72˚C for 28 sec 72˚C for 30 sec	400 bp
Nkx2.2-CreER[T2] (homozygous)	Cre 5' (TCG ATG CAA CGA GTG ATG AG) Ra-KO-a (CCC TTG TGG TCA TGC CAA AC)	Cre 3' (TTC GGC TAT ACG TAA CAG GG) Ra-KO-b (GCT TTT GCC TCC ATT ACA CTG G)	94˚C for 4min Cycle (x20): 94˚C for 30 sec 61˚C for 45 sec 72˚C for 1 min 72˚C for 10 min	460 + 420 bp [**]

(cont.)

Transgenic Line	Forward Primer (5' → 3')	Reverse Primer (5' → 3')	Program	Product size
Nkx2.2-KO / Nkx2.2-CreER[T2] interbreeding [*]	Gen mNkx2.2 F2 (CCCCAGTCACAGC CTACATT)	Gen mNkx2.2 R2 (AAAACCCCGTCTTT GTGTTG)	94˚C for 4min Cycle (x37): 94˚C for 30 sec 62˚C for 45 sec 72˚C for 1 min 72˚C for 10 min	300 bp

[*] – To detect Nkx2.2-KO heterozygous in an Nkx2.2-CreERT2 background, PCR conditions were re-designed to amplify part of the endogenous Nkx2.2 first exon which is omitted from the PAC DNA in the Nkx2.2-CreERT2 transgenic line. [**] – 2 pairs of primers were used simultaneously; the efficiency of PCR amplification between those two set of primers were such that allowed to distinguish an heterozygous from an homozygous sample.

2.8.4. Southern Blot Genotyping

Southern blotting was carried out on genomic DNA extractions from putative founder mice to confirm the presence of the transgene. 20µl of genomic DNA was used in an appropriate restriction enzyme digest and the resulting fragments electrophoresed, blotted and analysed as described above.

2.8.5. Mouse Breeding

Mice were maintained on a ~12 hour light-dark cycle (6pm-7am, twilight for first and last hours). Breeding pairs were caged together overnight from 6pm; noon the following day was designated embryonic day 0.5 (E0.5); otherwise breeding protocol is described in the respective section.

In pilot trials, we found that ~90% of successful couplings took place between 9:30pm and 1:30am (63% [19/30] of successful 4-hour-matings compare to 71% [12/17] of effective O/N matings).   Nonetheless, we also observed that 34% of couplings could happen between 6:30pm and 10:30pm (24% [4/17] of successful 4 h mating compare to 71% [12/17] effective O/N mating) indicating that there is a considerable chance of conception before 9:30pm. For this reason, embryos harvested from an O/N mating were carefully staged (see below).

During the optimisation studies for CreER^{T2} activation by tamoxifen (TM) administration, homozygous reporter strains (please, see table 2.3) and Nkx2.2-CreER^{T2} mice were maintained separately and inter-crossed to yield double-heterozygous offspring.

Subsequent work was performed on mice containing two copies of both Nkx2.2-CreERT2 and *Rosa26-YFP* as a mean to improve the efficiency of TM-induced transgene activation.

Compound mouse lines were inter-crossed until mutant strains (knock-outs and knock-ins) were in a background of double-homozygous *Nkx2.2-CreER^{T2} : Rosa26-YFP*.

The stages of embryos with different genotypes were matched by somite numbers (until E11) or using morphological features specific to developmental stages older than E11.5-old embryos (e.g. early sign of fingers at E12 or fingers separate distally at E14)Theiler 1972.

Table 2.3 - Summary of mouse strains used in this Thesis.

The table includes a brief description of the transgenic/mutant lines used and its source.

Name	Allele type	Brief description	Reference
Nkx2.2-CreER^{T2}	Transgenic (PAC)	Tamoxifen-inducible form of Cre recombinase under control of Nkx2.2 promoter	Taveira-Marques et al. 2010; Taveira-Marques 2010
Olig2-IRES-Cre	Targeted knock-in	Constitutive Cre recombinase targeted in Olig2 ~130bp downstream of the initiation codon	*IRES-Cre-lox-PGK-Neo-lox* cassete provided by D.H. Rowitch; knock-in mice produced by N. Kessaris (unpublished)
Ngn3-Cre	Transgenic (BAC)	nls-Cre-SV40pA sequences under control of Ngn3 promoter	Schonhoff et al. 2004
Dbx1-iCre	Transgenic (PAC)	Codon-improved Cre recombinase under control of Dbx1 promoter	Fogarty et al. 2005
Nkx2.2 null	Targeted knock-out	Targeted disruption of the entire ORF of Nkx2.2	Briscoe et al. 1999
Olig2 null	Targeted knock-out	Targeted deletion of most of the Olig2 coding region	Lu et al. 2002

(cont.)

Name	Allele type	Brief description	Reference
$Smo^{flox/flox}$	Targeted conditional knock-out	Smoothened conditional allele	Long et al. 2001
Rosa26-LacZ	Targeted knock-in	*lacZ* gene under the control of the ubiquitous Rosa26 promoter	Soriano 1999
Rosa26-YFP	Targeted knock-in	YFP under the control of the ubiquitous Rosa26 promoter	Srinivas et al. 2001
Rosa26-GFP	Targeted knock-in	EGFP under the control of the ubiquitous Rosa26 promoter	Mao et al. 2001
Z/EG	Transgenic	EGFP under the control of the pCAGGS promoter	Novak et al. 2000

All mice used in this thesis were maintained on a C57BL/6/CBA background. Mouse colonies were maintained at the animal facilities of the Wolfson Institute for Biomedical Research, University College London. All animal work was carried out in accordance with United Kingdom legislation.

2.9. Staining Protocols

2.9.1. In situ hybridisation analysis

2.9.1.1. Tissue fixation and preparation

Tissue required for in situ hybridisation analysis was initially fixed overnight in 4% paraformaldehyde (4% PFA, in phosphate buffered saline [PBS] diethylpyrocarbonate-treated, [DEPC-treated]) or, sometimes, for smaller time periods (over fixation is known to reduce probe penetration into the tissue). In the case of postnatal tissue, animals were terminally anaesthetised with pentobarbitone (Pentoject) i.p. Once unconscious, animals were perfused with PBS via the left ventricle of the heart at a slow and steady pace until

most of the blood was flushed out. This was immediately followed with 4% PFA to fix the tissue. Following perfusion fixation, the tissue of interest was dissected out and then left in 4% PFA overnight or less. Once fixed the tissue was cryoprotected by overnight treatment with a 20% w/v sucrose solution in PBS. This 20% sucrose was made RNase free by DEPC treatment (diethyl pyrocarbonate, added to solution at 1/1000th volume and left for at least one hour, then autoclaved). After sucrose treatment, tissues were embedded in OCT™ compound (RA Lamb), frozen in isopentane on dry ice and stored at -80°C.

Embryonic tissue was treated in exactly the same way except that perfusion step was omitted. Embryonic tissue was simply removed from the pregnant mother euthanised by a schedule 1 method, and placed in 4% PFA. All other steps were as those for postnatal animals.

Whole-mount *in situ* hybridization was performed on E11.5 brainstems from which the meninges were removed. Dissected brainstems were fixed in 4% paraformaldehyde, 0.1% Tween in PBS-DEPC-treated for 2 h at room temperature, washed, progressively dehydrated in increasing concentrations of alcohol, and then rehydrated before treatment with proteinase K at 10ug/ml in 0.1% Tween : PBS-DEPC-treated for 11minutes at room temperature. After rinsing briefly with 0.1% Tween : PBS-DEPC-treated, brainstem were further fixed in 4% paraformaldehyde and washed before hybridisation.

2.9.1.2.   Generating mRNA probes for in situ hybridisation

To prepare probes for in situ hybridisation, a plasmid template was required. cDNA templates were obtained from collaborators, the IMAGE consortium, or by PCR amplifying genes of interest cloned into the TOPO® vector. The template was linearised at an appropriate point using restriction enzyme digestion. 10ug of template was digested with 100 units of linearising restriction enzyme in a total volume of 100μl. Unless the linearizing restriction enzyme had star activity, digestions were done O/N. The resulting linear fragment was purified using phenol-chloroform extraction and ethanol precipitation or, alternatively, reaction was purified using the kit illustra GFX PCR DNA and Gel Band Purification kit(GE Healthcare). Working solutions were made with DEPC-treated water (three times autoclaved to remove any traces of DEPC) to ensure that the template remained RNase free. RNA transcription reaction was carried out using 20 units of RNA polymerase (T3 or T7, depending on which gave the desired strand synthesis), 800 ng – 1 μg template, 5μl of 5x transcription buffer (Promega), 7.5 μl dithiothreitol (DTT, 100 mM), 2.5μl RNA labelling mixture (DIG labelling, Roche), 1 μl RNasin (RNase inhibitor, Promega), DEPC-treated water added up to a total volume of 25 μl. This mixture was incubated at

37°C for 2.5 hours. The success of the transcription was checked by running 1µl of the reaction mixture on a fresh made 1% agarose gel to ensure the presence of a transcript at the correct size, quality of probe and to quantify by comparing it to a control (e.g. a tested probe of same size). Finally, the reaction mixture was diluted with 75µl DEPC-treated water, aliquoted in 2µl aliquots and stored at -80°C.

Table 2.4 - List of mRNA probes used for *in situ* hybridisation.

Probe	Source	Amplified fragment	Linearise with	Transcribe with
CreER^{T2}	Bill Richardson (UK)	Full cDNA sequence	Not I	T7
Hoxb1/Hox2.9	Robb Krumlauf (USA)	NM_008266.4 (1318bp - 353bp)	Cla I	T7
Krox20/Egr2	Pascale Gilardi-Hebenstreit (France)	NM_010118.2 (1135bp - 1897bp)	BamH I	T3
Nkx2.2	John Rubenstein (USA)	Full cDNA sequence	Not I	T7
Sim1	Katsuhiko Ono (Japan)	NM_011376 (1480bp – 2108bp)	Xba I	T7

2.9.1.3. Single in situ hybridisation using NBT/BCIP chromogenic detection

Tissue blocks were sectioned in a Bright OTF5000 cryostat. Coronal sections were typically cut to a width of 15µm. Sections were collected on SuperFrost® Plus slides (VWR International) and dried for at least one hour before used. Probe aliquots were defrosted, and the probe, usually diluted 1/1000, was added to hybridisation buffer containing 50% deionized formamide, 10% dextran sulphate (Fluka) , 0.1mg/ml yeast tRNA, 1x Denhardt's solution (Sigma), and 1x salt solution (10x salt stock, 2M NaCl, 50mM EDTA, 100mM Tris-HCl pH 7.5, 50mM $NaH_2PO_4.2H_2O$, 50mM Na_2HPO_4, DEPC treated). The diluted probe was denatured at 70°C for 5 minutes and then vortexed and pulse centrifuged and immediately applied to the slides. The slides were placed in a hybridisation box, the base of which contained 2 sheets of 3MM paper (Whatman) wetted with hybridisation buffer. After application of the probe, each slide was covered with a coverslip (previously baked at 200°C

O/N) and the hybridisation box was sealed closed with tape. Hybridisation was carried out at 65°C overnight. After hybridisation, slides were placed in wash solution (50% formamide, 1x SSC, 0.1% Tween-20) in a coplin jar for 5 minutes at 66°C to remove the coverslips. The slides were then washed a further two times for 30 minutes each at 65°C. The slides were next washed in room temperature 1x MABT (5x stock, 0.5M maleic acid, 0.75M NaCl, 1M NaOH [pH7.5], 0.5% Tween 20) twice for 30 minutes each. The sections were then blocked in blocking solution (8g blocking reagent, Roche cat no 1-096-176, 100ml 5x MABT, 200ml distilled water, heated to 65°C to dissolve then 80ml heat treated sheep serum added and finally made up to 400ml with distilled water) for at least one hour at room temperature. Next, an anti-Digoxigenin alkaline phosphatase conjugated (Roche) antibody was diluted 1/1500 in blocking solution and applied to the sections in a humidifier chamber overnight at 4°C. The sections were then washed 5 times for 20 minutes in 1x MABT, followed by 2 ten minute washes in staining buffer (0.1M NaCl, 0.05M $MgCl_2$, 0.1M Tris pH 9.5, 0.1% Tween-20). The colour reaction was developed by placing the slides in a solution containing 20ml staining buffer, 1ml 1M $MgCl_2$, 87µl NBT (1g 4-nitro blue tetrazolium chloride crystals, plus 7ml dimethyl formamide and 3ml distilled water), 67µl BCIP (BCIP from Roche, 1g plus 20ml dimethyl formamide), and 20ml of a 10% polyvinyl alcohol solution (10% w/v polyvinyl alcohol in distilled water with 0.1M NaCl, 0.1M Tris pH 9.5 and 0.1% Tween-20). Reactions were incubated in the dark at 37°C and periodically checked for development of a blue precipitate on the sections. In cases of less abundant transcripts, reactions were allowed to proceed overnight. Once reactions had proceeded to a suitable point, they were quenched with excess PBS. After this, the sections were dehydrated through alcohols before being treated with xylene and mounted in DPX mountant (Fluka) under a coverslip.

2.9.1.4. Double fluorescent in situ hybridisation

Double in situ hybridization on cryostat sections was done with DIG- and fluorescein-labeled mRNA probes. The probes were detected with alkaline phosphatase (AP)- or horseradish peroxidase (POD)-conjugated anti-DIG (1:1000) or anti-FITC (1:1000) Fab Fragments (Roche), accordingly. For double-labelling, AP was detected using Fast Red (Roche; one tablet dissolved in 2 ml of 0.1M Tris pH8. 0.4M NaCl) and POD was detected with fluorescein amplification reagent, as recommended by the manufacturer (Perkin Elmer; 10-min incubation in fluorophore tyramide working solution). After developing the in situ colour reagents sections were counterstained with Hoechst 33258 dye (Sigma, 1/1000 dilution, 5 minutes at RT), washed and coverslipped with mounting medium (Dako Cytomation Ltd).

2.9.1.5.   Whole-Mount in situ hybridization (Chromogenic detection)

Brainstems were overnight hybridized with 100-200 ng/ml digoxigenin (DIG)-labelled RNA probe in Hyb-mix [50% formamide : 5x SSC pH4.5 : 2% SDS : 2% BBR (Roche)] at 70˚C with rocking. Followed by washes with Solution X (50% formamide : 2x SSC pH4.5 : 1% SDS) and 1x MABT, digoxigenin detection with alkaline phosphatase-conjugated antibody (Roche 1:2000 diluted in 20% serum/2% BBR/ 1x MABT) was followed by further washes with 1x MABT and NBT/BCIP staining (Roche) to reveal signal. Finally, brainstems were post-fixed in 4% PFA for 20minutes at RT, incubated overnight at 4 ˚C in PBS/80% glycerol and flat mounted in same medium.

2.9.2. Immunohistochemistry

2.9.2.1.   Tissue fixation and preparation

Embryos were fixed in 4% (w/v) paraformaldehyde (PFA) in phosphate-buffered saline (PBS) at 4˚C. Postnatal animals were perfused with 4% (w/v) PFA through the right ventricle of the heart under terminal anaesthesia as above. Spinal cords and brains were dissected out and were immersed in 4% PFA in PBS at 4˚C.   Generally, fixation times for immunohistochemistry were varied according to the age of the embryo and the epitope in question. Tissue was cryo-protected overnight at 4˚C in DEPC-treated 20% sucrose (w/v) in PBS, embedded, frozen in isopentane on dry ice and stored at -80˚C as described above.

Coronal cryo-sections (10 to 20 μm) were cut on a cryostat, collected on slide and let to dry before proceeding with protocol (designated as "dry sections" in table 2.5). Alternatively, PBS was applied to sections immediately after collecting a ribbon of 3-4 consecutive sections onto a slide, in this way avoiding sections to dry (named as "wet sections" in table 2.5).

For post-natal (~P10 and above) and adult tissue, 30 μm coronal sections were picked up with a damp paint brush and floated in PBS, and treated as floating sections throughout the protocol (referred to "floating sections" in table 2.5). After immunohistochemistry, floating sections were transferred onto glass slides and air dried before mounting.

For immunolabelling on whole brainstems, brainstems were dissected in cold PBS and fixed for 2 h at 4 ˚C in 4% PFA with rocking. For some antibodies used, the tissue was less severely fixed in order to preserve the epitope structure of the antigen of interest. For cell permeabilisation, tissues were dehydrated at room temperature in PBS-EtOH solutions

progressively more concentrated in ethanol (e.g. 25%, 50%, 100% [2 times]) for 10min each solution, with rocking. Samples were stored in 100% ethanol at -20 °C for at least several months. Brainstems were rehydrated before incubation with primary antibody.

2.9.2.2. Detection of antigen on tissue sections

For immunohistochemistry, sections were pre-treated with blocking solution (10% heat-inactivated serum (v/v), 0.1% Triton X-100 (v/v BDH) in PBS), and then incubated sequentially in primary antibody and secondary, all in blocking solution, for overnight at 4°C and for 1-2 h at 20–25 °C, respectively. The primary antibodies used are listed in table 2.5.

Secondary antibodies used were Alexa Fluor 488–, 568– or 647–conjugated (Invitrogen, 1:1,000), Cy3- or FITC-conjugated goat or donkey antibody to guinea pig IgG (Chemicon, 1:500).

Following antibody treatment, sections were stained with Hoechst (Sigma) and post-fixed for 5-20 minutes in 4% PFA. Sections were mounted under coverslips in mounting medium (Dako Cytomation Ltd).

After incubation with primary, secondary, Hoechst and 4% PFA, sections were washed thoroughly (at least 3 times 10 minutes) in PBS containing 0.1% Triton X-100 or PBS (just before mounting).

2.9.2.3. Immunohistochemistry of Whole-Mount Mouse Embryos

Brainstems were washed in PBS, followed by 1 hour incubation at RT in blocking buffer (10% heat-inactivated serum, 0.1% Triton X-100 in PBS) with rocking, twice. The samples were then incubated 48 h at 4 °C in a primary antibody solution (primary antibody diluted in the blocking solution) with rocking. Brainstems were subsequently washed for 8 h at 4 °C in PBS/0.1% Triton X-100 and incubated with the appropriate Alexa Fluor dye (1:1000; Invitrogen) for 48 h at 4 °C with rocking. Following antibody incubation, samples were washed for 24 h at 4 °C in PBS, 0.1% Triton X-100 and counterstained with Hoechst 33342 (1/1000; Sigma). Finally, brainstems were incubated overnight at 4 °C in PBS/80% glycerol and flat mounted in same medium.

Table 2.5 - List of primary antibodies used in this thesis.

In this table is shown all the primary antibodies used for immunohistochemistry, from which species they were raised in, their working dilutions, sources and required protocol conditions. Abbreviations used: BCBC (Beta Cell Biology Consortium), DSHB (Developmental Studies Hybridoma Bank), M (Mouse), GP (Guinea-pig).

Antibody name	Raised in	Working dilution	Required protocol conditions	Source
5-HT (serotonin)	Rabbit	1:5000	Any	Sigma-Aldrich
APC (CC-1)	M IgG2b	1:200	Standard (i.e. o/n fixed tissue, o/n antibody incubation)	Calbiochem
ChAt	Goat	1:100	Non-sucrosed, non-frozen, o/n fixed tissue	Chemicon
Cre	M IgG1	1:1000	Light fixation (e.g. 1h fixation for a E11.5 body)	Chemicon
Gata3	M IgG1	1:30	Any	Santa Cruz
GFAP	M IgG1	1:400	Any	Sigma-Aldrich
GFAP	Rabbit	1:500	Any	DakoCytomation
GFP	Rabbit	1:6000	Any	AbCam
GFP	Chick	1:1000	Any	Aveslab
Human Olig2	Goat	1:500	Any	R&D Systems
Lim3	Rabbit	1:300	Any	Gift from T. Jessell
MNR2	M IgG1	1:5	Light Fixation (e.g. 20min for a E10.5 body)	DSHB
NeuN	M IgG1	1:400	Any	Chemicon
Nkx2.2	Rabbit	1:5000	Any	Gift from T. Jessell
Nkx2.2	M IgG2b	1:10	Light Fixation (e.g. 20min for a E10.5 body)	DSHB
Nkx6.1	M IgG1	1:500	Light fixation (e.g. 45min for a E12.5 body)	BCBC

(cont.)

Antibody name	Raised in	Working dilution	Required protocol conditions	Source
nNOS	Rabbit	1:500	Any	Zymed Lab.
nNOS	Sheep	1:2000	Any	Gift from P. Emson
Pax6	Rabbit	1:2000	Any	Chemicon
PDGFRα	Rat	1:500	Light fixation (e.g. 45min for P10 spinal cord)	BD Biosciences
Phox2b	Rabbit	1:2000	2h fixation at RT	Gift from J.-F. Brunet
Rat Isl1 (39.4D5)	M IgG2b	1:100	Light Fixation (e.g. 20min for a E10.5 body)	DSHB
RC2	M IgGM	1:5	Any	DSHB
S100β	M IgG1	1:400	Any	Sigma-Aldrich
Sox10	GP	1:4000	Standard	Gift from M. Wegner

2.9.3. β–Galactosidase staining

2.9.3.1. Tissue fixation and preparation

Mouse embryos were dissected out, rinsed in 1 x PBS, and then fixed in X-Gal fixative (1 % formaldehyde, 0.2 % glutaraldehyde, 2 mM $MgCl_2$, 5 mM EGTA in 1 x PBS) by various length of time. For example, E11 embryos were fixed during 1 h, E12.5 and E13.5 for 2 to 3 h, and half P8 brain for around 3h. Embryos more than 14.5 days old were cut into two or three pieces to equivalent size of E11-13.5 embryos and fixed accordingly. After fixation, embryos were incubated in 20 % sucrose until they sunk and subsequently embedded in Tissue Tek O.C.T. compound (SAKURA).

2.9.3.2. Detection on cryostat tissue sections

Frozen sections were cut 20-30µm thick on a Bright OTF 500 cryostat. Sections from a negative control were processed simultaneously with the experimental ones to check for any endogenous β-Gal activity. Sections were collected on SuperFrost® Plus slides (VWR International) and dried for one hour at least. If the sections were not going to be used immediately they were stored at -80°C. The sections were covered with 400 µm of X-Gal fixative (1% (v/v) formaldehyde, 0.2% (v/v) Glutaraldehyde, 2mM MgCI2, 5mM EGTA, IX PBS) in a humidified chamber, and then incubated for 20' at room temperature (X-Gal fixative stock solution could be used for a week if stored at 4°C and protected from light). The slides were then washed three times for ten minutes each with wash buffer (0.1 M Phosphate buffer pH 7.3, 2 mM $MgCl_2$, 0.1 % Sodium deoxycholate, 0.02 % NP4O). After washes, slides were incubated in freshly prepared LacZ staining buffer inside coplin jars at 30°C overnight and protected from light. This incubation was sometimes longer than overnight if the staining was still weak, it never acquired background. The LacZ staining buffer stock (1 ml of 50 mg/ml X-Gal [5-bromo-4-chloro-3-indolyl-B-D galactosidase, Molecular Probes (Invitrogen) 2007 dissolved in dimetylformamide], 82 mg K_3Fc (CN_6) (Sigma), 105 mg K_4Fe (CN_6) $3H_2O$ (Sigma), diluted in ~ 49 ml wash buffer) was prepared by mixing all the components, without the need to filter. After staining, the slides were washed thoroughly in 1 x PBS, post-fix in X-Gal fixative by 10 mm at room temperature, washed again with 1 x PBS three times by 5 minutes each, dehydrate through alcohols and xylene (30 % ETOH by 15", 60 % ETOH by 15", 80 % ETOH by 30", 95 % ETON by 1', 100 % ETOH by 1', Xylene by 1' [x2]), and then mounted in DPX mountant (Fluka). The β- Gal staining on sections started to diffuse after two or three months.

2.9.4. Retrograde labelling from sympathetic ganglia

Sympathetic MNs in Nkx2.2 CreERT2 : Rosa26 YFP mice were retrogradely labelled with 1,1 dioctodecyl-3,3,3',3'-tetramethylindocardocyanine (DiI, Invitrogen). Eviscerated neonates were fixed by immersion overnight in 4% (w/v) PFA at 4°C. A tiny crystal of DiI was placed inside a single sympathetic chain ganglion at thoracic level T3-T6 and the preparation was incubated in PBS containing 0.04% (w/v) sodium azide for 4 days at 37°C. Floating vibratome sections (400 µm) were immuno-labelled for YFP (rabbit anti-GFP; AbCam, 1:6,000) as described above, at 4°C without Triton X 100.

2.9.5. Electron microscopy

For pre-embedding immuno-electron microscopy, newborn Nkx2.2 CreERT2 : Rosa26 YFP mice that had received tamoxifen at E12.5 and E13.5 were anesthetized and perfused transcardially with phosphate-buffered saline (PBS) followed by 4% (w/v) paraformaldehyde/ 0.1% (v/v) glutaraldehyde in 0.1 M PBS. After dissection, spinal cords were immersed in 4% paraformaldehyde/ 0.1% glutaraldehyde in 0.1 M PBS overnight at 4°C. 90 μm-thick vibratome sections of spinal cord at thoracic level T10-T13 were pre-incubated with 10% (v/v) sheep serum in PBS containing 0.02% (w/v) saponin for 2 hours at 20–25 °C, then incubated with shaking overnight at 4°C with rabbit anti-GFP IgG (1:6000, Abcam) followed by biotin-conjugated anti-rabbit IgG (1:200, Jackson Immuno Research Labs) overnight at 4°C with agitation. Slices were then subjected to avidin/ biotin enhanced immuno-peroxidase (ABC Kit, Vector PK-6100) using 3,3'-diaminobenzidine (Sigma) and nickel ammonium sulphate (Alrich) as contrast agents. Stained sections were post-treated with1% (w/v) osmium tetroxide in 0.1 M phosphate buffer pH7.3 at 4oC for 1 hour, dehydrated in a graded ethanol-water series, cleared in propylene oxide, infiltrated with Araldite resin and finally flat-embedded between Melinex sheets. Semi-serial ultra thin sections of the whole vibro slice were cut at 70-80 nm using a diamond knife on a Reichert Ultracut E microtome. Sections were collected on 300 mesh grids and stained with uranyl acetate and lead citrate. Electron micrographs were taken in a Joel 1010 transmission electron microscope and recorded using a Gatan Orius CCD camera.

2.10. Tamoxifen induction

Cre-ER^{T2} activation was routinely induced by the oral administration of tamoxifen since it was found oral gavage was the most suitable technique of administration of tamoxifen (see Chapter 3). Tamoxifen (TM, Sigma, T5648) was dissolved in pure corn oil at a max concentration of 40mg/ml using a sonicator (Decon model FS100B). A step of sonication at 30°C for 45min was usually enough to get tamoxifen into solution. If more concentrated tamoxifen solution were needed (for example up to 100mg/ml), then tamoxifen (TM) was dissolved in a corn oil solution containing 10% (v/v) ethanol. Very concentrated TM solutions were also sonicated at 30°C for 45min (sometimes for even less time). A further step of sonication at 37°C for 10- 15 min was sometimes needed, in particular for the 100mg/ml TM solution, to get TM completely into solution. At 100mg/ml the TM solution was not that so stable and it was used immediately. Another reason for adding ethanol is that it is known to

improve induction levels. Care was taken not to exceed 10µl of ethanol per dose due to the effects of ethanol on vertebrate embryogenesis (further discussed in Zhou et al. 2003; Sari et al. 2004; Yelin et al. 2005; Parnell et al. 2006; Yelin et al. 2007).

The tamoxifen stock was administered at different concentration to the pregnant female on one or more occasions. No more than 100µl of total volume (hence, 10µl of ethanol) was given to each female per dose (pregnant females were weighed prior to administration of TM and the concentration of the stock solution was adjusted to the desired dose accordingly). Tamoxifen usually prevented normal parturition (please, see section 3.2.7) so, for postnatal analyses, litters were delivered surgically and fostered.

2.11. Data analysis

2.11.1. Microscopy

Light microscopy images were captured digitally in a Zeiss Axioplan microscope with a Hamamatsu digital camera on a Dell computer by using the SimplePCI imaging software.

Confocal images were acquired under one of three confocal systems: a TCS SPI confocal microscope (Leica Microsystems), a UltraView ERS microscope (Perkin Elmer), or a TCS SPE confocal microscope (Leica Microsystems).

Confocal Z-stacks of stained sections were recorded at 0.5-1 µm increments whereas confocal Z-stacks of whole-mount at 3-6 µm increments.

XZ and YZ views were reconstructed using Volocity software (Perkin Elmer) or Leica LAS AF Lite Software.

Composite images were assembled using Adobe Photoshop CS 8.0 software and/or Microsoft ICE (Image Composite Editor).

2.11.2. Quantification

Protein colocalisation (multiple fluorochromes) was assessed in the confocal microscope. At least three animals/embryos were used for each genotype/TM-induction. A minimum of three 4 µm-thick Z-stack sections for each specific condition were immunolabeled to count triple or double-positive cells.

Counts were done manually and were expressed as average ± SEM. T-test was used for statistical analysis in this thesis (Microsoft Office Excel 2003).

Chapter 3 - Generation and characterization of Nkx2.2-CreER^{T2} transgenic mice

3.1. Introduction to Nkx2.2

The *Nkx2.2* gene (Nk-2 transcription factor related, locus 2 [Drosophila] gene) was first isolated as a homeobox-containing gene with a pattern of expression restricted to longitudinal

© Sidney Harris
Sciencecartoonsplus.com

columns of cells along the entire developing CNS axis (Price et al. 1992; Shimamura et al. 1995). Nkx2.2 is a member of the mouse Nkx-2 family whose homeobox domains are most homologous to that of the Drosophila Nk-2 gene. Members of the Nk family share two regions of homology outside the homeobox domain (Harvey 1996): 1) a region of 10 amino acids (aa) located near the N terminus – the TN (tin) domain (Rudnick et al. 1994) and 2) 17aa found downstream of the homeobox domain – the Nk2 specific domain (NK2-SD also called the NK2 domain) (Price et al. 1992). The NK2-SD domain has an important role in transcription factor functions (Watada et al. 2000). Interestingly, the Nkx2.2 homeobox domain contains two nuclear localization signals (NLS) which act cooperatively in mediating complete nuclear transport of Nkx2.2 (Hessabi et al. 2000). The mouse *Nkx2.2* gene has
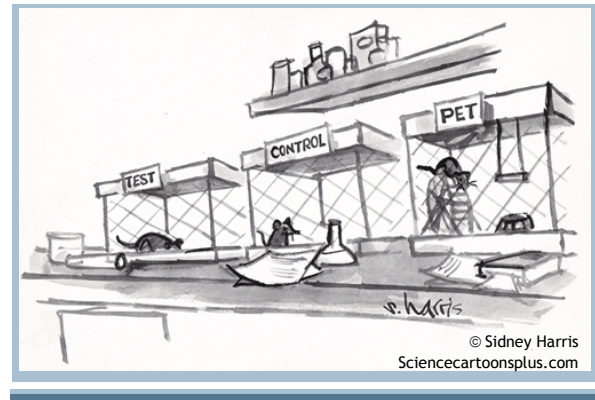
three transcript variants[**] and is encoded by two or three exons, depending on transcript, spanning a region of maximum 11.09 Kb on mouse chromosome 2. Identification and characterization of an *Nkx2.2* enhancer revealed a region sufficient to account for the normal ventral Nkx2.2 expression in the neuroepithelium. This region is directly regulated by Wnt-Tcf repressor activity and positive Shh-Gli signalling and implicates graded Shh and Wnt signalling in defining the p3 domain (Lei et al. 2006; Vokes et al. 2007).

Mice homozygous for *Nkx2.2* mutation exhibit different phenotypes (see below for a detailed description). Because of functional redundancy between *Nkx2.2* and its family gene *Nkx2.9* , mice carrying only one *Nkx2.2* allele are indistinguishable from wild-type animals (Sussel et al. 1998; Briscoe et al. 1999). Accordingly, $Nkx2.2^{+/-}$: $Nkx2.9^{-/-}$ compound-mutant mice, lacking the compensatory activity of Nkx2.9, have impaired normal locomotor behaviour and show moderate increase in motorneurons from the medial motor column, at the expenses of reduction, albeit not complete, of mature $Sim1^+$ V3 interneurons (Holz et al. 2010).

Nkx2.2 is expressed in the CNS but its pattern of expression changes dramatically throughout development. At first, Nkx2.2 is detected in the most ventral region of the neural tube on either side of the central canal (Shimamura et al. 1995). This region later becomes the p3-domain (Briscoe et al. 2000), in which Nkx2.2 activity, together with Nkx2.9,play the defining role (Briscoe et al. 1999; Holz et al. 2010)[††]. Apart from playing a role within the p3 domain, Nkx2.2 has also been implicated in the formation of the floor plate (Lek et al. 2010). In the developing spinal cord, Nkx2.2-expressing p3 progenitors give rise to Sim1-expressing V3 INs in the ventral cord, whereas in the hindbrain they give rise to visceral MNs (vMNs) followed by 5HT-expressing serotonergic neurons (Ericson et al. 1997b; Briscoe et al. 1999; Pattyn et al. 2003a). Nkx2.2 initially perdures in V3 INs (Briscoe et al. 1999; Zhang et al. 2008), but is then rapidly down-regulated in migratory V3 INs as well as post-mitotic visceral MNs and serotonergic neurons (Pattyn et al. 2000; Cheng et al. 2003; Pattyn et al. 2003a). While V3 IN generation is dependent on the selective expression of Nkx2.2 (Briscoe et al. 1999; Briscoe et al. 2000), Nkx2.2 activity is sufficient, but not necessary (Briscoe et al. 1999), to trigger vMN generation via activation of Phox2b (Pattyn et al. 2000; Pattyn et al.

[**]   More recently a fourth transcript variant has been identified (http://www.ensembl.org/Mus_musculus/Transcript/Summary?db=core;g=ENSMUSG00000027434;r=2:147003284-147019979;t=ENSMUST00000067075; accessed on June 2011). This new variant, however, was not considered in Figure 3.7.

[††] Either gene alone is sufficient to restrict Olig2 expression to the pMN domain, but not when both genes are knocked out and/or down-regulated (see Figure 1.2 Panel B).

2003b). On the other hand, Nkx2.2 is necessary but not sufficient for production of serotonergic neurons (Briscoe et al. 1999; Pattyn et al. 2003a), since it acts cooperatively with different co-factors, depending on the level of the hindbrain being considered (Cheng et al. 2003; Craven et al. 2004). Additionally, SLIT1, a gene expressed in ventral radial glia and white matter astrocyte precursors, was found to require Nkx2.2 activity for its expression (Hochstim et al. 2008; Genethliou et al. 2009).

Nkx2.2 is expressed in cells of the oligodendrocyte lineage too. The levels of expression of Nkx2.2 vary in oligodendrocyte lineage cells during development and in adulthood and its intensity controls their proper developmental – too much or too little of Nkx2.2 can affect OL differentiation (Kitada et al. 2006; Liu et al. 2007). Embryonically, dorsal expansion of Nkx2.2 into the Olig2$^+$ pMN domain is associated with the initiation of gliogenesis (Zhou et al. 2001) as the interaction between Olig2 and Nkx2.2 proteins inhibits V3 IN development and promotes an OL fate (Sun et al. 2001a); nevertheless, transfection of Nkx2.2 alone has been shown to be insufficient to impose an OL character (Zhou et al. 2001). Accordingly, Nkx2.2 was found to form a physical complex with Olig2 in mammalian cells and yeast two-hybrid assay (Sun et al. 2003). Nkx2.2 can also couple with other bHLH proteins, other than Olig2, to drive OL production. It has been suggested that Mash1 can cooperate with Nkx2.2 to specify OLPs and direct differentiation to mature OLs (Sugimori et al. 2007; Sugimori et al. 2008). Immature pre-myelinating OLs still express Nkx2.2. For this reason mutation of *Nkx2.2* causes a delay and a dramatic decrease in the number of PLP$^+$ pre-myelinating OLs and, subsquently, MBP$^+$ mature myelinating OLs (Qi et al. 2001). Besides activating PLP expression (Fu et al. 2002), Nkx2.2 prevents the precocious expression of MBP in pre-myelinating OLs (Wei et al. 2005), allowing MBP expression only in mature OLs after Nkx2.2 expression is down-regulated (Xu et al. 2000). All in all, Nkx2.2 plays a crucial role during OL proliferation and differentiation but not in mature myelinating OLs.

The dynamic changes of Nkx2.2 expression during development are recapitulated in remyelinating episodes (Fancy et al. 2004; Watanabe et al. 2004). Two recent reports show a transient-regulation of Nkx2.2 expression in dividing OLPs and immature OLs, but down-regulation in mature remyelinating OLs. Interestingly enough, and in contrast to development, the regulation of Nkx2.2 was shown to be independent of endogenous Shh (Fancy et al. 2004).

Moreover, Nkx2.2 expression has been detected in the ventral forebrain (Price et al. 1992), thalamus (Vue et al. 2007), hypothalamus (Kurrasch et al. 2007) and retina (Fu et al. 2001) too. Nkx2.2 is also expressed outside the CNS. Its expression has been identified in heart, lung, thyroid and pancreas (Lints et al. 1993; Rudnick et al. 1994; Kimura et al. 1996). In the pancreas, Nkx2.2 plays a vital role in the final differentiation of pancreatic beta-cells,

the exclusive source of insulin (Cissell et al. 2003, Sussel et al. 1998, Wang et al. 2004). In *Nkx2.2* null mice, beta-cells are markedly reduced, which leads to diabetes shortly after birth and eventually death (Sussel et al. 1998).

Besides its role during patterning of the neural tube (see section 1.3.1.1), transcriptional repressor activity of Nkx2.2 was also found to regulate general activator proteins, such as Sp1 and E2F, capable of driving transcription of proneural bHLH protein Hb9, a protein specifically expressed in MNs (Lee et al. 2004). These results provide further support for the derepression model of gene regulation in the neural tube (see section 1.3.1.1). Nkx2.2 can also act as a transcriptional activator to promote target gene expression (Watada et al. 2000). In particular, the insulin gene was shown to be directly activated by Nkx2.2 in differentiated pancreatic beta cells (Cissell et al. 2003).

3.2. PAC transgenesis

3.2.1. Identification of a suitable probe for screening a genomic PAC library

In order to find a cDNA fragment specific to the *Nkx2.2* gene that could allow us to screen a genomic PAC library for clones containing *Nkx2.2*, small pieces of DNA were isolated from a full length *Nkx2.2* cDNA and used as probes on mouse genomic Southern blots. The fragment that hybridized to single bands corresponding to the *Nkx2.2* locus was then used to screen a Mouse genomic P1 Artificial Chromosome (PAC) library. The selected probe was a 620bp Not I/Xho I fragment that spanned the entire Exon I (see Figure 3.1).

3.2.2. Isolation and characterization of Nkx2.2 PACs

PACs are P1-derived artificial chromosomes that were developed for cloning large genomic fragments into Escherichia coil (*E. coli*). Despite their large size, PACs can be propagated and manipulated in bacteria. PACs have their own inherent advantages when it comes to using them for mouse transgenic studies. Because PACs can contain large DNA fragments, up to 200-300Kb, they are unlikely to be silenced, i. e. they are less likely to be subject to positional effects. PAC DNA can easy be purified and modified directly in *E. coli* by recombineering technologies (see section 3.4).

3.2.2.1. PAC library screening

A mouse genomic PAC library (RPCI21) was obtained from the UK HGMP Resource Centre. This had been constructed with fragments of female 129/SvevTACfBr mouse spleen genomic DNA ligated into the pPAC4 vector (see vector pPAC4 map, in http://www.chori.org/bacpac/ppac4.htm). The library contains 128,000 clones, in 336 microtitre plates, that grew in LB broth with kanamycin (25 µg/ml) and 7.5% glycerol. The resulting culture was plated out and then gridded in a 4x4 array on 22.2x22.2 cm Hybond N nylon membranes (Amersham) using a Genetix Qbot robot. Each clone was spotted twice to give 36,864 spots on each membrane. 7 filters, each divided into 6 panels, which, in turn, contain 24x16 of the 4x4 array, cover the whole library. Clones spotted on the filters had been processed by SDS treatment, denaturation and neutralisation, dried and UV crosslinked. To screen for the presence of *Nkx2.2* PACs, the membranes were hybridised overnight with the above mentioned labelled radioactive probe. The subsequent pattern of spots observed on the autoradiography films enabled us to identify the *Nkx2.2* PAC clones. Four *Nkx2.2* PAC clones were identified from the whole PAC library (see Figure 3.2). To each of the clones was assigned an identification number (see Table 3.1).

Table 3.1 - Naming PACs.

Description	ID
512 - D5 Mouse PAC (RPCI 21) clone	1
544 - M7 Mouse PAC (RPCI 21) clone	2
637 - P21 Mouse PAC (RPCI 21) clone	3
638 - P21 Mouse PAC (RPCI 21) clone	4

3.2.2.2. Checking authenticity of PAC clones

PAC DNA was isolated as described in materials and methods (mini-prep protocol). To confirm the identity of the clones, the PACs were digested with BamHI and XhoI (as with the genomic digestion mentioned above) and analyzed by Southern blotting using the 620bp

NotI/XhoI *Nkx2.2* cDNA fragment as a probe (see Figure 3.1). Hybridization of the probe to a 3 kb or a 2.2 kb band (respectively for BamHI and XhoI) confirmed the identity of the clones. Large quantities of each PAC DNA were prepared.

3.2.2.3. Molecular characterization of Nkx2.2 PACs

To identify the size of the genomic DNA inserts the purified PAC DNA was digested with the following infrequent restriction endonucleases: NotI, which is able to release the insert, and SalI enzyme. Digested PAC DNA was analysed by pulse field gel electrophoresis (PFGE). From PFGE, the four clones (PAC ID:1, ID:2, ID:3 and ID:4) were estimated to contain genomic fragments of approximately 200 Kb, 150 kb,. 170 kb and 170 Kb respectively (see Figure 3.3).

3.2.2.4. Mapping the ends of the genomic inserts by inverse PCR

The extremities of the purified PACs were further characterized by inverse PCR using primers and conditions provided by N. Kessaris. This was carried out to determine which regions of the mouse genome each PAC contains and its orientation.

The inverse PCR strategy can be summed up in the following four steps:

Step 1. PAC DNA was digested using a variety of restriction enzymes that were supposed to cut inside the regions of the vector immediately flanking the genomic insert (the 5' and 3' end vector-insert junction) and at unknown locations within the genomic insert. It was necessary to use a variety of restriction enzymes since it is unknown which restriction sites do exist in the ends of the genomic insert.

Step 2. The digested PAC DNA was diluted and self-ligated using T4 DNA ligase. Circularization serves to reorient the vector arm templates in a manner that permits the vector arm primers to anneal in the appropriate orientation in the next step of PCR amplification.

Step 3. Sets of 5' and 3' end vector arm primers were used to amplify the 5' and 3' end vector-insert junction fragments, respectively. To confirm the authenticity of the resulting PCR products, nested PCR was carried out with two sets of 5' and 3' end vector arm primers.

Step 4. The amplified products were purified by gel electrophoresis, subcloned into appropriate plasmid, and sequenced. The DNA sequencing results were blasted to *Nkx2.2* gene sequence (in www.ensembl.org) thus allowing us to locate the identity of the genomic insert in the mouse *Nkx2.2* gene.

It should be noted that the 5' end arm of the pPAC4 vector is arbitrary and does not necessarily correspond to the 5' end of the genomic insert. An example of an inverse PCR strategy is given in Figure 3.4.

PAC clone ID:1 : PFGE and inverse PCR data showed that clone ID:1 contain a genomic DNA fragment that was 206 Kb in length. In fact clone ID:1 contained 100 Kb upstream of *Nkx2.2* and 106 Kb downstream, positioning *Nkx2.2* roughly in the middle. This clone ID:1 was identified as the most suitable clone for our study as it was the most likely to contain all the regulatory elements for correct expression of the *Nkx2.2* homeogene (see Figure 3.5). Although not shown here, the original PAC ID:1 clone obtained from HGMP contained a large deletion of approximately 100 Kb, missing out *Nkx2.2* altogether but otherwise mapping precisely in the Nkx2.2 genomic region by inverse PCR. This suggested that the PAC clone had undergone recombination resulting in this deletion. The same PAC clone was ordered again from HGMP and this time the correct 206 Kb genomic clone was obtained without recombination.

Nkx2.2 PAC ID:1 also contained the related gene *Nkx2.4*. In order to avoid overexpression of this gene in our mouse transgenics, *Nkx2.4* had to be removed (see section 3.3.3)

PAC clone ID:2 : This PAC clone contains 60 Kb upstream and 96 Kb downstream of *Nkx2.2*. Because of its smaller size and short region upstream (60 Kb) of *Nkx2.2* I decided not to use this PAC in further work (see Figure 3.5).

PAC clone ID:3 and ID:4 : Inverse PCR for these PACs anchored one of their ends 160 Kb away from *Nkx2.2*. The other end of the PAC did not match any known sequences in the mouse genome suggesting that they fall within as yet non-sequenced region. However, PFGE showed that these two PACs were identical and contained only approximately 10 Kb downstream of *Nkx2.2* making them unsuitable for *Nkx2.2* transgenics (see Figure 3.5).

3.2.3. Construction of targeting vectors

3.2.3.1. Basic targeting vector designs

In the present study I needed to construct two targeting vectors. The fundamental elements of them are the homology to the target DNA, a positive selection and two unique restriction sites one on either side of the two homologies for isolating of the targeting cassette without vector sequences. The two targeting vectors were named *Nkx2.2-CreER^{T2}* and *Nkx2.4*. The former was used to replace part of the *Nkx2.2* coding sequence with tamoxifen-inducible Cre recombinase (Cre-ER^{T2}) and the latter was used to delete the *Nkx2.4* gene from the PAC.

3.2.3.2. The Nkx2.2 targeting vector

The *Nkx2.2-CreER^{T2}* targeting vector was designed to drive homologous recombination and replace part of *Nkx2.2* sequences with *Cre-ER^{T2}*. In addition to Cre recombinase and two regions of homology to the target DNA, which is where recombination will occur, the targeting vector also contains a positive selection marker. In this case, the selection marker used was chloramphenicol (Cm) flanked by FRT sites. This marker is used to select correctly targeted clones and is removed prior to microinjection into mouse embryos. The process of removing the chloramphenicol marker is similar to the *Cre/loxP* system. The strain of bacteria EL250, used for PAC manipulation contains an arabinose inducible *flpe* gene. The expression of Flpe (a genetically enhanced, site-specific Flp recombinase) can be induced by arabinose to remove the selection marker Cm that is flanked by the site-specific recognition sites of the recombinase, the FRT sites (Buchholz et al. 1998) (see Figure 3.6).

Cloning strategy for construction of the Nkx2.2 targeting vector (see Figure 3.7 and Table 2.1):

Step 1. 5' homology (357bp) was obtained by PCR amplification using Nkx2.2 PAC clone ID:1, as template, and the set of primers (Nkx2.2 5'AscF1, Nkx2.2 5' NcoR1). In this step BstAPI restriction site was added to the 3' end of the 5' homology. 5' homology was cloned into pCRII-TOPO and sequenced;

Step 2. This involved the amplification of the 5' end of *Cre-ER^{T2}* (400bp) using pCre-ER^{T2} as template (kindly provided by Pierre Chambom) and the set of primers (CreERT2BstAPIF1, CreBamR1). In this step BstAPI restriction site and the 23bp upstream of *Nkx2.2* ATG was

added to the 5' end of the 5' end of *Cre-ER*^{T2}. The 400bp fragment was then cloned into pCRII-TOPO and sequenced;

<u>*Step 3.*</u>   The 5' homology and the 5' end of *Cre-ER*^{T2} fragments were inserted in pBluescriptIISK PacI AscI (pBluescriptIISK with a modified MCS to introduce PacI and AscI. kindly provided by N. Kessaris) in a three way ligation. For this, the 320bp BstAPI/AscI fragment, isolated from the plasmid that resulted from Step 1, and the 388bp BstAPI/BamHI fragment, isolated from plasmid that resulted from Step 2, were cloned into the BamHI/AscI sites of pBluescriptIISK PacI AscI at the same time;

<u>*Step 4.*</u>   This step involved cloning the whole *Cre-ER*^{T2} cassete into pBluescriptIISK (kindly performed by Françoise Jamen). For this, 2Kb EcoRI fragment was isolated from plasmid pCre-ER^{T2} and inserted in BamHI fragment of pBluescriptIISK by a blunt ended ligation;

<u>*Step 5.*</u>   In this step BamHI/NotI *Cre-ER*^{T2} fragment from Step 4 was inserted in plasmid from Step 3 as BamHI/NotI. At this stage I have already placed 5' homology in the 5' end of the *Cre-ER*^{T2} cassette;

<u>*Step 6.*</u>   3' homology (470bp) was obtained by PCR amplification using *Nkx2.2* PAC clone ID:2, as template, and the set of primers (Nkx2.25'AscF1, Nkx2.25'NcoR1). In this step, NotI and PacI were added to the 5' and 3' end, respectively. 3' homology was cloned into pCRII-TOPO and sequenced, having the sequencing result been blasted to the mouse *Nkx2.2* gene to check the accuracy of the amplified fragment;

<u>*Step 7.*</u>   This step involved the insertion of 3' homology into plasmid from Step 5 as NotI/PacI;   The isolation of the 3' homology fragment was carried out by PacI digest followed by NotI digest.

<u>*Step 8.*</u>   Finally, the positive selection marker chloramphenicol was isolated from pPI22 (kindly provided by Palma Iannarelli) as a NotI fragment and subsequently cloned into the plasmid from Step 7 previously digested with NotI. Additionally, the construct 5' homology – Cre-ER^{T2} - FRT - Cm - FRT - 3' homology was further digested with MluI and its restriction site removed by blunt ended ligation. The construct 5' homology – Cre-ER^{T2} - FRT - Cm - FRT - 3' homology is now complete.

3.2.3.3. The Nkx2.4 targeting vector

The reason for removing *Nkx2.4* coding sequence was to avoid possible adverse effects of introducing an extra copy of the Nkx2.4 gene into the mouse genome. In *Xenopus* it has

been shown that *Nkx2.4* expression is strictly segregated to the ventral half of the neural tube at all stages and that the expression of *Nkx2.4* overlaps that of *Nkx2.1* in the ventral diencephalon (Small et al. 2000). Overexpression of *Nkx2.4* could conceivably affect embryonic development and hence interfere with the normal expression of the *Nkx2.2* gene (see Figure 3.8).

The targeting vector was designed to recombine at the *Nkx2.4* locus and replace it with chloramphenicol resistance. The *Nkx2.4* targeting vector was also designed in such a way as to insert a MluI restriction site for linearization of the selected PAC clone.

Cloning strategy for generating the Nkx2.4 targeting vector (see Figure 3.9 and Table 2.1):

Step 1. 5' homology (516bp) was obtained by PCR amplification using *Nkx2.2* PAC clone ID:1, as template, and the set of primers (Nkx2.45'PacF1, Nkx2.45'MluR1). In this step PacI and MluI restriction sites were added to the ends. 5' homology was cloned into pCRII-TOPO and sequenced;

Step 2. This involved the amplification of the 3' homology (681 bp) using *Nkx2.2* PAC clone ID:1, as template, and the set of primers (Nkx2.43'HindF1, Nkx2.43'AscR1). In this step HindIII and AscI restriction site were added to the ends. 3' homology was then cloned into pCRII-TOPO and sequenced;

Step 3. Finally, the 5' homology, the 3' homology and the positive selection marker chloramphenicol were inserted in pBluescriptIISK PacI AscI (pBluescriptIISK with a modified MCS to introduce PacI and AscI) in a four way ligation. For this, the 516bp EcoRI/PacI fragment, isolated from the plasmid that resulted from Step 1, and the 681 bp AscI fragment, isolated from plasmid that resulted from Step 2, and chloramphenicol cassette isolated from pPI22 fragments (kindly provided by Palma Iannarelli) were cloned into the PacI/AscI sites of pBluescriptIISK PacI AscI at the same time; the construct 5' homology – Cm - 3' homology is now complete.

3.2.4. PAC modification by homologous recombination in bacteria

<u>Brief introduction</u>

Highly efficient phage-based *E. coli* homologous recombination systems that enable modification and subcloning of PAC DNA without requiring restriction enzymes or DNA ligase, have been recently developed. This so-called recombinogenic engineering or recombineering, uses phage recombination functions to induce homologous recombination using homologies of 50bp (or less). The two most known phage-encoded recombination systems are *Rac* encoded *RecET* system and λ-encoded Red system (Copeland et al. 2001). In turn, there are two ways that *Red* recombination can be induced: through a plasmid system or through a defective prophage. The latter was the one I used.

In the defective λ-prophage-based system, *gam*, *bet* and *exo*, the three genes required for *Red* recombination, are expressed from λ-prophage which is integrated into the *E. coli* chromosome, and their expression is under the tight control of the temperature sensitive *λ-cI857* repressor. At 32°C, when the repressor is active, the expression of these genes is undetectable. However, when cells are subjected to 42°C for 15 min, the repressor is inactivated and the genes are co-ordinately expressed from the *λ-pL* promoter at very high levels, making it possible to achieve greater than 10^4 recombinants per 10^8 electroporated cells.

The recombinogenic bacteria strain EL250 that I used in our recombination system is a modified DH10B strain (Gibco) containing the defective λ-prophage (Yu et al. 2000). This specialised *E. coli* strain was further engineered to include arabinose-inducible *flpe* gene, which catalyses the excision of an *frt* site-flanked sequence (in this study, the selectable marker chloramphenicol) in the presence of arabinose (Lee et al. 2001).

3.2.4.1. Removal of loxG site from pPAC4 backbone

The pPAC4 vector backbone contains a *loxG* site. Like *loxP*, *loxG* is a site-specific recognition sequence for Cre recombinase. So, it is possible that Cre-mediated recombination could occur between two *loxP* and two *loxG* sites. To avoid this I removed *loxG* from the pPAC4 vector backbone in *Nkx2.2* PAC clone ID:1. In addition, an SV40 promoter driving the expression of blastocidin-σ-methylase and an SV40pA were all removed from the vector backbone to minimise adverse effects introduced by this strong promoter.

Figure 3.10 shows where the ampicilin gene was inserted in the pPAC4 vector backbone. The targeting vector was kindly provided by N. Kessaris.

In order to confirm the removal of *loxG*, Southern analysis of the modified PAC DNA digested with PstI using as a probe the XhoI/BglII fragment from the plasmid shown in Figure 3.10. A difference around 7.5 Kb should be seen between modified and unmodified *Nkx2.2* PAC clone (see Figure 3.11).

3.2.4.2.   Removal of Nkx2.4 gene from recombinant PAC vector

The original plan for PAC modification was to first remove the *loxG* site and insert an ampicillin selection cassette. This would be followed by insertion of *Cre-ER^{T2}*, using for selection chloramphenicol flanked by FRT sites. This would allow us to remove the selection cassette using FIpe and subsequently delete *Nkx2.4* from the PAC using chloramphenicol again for selection.

Following insertion of *Cre-ER^{T2}* into the *Nkx2.2* locus various attempts were made to remove *Nkx2.4*, but all were unsuccessful, resulting in deletion of sequences from the recombinant PAC clone (see Figure 3.12).

It appeared that the presence of *Cre-ER^{T2}* fragment allowed the DNA to fold in such a way that permitted two homologous regions (as small as 50bp) distant from each other to recombine unexpectedly and delete a fragment from the full sequence of the recombinant PAC.

In an effort to overcome this unexpected recombination the plan was changed. Instead of first inserting *Nkx2.2* and then the *Nkx2.4* targeting vector, I did the other way round. The removal of *Nkx2.4* was carried out first by homologous recombination using *Nkx2.4* targeting vector and *Nkx2.2* PAC clone ID:1. In order to confirm the removal of the gene, Southern analysis of PAC DNA, isolated from the modified *Nkx2.2* PAC clone digested with HindIII, was carried out using as a probe the 5' homology of *Nkx2.4* gene (see Figure 3.12).

A difference around 2.5 Kb should be seen between modified and unmodified *Nkx2.2* PAC clone (Figure 3.12, left). Furthermore, to confirm the existence or not of deletions mini-preps were digested with SalI and NotI enzymes and run on PFGE (data not shown).

At this point of the study, I have a recombinant form of *Nkx2.2* PAC clone ID:1 from which *loxG* and *Nkx2.4* gene were removed. Because our recombinant PAC clone was already resistant to chloramphenicol and the selection cassette used in *Nkx2.2- CreER^{T2}* targeting

vector also carried   chloramphenicol resistance, correctly recombined clones containing *CreER^{T2}* had to be identified without selection. For this, colony lifts and hybridization with a probe specific to the *CreER^{T2}* gene were used in 2 rounds of enrichment (see Figure 3.13). Recombinant PAC clone integrity was confirmed by pulsed field gel electropholesis (PFGE). Afterwards, chloramphenicol selection was removed by inducing the expression of Flpe using arabinose, as described in materials and methods.

3.2.5. Injection of the recombinant PAC clone into mouse fertilised eggs by pronuclear injection

The recombinant PAC clone was linearised with MluI, purified (see materials and methods for protocol) and injected using a dilution of 1 in 20 into mouse fertilised eggs by pronuclear injection as described in materials and methods. In total 9 pregnancies were obtained by pronuclear injection of *Nkx2.2-CreER^{T2}* recombinant PAC clone, which resulted in 53 animals being born.

The resulting offspring were then analysed by PCR using the set of primers (CreBamHI, Nkx2.25'AscF1; offspring were also genotyped using primers from Table 2.2) and by Southern blotting using as probe 3' homology of *Nkx2.2*. In total four pups were positive for the transgene. The founders were named 4/1 , 5/4 , 7/5 , and 10/2 and were used to generate four independent transgenic lines.

As it is possible to see in Figure 3.14, the probe used for Southern blot picks up two bands. This is due to the fact that the fertilized eggs used in microinjection are derived from two mouse strains that exhibit a polymorphism at this locus. Additionally, it is shown by Figure 3.14 that only one copy of the transgene integrated into the genome of founder 7/5, as the intensity of the transgenic band is as strong as the intensity of either of the two corresponding endogenous bands of the *Nkx2.2* gene. Similarly, the other three lines were also found to carry a single copy of the transgene.

3.3. Transgene expression analysis

3.3.1. Characterizing the expression of the CreER^{T2} transgene in the embryonic spinal cord between E10.5 and E15.5

The expression of *CreER^{T2}* transgene in the four transgenic lines was first assessed by RNA in situ hybridization. Transgene expression is often dependent on its site of integration in the genome. The transgene can happen to integrate into a chromosomally active region of the genome, resulting in the expression of the transgene. Alternatively the transgene can integrate into a chromosomally silent region which could lead to the inactivation of the transgene. Consequently, the characterization of the *CreER^{T2}* expression pattern was carried out in all four transgenic founders and has shown that only one of these four lines – transgenic line 4/1 - expressed the transgene at appropriate levels and in the correct pattern at E10.5 (see Figure 3.15 - A and data not shown). I have selected line 4/1 for further study.

Some additional characterization of CreER^{T2} embryonic expression was further carried out at E10.5, E12.5, E13.5 and E15.5 to compare it with that of Nkx2.2 and Olig2 protein as well as with the expression of Sim1, a specific marker for V3 interneurons which are known to originate from the p3 domain (Fan et al. 1996; Sommer et al. 1996; Briscoe et al. 1999). At E10, expression of transgene was restricted to the VZ of p3 domain which is marked by the the expression of Nkx2.2 (see Figure 3.15 A). At this age Nkx2.2 and Olig2 expression domains were non-overlapping with a sharp boundary. Similarly, the dorsal limit of the transgene was observed to abut the Olig2 expression domain, the so-called pMN domain. On E10.5 *CreER^{T2}* mRNA and protein was still present in the VZ but was also detected in cells that had migrated from the VZ and settled in the ventral cord close to the midline (see Figure 3.15 E and data not shown). These cells were confirmed to be V3 interneurons by their co-expression with marker Sim1 (see Figure 3.15 E). Surprisingly, at more caudal regions of the spinal cord, where Hoxc9 expression defines thoracic spinal cord (Dasen et al. 2003), a small number of cells were found to express CreER^{T2} only (see Figure 3.15 B arrow heads). The number of CreER^{T2}-positive/Nkx2.2-negative cells increased from E10.5 to E12.5 and were more preeminent at the thoracic level of the spinal cord (see Figure 3.15 A, B, and E).

Until E12.5, more and more CreER^{T2}-positive cells had migrated dorsally and settled in the intermedio-lateral cord, while a few others had settled in a medial position near the central canal of the upper thoracic spinal cord (see Figure 3.16 B; around 2/3 [90 cells out of 141 per cord] of CreER^{T2}-positive cells that had left the VZ migrated dorsally whereas the other

1/3 remained ventral to p3 domain [51 cells out of 141 per cord]). At lower thoracic levels (caudal to T8), CreER^{T2}-positive cells were also observed in the dorsal cord (see Figure 3.16 C). Neither of the dorsally-migrating cell populations expressed Nkx2.2 (see Figure 3.16 A-D). The persistence of the CreER^{T2} transgene in migratory cells, and its failure to down-regulate at the same time as endogenous Nkx2.2, might reflect a greater stability of Cre transcripts and/or de-regulated transcription of the PAC transgene. Nevertheless, it is suggested that CreER^{T2} expression might actually be useful as a short-term p3 lineage marker. Supporting this idea, I found that at E15.5, the cluster of CreER^{T2}-positive cells in the dorsal cord was positioned at the same level as a dorsal population of Sim1-positive cells, which were absent in Nkx2.2 KO (see Figure 3.16 E, Figure 4.15 and data not shown). At E13.5, some Sim1-positive cells were found to migrate dorsally at upper cervical cord, resembling migratory CreER^{T2}-positive cells at the same level, which suggests that CreER^{T2} persists in p3-derived migratory neurons (see Figure 3.15 D). To further investigate whether CreER^{T2} could be used as a lineage tracer of the p3 domain, I then looked for supporting evidence for CreER^{T2} perdurance in the different differentiated cell populations known to be generated in the p3-domain of the hindbrain (Pattyn et al. 2003a; Guthrie 2007).

3.3.2. Enduring transgene expression in p3 derived neurons of the developing hindbrain after Nkx2.2 down-regulation

Given the fact that CreER^{T2} continues to be expressed in cells outside the domain of Nkx2.2 expression in the spinal cord, it was important to ascertain whether the transgene behaved likewise in the hindbrain (HB) where p3 progeny have been extensively studied and characterised (Briscoe et al. 1999; Pattyn et al. 2003a; Pattyn et al. 2003b). p3 progenitors from the HB are known to give rise to branchiomotor and visceral motor neurons and to later serotonergic interneurons expressing Phox2b and 5HT (among other markers) (Briscoe et al. 1999; Pattyn et al. 2000; reviewed in Chandrasekhar 2004; Guthrie 2007).

Similar to spinal cord, CreER^{T2} transcript and protein were analysed in HB at E11.5 and E13.5 and its expression pattern was compared with that of Nkx2.2, Phox2b and 5HT (see Figure 3.17). CreER^{T2} transcript expression was first analysed at E11.5 by whole-mount *in situ* hybridization. It was noted that its expression extended along the midline within the ventricular zone having also been observed in regions adjacent to the VZ (e.g. in rhombomere (r) 4, see Figure 3.17 A) or in postmitoic cells which had migrated laterally, settling within r2-r3 in a unique location known to be occupied by the trigeminal (V) neurons (BM neurons; Song et al. 2006 ; see also Figure 3.17 A). CreER^{T2} expression outside the VZ resembled that of Tbx20, a marker upregulated in post-mitotic BM/VM neurons but absent in

their progenitors and sMNs (Song et al. 2006). To further assess CreER^{T2} expression, transverse sections at E11.5 were cut and stained for Nkx2.2 and Cre proteins. While mimicking Nkx2.2 expression in the VZ (close-ups in Figure 3.17 B), CreER^{T2} expression was detected outside the VZ in post-mitotic cells that from their specific locations could be identified as the branchial facial (VII) BM neurons (white arrow heads in Fingure 3.18 B). Branchial facial (VII) BM neurons are generated within r4 and then migrate tangentially along the anteroposterior axis of the hindbrain into r6 before settling in the dorsolateral region of r6 (Song et al. 2006). Concurrently, Cre was observed to co-express with Phox2b, a marker involved in BM and VM neurons differentiation (Pattyn et al. 2000), in r6 (see Figure 3.17 C, r6). In fact, almost Phox2b positive cells, if not all, were also seen to co-localise with Cre (see Figure 3.17 C). Some cells, however, were only Cre-positive and lay in close proximity to the VZ. These cells could be stained for 5HT confirming their identity as serotonergic neurons (see Figure 3.17 D). All in all, these data show that there is perdurance of Cre expression in post-mitotic cells that are known to derive from p3 progenitors of the hindbrain and therefore that Cre expression can be used as a neuronal lineage tracer in the hindbrain. It remains to be proved whether CreER^{T2} behaves similarly in the spinal cord.

Visceral motor nerons can also be found along the spinal cord. Parasympathetic MNs are located in the sacral spinal cord while sympathetic motor neurons (SPNs) are found mainly in the thoracic spinal cord (Loewy 1990). This raises the question of whether the post-mitotic CreER^{T2} positive cells that settled in the intermedio-lateral cord of the spinal cord could be visceral motor neurons too. They were absent in the lower cervical region of the spinal cord but present at thoracic levels suggesting that they might be SPNs. To test this hypothesis, I carried out immunohistochemistry for Cre and nNOS/Isl1 at E12.5. I also performed stainings for HB9/Isl1 to differentiate SPNs from somatic MNs (Figure 3.18 B, see also Table 1.1). Indeed, nearly all Cre-positive cells co-stained for nNOS (Figure 3.18 A) whereas only a sub-population of them co-labelled with Isl1 (Figure 3.18 A, arrow heads). This might be because those Cre-positive cells were themselves in different stages of maturation/differentiation rather than being different sub-types of SPNs (Isl1 has been shown to be essential to the overall assignment of visceral spinal motor neuron identity) (Pfaff et al. 1996). A few SPNs could be seen to express HB9 too (Figure 3.18 B, arrows), which was not surprising since HB9 has been implicated in the differentiation of visceral MNs, mainly determining subclass identity of SPNs - SPNs located in the intermediolateral nucleus versus central autonomic nucleus (Arber et al. 1999). This seems to be a peculiarly of visceral MN of the spinal cord, though, as cranial visceral MNs do not express HB9 (Briscoe et al. 1999). Moreover, HB9 has been shown to be expressed in visceral MNs at some point of

their development because visceral MNs are all labelled in Hb9-GFP mouse during adulthood (Wilson et al. 2005).

All in all, these data imply that p3 progenitors generate not only V3 interneurons but also SPNs and a class of unidentified dorsal neurons (quite possibly Sim1 positive). This was unexpected because SPNs have been presumed to share the same progenitors as sMNs – originating in pMN, not p3 (Briscoe et al. 1999; Thaler et al. 2004). However the possibility remains that SPNs might activate *Nkx2.2-CreER^{T2}* ectopically after they leave the VZ, and are not genuinally derived from p3 Nkx2.2-expressing progenitors in the VZ. To tackle this potential complication a panoply of mutants mice were studied, something I will discuss in Chapter 4.

3.3.3. Characterization of transgene expression during gliogenesis

Olig2 expression in the rodent ventral neural tube initiates in a region adjacent to the developing floor plate (Takebayashi et al. 2000; Jeong et al. 2005; Dessaud et al. 2007; Ribes et al. 2010). Subsequently, Nkx2.2 is upregulated and, by repressing Olig2, establishes its unique domain of expression that ultimately becomes ventral and non-overlapping to the that of Olig2. By E10.5, Nkx2.2 and Olig2 can be seen forming mutually exclusive and adjacent domains (see Figure 3.19 A) - Nkx2.2 domain being sandwiched between the floor plate and Olig2. At this age Nkx2.2 and Olig2 domains – the p3 and pMN progenitor domains, respectively – become neurogenic.

Sim1-positive V3 INs derive from p3-progenitors around E10 [‡] and their generation continues for at least two days. Being known to be a transcription factor crucial to V3 INs specification (Briscoe et al. 1999), Nkx2.2 remains strictly regulated within the p3 domain during these stages of development. However, around E12.5 Nkx2.2 is upregulated inside the Olig2 domain and a new region of overlap between Nkx2.2 and Olig2 is formed (see Figure 3.19 B). This region has been named p*, to differentiate it from the p3 and pMN domains (Zhou et al. 2001). Both regions p* and pMN are known to give rise to oligodendrocyte precursors (OLPs), which then migrate away from the VZ to populate the entire spinal cord (Zhou et al. 2001; Fu et al. 2002). From E12.5, it was observed that Nkx2.2

[‡] At 28 somites (E10), Sim1 expression has just started and can be seen weakly expressed in a few cells flanking the most ventral region of the spinal cord. By 38 somites, Sim1 expression is strong and abundant within the V3 IN population (data not shown).

co-labels with Sox10 and PDGFRα within the Olig2^{+} neuroepithelial domain, although there are Sox10^{+} cells that are Nkx2.2-negative but Olig2-positive (asterisk in Figure 3.19 D; see also Figure 3.19 C). At least 60% of the cells that express Sox10 co-express Nkx2.2 within the Olig2^{+} neuroepithelial domain. As OLPs migrate away from the VZ, Nkx2.2 appears to be translocated from the nucleus to the cytoplasm (arrow heads in Figure 3.19 E). Nkx2.2 is downregulated eventually during migration, whereas OLPs express Olig2 throughout their development (Richardson et al. 2006; Richardson et al. 2011). Nevertheless, expression of Nkx2.2 returns once again to differentiating oligodendrocytes. At this stage, Nkx2.2 plays an important role in oligodendrocyte maturation which takes place mainly after birth in the sub-pial white matter (Qi et al. 2001).

Expression of the *Nkx2.2 CreER^T2* transgene in the neuroepithelium was found not to overlap with the Olig2 expression domain after E12 (see Figure 3.15 B and C). The transgene also was not up-regulated with *Nkx2.2* in differentiating oligodendrocytes (Qi et al. 2001 and data not shown). While this prevents us from using it for studies of oligodendrogenesis within the p*/pMN domain, *Nkx2.2-CreER^T2* mice were still useful to answer the question of whether some, if any, oligodendrocytes are ever produced by p3 progenitors. This is a point to be dealt with in the following chapter, Chapter 4.

3.4. Optimization studies for CreER^T2 activation

In order to label *Nkx2.2*-expressing cells it is necessary to cross *Nkx2.2-CreER^T2* mice to a Cre dependent reporter and to activate *CreER^T2* by TM administration. Different methods of TM administration were employed in pilot studies in an effort to determine the most efficient and least toxic way to activate Cre during embryogenesis (note that TM is known to have antiestrogenic properties therefore it can interfere with pregnancy; see text-box below). The efficiency of TM is dependent on the route of administration. There are currently three methods for administration of TM in pregnant females: intraperitoneal injection, oral administration through food and oral administration by gavage. I found that oral gavage was the most suitable technique of administration of TM. Highly dependent on the reporter mouse strain used and influenced by the weight and the age of the pregnant female and the precise time when transgene activation was needed, the optimum TM dose was found to be the highest dose that could be tolerated without inducing spontaneous abortion. For longer-term fate map analyses, it was necessary to use a lower dose of TM.

Comparative studies of TM induction with different reporter lines have shown that Rosa26-LacZ and Rosa26-YFP reporter mice were more suitable Cre reporter lines than Rosa26-GFP and Z-EG, the two latter having a very low recombination efficiency in my hands (see Figure 3.20). Also late weaned and/or previously pregnant, ~2-3-month-old females weighing more than ~ 24g frequently seem to hold the pregnancy to term better when compared to younger females (see Figure 3.21). Presumably absortion of TM by body fat might reduce the side effects of TM for the pregnancy by preventing it from binding with the oestrogen receptors in the endometrium, uterine tissue and mammary gland, structures highly important during pregnancy (Robinson et al. 1991; Wade et al. 1993; Sairam et al. 2002; Buchanan et al. 2007, and also see text-box below). In an attempt to apply some statistical analyses to the data of Figure 3.21, non-parametric measures, namely Logistic regression and Spearman's rank correlation coefficient, were carried out using SPSS software.   Spearman's rank correlation coefficient (*sr*) can be used to measure the statistical dependence between a binary variable and a continuous variable. I coded the occurrence of pregnancy as a binary variable (0 is abort and 1 is pregnant) and considered the female's age (in months), her weight on the day of TM administration (in grams), TM dosage (in mg per Kg of female's body weight), and the time of TM injection (varying between 6.5 and 10.5) as continuous variables. As seen in Table 3.2, there is no significant correlation between pregnancy and continuous variables age, weight and TM dosage. However, the time of injection appears to moderately influence the propability that the female will abort, *sr* = 0.401, *p* = 0.0001.

Table 3.2 - Spearman's rank correlation coefficients between a binary variable (pregnancy) and continuous variables (age and weight of pregnant female, dose and time of tamoxifen administration).

Spearman's rank correlation coefficients values vary from -1 to +1.

Parameter	Age	Weight	TM Dosage	Time of Injection
Correlation coefficient (*sr*) with pregnancy	0.086	0.075	0.148	**0.401**
p value	0.465	0.559	0.153	**0.0001**
Sample size (n)	74	63	95	95

Similar conclusions were also drawn when using Logistic regression analysis. Table 3.3 and Table 3.4 summarise the results. Logistic regression evaluates the probability of a categorical dependent variable, in this case the probability of pregnancy after E13.5 (0 is abort and 1 is pregnant), on the basis of continuous independent variables (age and weight of pregnant female, dose and time of tamoxifen administration). The study was done in 2 steps. Because age and weight are correlated to some extent (*sr* = 0.4 , *p* = 0.015) I entered age and weight in the first step of the logistic regression to account for any variance due to these two variables. These were observed to be statistically non-significant (*p* = 0.603). However, adding time and dose of tamoxifen injection into de model revealed to significantly improve the outcome (*p* = 0.015). The fitness of the model is however poor (Chi-square = 12.276) possibly due to some missing data.

Table 3.3 - Summary statistics of Logistic regression

	Chi-square	df	*P*
Model at Step 1 (age + weight)	1.013	2	0.603
Model at Step 2 (age + weight + time of injection + TM dosage)	12.276	4	0.015

Table 3.4 - Unique contribution of individual variables at step 2

Individual Variables	B	df	*p*
Age	-0.171	1	0.896
Weight	0.001	1	0.998
TM dosage	0.05	1	0.094
Time of injection	0.599	1	0.565
Constant	-12.362	1	0.304

I found that even at the optimum dose of TM, pregnant females did not enter labour normally at the appropriate time, so for postnatal analyses, pups were surgically removed from their mothers and reared by a foster mother (protocol described in Nagy et al. 2001). Initially, females were left to give birth naturally and if birth didn't happened by E19.5

litters were delivered by Caesarean section and fostered. Subsequent litters subjected to the same protocol conditions were delivered at E18.5. As some embryos might die during gestation due to TM effect, both mother and father were homozygous for the transgene(s) in order to increase the chances of getting more material to analyse. Additionally, protein-enriched food was given to the pregnant females (>19% protein extruded rodent diet 2019, Harlan Teklad) to help them to hold the pregnancy better.

Text-box - The effects of tamoxifen on pregnancy

The pharmacological aspects of TM are complex and biologically context-dependent Furr et al. 1984. TM has anti-estrogenic properties because it binds to the oestrogen receptor (ER). The binding prevents the receptors from recycling thereby reducing the number of receptor molecules available for subsequent 17-ß-estradiol activity. However, the drug as well as its metabolised form, 4-hydroxytamoxifen, are themselves also biologically active compounds. Both drugs can behave either as pure agonists, partial agonists, or as antagonists depending on both tissue and specie. For example, TM opposes oestrogen action in the breast and mouse mammary glands whereas it manifests estrogenic activity in the mouse uterine tissues and skeleton. The pharmacological behaviour of TM also depends on the dose administered. In the rat uterus TM is an agonist at low concentrations and antagonist at higher concentrations, hence its partial agonist effect. Moreover, biological activity of TM differs among genes, depending on the mechanism of gene regulation TM may appear either as agonist or antagonist. The diverse biological activity of TM among tissues or cells or genes of a specie and between species, led scientists to classified it as a selective oestrogen receptor modulator (SERM).

The differential biological activity of TM stems from the fact that oestrogen receptors are ligand-regulated transcriptional factors and that cells possess the ability to distinguish among different ER–ligand complexes. The binding of the ligand induces activating changes in the transcriptional inactive ER that allow ER to interact with specific oestrogen response elements within the regulatory region of a target gene. The conformational changes of ER are dependent on the ligand, and the ability of ligand-bound ERs to regulate target gene transcription is determined by the cell- and tissue-specific expression of both coactivator and corepressor proteins involved in the ER signalling cascade. In addition, the discovery of more than one receptor, specifically ERα and ERβ, together with the discovery of two distinct transcriptional activating functions (AF1 and AF2) within the ERα, which are affected differently by TM, help to further explain the diverse nature and the magnitude of

the estrogenic properties of TM (McDonnell et al. 2002). Interestingly enough, the effects of TM are also dependent on the presence or absence of other hormones, like oestrogen (E) or progesterone (Kohlerova et al. 2004).

As a result of the anti-estrogenic properties of TM, the high concentrations of TM that sometimes are required to activate Cre-ER^{T2} are quite close to interfere with pregnancy, often resulting in abortion or failure of birth. Abortion is often a consequence of the agonist effect of TM in the mouse reproductive tissues. Indeed, and consistent with previous findings (Sadek et al. 1996), increasing TM levels increases the risk of foetuses aborting and reduces the sizes of litters. It is likely that the high levels of TM and its agonist effect on mouse reproductive tissues might resemble the high quantities of E that are known to cause foetal death or reduce foetal growth by blocking decidualisation (Milligan et al. 1997). Abortion can also be a consequence of the effect of TM on suppressing progesterone receptor (PR) synthesis levels. Total or partial inhibition of PR has been observed in hypothalamus, mammary glands and uterus of TM-dosed mice (Muldoon 1987; McKenna et al. 1992). In addition, TM or E has been reported as an effective competitor for progesterone binding sites in the mouse brain (Bukusoglu et al. 1996). So, it is not surprising that the blockage of PR, and hence progesterone signalling cascade, has been shown to induce abortion or resorption of foetuses (Milligan et al. 1997). Even as abortion does not happen until birth, failure of birth might happen on induced pregnant females. Such incident might again be due to the antagonist properties of TM in the mouse uterus and brain. It has been shown in rat that tamoxifen interference with normal oestrogen activity can disrupt the onset of labour (Downing et al. 1981). Moreover, it has been shown that TM acts on various hormones, a group of proteins also termed "contraction-associated proteins", which are involved in the mechanism of parturition. For example, production of prostaglandins, responsible for stimulating contractions of the myometrium, is stimulated by E near birth and can be inhibited by TM. The effect of TM can be reversed by administering natural or synthetic prostaglendins (Furr et al. 1984 and therein). Fos levels, which only show significantly higher transcript levels during labour, decrease considerably after TM treatment (Wu et al. 2007). A third example is oxytocin, which also plays a role during parturition, given the influence of oxytocin on uterine contractions. Even using supramaximal concentrations of oxytocin, this hormone can not override TM inhibitory effect on contractile responses of the myometrium (Lipton et al. 1984). On the whole, TM can create inbalances in the hormonal levels of pregnant females that can alter the normal course of the pregnancy.

It is therefore difficult to predict the outcome of TM treatment on the induced pregnant females because the spectrum of biological actions of TM ranges from full agonist to complete antagonist to oestrogen action. It seems that the ultimate effect of TM action depends considerably more on the time of injection and, to a lesser degree, on the TM dose, and hence a pool of females no less than 3 in number was dosed when testing each induction protocol. As previously reported, induction by TM did show a dose-dependent response on the level of induction obtained (Hayashi et al. 2002) (see Figure 3.22). However, that usually happens at the expenses of adverse effects for the pregnancy. Nonetheless, it was often possible to find a situation where successful pregnancy could coexist with good Cre induction. Reproducible recombination with few or no side effects for pregnancy was frequently achieved using 200mg/Kg body weight (bw) of TM in a variety of our reporter transgenics, meaning that such concentration of TM represents a good starting point when optimising Cre induction in new transgenic lines. It is worth mentioning that for some of our transgenics, 200mg/Kg bw gave nearly complete induction whereas in other transgenic lines the same concentration was barely enough to induce any Cre recombination.

The possibility of Cre recombinase activity in the absence of TM induction was also considered. Unlike other reports (Imayoshi et al. 2006), my *Nkx2.2-CreER*^{T2} line exhibited no background recombinase activity (data not shown), recombination being completely dependent on TM administration.

Several abnormalities have been linked to Cre genotoxicity in the mouse both *in vitro* and *in vivo*. *In vitro* studies involving the use of cultured cells lacking exogenous *loxP* sites have reported "illegetimate" recombination events resulting in chromosomal rearrangements, aneuploidy, decreased growth and cytopathic effects. Reports of Cre-site infidelity in transgenic mice have also been recently published. For example, a study by Schmidt *et al*. links male sterility to chronic high-level expression of Cre in the spermatids of transgenic animals. Also, Cre toxicity effects can compromise normal tissue development as described by Forni et al. (2006). In that study, a form of hydrocephalus is attributed to a toxic threshold of nuclear Cre expression in neurogenic cells of *Nestin-NLS-Cre* mice. The development of hydrocephaly was observed to be dependent on TM treatment when using *Nestin-CreER*^{T2} transgenic line and this was aggravated at higher TM doses, presumably because high TM induced more efficient nuclear accumulation of CreER^{T2} (Schmidt et al. 2000; Forni et al. 2006).

However, in my studies such aberrations due to Cre genotoxicity seemed not to be important. The fact that my transgenic line only carries one copy of the transgene (or two copies in the homozygotes) might explain the lack of Cre toxicity. Homozygous mice for Cre

recombinase induced at embryonic ages live as long as one year of age without showing any aberrant phenotype. Also, any embryos that showed morphologic defects or striking abnormalities were rejected from the present studies. The results reported in this thesis using *Nkx2.2-CreER^{T2}* transgenic line were in any case always compared with/validated by control experiments.

3.5. Discussion

3.5.1. Assessing Nkx2.2-CreER^{T2} transgene expression

To fate map the progeny of Nkx2.2-expressing p3 progenitors I generated an Nkx2.2-CreER^{T2} PAC transgenic line by pronuclear injection. Although the expression of Nkx2.2 is initially confined to the p3 domain, soon after E12.5 the domains of Nkx2.2 and Olig2 (which demarcates the pMN domain) switch from being mutually exclusive to overlapping (Zhou et al. 2001). Moreover, later in development Nkx2.2 has also been reported to be expressed in differentiating oligodendrocytes (Qi et al. 2001). I therefore made use of the tamoxifen-inducible form of Cre recombinase (CreER^{T2}) (Indra et al. 1999) to dissociate the different phases of Nkx2.2 expression by timed administration of tamoxifen. The restricted expression pattern of Nkx2.2 in the neuroepithelium was faithfully recapitulated by CreER^{T2} transgene in founder mouse lines up to E12.5. However, the transgene failed to mimic the dorsal expansion of Nkx2.2 expression into the Olig2 domain during the gliogenic phase (at E12.5 and thereafter) and it was not observed being upregulated either in OLPs or in differentiating OLs. Instead, the transgene expression was carried over in post-mitotic neuronal cells that appear to emanate from the p3 domain. The fact that CreER^{T2} expressing cells of the hindbrain co-labelled with neuronal markers such 5HT and Phox2b, specifically expressed in serotonergic neurons and branchial/visceral motor neuons, respectively, which are known to derive from p3 progenitors of the hindbrain, supports the hypothesis that Cre could be used as a neuronal lineage tracer of the p3 domain in the hindbrain and, by extension, in the spinal cord too. If so we have to conclude that p3 progenitors generate SPNs, the visceral motor neurons of the thoracic spinal cord, because they co-express Cre as well as their specific marker nNOS. This is unexpected because SPNs have long been thought to share the same origin as sMNs – the pMN domain. Other unidentified cells, possibly Sim1-positive interneurons and/or other interneurons, could also come from p3 progenitors as Cre-expressing cells are seen migrating away in a pattern that does not resemple SPNs (e.g. the expression pattern differs from the one of Chat staining).

Nonetheless, it remains possible that the Nkx2.2- CreER[T2] transgene might be activated ectopically in those post-mitotic neuronal cells after they migrate away from p3 domain. Further studies are needed to iron out this potential complication (see chapter 4 for further discussion).

How can we explain the aberrant and unexpected behaviour of the *Nkx2.2-CreER[T2]* transgene? It is known that the insertion site of the transgene can influence the dynamics of expression (Clark et al. 1994). It is also possible that regulatory elements that control *Nkx2.2* might not be present in the transgene so as to ensure an accurate expression throughout development. Actually, a study of functional screening for Shh regulatory elements uncovered that each of the 6 enhancers that play different roles during development are distributed as far apart as 400 kb (Jeong et al. 2006). It is then possible that the chosen PAC, which spans merely 200kb, might not contain all the regulatory elements needed to mimic expression of Nkx2.2 exactly. In addition, one cannot exclude the possibility that even though only ~50bp of genomic DNA is replaced by the CreER[T2] insert that could itself result in a detrimental effect on the transcriptional regulation of the transgene.

3.5.2. Tamoxifen recombination efficiency studies

Successful activation of Cre was found to be dependant on the levels of Cre expression, Cre-conditional reporter used, TM concentration, weight of pregnant female and stage of induction. Different methods for administration of TM were employed and oral gavage was chosen as the most suitable and most reliable. I have found with *Nkx2.2-CreER[T2]* line that *R26R-YFP* (Srinivas et al. 2001) consistently gives higher recombination rates when compared with other Cre-conditional reporters. Young et al. (2010) put forward a plausible explanation that could explain the utterly disparate Cre-recombination activity levels observed between, for example, *R26R-YFP* (very high) and *R26R-GFP* reporter line (Mao et al. 2001) (virtually no recombination). The fact that *R26R-GFP* contains 3 lox sites instead of 2 as in *R26R-YFP* together with transient activation of CreER[T2] only upon TM administration could hamper efficient activation of reporter gene (Young et al. 2010). Nevertheless, the *R26R-GFP* reporter has often been reported to successfully recombine in constitutive Cre lines (e.g. Fogarty et al. 2005), so the activity of CreER[T2] is probably reduced compared to the Cre protein.
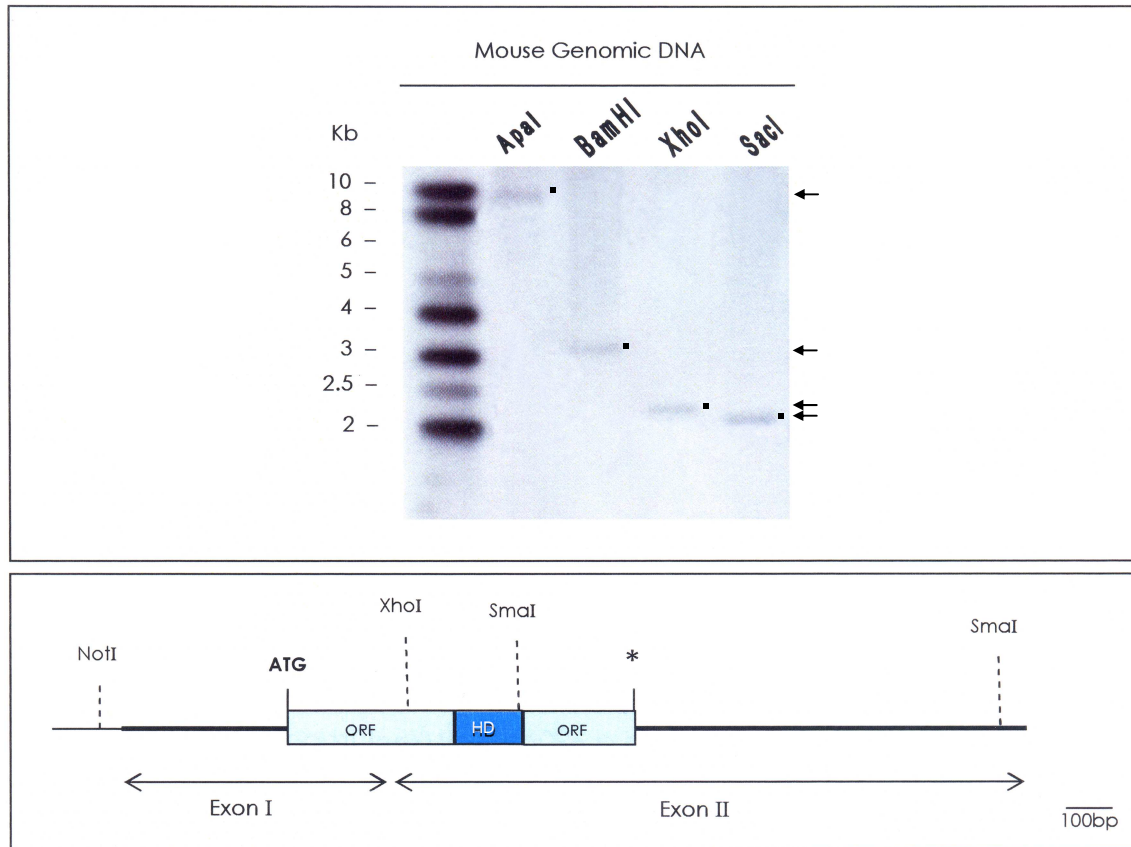
Figure 3.1 - Southern analysis of mouse genomic DNA using a NotI-XhoI fragment from mouse *Nkx2.2* cDNA as a probe. Above: Southern blot of mouse genomic DNA digested with ApaI, BamHI, XhoI or SacI and hybridized with the mouse Nkx2.2 cDNA fragment (620bp NotI/XhoI fragment). The membrane was exposed to a Hiperfilm™ MP at -70°C, overnight. Size markers are shown on the left. Below: Diagram of the mouse Nkx2.2 cDNA showing the position of the probe and the localization of the open reading frame (ORF), the position of the homeodomain (HD), and the positions of the exon I and exon II. The NotI site lies in the vector backbone sequence just upstream of the cDNA insert. The scale bar is 100bp.
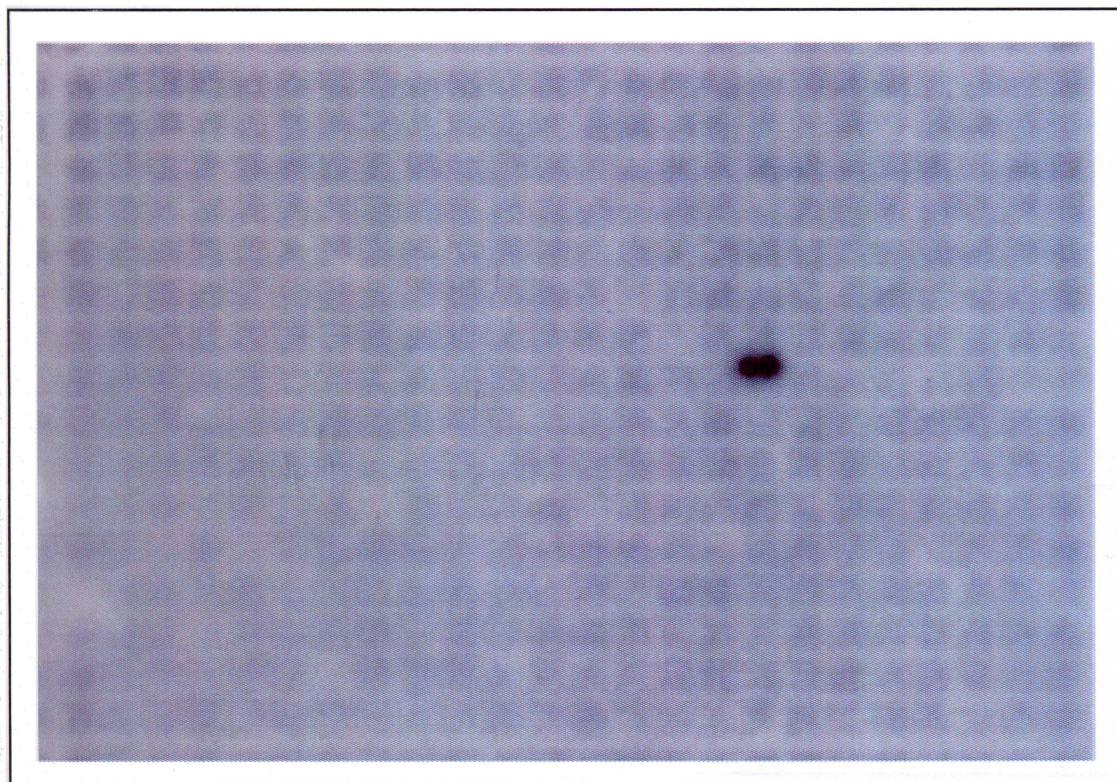
Figure 3.2 - One of the six panels of a membrane mouse PAC hybridised with mouse *Nkx2.2* **cDNA fragment (620bp NotI / XhoI fragment from pNkx2.2).** The membrane shows a positive signal (in duplicate) which corresponds to a *Nkx2.2* PAC clone. The membrane was exposed to a Hyperfilm™ MP at -70°C, overnight.
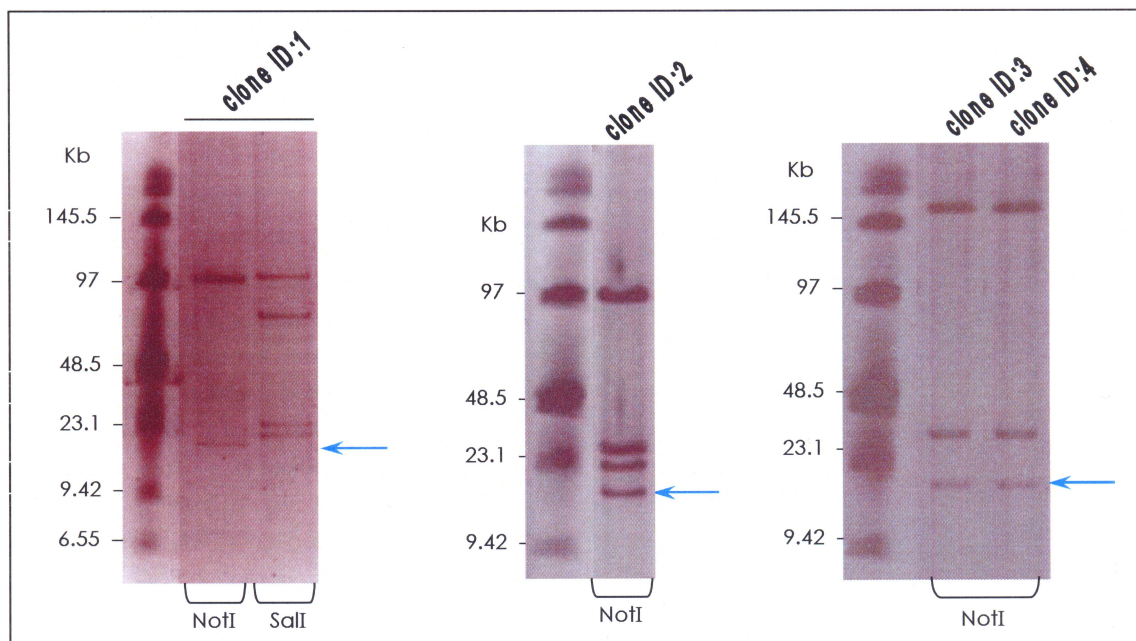
Figure 3.3 - Pulsed field gel electrophoresis of PAC DNA from the 4 selected *Nkx2.2* PAC clones digested with NotI and SalI enzymes. The band corresponding to the backbone of the pPAC4 vector (16.7 Kb) is indicated by the blue arrow. Size markers are shown on the left side of each gel photo. See text for more details.
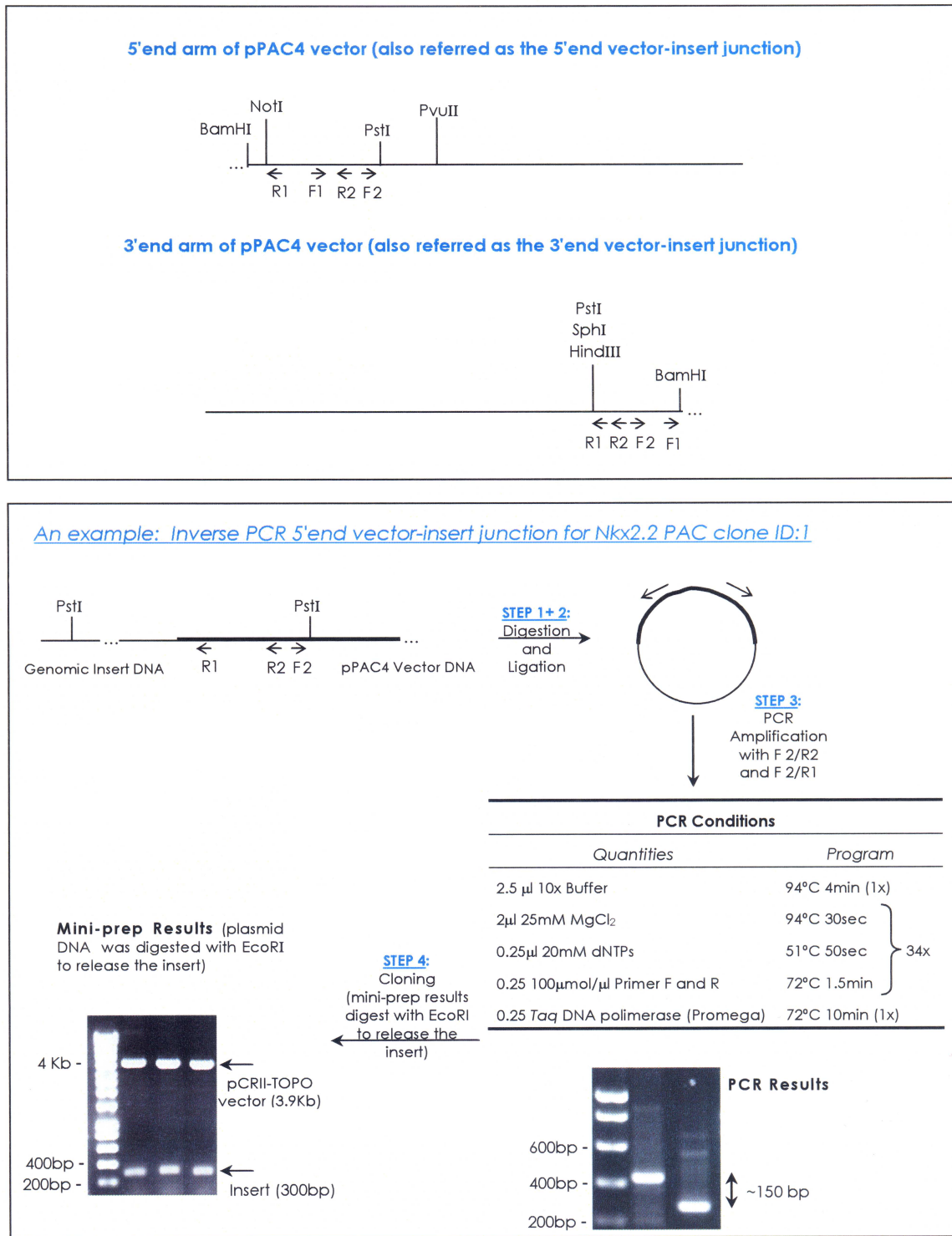
Figure 3.4 - Inverse PCR strategy. Above: schematic representation of the location of restriction sites of selected enzymes to carry out inverse PCR procedure (the sequence of the primers is shown in Table 2.1). Below: an example of inverse PCR.
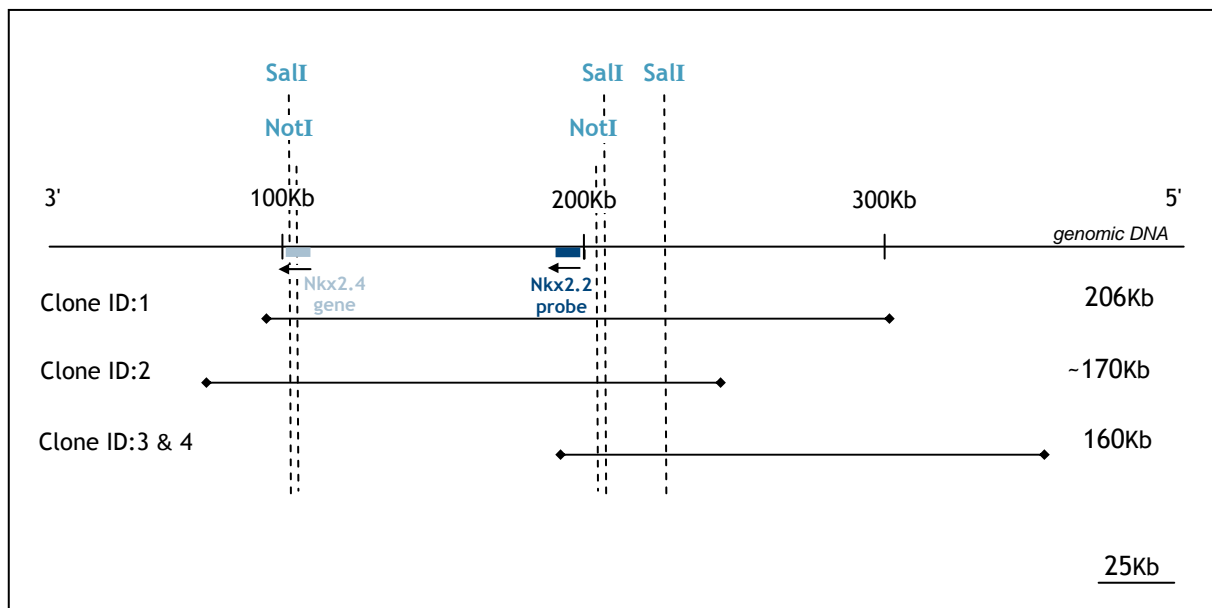
Figure 3.5 - Structures of the selected *Nkx2.2* PAC clones. The 620bp NotI/XhoI probe from pNkx2.2 is represented by a dark blue bar (not to scale) and Nkx2.4 gene is represented by a light blue bar (not to scale). Note that SalI enzyme cuts the PAC backbone only once. The scale bar is 25Kb. Arrows indicate direction of transcription.
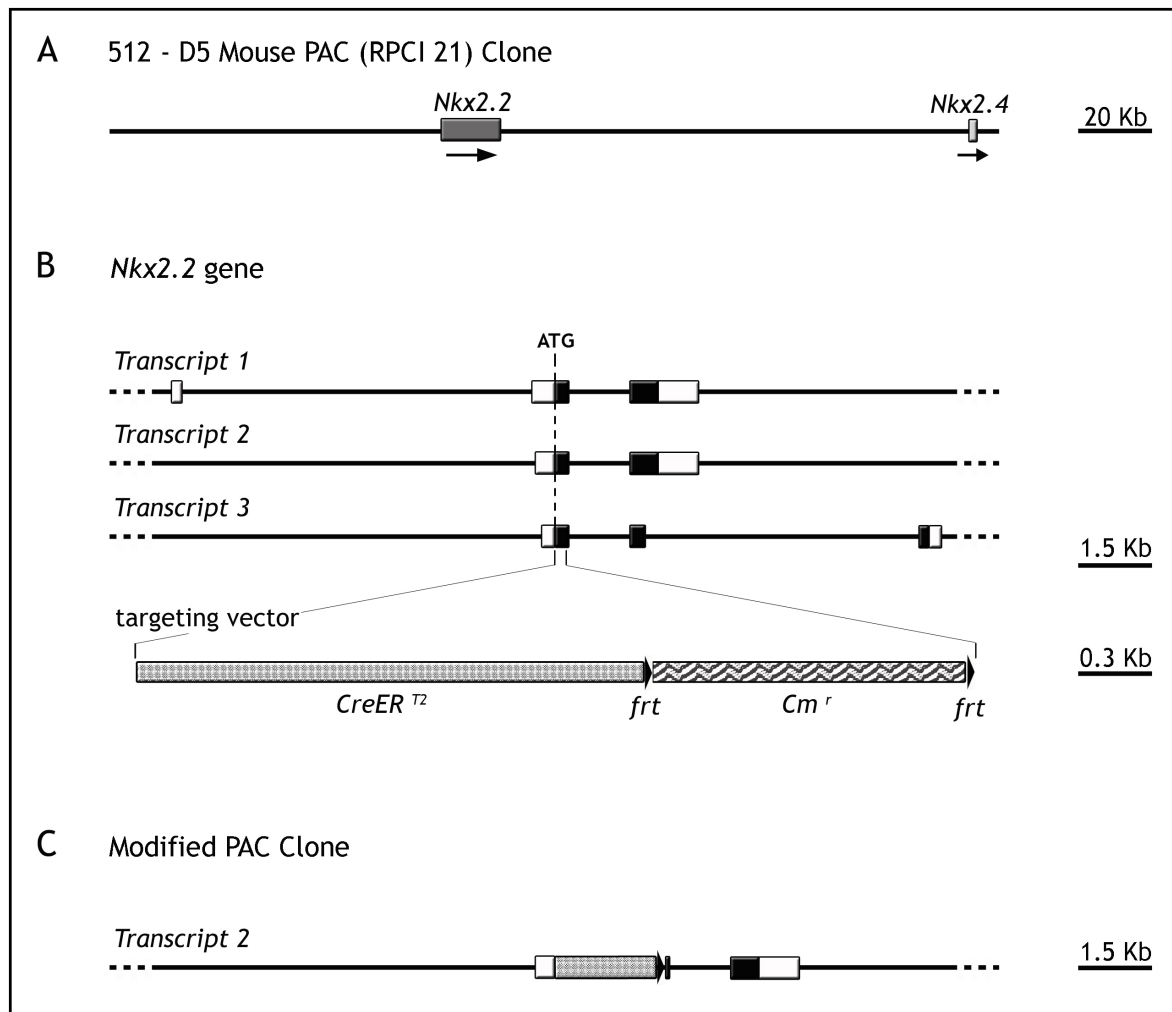
Figure 3.6 - The genetic strategy used to generate *Nkx2.2-CreER^{T2}* mouse line. (A) Map of the genomic region of the unmodified PAC insert and the positions of *Nkx2.2* and *Nkx2.4* genes. (B) The endogenous *Nkx2.2* locus (including its three transcript variants) and the relative location of the targeting vector containing the *CreER^{T2}* gene and a bacterial cloramphenicol resistance cassette (Cm^r) flanked by FRT sites (arrowheads). The ATG of the *Nkx2.2* gene coincides with the ATG of the *Nkx2.2-CreER^{T2}* gene. Exon structure is represented by boxes – black regions denote the open reading frame. (C) The Cm^r cassette was removed before microinjection of the modified PAC (exemplified for "Transcript 2"). Note that the FRT site is not to scale.
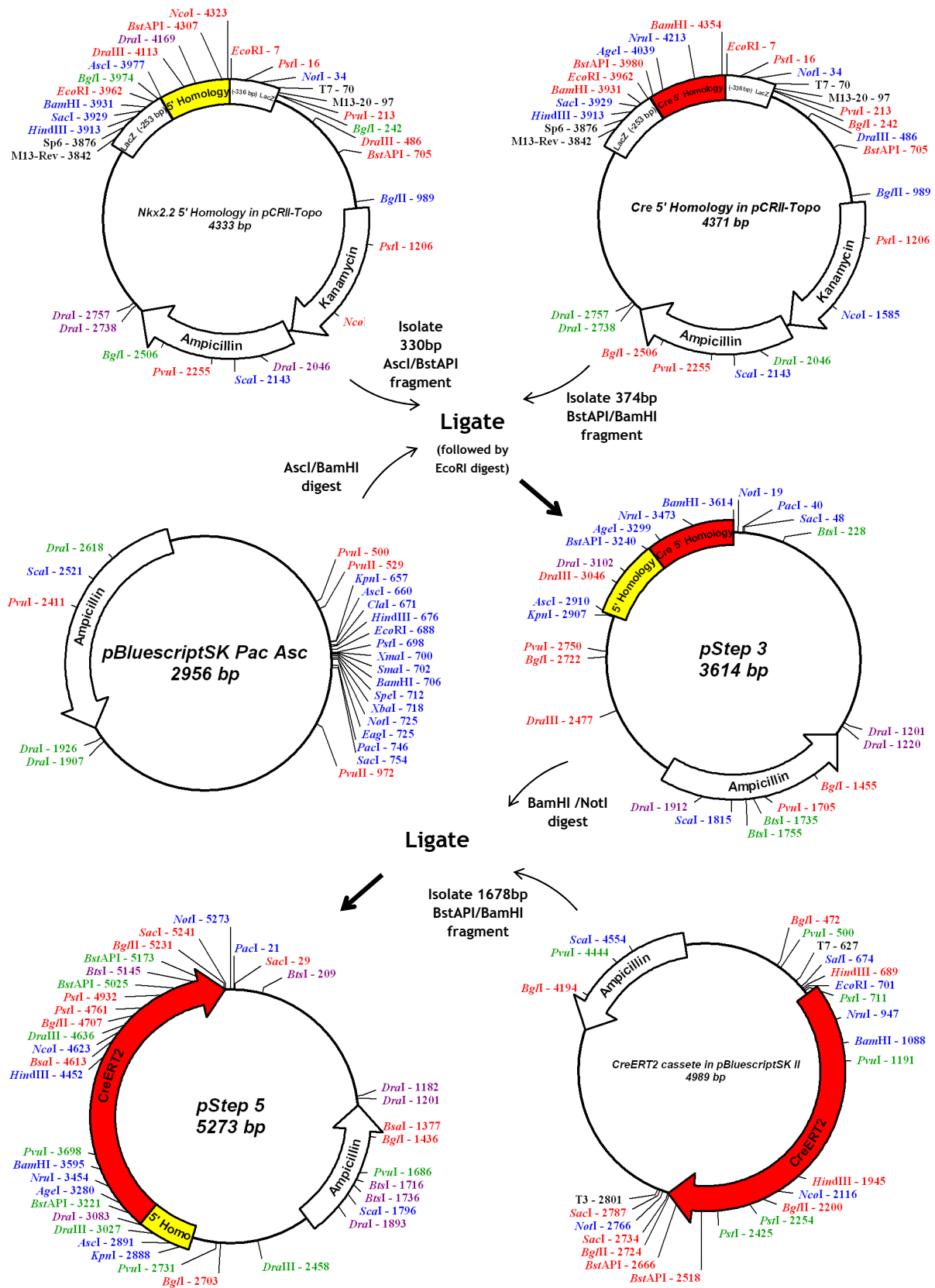
Figure 3.7 - Construction of *Nkx2.2* targeting vector. See section 3.2.3.2 for a description.
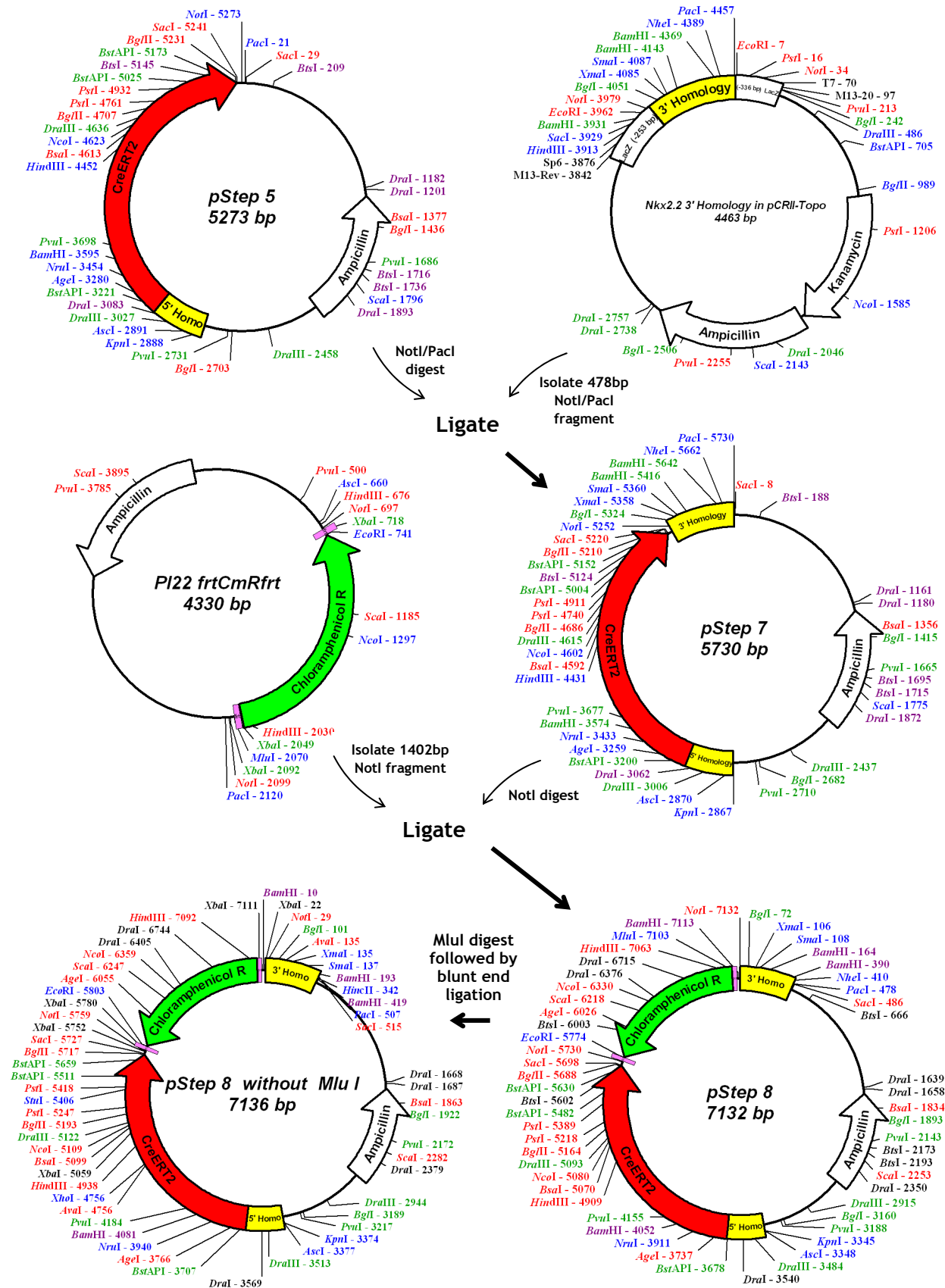
Figure 3.7 (cont.) - Construction of *Nkx2.2* targeting vector. See section 3.2.3.2 for a description. The *frt* sites are represented in pink in the PI22 plasmid.
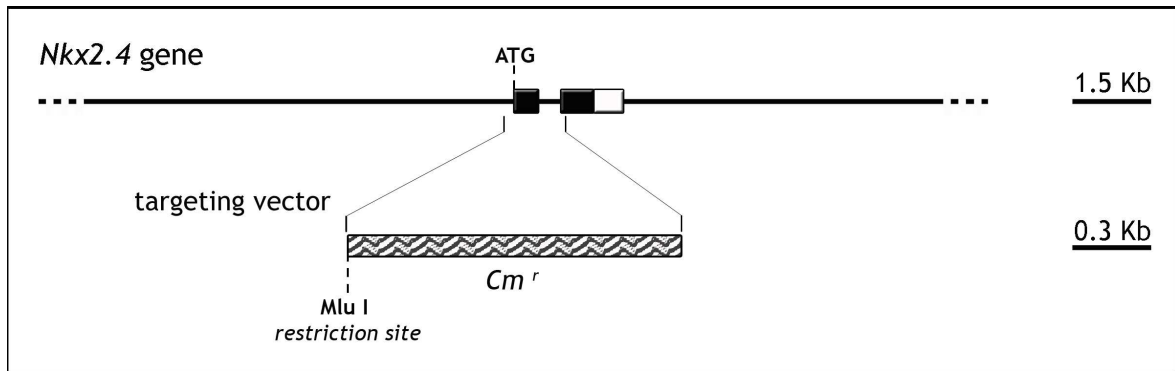
Figure 3.8 - The *Nkx2.4* targeting vector. Alignment with *Nkx2.4* gene from which there is only one transcript identified to date (see text for details).
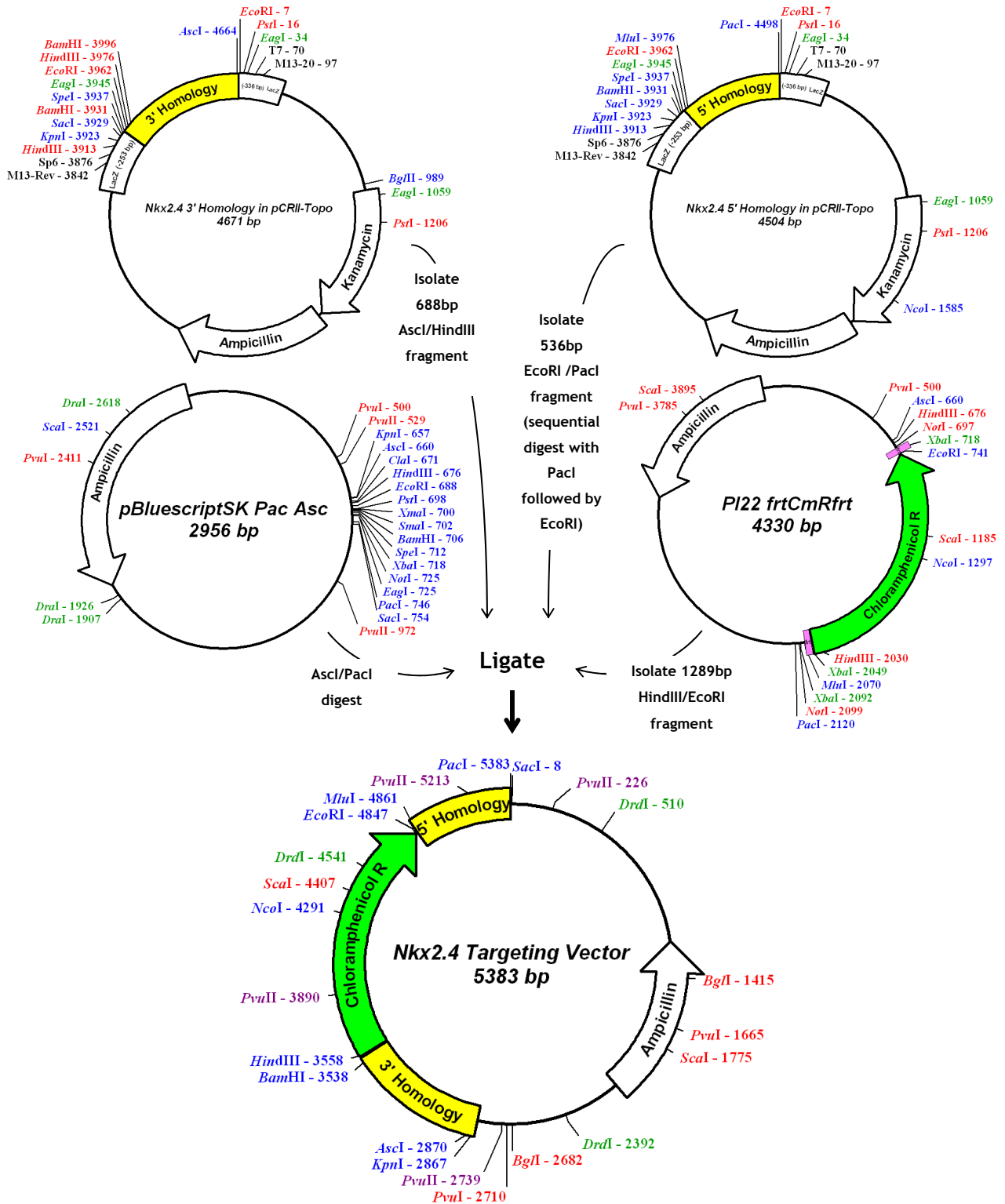
Figure 3.9 - Construction of *Nkx2.4* targeting vector. A 4-way ligation was carried out to combine the 536bp *Nkx2.4* 5' homology, the 688bp *Nkx2.4* 3' homology, the 1289bp Cm^r cassette from PI22, and a modified pBluescript vector named pBluescriptSK PacAsc to produce *Nkx2.4* targeting vector. The ligation was digested with NotI before plating in the presence of chloramphenicol to reduce contamination from the plasmid backbones. The *frt* sites are represented in pink in the PI22 plasmid.
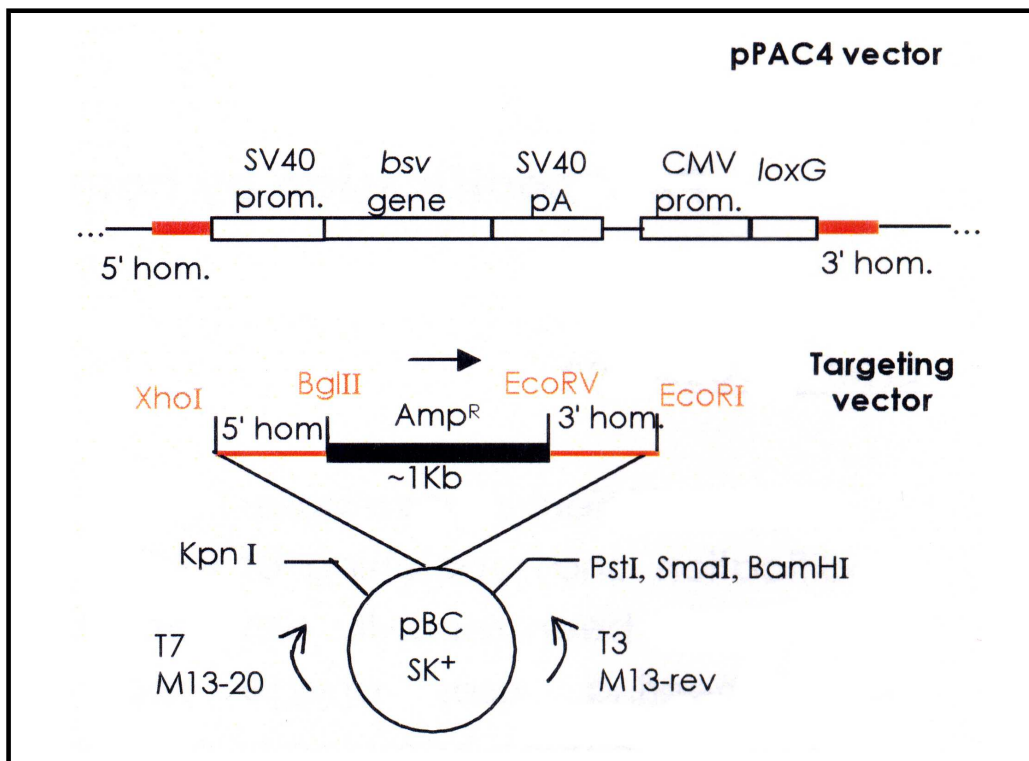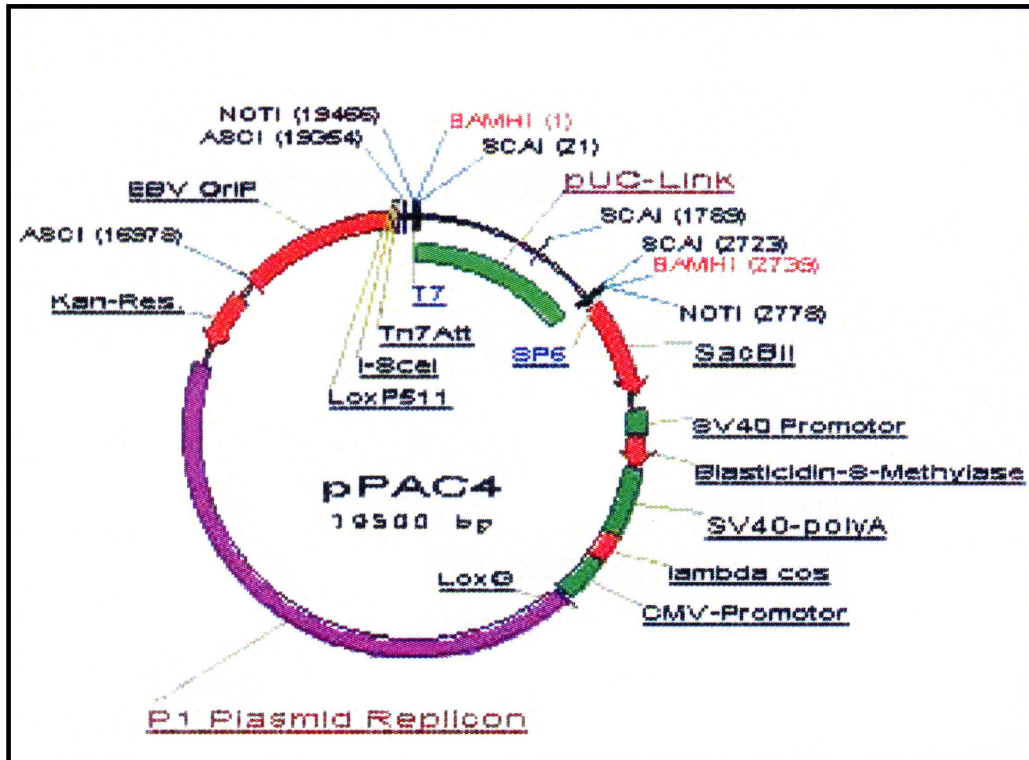
Figure 3.10 - Schematic representation of pPAC4 vector map (top panel), and strategy cloning of ampicillin gene into pPAC4 vector backbone (bottom panel). See text for details.
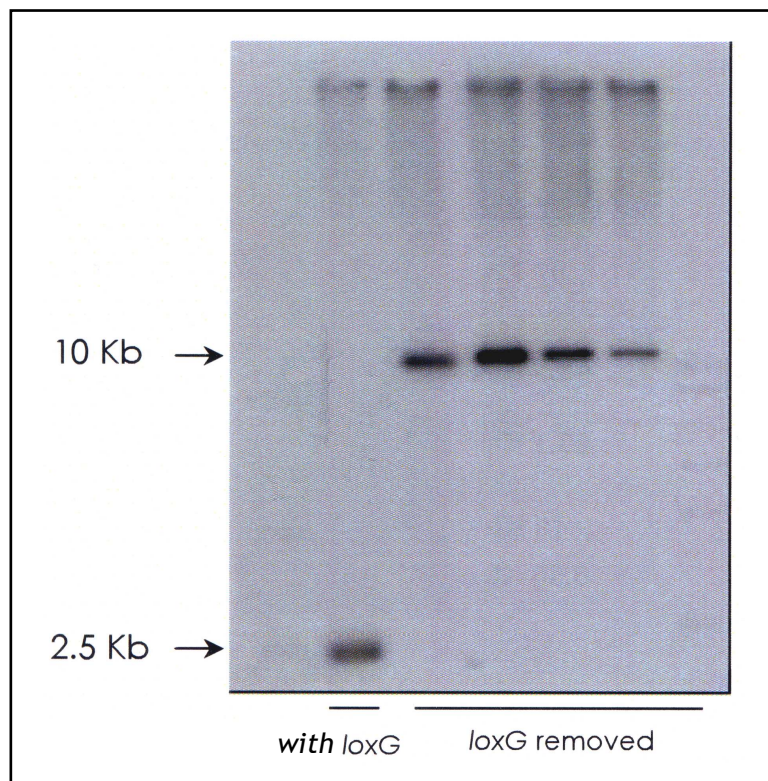
Figure 3.11 - Checking removal of *loxG*. Southern analysis of PstI digested PAC DNA from modified *Nkx2.2* PAC clone ID:1 using XhoI/EcoRI fragment containing ampicilin gene (4 mini-preps plus the negative control are shown). Size markers are shown on the left. See section 3.2.4.1 for a description.
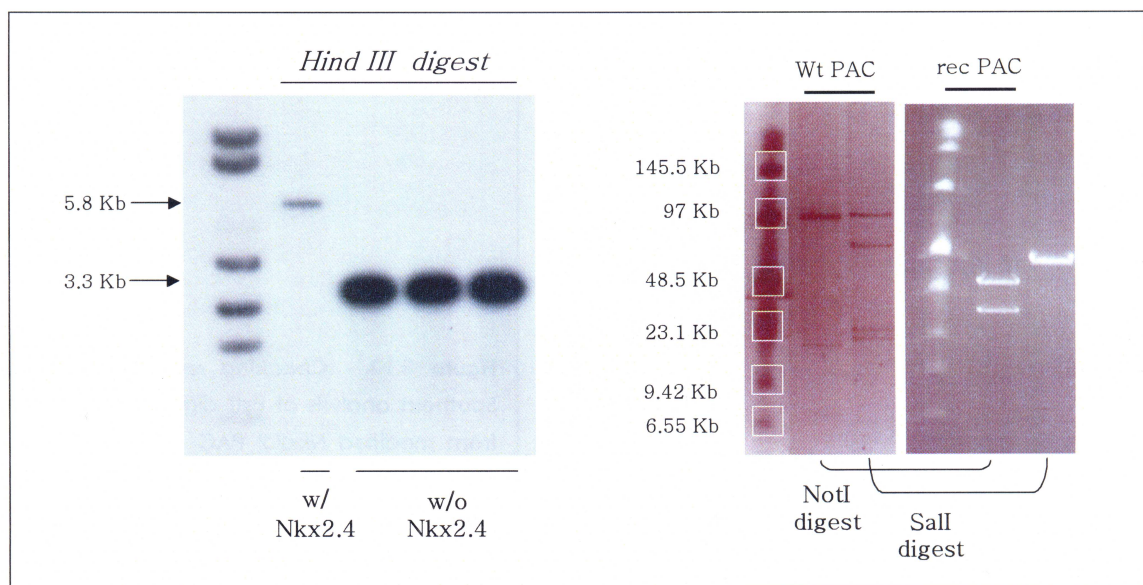
Figure 3.12 - Removal of *Nkx2.4* gene by homologous recombination. On left: Southern analysis of HindIII digested PAC DNA from modified *Nkx2.2* PAC clone ID:1 using 5' homology of *Nkx2.4* gene as a probe (3 mini-preps plus the negative control are shown). On right: Pulse field gel electrophoresis of PAC DNA from unmodified *Nkx2.2* PAC clone ID:1 (wt PAC) and from recombinant *Nkx2.2* PAC clone ID:1 after removal of *loxG* and *Nkx2.4* (rec PAC, only one PAC preparation is shown). PAC DNA was previously digested with NotI and SalI enzymes. Size markers (white squares) or the expected fragment sizes (arrows) are shown on the left of each gel photo.
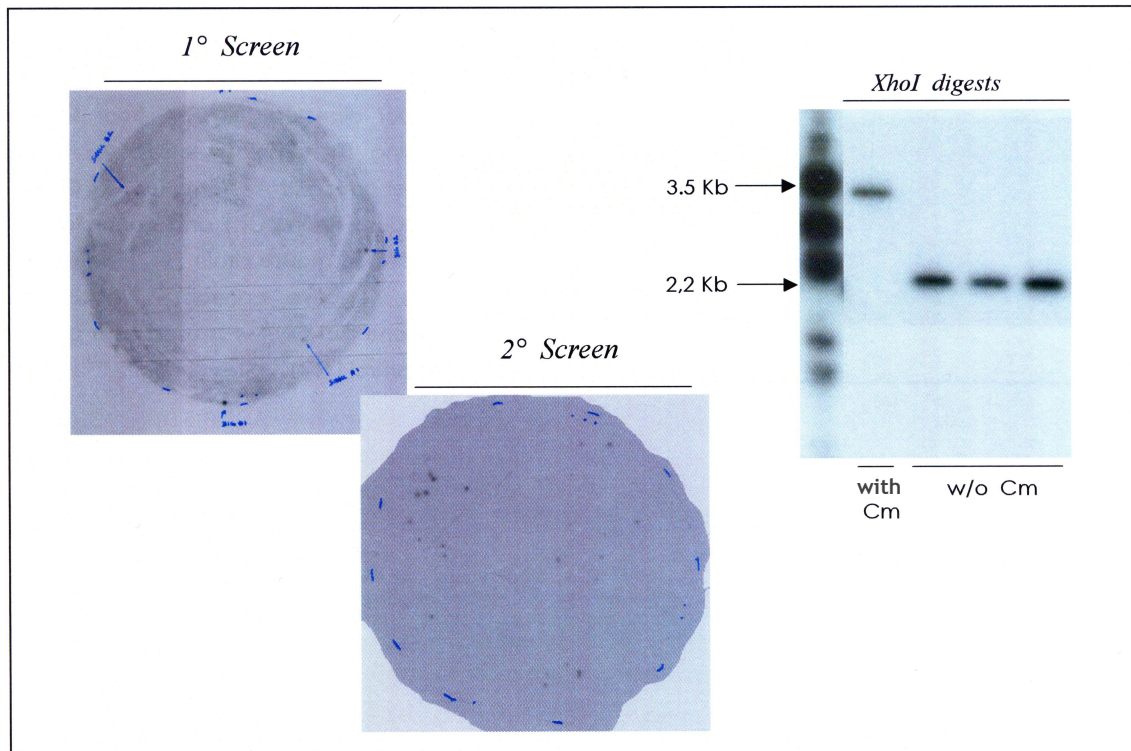
Figure 3.13 - Insertion of *Nkx2.2-CreER*^{T2} targeting vector by homologous recombination and removal of chloramphenicol cassette. Left: Primary and secondary screens of small libraries of *Nkx2.2* PAC clone ID:1 without loxG and *Nkx2.4* gene and with or without *Nkx2.2-CreER*^{T2} targeting vector inserted were performed using a specific probe to *CreER*^{T2} gene. Right: Southern analysis was carried out to confirm the removal of Cm[r] cassette. XhoI PAC DNA digests were probed with 3' homology of *Nkx2.2* gene (3 mini-preps plus the negative control are shown). The expected fragment sizes are shown on the left.
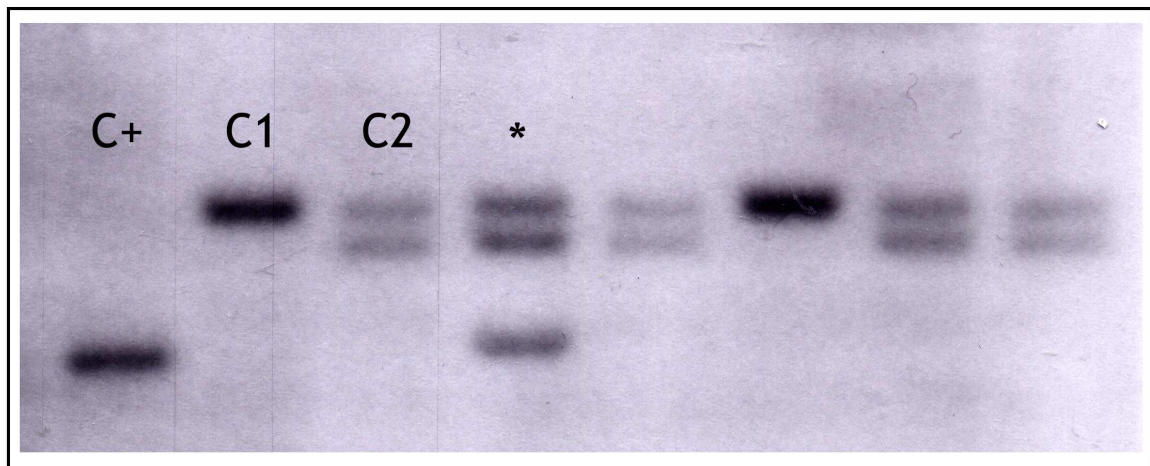
Figure 3.14 - Genotyping of a candidate for *Nkx2.2-CreER^{T2}* transgenic line. Southern analysis of SacI digested tail DNA from 5 pups using 3' homology of *Nkx2.2* gene. Genomic DNA from (B6 x CBA)F1 mouse strain (C1) and genomic DNA from B6 mouse strain (C2) were used as negative controls. *Nkx2.2* PAC clone ID:1 DNA was used as a positive control (C+). A founder is marked with an asterisk.
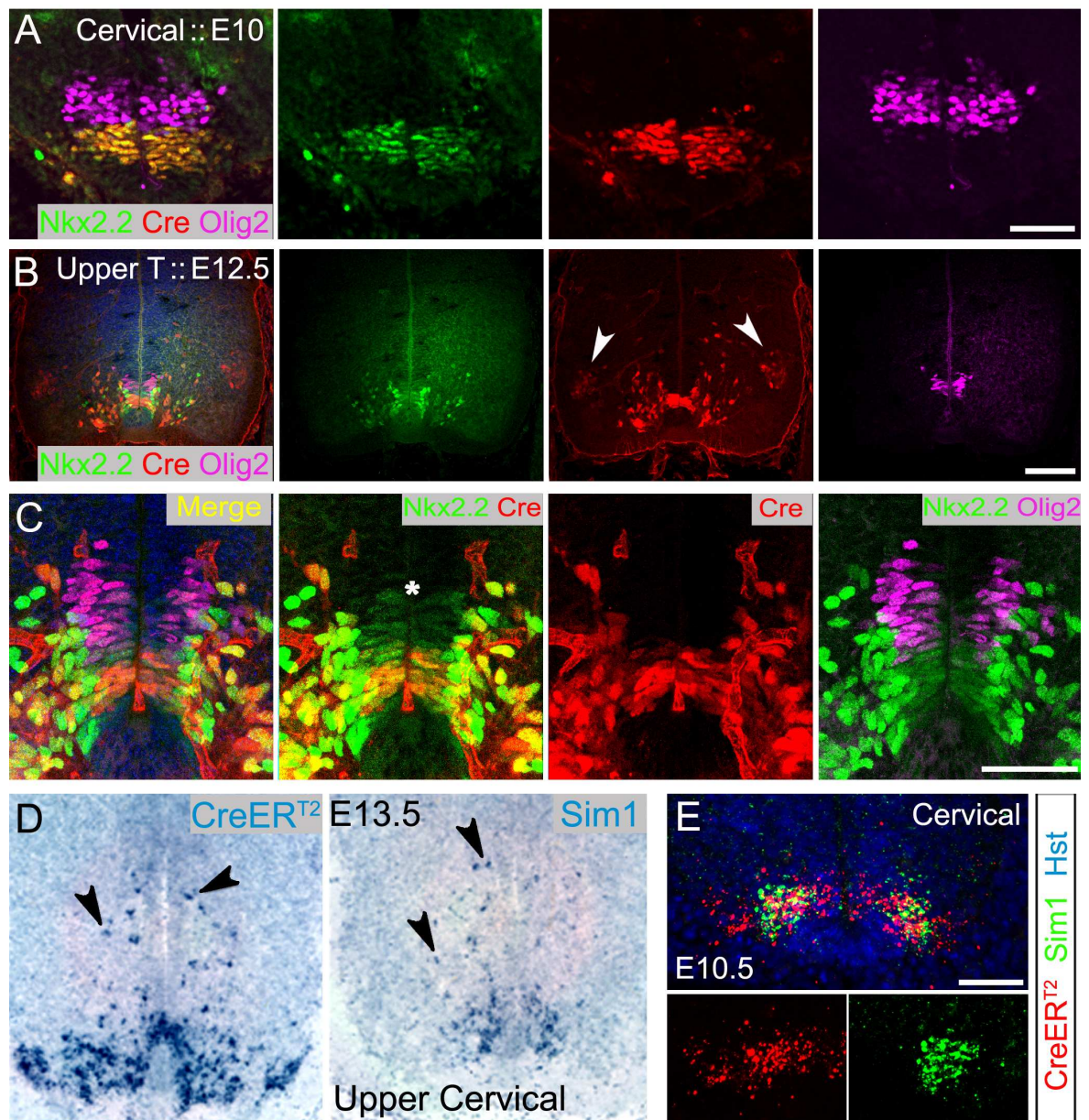
Figure 3.15 - Defining the limits and pattern of *CreER^{T2}* expression. (A-C) Expression of the endogenous *Nkx2.2*, *Olig2*, and the *CreER^{T2}* transgene revealed by immunohistochemistry. Transverse sections of the cervical spinal cord at E10 (A) and upper thoracic spinal cord at E12.5 (B, C). Cre transgene does not mimic *Nkx2.2* expression pattern regarding its overlap with *Olig2* at E12.5 (C; the dorsal limit of *Nkx2.2* expression domain is marked with an asterisk). (D-E) *CreER^{T2}* transcript expression in a pattern resembling that of migratory Sim1-positive cells (D) and V3 interneurons located in the ventral horn (E). *In situ* hybridization probes and antibodies used are as indicated. Tamoxifen was administered ~5hours before harvesting to assure translocation of CreER^{T2} protein into the nucleus without YFP reporter activation. See text for more details. Scale bars in A, C & E, 50μm and in B, 100μm.
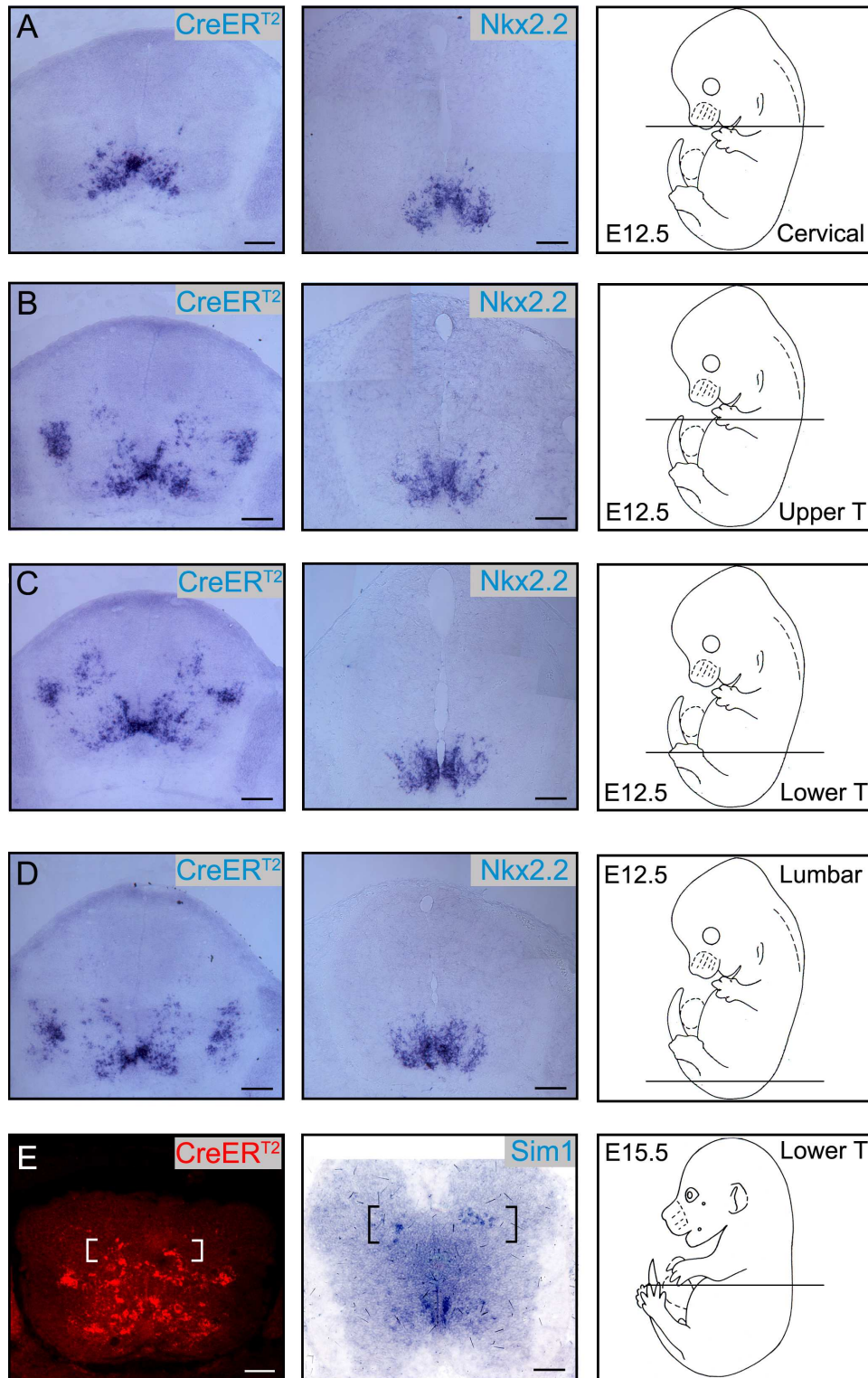
Figure 3.16 - **Characterisation of *CreER^{T2}* transcript expression at E12.5 and E15.5.** Differences between *CreER^{T2}* and *Nkx2.2* expression were assessed by *in situ* hybridisation at various levels of the spinal cord (A-D; see text for more details). A dorsal cell population is present at lower thoracic spinal cord but absent at other levels of the spinal cord. This same dorsal cell population seem settling at the equivalent position of dorsal Sim1-positive cells (brackets in E). Scale bars in A-D, 100μm.
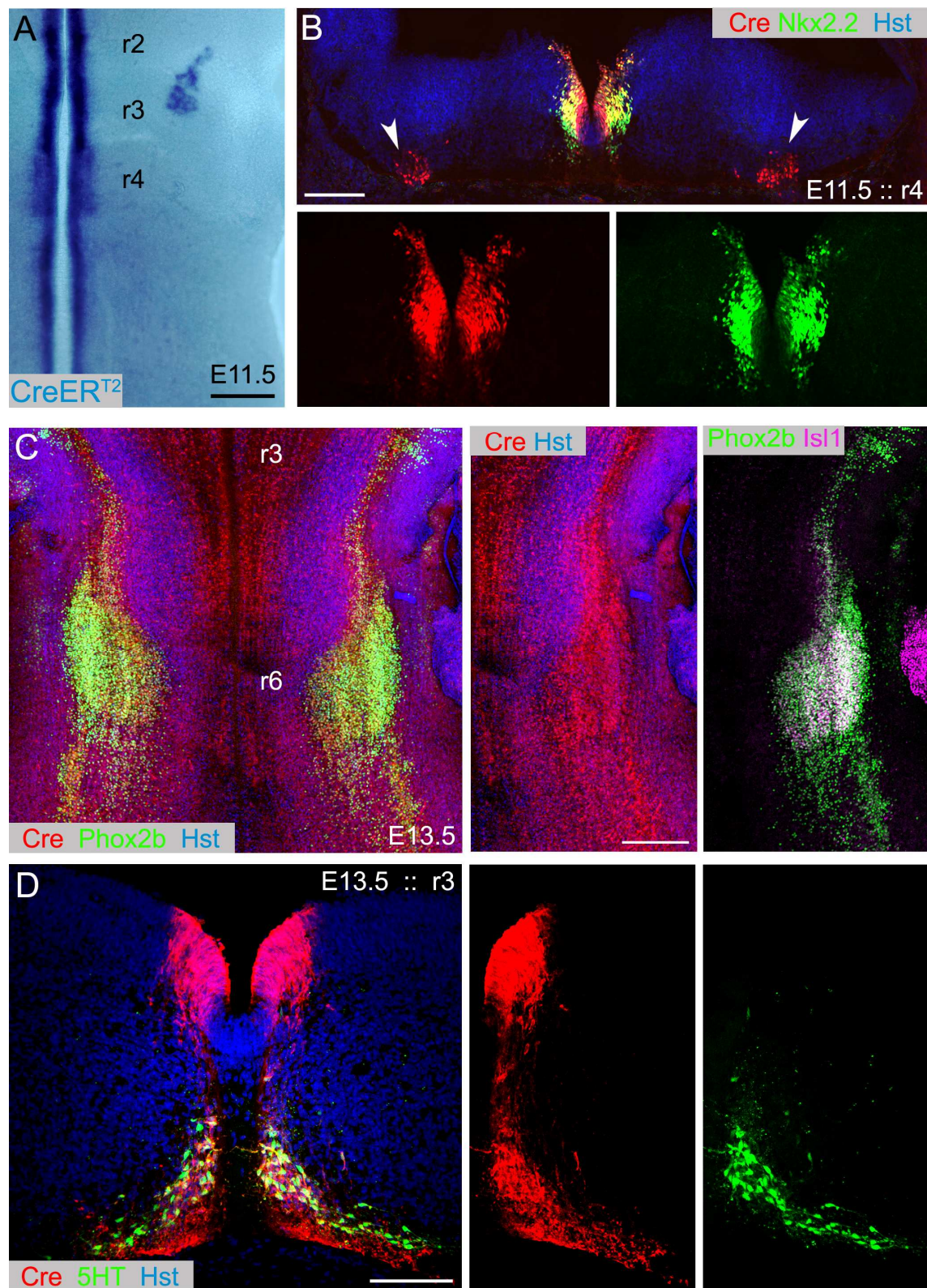
Figure 3.17 - *CreER^{T2}* expression in the hindbrain. *CreER^{T2}* expression was assessed in flat-mounted hindbrains at E11.5 by *in situ* hybridization (A) and at E13.5 by immunohistochemistry (C). Transverse sections of E11.5 (B) and of E13.5 hindbrains (D) were analysed for Cre protein expression at rhombomere (r) 4 and r3 (B and D, respectively). mRNA probes and antibodies used are as indicated. Sections were counterstained with Hoechst 33258 (Hst). Scale bars in A &C, 250μm and in B & D, 100μm.
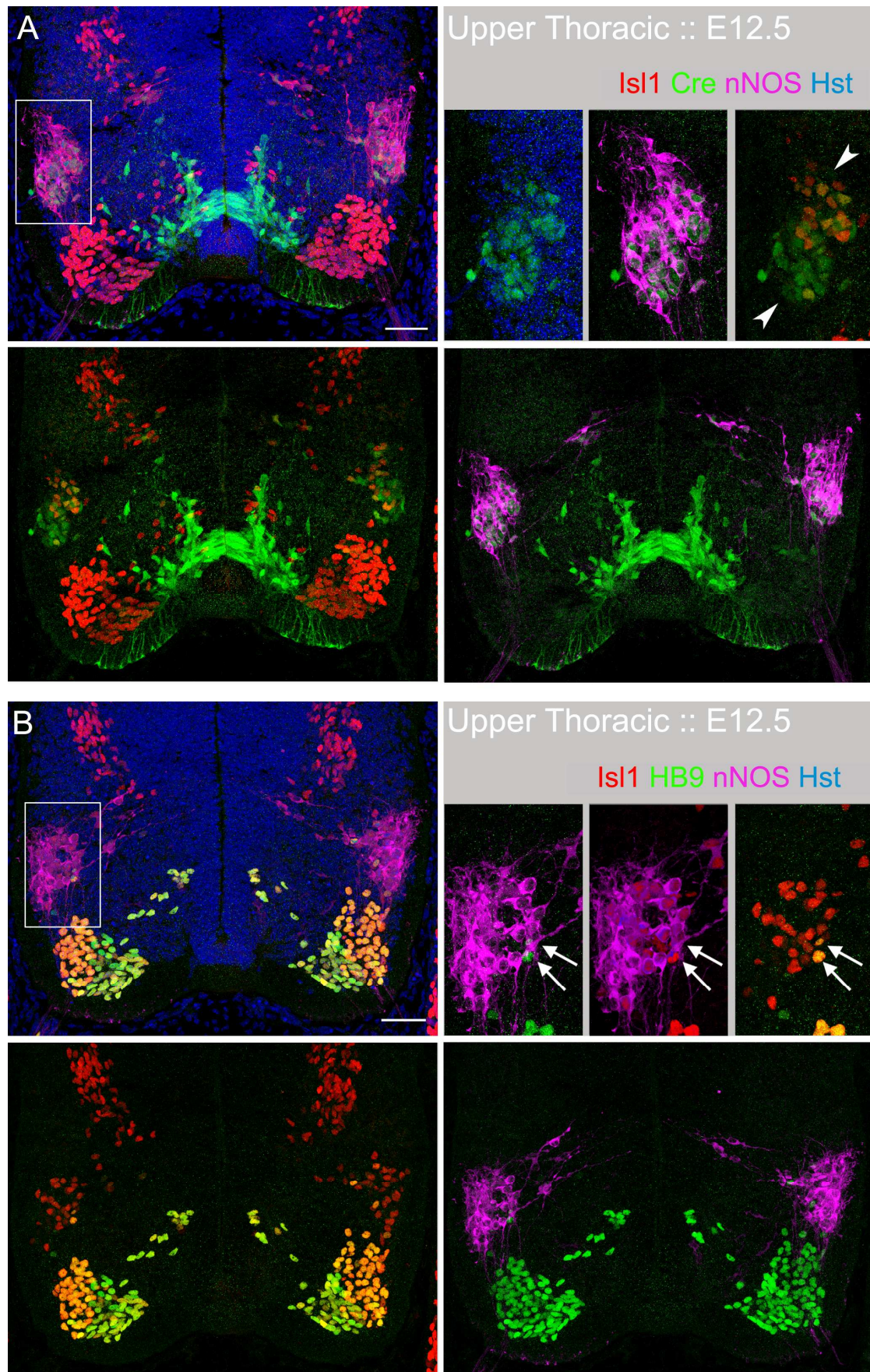
Figure 3.18 - Marking SPNs, but not sMNs, by Cre labelling. Consecutive and transverse sections of E12.5 spinal cord at upper thoracic level. Antibodies used are as indicated. See text for more details. Scale bars in A &B, 50μm.
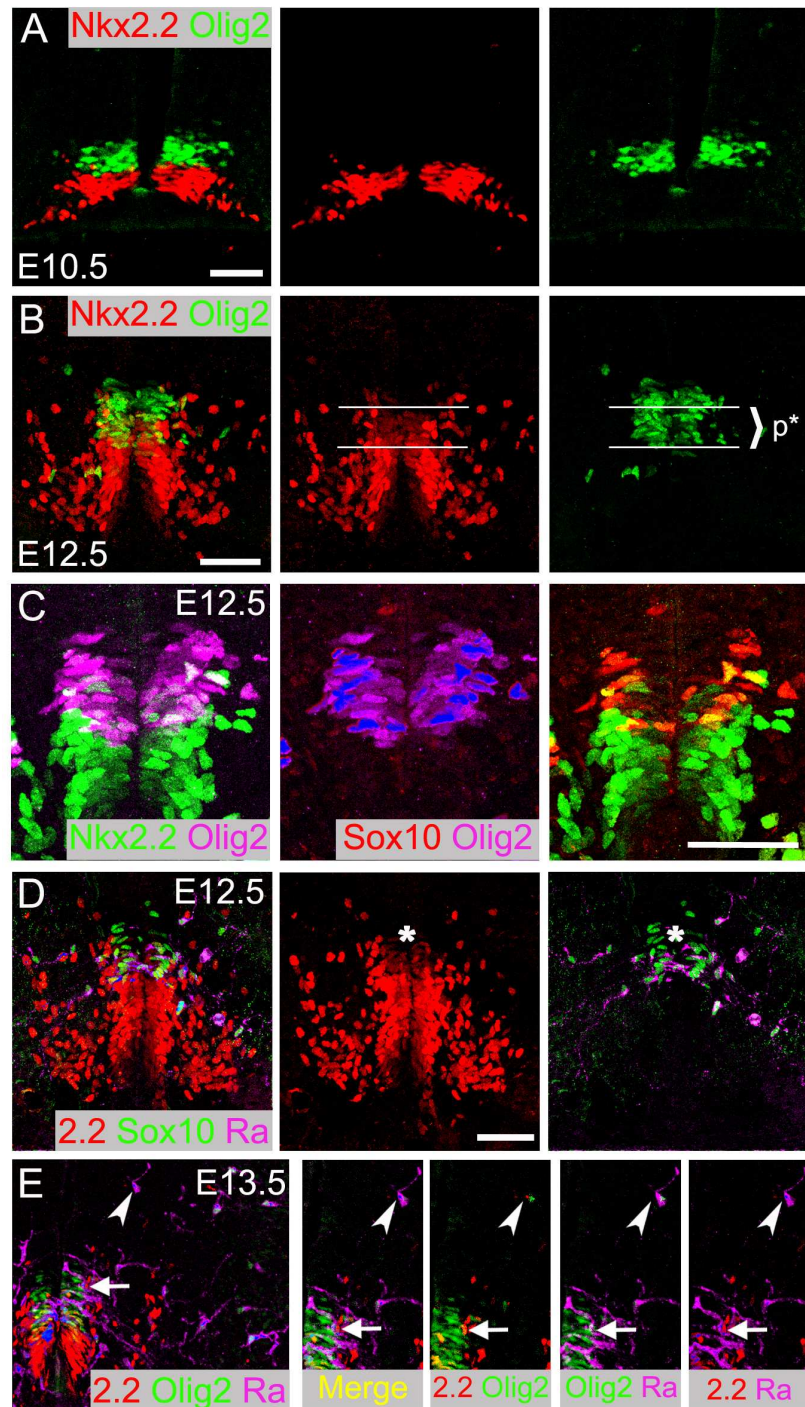
Figure 3.19 - Dynamic expression of Nkx2.2 and Olig2 in the ventral spinal cord. Nkx2.2 and Olig2 expression domains change from mutually exclusive (A) to overlapping domains (B-D). Specific OLP markers, Sox10 and PDGFRα, were detected within this overlapping domain at E12.5 (C and D). Translocation of Nkx2.2 from nucleus to the cytoplasm can be observed as OLPs detach from the VZ (arrow heads in D, and most notably in Nkx2.2/Olig2 close-up). Asterisk in D demarcates the dorsal limit of Nkx2.2 expression; albeit weaker in signal intensity, Nkx2.2 dorsal region of expression is up-regulated within the PDGFRα expression domain. See text for more details. Scale bars in A-D, 50μm.
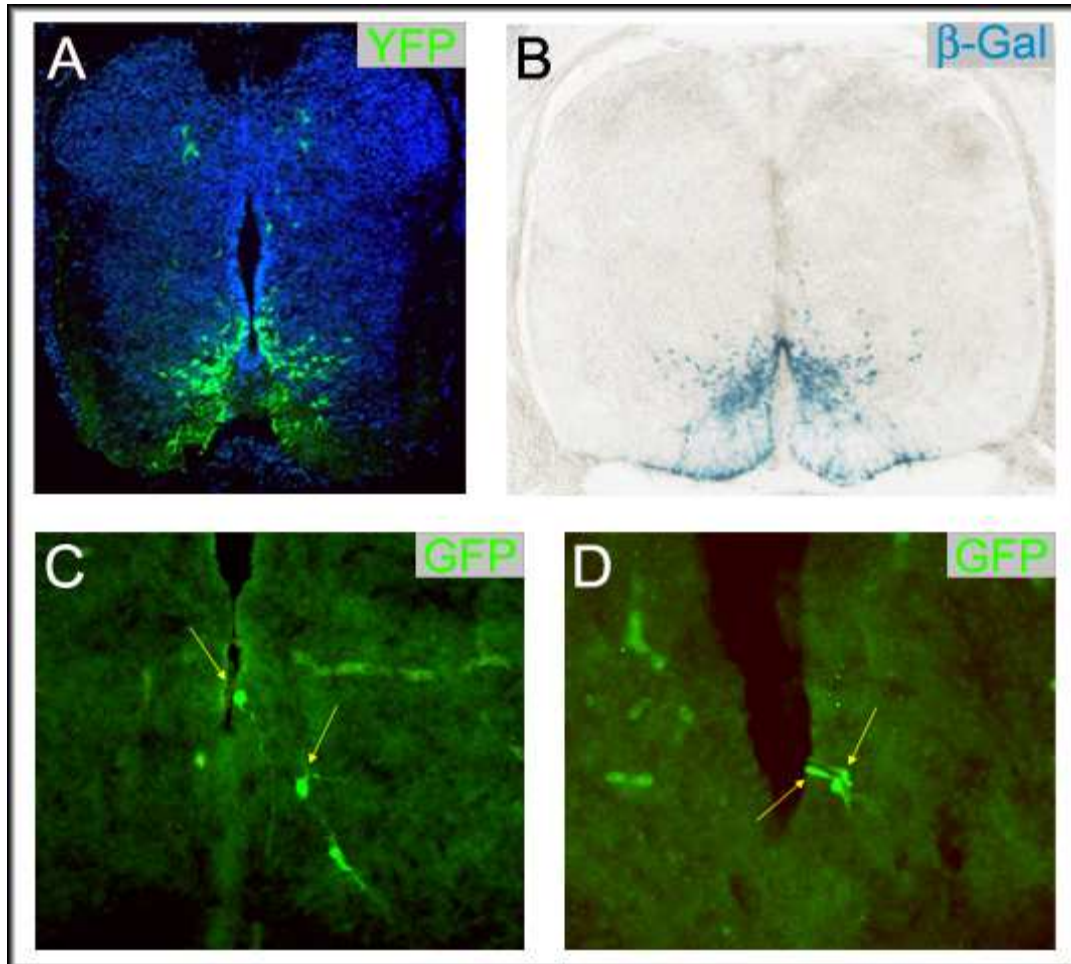
Figure 3.20 - Recombination efficiencies in various Cre-reporter lines. (A-B) Reporter gene activation in *Rosa26-YFP* (A) and *Rosa26-LacZ* (B) mice. Transverse sections of ventral spinal cord immunolabelled for YFP (A) or developed for β-galactosidase enzyme activity (B) at embryonic day 14.5 (E14.5), after administration of 200mg/Kg (A) or 280mg/Kg (B) of TM at E8.5. (C-D) Reporter gene activation in *Rosa26-GFP* mice. Immunofluorescence detection of GFP (arrows) in a few cells of the ventral spinal cord at E14.5 after administration of 200mg/Kg bw (C) or 400mg/Kg (D) of TM at E8 (transverse section).
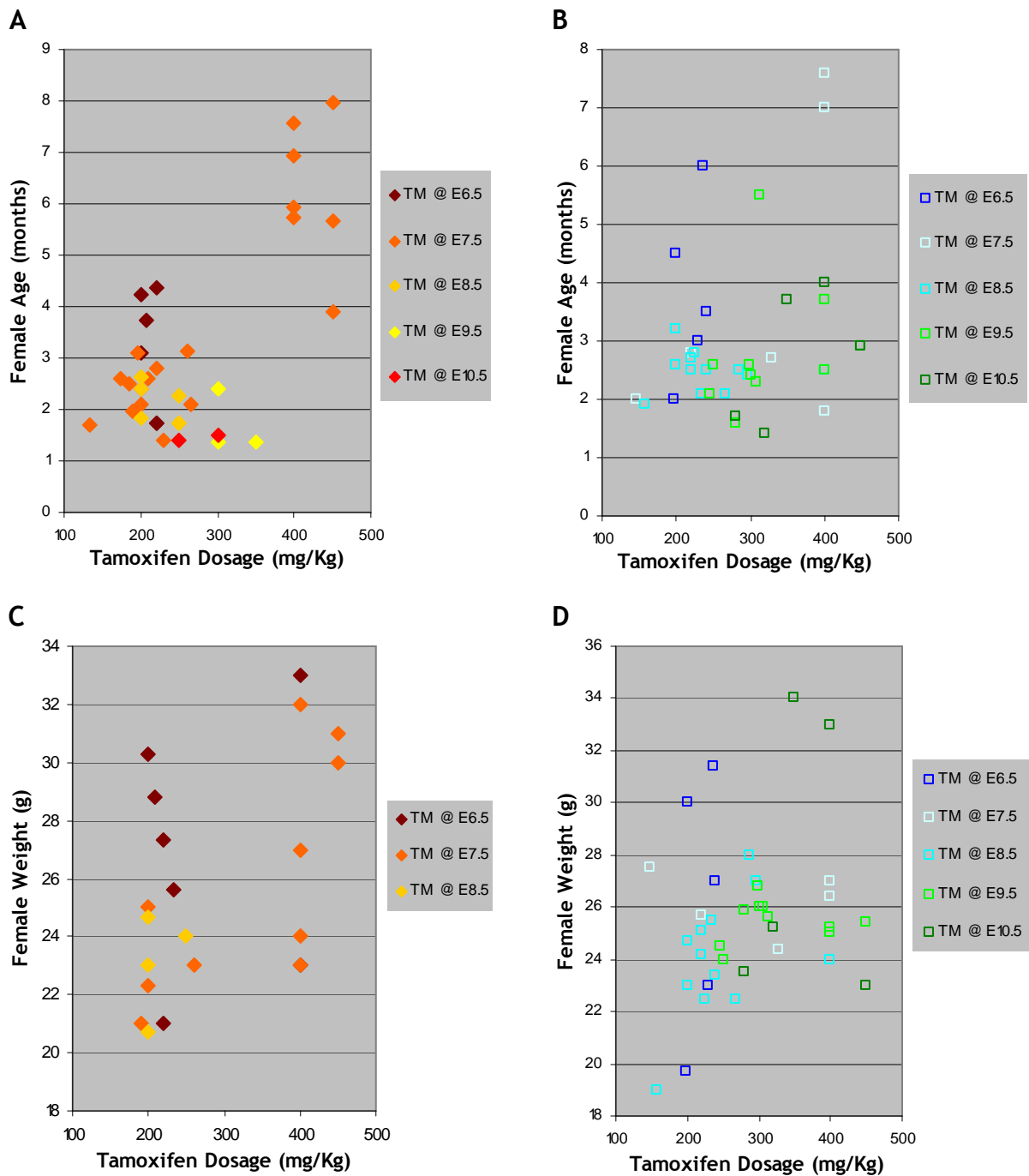
**Figure 3.21 - TM administration-induced spontaneous abortion while influenced by dosage and time of injection and female's age and weight.** Some critical TM dosages used in the experiments were plotted on a graph. Every dot represents a single TM administration to a pregnant female with the age/weight at the time of TM injection specified in the y-axis. Some females aborted beyond E13.5 after TM administration (A, C), while others were able to hold long term pregnancies (B, D; harvest after E13.5). TM is likely to have a more detrimental effect on early stages of development or/and possibly on younger and lighter females too. TM dosages were decided by taking the negative effects of TM on pregnancy in account, but aiming at reducing the length of time in each experiment. The fact that older females are less prone to breed was also taken into consideration.
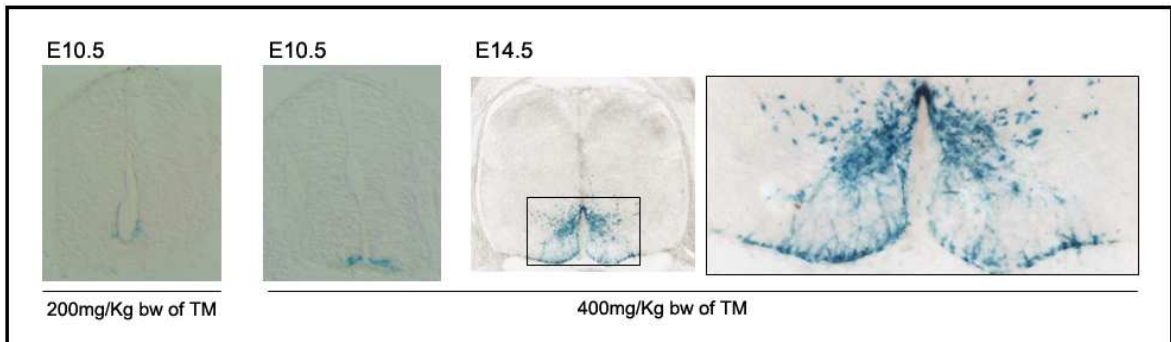
**Figure 3.22 - The level of recombination following TM administration is dose-dependent.** Transverse sections of ventral spinal cord stained histochemically for β-galactosidase enzyme activity with X-Gal at specific embryonic day (E) after administration of the indicated dose of TM at E8. At E10.5 there is barely detectable recombination with 200mg/Kg TM compared to 400mg/Kg bw (body weight, bw).

Chapter 4 - Fate mapping analysis

4.1. Glia contribution from the p3 domain

4.1.1. A proportion of radial glial cells derive from the p3 domain

To fate map p3 progenitors, *Nkx2.2-CreER^{T2}* and *Rosa26-YFP* mice were crossed.   I administered a single dose of tamoxifen at specific embryonic days and immunolabelled for YFP at progressively later times.   For example, when tamoxifen was delivered E7.5 and animals analysed at E11.5, this is referred to as E7.5 → E11.5.   Initial studies were concentrated on the lower cervical spinal cord (C5 – C8).   Radial glia were the first cell type to express YFP and their long slender processes were invariably located close to the ventral midline (Figure 4.1).   YFP-labelled cells were densely packed in the most ventral region of the spinal cord.   Figure 4.1 shows the presence of YFP in radial glial fibres in E7.3 → E11.5 mice.   These fibres can be seen to co-label with radial glial cell marker RC2 and to project radially to the pial surface, as described by Camillo Golgi in 1885 (for review see Bentivoglio et al. 1999).   Even at E14.5, YFP-labelled radial glial fibres were still visible (data not shown; instead see Figure 3.23).   In E7.3 → E11.5 cords a few cells had migrated out and lay just outside the VZ, remaining ventrally and close to their point of origin.   They could possibly be Sim1 - expressing V3 INs that are known to accumulate in the ventral horn (Briscoe et al. 1999); however, I could not ascertain it because neither neuronal marker NeuN is expressed at this age nor co-labelling of Sim1 with YFP is technically achievable for the time being.

4.1.2. Production of oligodendrocytes and astrocytes from the p3-domain

At lower cervical spinal cord, I observed that all p3-derived cells of E6.8 → P12.5 *Nkx2.2-CreER^{T2} : Rosa26-YFP* cords were invariably located close to the ventral midline in a "wedge" distribution which persisted until adult stages, suggesting that the majority of p3-derived cells migrate radially from the VZ (Figure 4.1 B-F and data not shown). To identify the various cell types produced from *Nkx2.2*-expressing progenitors, I have carried out double-immunolabelling for YFP together with different cell lineage markers. Neurons were identified with neuronal marker NeuN (Mullen et al. 1992), astrocytes by the expression of GFAP (Debus et al. 1983) or S100β (Matus et al. 1975), oligodendrocytes for the presence of CC1 (Bhat et al. 1996) and Sox10 (Kuhlbrodt et al. 1998) or Olig2 (Lu et al. 2000), the latter markers also expressed by OLPs. Many of the YFP-positive cells found within the wedge-shaped area flanking the ventral midline co-labelled for glial markers (Figure 4.1 B-F). The vast majority of all those cells were seen to colocalise with astrocytic markers GFAP and S100β. Colocalisation of YFP and GFAP was observed in the ventral funiculus and in the ventral commissural axon tracts and in cells with fibres radially orientated (Figure 4.1 C). Their position together with their morphology identifies them as GFAP-positive fibrous astrocytes. Moreover, the arrangement of the p3-derived fibrous astrocytes arrangement resembles that of radial glial processes present from earlier times, suggesting they might be produced via direct trans-differentiation of radial glia (Voigt 1989). Colocalisation of YFP and S100β were mainly seen in the ventral horn gray matter (Figure 4.1 D). These cells possess a unique morphology characterised by a relatively small S100β^+/YFP^+ cell body surrounded by a dense network of YFP-only positive processes, identifying them as protoplasmic actrocytes. p3-derived protoplasmic astrocytes in gray matter were invariably associated with NeuN positive neurons, of which some were also YFP-positive. The few NeuN-positive cells co-labelling for YFP were found to occupy laminae VII and VIII (Figure 4.1 B), which allows them to be identified as ventral V3 INs (Briscoe et al. 1999; Zhang et al. 2008). Finally, a small proportion of YFP^+ cells co-expressed the oligodendrocyte lineage marker Sox10, within which some were co-labelled for oligodendrocyte precursor (OLP) marker PDGFRα (data not shown; Pringle et al. 1992) and others co-expressed CC1, a marker of differentiated oligodendrocytes (Figure 4.1 F).

Most importantly, the domain of YFP activation is located ventrally but outside the pMN domain (see Figure 3.16 C), a domain demarcated by Olig2 expression and which is thought to be the primary source of oligodendrocytes in the spinal cord (Lu et al. 2002; Takebayashi et al. 2002; Zhou et al. 2002; Tripathi et al. 2011). The generation of oligodendrocytes from

Nkx2.2-positive progenitors has been reported in chick (Soula et al. 2001; Gotoh et al. 2011). Even if remote, there is the possibility that the YFP-labelled olidendrocytes in *Nkx2.2-CreER^{T2} : Rosa26-YFP* cords could come from progenitor cells that after being produced in the p3 domain migrate into the *Olig2*-expressing progenitor domain at a time when Nkx2.2 is known to expand into the pMN domain. To be sure that oligodendrocytes labelled in *Nkx2.2-CreER^{T2} : Rosa26-YFP* cords are p3-derived I analysed E6.8 → E12.5 cords for colocalisation of YFP with Olig2 within the VZ. Figure 4.2 shows that YFP-positive progenitors stay restricted to the p3 domain and they do not co-express Olig2. Since I showed that the expression of the transgene does not expand dorsally (into the p* domain) as the endogenous *Nkx2.2* expression does (see section 3.3.3 and Figure 3.16 C), I conclude that Nkx2.2 is up-regulated in cells of the pMN domain and progenitors from p3-domain do produce a few oligodendrocytes in mice.

To further confirm that the generation of oligodendrocytes originate from the p3 domain and to investigate their distribution at earlier and later developmental stages, the expression of YFP and oligodendroglial markers, Olig2 or Sox10, were examined in E10.5 → E12.5 (Figure 4.3), E10.5 → E14.5 (Figure 4.4), E10.5 → E16.5 (Figure 4.5), E10.5 → P1.5 (Figure 4.6), and E10.5 → P12.5 (Figure 4.7) *Nkx2.2-CreER^{T2} : Rosa26-YFP* spinal cords. The production of p3-derived oligodendrocytes seems to begin as early as E12.5 (Figure 4.3) increasing gradually in number (Figure 4.4 – 4.5). Postnatally, cells co-expressing YFP and Sox10 were concentrated mainly in the ventral funiculus (Figure 4.7). However, YFP-positive oligodendrocyte cells were also found scattered in other areas of the cord, such as the dorsal horn and funiculus (Figure 4.6 and 4.7), intermediate zone (Figure 4.7) and lateral funiculus (Figure 4.8). At least some of them had attained a more mature phenotype as demonstrated by their labelling with CC1 (Figure 4.6). Although a matter of speculation, it is worth observing that p3-derived oligodendrocytes tended to position themselves along the neuronal processes of p3-derived neurons (Figure 4.8).

Restricted astrocytic distribution of YFP-positive cells in the ventral cord was still observed in E15.5 → P1 *Nkx2.2-CreER^{T2} : Rosa26-YFP* cords (Figure 4.9 A). In E17.5 → P2 cords YFP^{+} astrocytes could still be seen in the ventral gray and white matter. Some other YFP^{+} cells were noted in the ependymal layer (see below). Taken together, these data indicate that generation of astrocytes and ependymal cells still takes place after E17.5 (Figure 4.9 B).

4.2. Remnants of embryonic p3 domain in the adult ependymal layer

Previous works suggest that the ependymal cells around the central canal of the postnatal/adult spinal cord are derived from ventral Nkx6.1-expressing neuroepithelial domain of the embryo. This is not only because ependymal cells express Nkx6.1 but also because fate mapping studies of progenitor domains more dorsal than the Nkx6.1-expressing domain show that they do not contribute to the ependymal layer (Fu et al. 2003; Fogarty et al. 2005; Fogarty 2006). Consistent with this, YFP$^+$ cells were found to be invariably located in the ventral half of the epithelial cell layer surrounding the postnatal central canal in postnatal *Nkx2.2-CreER^{T2} : Rosa26-YFP* spinal cords (Figure 4.10). These postnatal ependymal cells could be fate mapped as late as E17.5 (that is after tamoxifen administration at E17.5) (Figure 4.9). Making use of a knock-in mouse generated within the Richardson lab, which express Cre under the control of Olig2 promoter (D.H. Rowitch / N Kessaris, unpublished), I could show that ependymal cells are also derived from the pMN domain. These ependymal cells were also found in the central and ventral parts of the postnatal ependymal layer, implying that dorsal ependymal cells are derived from the p2 domain [since the Dbx1 domain (p1, p0, dp6 and dp5) does not contribute (Fogarty et al. 2005)] (Figure 4.10). The most ventral cells of the postnatal ependymal layer are not labelled in *Olig2-Cre : Rosa26-YFP* mice[§§], and they possibly come from floor plate progenitors (Figure 4.10).

4.3. Defining the neuronal lineages of the p3 domain

The unexpected possibility of perdurance of CreER^{T2} in neurons derived from p3 progenitors fits in with the co-labelling of Cre with 5HT and Phox2b observed in the hindbrain (Figure 3.18 and section 3.3.2). To test whether CreER^{T2} expression could be a result of ectopic activation in post-mitotic neuronal cells after they had left the VZ, I have analysed YFP expression in thoracic spinal cords in early-induced *Nkx2.2-CreER^{T2} : Rosa26-YFP* cords.

[§§] In *Olig2-Cre : Rosa26-YFP* mice, both p3 and pMN progenitor domains are fate mapped (Dessaud et al. 2007; also see section 4.3.5)

The defined time of onset of Nkx2.2 protein expression at around E8.5 (Jeong et al. 2005) permitted me to estimate that of CreER^{T2} protein, which can only take place at or after E8.5. The estimated serum lifetime of tamoxifen *in vivo* does not exceed 2 days (Robinson et al. 1991; Danielian et al. 1998; Buchanan et al. 2007). I therefore examined the p3 derived neuronal cells by administering tamoxifen before E6.5, early enough to avoid Cre-recombination in cells other than p3 progenitors in the VZ, and searched for the expression of YFP and neuronal markers (nNOS and NeuN) in E5.5/6.5 → E13.5 *Nkx2.2-CreER^{T2} : Rosa26-YFP* spinal cords (Figure 4.11). YFP-positive cells were observed to mimic the Cre expression pattern, although only a subset of p3 precursors was labelled because of inefficient recombination (Figure 4.11 A). Some of the YFP-positive processes could be seen crossing the ventral midline (Figure 4.11 A arrow). These processes belong to V3 INs that settle ventrally close to the floor plate (also labelled for YFP) and are known to be commissural neurons (Zhang et al. 2008). Other YFP-labelled cells were located laterally and medially in the intermediate cord and co-expressed nNOS (Figure 4.11 A) and NeuN (not shown). These cells could not be found in cervical spinal cord (not shown) and had spindle-shaped soma often nested in the intermediolateral nucleus (IML), providing evidence of their SPN identity (Cabot 1990; Joshi et al. 1995). SPNs can be retrogradly labelled with Di-I crystals applied to sympathetic chain ganglia. Figure 4.11 B shows retrograde labelling from nerve terminals in the sympathetic chain ganglia of P0.5 *Nkx2.2-CreER^{T2} : Rosa26-YFP* mice TM-induced at ~E10.5[***]. YFP- and Di-I positive cell can be seen in the IML nucleus and in other cells in the intermediate medial spinal cord (arrow heads in Figure 4.11 B), demonstrating that some YFP-positive cells are true SPNs.

In E6.8 → P12.5 *Nkx2.2-CreER^{T2} : Rosa26-YFP* spinal cords, at lower thoracic level (around T8), some YFP-positive cells were identified as being neurons through their expression of neuronal marker NeuN (Figure 4.12 arrows). The fact that these cells were located in the deep dorsal horn demonstrates that the dorsal CreER^{T2} expressing cells (Figure 3.17) do come from the p3 domain, then migrate to the dorsal horn and can persist postnatally. As I mentioned earlier, dorsal CreER^{T2} expressing cells probably correspond to a group of interneurons that settle dorsally and express Sim1 during their development (Figure 3.17). It is an interesting idea that these interneurons might participate in local spinal circuits with SPNs ("sympathetic interneurons").

[***] Repetitive administration of TM at later stages was carried out to allow long term pregnancy while providing a good level of recombination.

4.3.1. Tracing dorsal INs but not SPNs in Ngn3-Cre : Rosa26-YFP mice

Ngn3 transcripts were expressed in p3 from E10.5 to E12.5, and more weakly in p1 to dp5 (Figure 4.13 and 4.14). Ngn3 is known to label Sim1-expressing V3 INs (Briscoe et al. 1999), hence the appearance of YFP-positive cells in the ventro-medial cord in *Ngn3-Cre : Rosa26-YFP* cords. A small number of dorsal neurons was also YFP-labelled in *Ngn3-Cre : Rosa26-YFP* and they possibly are the same dorsally positioned group of YFP$^+$ cells in *Nkx2.2-CreER^{T2} : Rosa26-YFP* spinal cords described above (Figure 4.13). On the contrary, *Ngn3-Cre : Rosa26-YFP* mice did not reveal YFP-positive SPNs at any age, suggesting that SPNs are specified before the onset of *Ngn3* expression, that is before E10.5 (Figure 4.14). Here, it is worth mentioning, that the dorsal expression domain of *Ngn3* in the neuroepithelium is unlikely to be the source of the above-mentioned dorsally positioned neurons because the latter are not fate-mapped in *Dbx1-Cre : Rosa26-YFP* mice (Fogarty et al. 2005; data not shown).

4.3.2. Lack of dorsal p3-derived neurons in *Nkx2.2* null mice

If the dorsal CreER^{T2} expressing cells found at lower thoracic levels of the cord (T8 and more caudal) were indeed p3 derived cells and putatively Sim1-expressing neurons, one might expect they would not be present in *Nkx2.2* null mice. Confirming this expectation I found that the dorsal CreER^{T2} expressing cells as well as Sim1$^+$ V3 INs, known to derive from Nkx2.2-positive progenitors (Briscoe et al. 1999), were missing in *Nkx2.2* mutants (Figure 4.15). Incidentally, p3-progenitors (strong labelling in ventral midline) together with SPNs and some unidentified ventral CreER^{T2}-expressing cells were still present in mice lacking *Nkx2.2*. The existence of p3-progenitors suggests that other unidentified factors act to specify and maintain the p3 domain.

4.3.3. SPN production does not require Nkx2 activity

It is shown that Nkx2.2-expressing precursors generate Sim1-positive V3 interneurons in the spinal cord, and serotonergic interneurons and visceral motor neurons in the hindbrain (Ericson et al. 1997b; Briscoe et al. 1999). Nkx2.2 activity is required not only for the formation of Sim1-positive V3 interneurons in the spinal cord but also for the production of p3-derived serotonergic interneurons in the hindbrain (Briscoe et al. 1999). Meanwhile, Nkx2.2 null mice do not lack p3-derived visceral motor neurons (vMNs) of the hindbrain and it was suggested that this reflects a redundancy in activity of the closely related Nkx2.9

(Briscoe et al. 1999). Since Nkx2.9 is expressed both in the p3 domain of the spinal cord and in the hindbrain (Pabst et al. 1998), I tested the possibility that Nkx2.9 compensates for the loss of Nkx2.2 activity in Nkx2.2 null cords. However, I found that SPNs form in mice that lack either Nkx2.2 or Nkx2.9 or both, judging by the expression of nNOS at E13.5 (Figure 4.16).

4.3.4. SPN development depends on sonic hedgehog signalling in Nkx2.2-progenitors

SHH activity is necessary for normal formation of most ventral progenitor domains in neural tube. Alteration of SHH signalling through disruption of *Smo* (encoding the SHH signalling receptor Smoothened) results in changes to the properties and/or fates of the ventral progenitors. In an attempt to specifically impair specification of Nkx2.2-expressing progenitors, *Nkx2.2-CreER^{T2}* mice were crossed with *Smo^{flox/flox}* mice to ablate SHH signalling within p3 domain. E6.5/7.5 → E13.5 *Nkx2.2-CreER^{T2}* : *Smo^{flox/flox}* cords were then examined for the expression of nNOS and HB9, which mark SPNs and sMNs, respectively. I found that the number of PGNs decreased by 52% +/- 6% (mean +/- s.e.; n=3), without significant variation in the number of sMNs (Figure 4.17), reinforcing the idea that SPNs and sMNs have separate developmental origins.

In *Shh* null mice, the most ventral progenitor domains (p3, pMN and p2) are lost and instead the ventral-most region adjacent to the floor plate acquires p1-domain characteristics and up-regulates *Dbx1* (which is normally expressed in progenitor domains occupying either sides of the dorsoventral midline; Pierani et al. 1999). To confirm whether the observed reduction in SPN numbers corresponded to a loss of Shh activity in the p3 domain, I analysed E6.5/7.5 → E11 *Nkx2.2-CreER^{T2}* : *Smo^{flox/flox}* cords for the expression of *Dbx1*. I identified a few cells expressing *Dbx1* ectopically in the most ventral region of the spinal cord where p3-domain was supposed to form, implying that Shh was missing in those Dbx1-labelled progenitor cells (Figure 4.18).

4.3.5. Olig2 loss of function impairs generation of both SPNs and sMNs

Current understanding of the developmental origin of SPNs is that they are formed from the same pool of Olig2-expressing progenitors as somatic motor neurons (Lu et al. 2002;

Takebayashi et al. 2002; Zhou et al. 2002). To confirm that SPN generation requires Olig2, I analysed Olig2 mutant cords for the presence of SPNs and found that both SPNs and sMNs were missing (Figure 4.19), as previously described (Lu et al. 2002; Takebayashi et al. 2002; Zhou et al. 2002). Figure 4.19 also shows some nNOS-positive cells scattered throughout the ventral cord of Olig2 null mice that were missing in control littermates. Although they express nNOS, these cells are unlikely to be misplaced SPNs since Isl1- as well as Hb9-positive cells are not present in Olig2 null cords (Zhou et al. 2002; Lu et al. 2002)[†††]. Nonetheless, expression of nNOS is not retricted to autonomic motor neurons because ventral neurons in laminae VII, VIII, IX have also been shown to express nNOS (Reuss et al. 2001). On a more speculative note, those nNOS-positive cells scattered in the ventral cord of Olig2 null mice could arise from progenitor domains affected by the loss of the Olig2-expressing pMN domain. In Olig1/2 null mice, for example, pMN domain is converted into a "p2-like" domain with concomitant increase in Chx10-expressing V2 INs (Lu et al. 2002; Zhou et al. 2002), while other nearby domains, such p1 and p3 domains, are unaffected.

Therefore, paradoxically, SPNs seem to derive from Nkx2.2-expressing progenitors yet also require OLIG2 for their development. A possible explanation for this lies in the fact that Nkx2.2-positive cells are known to express Olig2 at very early developmental stages (Jeong et al. 2005; Dessaud et al. 2007), so it is possible that SPNs derive from progenitors that transiently express both Nkx2.2 and Olig2. Another possible explanation might be that the requirement for Olig2 in SPN generation is not cell-autonomous – i.e. some interaction between the Olig2-expressing cells and Nkx2.2-expressing progenitors might be required for SPN production.

To determine wether SPNs descend from Olig2-expressing progenitors, *Olig2-Cre : Rosa26-YFP* spinal cords were examined for the expression of YFP and SPN markers, such nNOS. YFP-labelled cells (presumed SPNs) were then seen in the IML, co-expressing nNOS, and in the ventral horn where sMNs are known to settle (Figure 4.20), confirming that SPNs as well as sMNs derive from Olig2-expressing progenitors. Therefore, my results suggest segregated origins for autonomic versus somatic motor neurons, in that SPNs are generated by progenitors with a history of both Nkx2.2 and Olig2 expression, whereas sMNs originate from progenitors that only express Olig2. In the hindbrain, where sMNs and vMNs are known to be derived from separate progenitors domains (pMN and p3 respectively) (Osumi et al. 1997;

[†††] Isl1 and Hb9 have been reported to be crucial genes to the development of SPNs (Pfaff et al. 1996; Arber et al. 1999).

Ericson et al. 1997b), it also seems that p3 progenitors express Olig2 transiently during early development because I was able to observe YFP-positive p3-derived neurons (Phox2b and 5HT-expressing neurons) in *Olig2-Cre : Rosa26-YFP* mice (Figure 4.20).

4.4. Discussion

4.4.1. Summary of the results

Using *Cre-loxP* technology I have fate-mapped the *Nkx2.2*-expressing p3 domain of the embryonic neural tube and shown that it generates neurons, oligodendrocytes, astrocytes and ependymal cells. A population of radial glial cells are also p3-derived and are presumably the first to be generated, followed by neurons and glia. Different populations of p3-derived neurons were identified in the spinal cord: 1) *Sim1*-expressing V3 INs, 2) an unidentified dorsally-located *Sim1*-positive neuronal population, and 3) the pre-ganglionic motor neurons of the sympathetic nervous system (SPNs). The majority of p3-derived glia were invariably found within a wedge-shaped area close to their site of origin, although a few oligodendrocytes were seen scattered throughout the spinal cord. p3-derived astrocytes included two subtypes - fibrous and protoplasmic astrocytes. p3-derived fibrous astrocytes were GFAP-positive and settled in the ventral funiculus whereas most protoplasmic astrocytes expressed S100β and very little or no GFAP, and occupied the ventral gray matter. These cells have small cell bodies surrounded by a dense mass of fine branching processes. Finally, ependymal cells originating in the p3 domain were occasionally detected and found embedded in the neuroepithelial cell layer that surrounds the postnatal central canal.

4.4.2. Segregated origins for somatic and autonomic motor neurons

The inducible Cre recombinase is a valuable tool for fate-mapping experiments inasmuch as it enables us to label progenitor cells and all its progeny in a spatio-temporally controlled manner. However, the technique involves the use of tamoxifen (TM) for activating Cre-recombinase which raises some problems. It has been reported that the serum lifetime of TM is approximately 24hours (Danielian et al. 1998); however, higher doses can last longer in mother's serum (Robinson et al. 1991). To test whether recombination of the *Rosa26-YFP* reporter in SPNs could be a result of ectopic activation of *CreER^{T2}* in SPNs or in their

migratory restricted-precursors, I administered TM early enough to not get labelled those migratory restricted-precursors (*CreER*[T2]–positive cells). For that I assumed that TM would not last more than 2 days, based on the available published data. In this context, it would be important to ascertain that the administered TM dose in those early fate-mapping experiments does not indeed exceed 2 days in mother's serum.

Additional supporting evidence for a p3-derived origin of SPNs relies on partial ablation of SHH signalling in p3 progenitors, through conditional deletion of the Smo receptor in *Nkx2.2-CreER*[T2] *: Smo*[flox/flox] mice. Depletion of SPNs without altering sMNs numbers and/or distribution. The specific deletion of *Smo* in p3 progenitors was then confirmed by the ventral ectopic activation of *Dbx1*, which is known to be up-regulated in the absence of SHH signalling at more dorsal regions of the spinal cord (Pierani et al. 1999). Despite the very small number of *Dbx1*-positive cells observed within the p3 domain, the number of nNOS-positive SPNs was significantly decreased by ~50%. This discrepancy could be explained by the lapse of time needed to activate the targeted disruption of SHH signalling in p3 progenitors. DBX1 is known to be expressed only in the neuroepithelium and downregulated immediately after cells migrate away from the VZ (Pierani et al. 2001). If total disruption of SHH signalling occurs in the neuroepithilum, then that results in up-regulation of *Dbx1* expression in p3-progenitors. But, the same does not accur if complete ablation of Shh signalling happens in cells already migrated away from the VZ, which are no longer competent to express *Dbx1*. Another potential pitfall could derive from the perdurance of *Smo* expression in migratory cells leaving the VZ. This is not expected however to happen having in mind similar studies in forebrain. It has been reported that SHH signalling does not have any effect on migration/maturation of interneuron populations of the brain but only during their specification in timed-deletion of *Smo* experiments (Fuccillo et al. 2004; Xu et al. 2010). A similar experimental stategy could be used to assess that deletion of *Smo* is restricted to p3-progenitors – which would include administer TM at later times of development (for example E8.5/9.5) and analyse for the presence of SPNs (expected to appear in normal numbers and distribution) at E13.5.

Despite deriving from Nkx2.2-expressing precursors, production of SPNs appears not to require NKX2.2 function since they are present in *Nkx2.2* null cords. They seem not to require NKX2.9 for their development either, as suggested previously for visceral MN development of the hindbrain (Briscoe et al. 1999), and they develop apparently normally even in the absence of both NKX2.2 and NKX2.9 (Figure 4.16). Presumably other factors are needed for SPN specification from p3-progenitors. For example, it is reported that in the hindbrain PHOX2b plays a key role in vMN differentiation (Pattyn et al. 2000). It is worth mentioning that a p3 Pax6-independent domain still persists in the absence of *Nkx2.2* and/or *Nkx2.9,* hence the lack of expansion of Pax6 expression domain in those mutants

(Genethliou et al. 2009; Holz et al. 2010). Since somatic MNs are known to derive from the *Pax6/Olig2*-expressing domain it implies that the presence of SPNs could be correlated with the lack of expression of *Pax6* in the p3 domain.

I also found that SPNs come from progenitors with a history of both *Nkx2.2* and *Olig2* because I was able to label them in *Nkx2.2-Cre-ER^{T2} : Rosa26-YFP* and *Olig2-Cre : Rosa26-YFP* cords. Since sMNs are known to derive from *Olig2*-expressing progenitors, that implies that separate pools of progenitors produce SPNs and sMNs. The expression of Olig2 in p3 progenitors is in agreement with previous studies demonstrating that OLIG2 is expressed in the most ventral regions of the neural tube at very early stages of development, overlapping with the Nkx2.2 expression domain between ~E8.5 and ~E9.5, before retreating from the most ventral region to form the pMN domain (Takebayashi et al. 2000; Jeong et al. 2005; Dessaud et al. 2007). Taken together, my results support separate origins for somatic and visceral motor neurons – the latter deriving from progenitors in the region of overlap between Nkx2.2 and Olig2 existing prior to ~E9.5, and the former from progenitors that never express *Nkx2.2*. My results also imply that a first level of subtype specification in MN development already occurs in the neuroepithelium, leaving room for further diversification of MNs as cells migrate away from VZ.

4.4.3. Glial cells generated within p3-domain

In mice, p3-derived progenitors give rise to oligodendrocytes, as in chick (Gotoh et al. 2011), as well as two types of astrocytes – fibrous astrocytes in white matter, as previously reported (Hochstim et al. 2008) and protoplasmic astrocytes in gray matter. p3-derived astrocytes migrate in a strictly radial fashion and settle only in the ventral spinal cord. p3-derived oligodendrocytes represent a very small fraction of the total spinal cord oligodendrocyte population (estimated to be ~3%) and they remain largely confined to the ventral funiculus; however, a sparse population of p3-derived oligodendrocytes can be observed postnatally. Both astrocytes and most of the oligodendrocytes settle close to their site of origin, the region to which their radial glia precursors originally project to, suggesting they are produced by transformation of radial glia as reported for Dbx1- and Msx3-derived glia (Fogarty et al. 2005; Fogarty 2006). Taken together the data obtained from *Dbx1-*, *Msx3-* and *Nkx2.2-* Cre lines, one can anticipate the following common features for the production of astrocytes: 1) both fibrous and protoplasmic astrocytes derive from common precursors (specially demonstrated with *Nkx2.2-CreER^{T2}* line; this Thesis) 2) they are all very much restricted in their migratory properties, settling close to or radially opposed to their respective progenitor domain and 3) there are multiple origins for

astrocytes along the neuroepithelium. A more exhaustive fate-mapping study throughout the various neuroepithelial domains of the spinal cord has been addressed elsewhere (Tsai et al. in preparation). The fact that astrocytes can arise from different progenitor domains opens the possibility of functionally distinct astrocytes being derived from different progenitor domains, as it is observed in interneuron development (Lewis 2006; Goulding 2009), but further studies will be needed to answer that and other questions.

Oligodendrocytes also can come from different regions of the neuroepithelium with different progenitor domains contributing in varying degree to the total number of spinal cord oligodendrocytes. The majority of oligodendrocytes (~80%) in the spinal cord come from the pMN domain (Richardson et al. 2006; Tripathi et al. 2011), whereas *Dbx1-* or p3-derived oligodendrocytes account for a comparatively small contribution (Fogarty et al. 2005; Tripathi et al. 2011; this Thesis). Although generated from various progenitor domains, oligodendrocytes derived from different sources have similar electrical properties (Tripathi et al. 2011), suggesting that they could substitute for each other if required. Fittingly, OLPs derived from different regions of the forebrain were shown to be functionally redundant, for example ventrally-derived OLPs were able to compensate for the loss of dorsally-derived OLPs (Kessaris et al. 2006). A similar situation has been recently described in the dorsal funiculus of the spinal cord where the original ventrally-derived oligodendrocytes are replaced by dorsally derived oligodendrocytes later in development (Tripathi et al. 2011). Some differences among species have been noted as well. Whereas in chick the majority of oligodendrocytes come predominantly or exclusively from the overlapping region of NKX2.2 and OLIG2 (Soula et al. 2001; Richardson et al. 2006), in rodents they arise from all parts of the Olig2-expressing pMN-progenitor domain. However, the primary source of oligodendrocytes in the rodent spinal cord might actually be the Olig2-, Nkx2.2-expressing p*-domain since substantial overlap with Sox10/ PDGFRa-expressing region is observed at E12.5 (Figure 3.20). Unfortunately, this cannot be teased out using my *Nkx2.2-CreER*^{T2} line since the transgene is not expressed in the p* domain as the endogenous gene is (Figure 3.16).
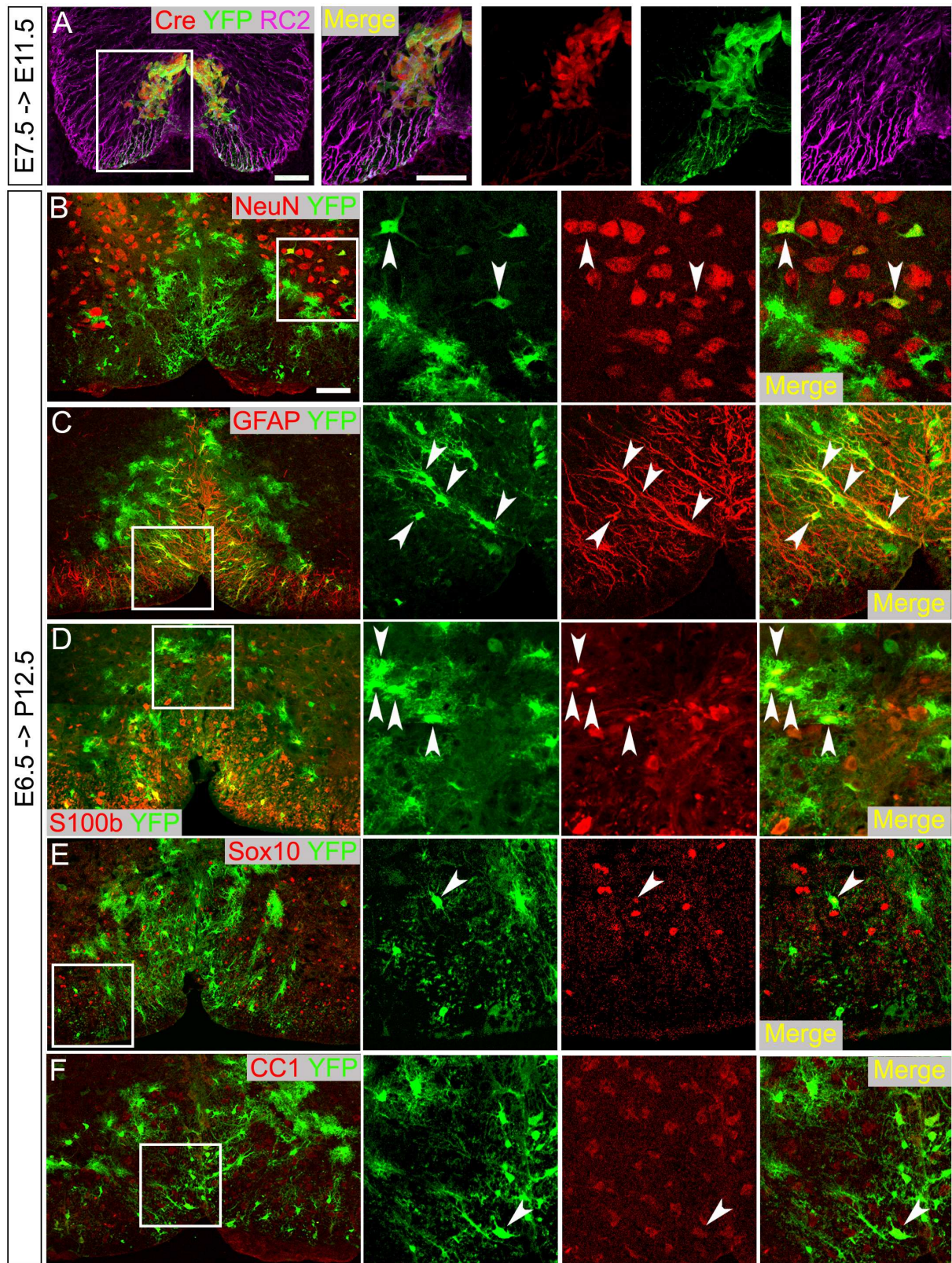
Figure 4.1 - p3 generates radial glial cells, neurons and glia. (A) A sub-population of radial glial cells (RC2-expressing cells) co-labels with YFP identifying them as p3-derived. Their processes project to the pial surface close to ventral midline. (B-F) Sub-populations of neurons (Neu[+]), astrocytes (GFAP[+] or S100b[+]) and oligodendrocytes (Sox10^{+} or CC1^{+}) are also YFP-labelled, hence p3-derived. See text for more details. Scale bars in A, 50μm and in B, 100μm.
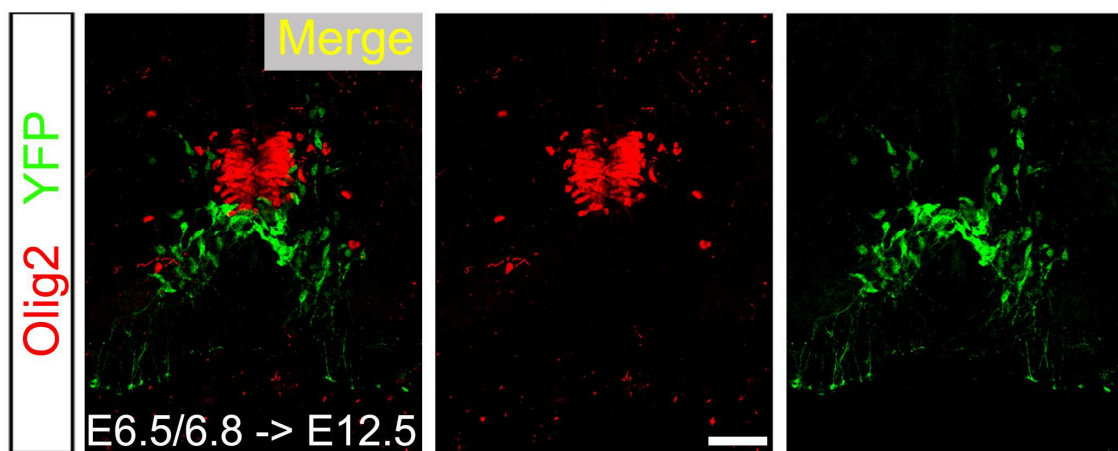
Figure 4.2 - *Nkx2.2*-expressing p3-derived cells do not migrate to the pMN domain during expansion of *Nkx2.2* into the *Olig2* domain. Transversal sections of *Nkx2.2-CreERT2 : Rosa26-YFP* cord immunolabelled for YFP and Olig2. No YFP-positive cells can be seen labelling with Olig2, which implies that YFP-positive cells do come from *Nkx2.2*-expressing p3 progenitors. Mother was induced at E6.5 and E6.8 and analysed at E12.5. Scale bar is 50μm.
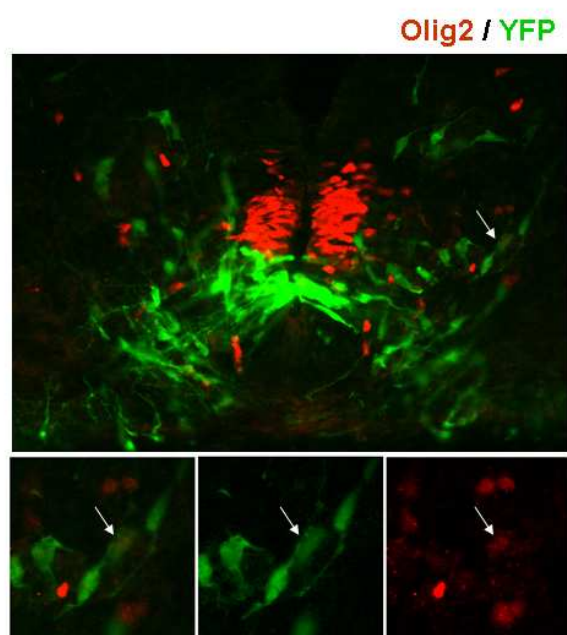
Figure 4.3 - Rare appearance of p3-derived OLPs at E12.5. Double labelling of YFP and Olig2 on transverse section at cervical levels of E12.5 spinal cord shows colocalisation in migratory oligodendrocyte precursors (arrow), albeit rare to find.
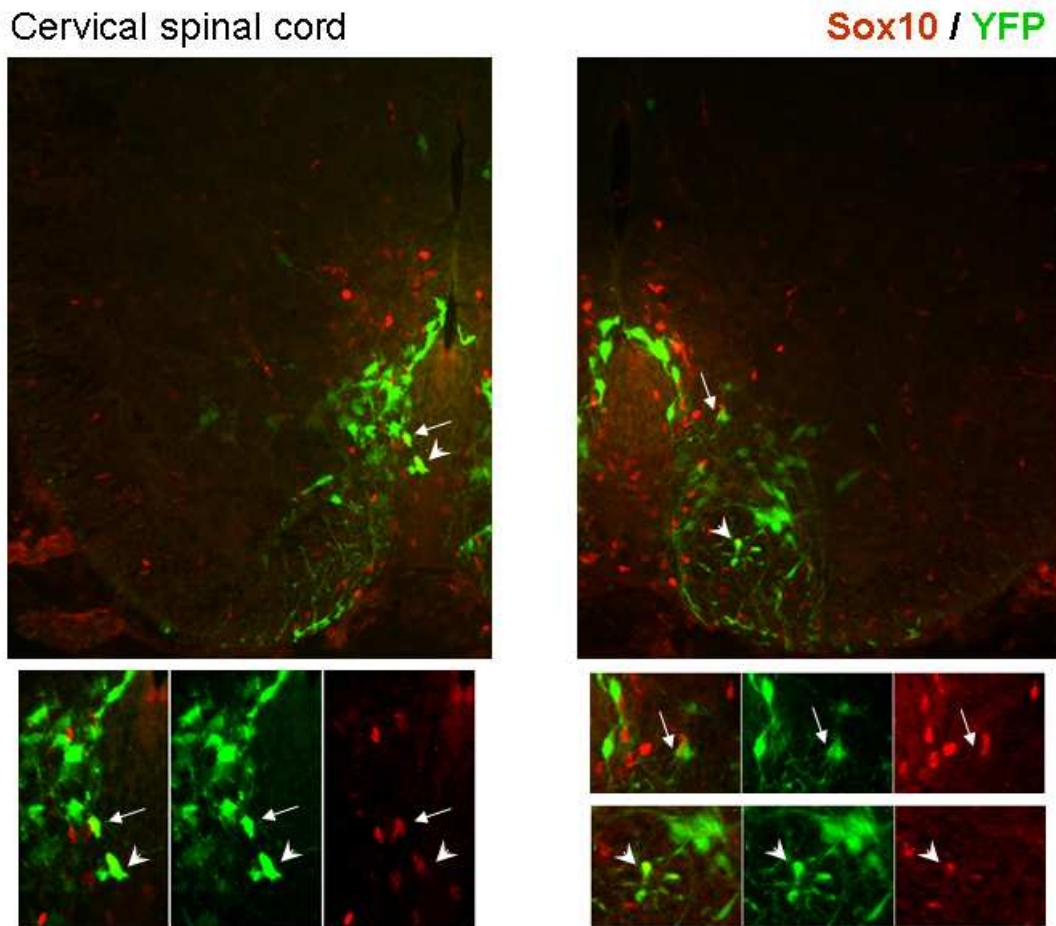
Figure 4.4 - A few more OLPs derive from p3 progenitors at E14.5. Transversal sections of cervical spinal cord of E10.5 → E14.5 *Nkx2.2-CreER^{T2} : Rosa26-YFP* mice immunolabelled for Sox10 and YFP.
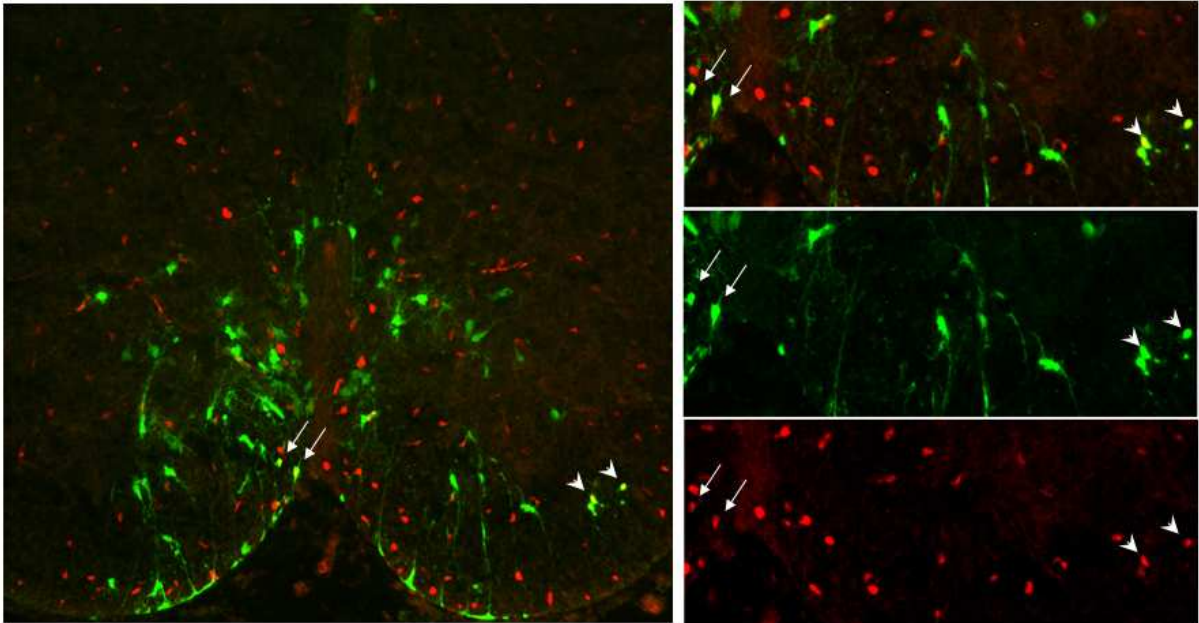
Figure 4.5 - p3-derived oligodendrocytes appear more often at later stages of embryogenesis. Double labelling of YFP and Sox10 (for example, see arrows and arrow heads) on transverse section at cervical levels of E16.5 spinal cord shows colocalisation in p3-derived oligodendrocyte located in the ventral funiculus possibly generated by trans-differentiation of radial glia. (see text for more details).
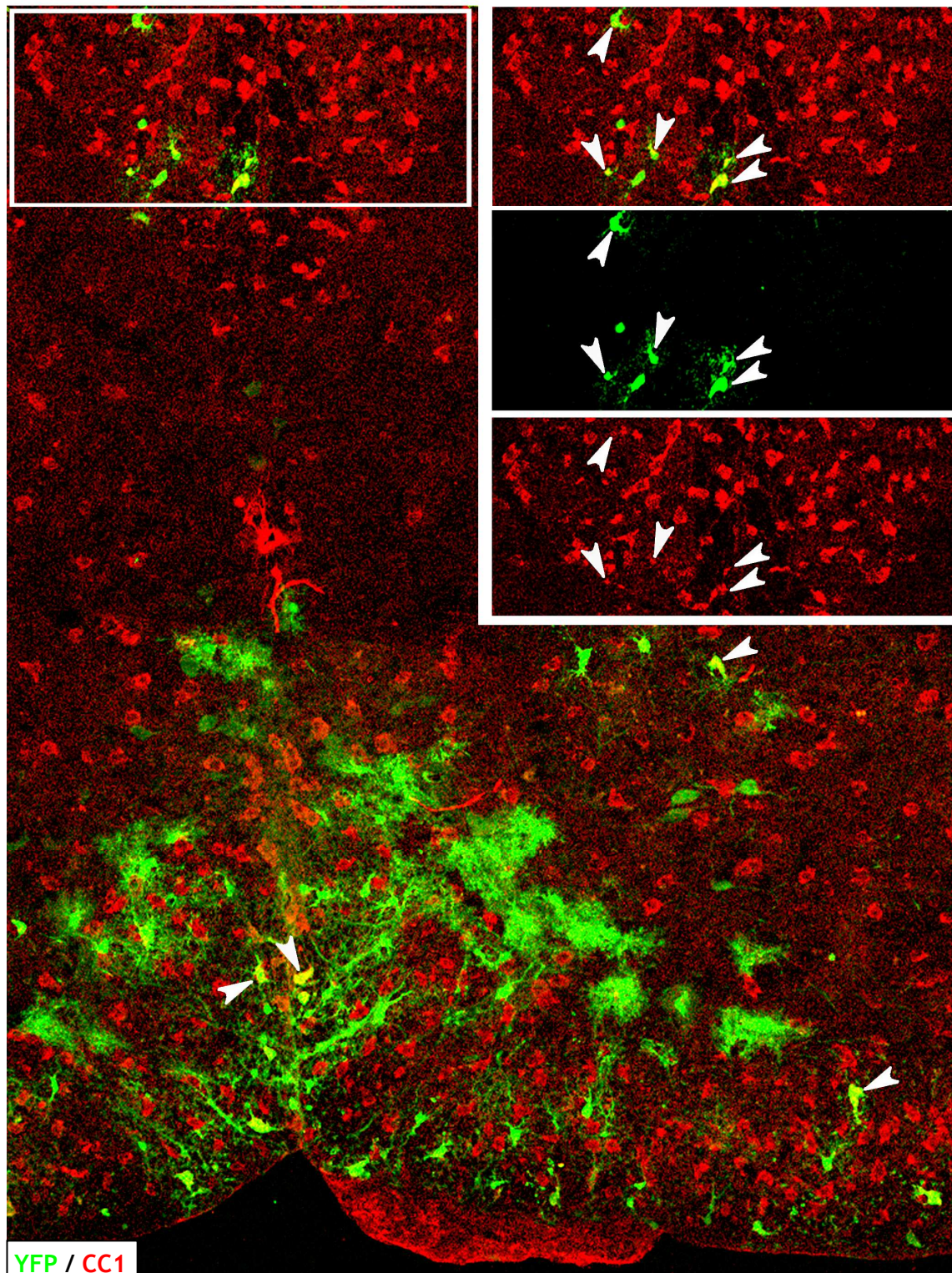
**Figure 4.6 - p3-derived OLPs can differentiate into mature oligodendrocytes.** Transversal section of E6.5 → P1.5 *Nkx2.2-CreER^{T2} : Rosa26-YFP* cervical spinal cord immunolabelled for YFP (green) and CC1 (red), a monoclonal antibody that recognises adenomatosis polyposis coli (APC) which is up-regulated in myelinating oligodendrocytes. Arrows show co-labelling of YFP (green) with CC1 (red).
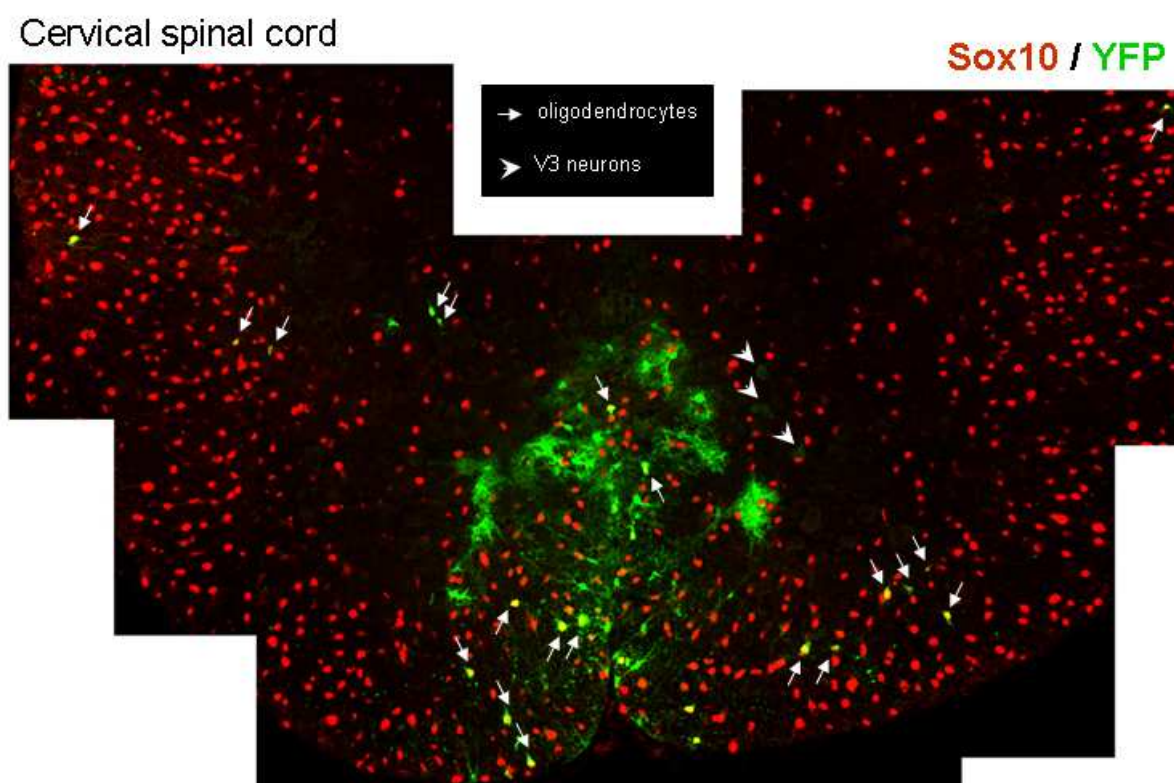
Figure 4.7 - Wide distribution (but low number) of p3-derived oligodendrocytes throughout the spinal cord. Transversal sections of cervical spinal cord of E10.5 → P12.5 *Nkx2.2-CreER^{T2} : Rosa26-YFP* mice immunolabelled for Sox10 and YFP.

Upper Thoracic Spinal Cord :: E14.5 → P13.5
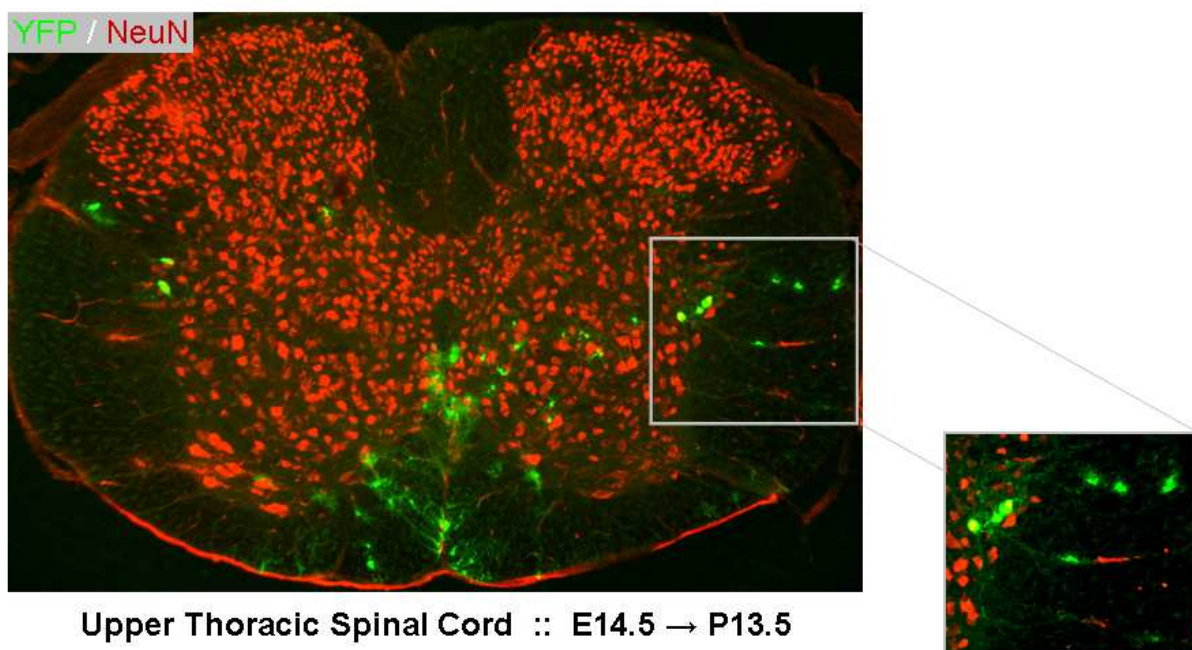
Figure 4.8 - Some p3-derived oligodendrocytes tend to position themselves along the neuronal processes of p3-derived neurons. Transversal sections of upper thoracic spinal cord of E14.5 → P13.5 *Nkx2.2-CreER^{T2} : Rosa26-YFP* mice immunolabelled for NeuN and YFP.
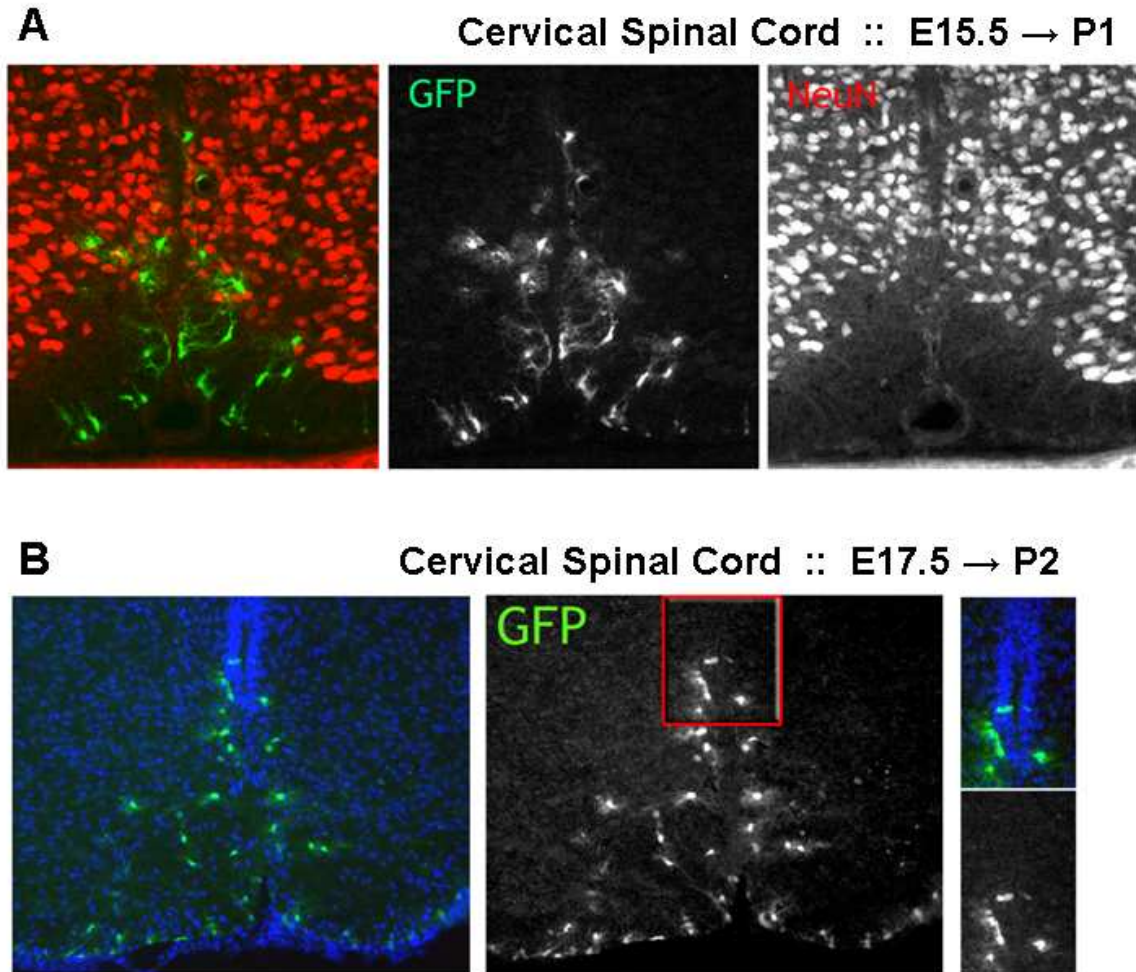
Figure 4.9 - Restricted distribution of p3-derived astrocytes to the ventral spinal cord during late embryogenesis. Transversal sections of cervical spinal cord of E15.5 → P1 (A) or E17.5 → P2 (A) *Nkx2.2-CreER^{T2} : Rosa26-YFP* mice. Antibodies used are as indicated. Sections were counterstained with Hoechst 33258 (blue staining).

YFP/GFAP/Hst
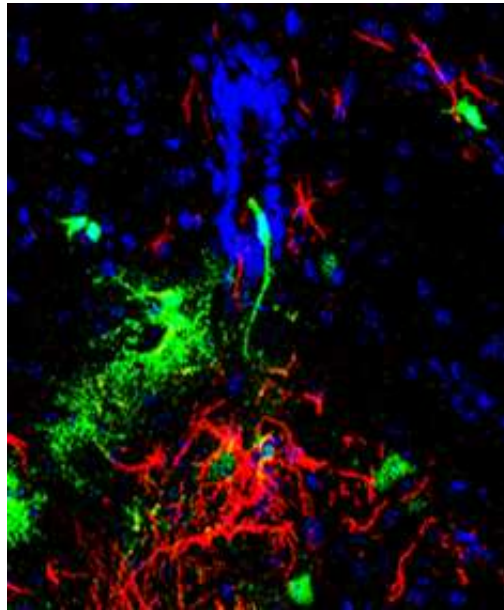
YFP/Olig2/Hst
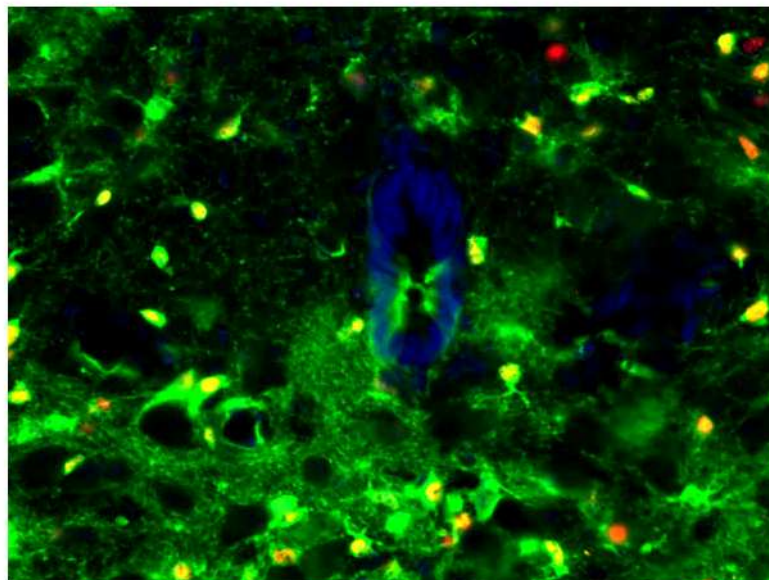
Figure 4.10 - Ependymal cells of the spinal cord derive from ventral progenitors only. Above: Transversal sections of cervical E6.8 → P12.5 *Nkx2.2-CreER^{T2} : Rosa26-YFP* cords. Below: Transversal sections *Olig2-Cre x YFP* at P10 (thoracic spinal cord). Antibodies used are as indicated. Sections were counterstained with Hoechst 33258 (Hst, blue).
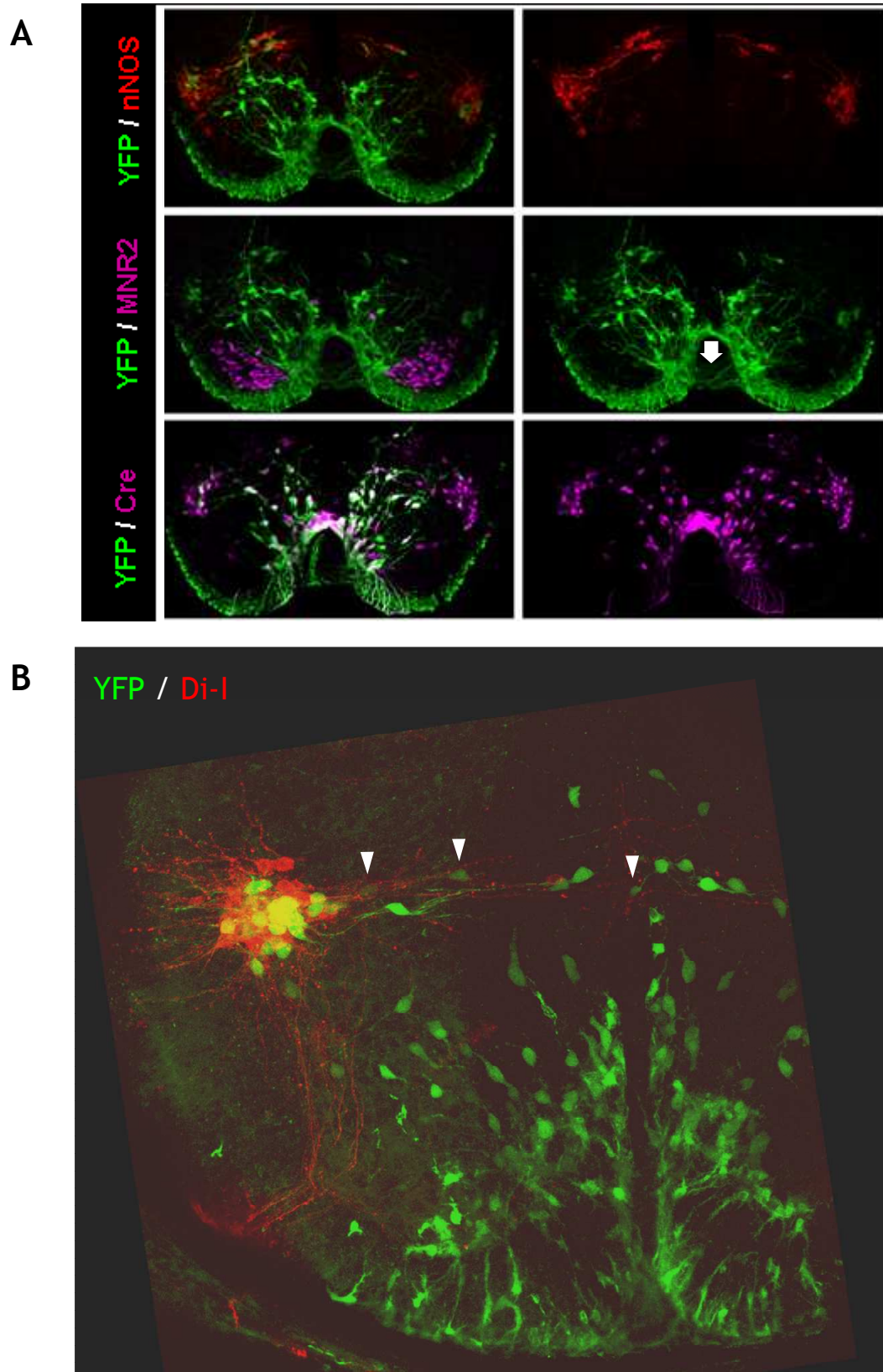
Figure 4.11 - Characterisation of YFP-labelled SPNs. Above: Transversal section of E5.5/6.5 → E13.5 *Nkx2.2-CreER^{T2} : Rosa26-YFP* thoracic spinal cord. Below: Retrograde labelling of SPNs in E10.5/11.5/12.5 → P0.5 *Nkx2.2-CreER^{T2} : Rosa26-YFP* thoracic spinal cord. Antibodies used are as indicated. See text for more details.
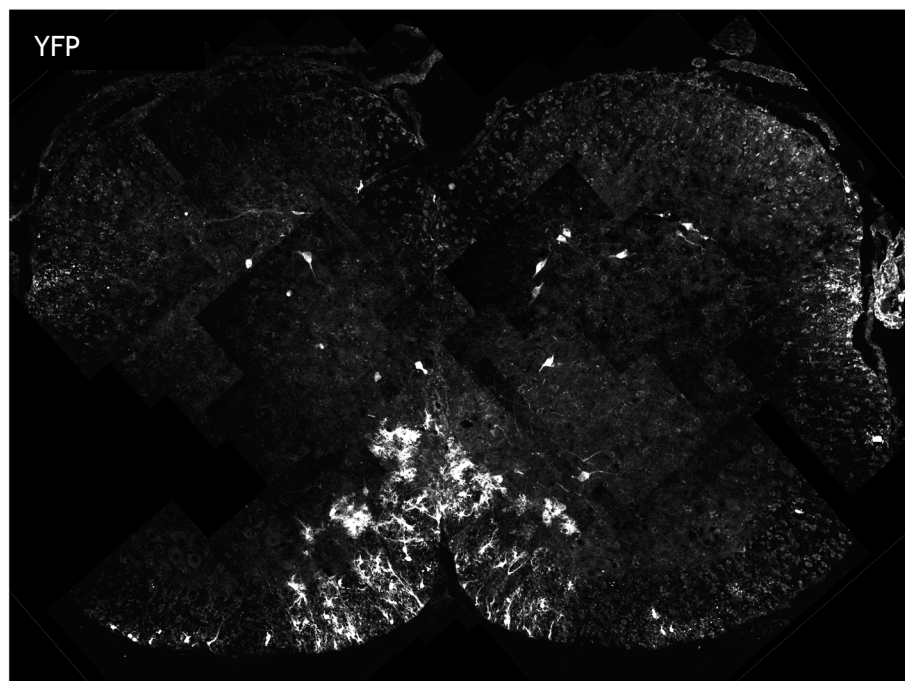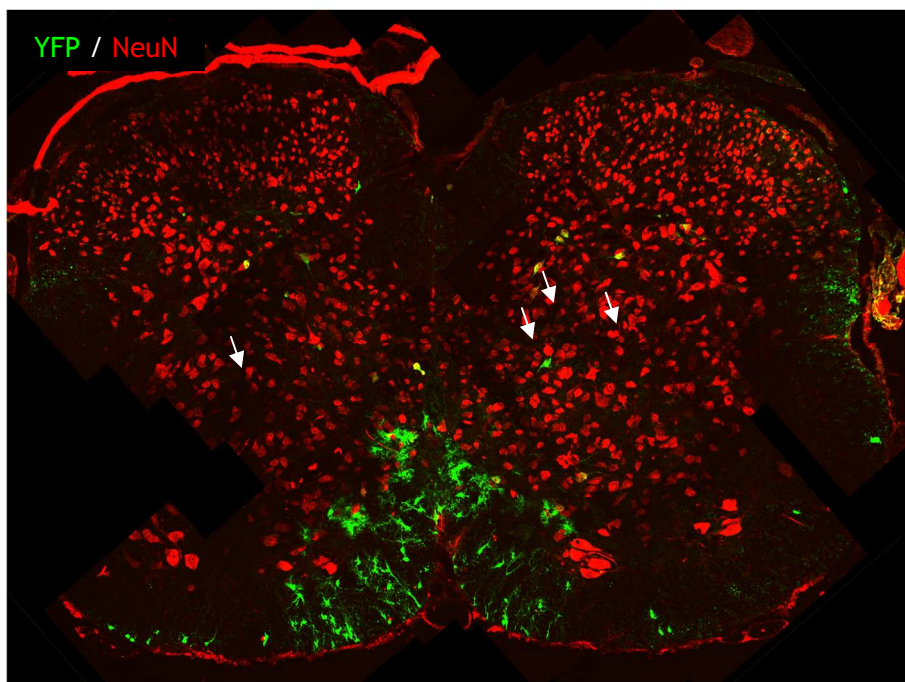
Figure 4.12 - YFP⁺, NeuN⁺ neurons in deep dorsal horn are p3 derived. E6.8 → P12.5 *Nkx2.2-CreER^{T2} : Rosa26-YFP* spinal cords, at lower thoracic level (around T8) immunolabelled for NeuN and YFP. Arrows point towards YFP⁺, NeuN⁺ neurons.
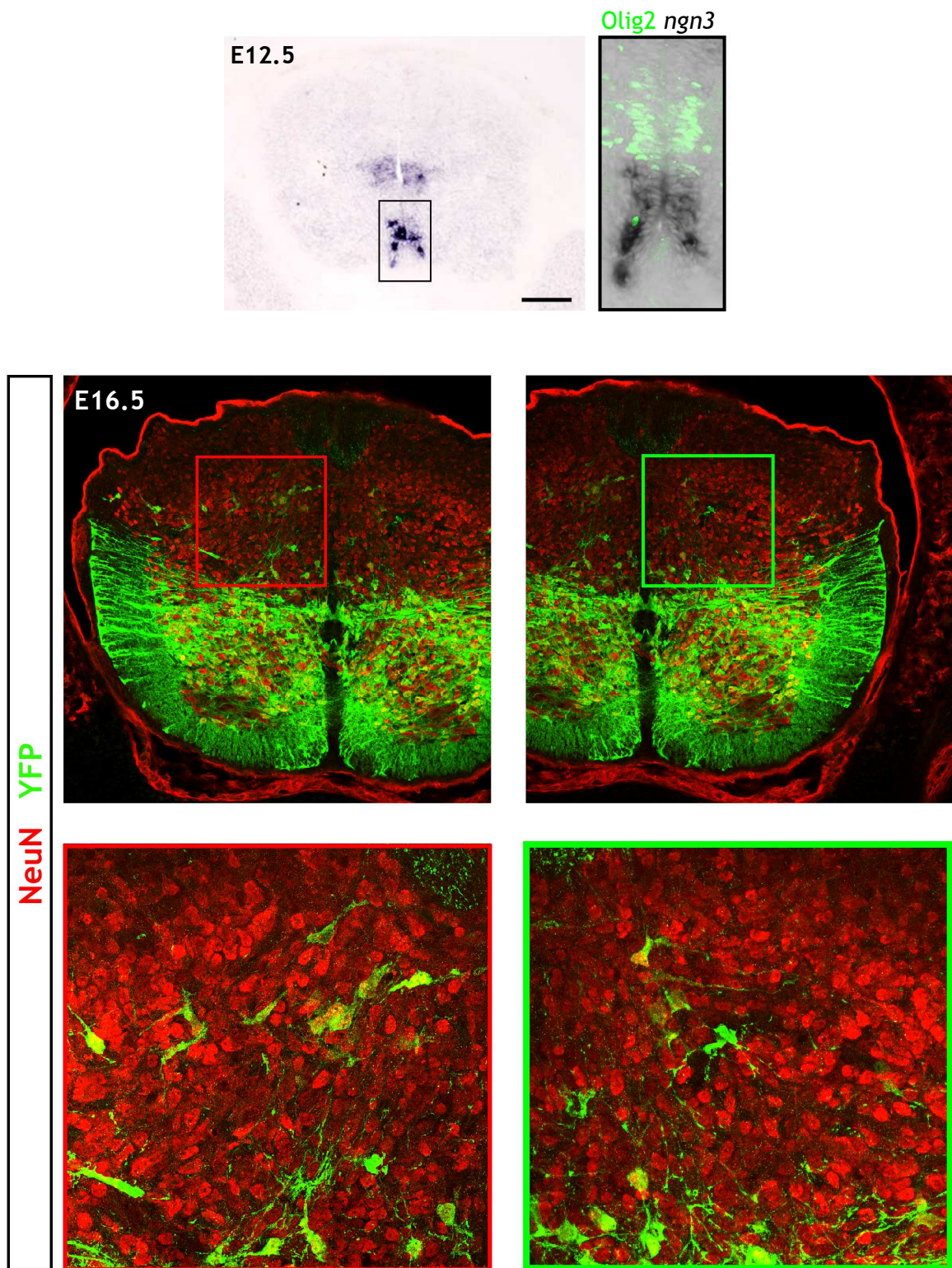
Figure 4.13 - Dorsal interneurons are labelled in *Ngn3-Cre : Rosa26-YFP* mice. Above: Expression of endogenous *Ngn3* at E12.5 revealed by *in situ* hybridization, further immunolabelled for Olig2. Below: Transversal section of E16.5 lower thoracic spinal cord of *Ngn3-Cre : Rosa26-YFP*. Antibodies used are as indicated. Scale bar in A, 200μm. Images kindly provided by Hui-Hsin Tsai (Rowitch lab, UCSF).
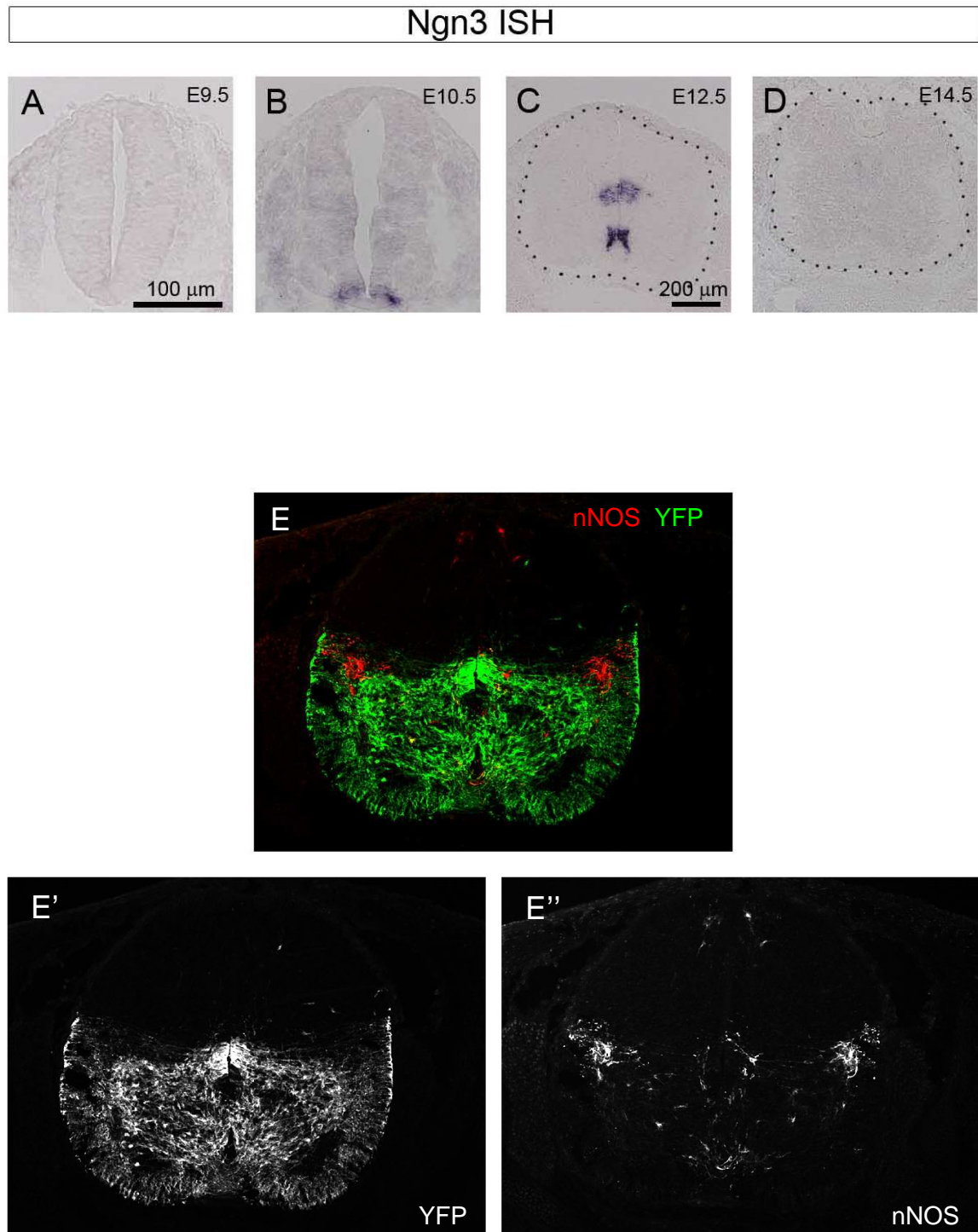
Figure 4.14 - SPNS are not fate-mapped in *Ngn3-Cre : Rosa26-YFP* mice. Above: Expression of endogenous *Ngn3* at different embryonic stages, revealed by *in situ* hybridization. Below: Transversal sections of E13.5 thortacic spinal cord of *Ngn3-Cre : Rosa26-YFP* mice immunolabelled for nNOS and YFP. Images kindly provided by Hui-Hsin Tsai (Rowitch lab, UCSF).
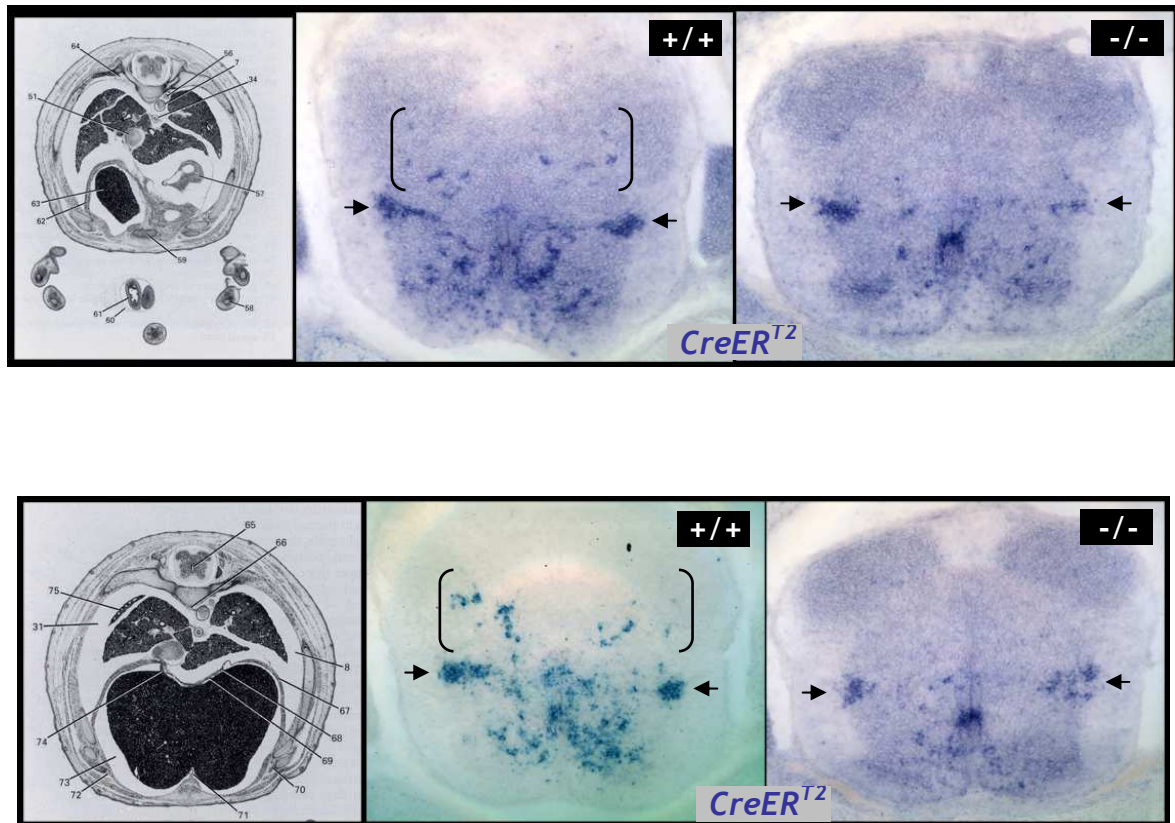
Figure 4.15 - Dorsal CreER^{T2}-expressing neurons as well as Sim1-positive V3 INs are missing in *Nkx2.2* mutants. CreER^{T2} transgene transcript at E15.5, revealed by *in situ* hybridisation. Transversal sections of *Nkx2.2* null mice (-/-) and respective wild type littermate (+/+) at lower thoracic levels of the cord (around T8, above, and more caudal, below). Arrows indicate SPNs and square brackets, dorsal CreER^{T2}-expressing neurons.
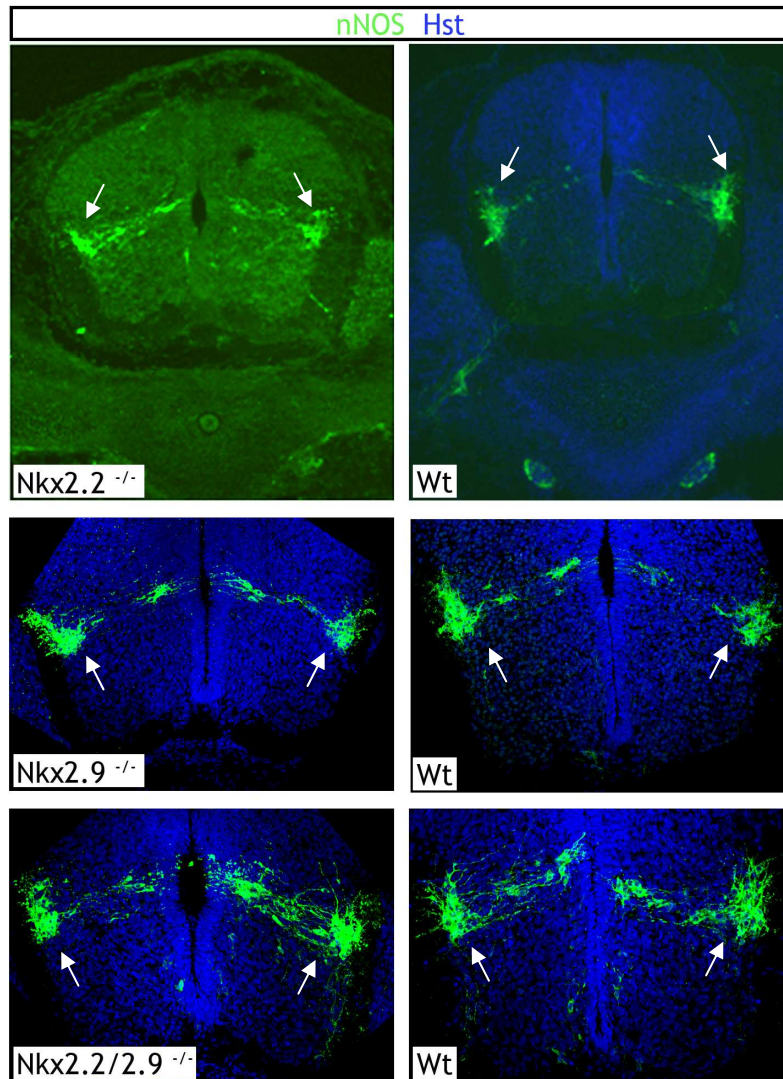
Figure 4.16 - Presence of SPNs in mice lacking either Nkx2.2 or Nkx2.9 or both genes. Transversal sections of thoracic spinal cord immunolabelled for nNOS at E13.5. SPNs (arrows) are generated in Nkx2.2, Nkx2.9 and Nkx2 double knock-out mice in normal numbers and distribution as the ones in the wild type (Wt) littermates. Cell nuclei were poststained with Hoechst 33258 (Hst, blue).
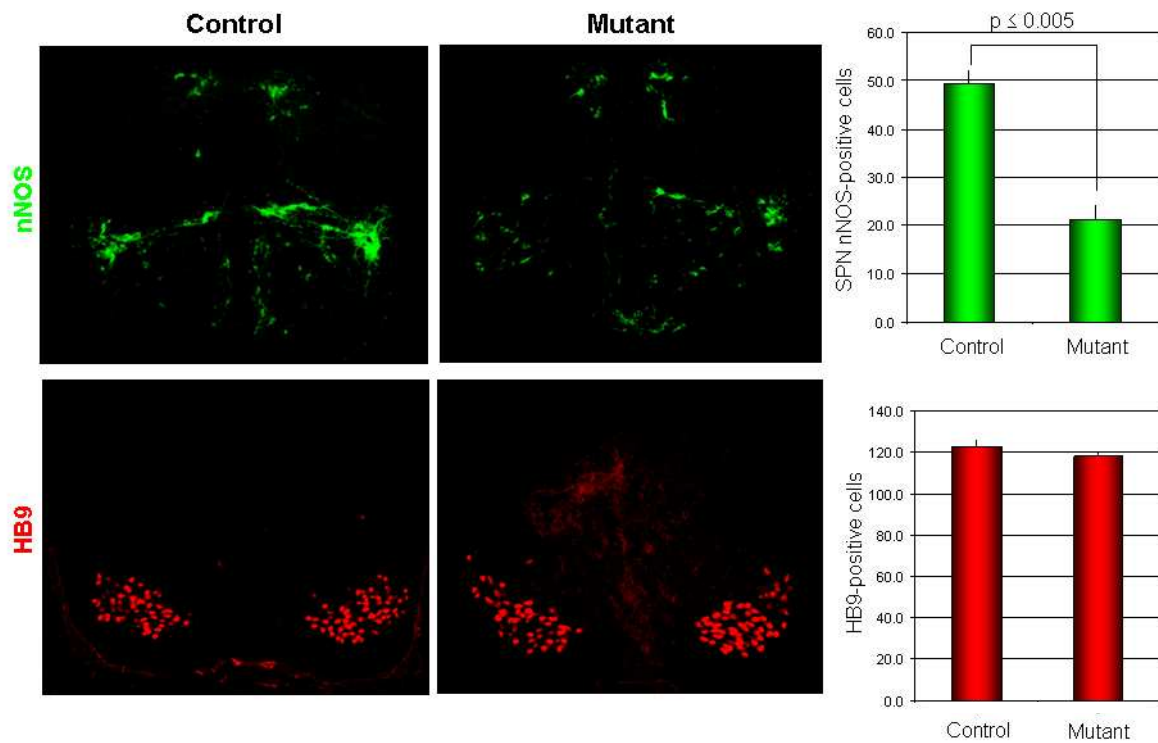
Figure 4.17 - Loss of SPNs, but not sMNs, due to the disruption of p3-progenitor specification. Tamoxifen was administered to pregnant mother twice at E6.5 and E7.5 and embryos analyzed at E13.5. Immunolabelling of consecutive sections of *Nkx2.2-CreER*[T2] : *Smo*[flox/flox] thoracic spinal cord for nNOS and HB9 to visualise SPNs and sMNs, respectively. Disruption of SHH signalling specifically in p3-progenitors only affects SPNs production, but not that of sMNs, suggesting that SPNs and sMNs come from separate progenitor pools.
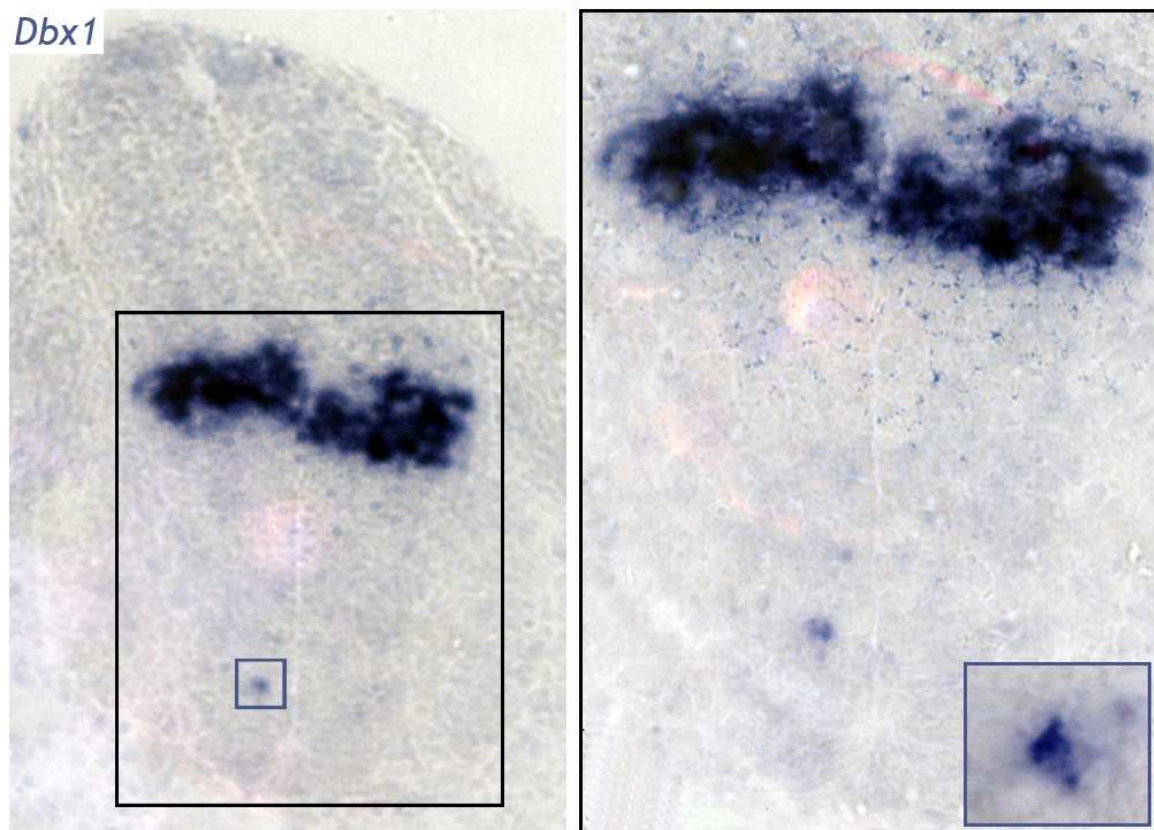
Figure 4.18 - Targeted loss of Shh signalling in p3 domain leads to ectopic activation of *Dbx1* in the ventral spinal cord. Expression of Dbx1 in E6.5/7.5 → E11 *Nkx2.2-CreER^{T2}* : *Smo$^{flox/flox}$* cords revealed by *in situ* hybridisation.

Olig2 $^{-/-}$ **Wt littermate**
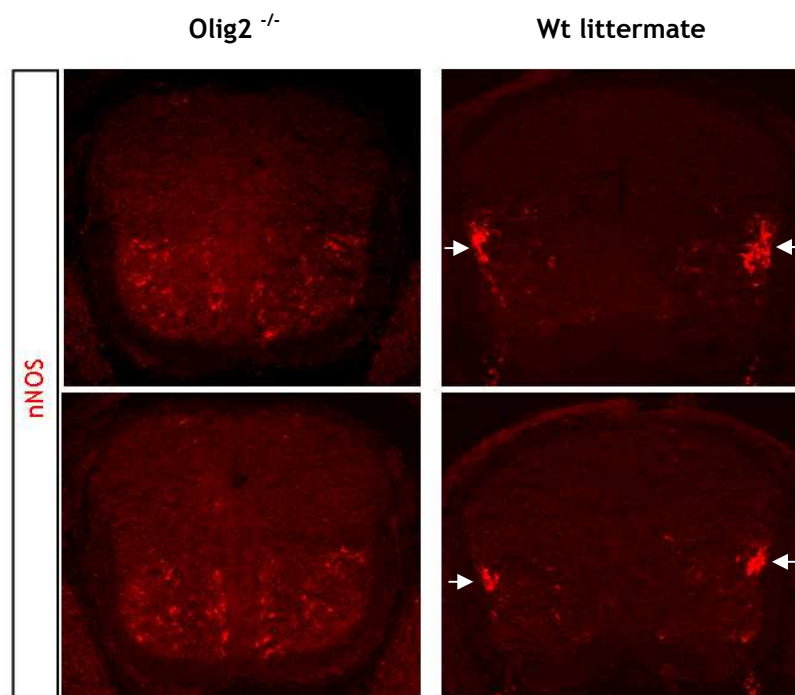
Figure 4.19 - Apparent absence of SPNs in *Olig2* null spinal cords. Immunoflourescence detection of nNOS in *Olig2* null spinal cords and respective control littermate. Two transverse sections of thoracic spinal cord are shown for each genotype. nNOS$^+$ cells are seen in Olig2$^{-/-}$ cords but they are not clustered in the intermediate cord where SPNs are normally found (arrows). The identity of these scattered nNOS$^+$ cells is not known.
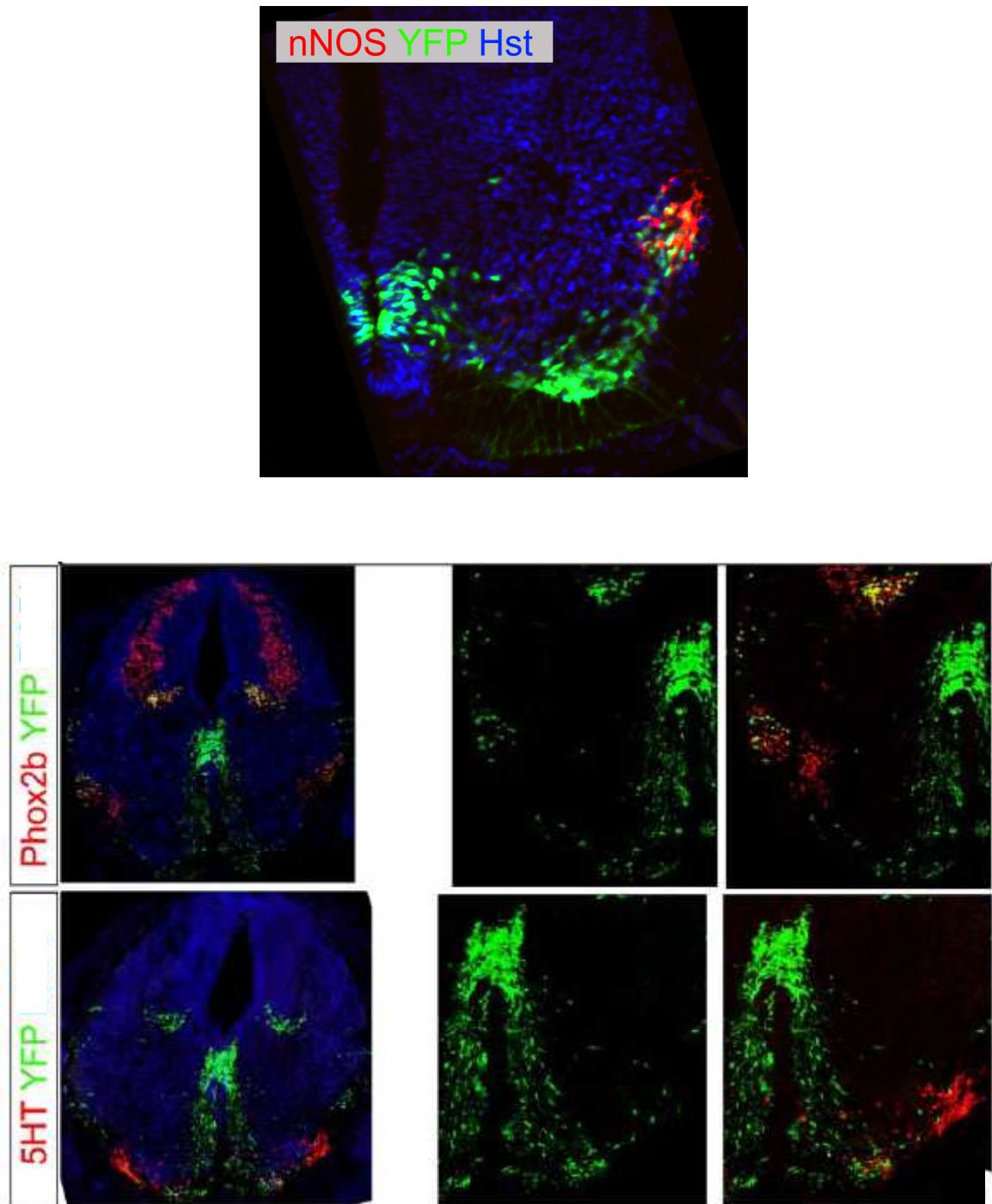
Figure 4.20 - Tracing visceral motor neurons in *Olig2-Cre mice*. Above: Transversal section of E12.5 thoracic spinal cord of *Olig2-Cre : Rosa26-YFP*. Below: Hindbrain of *Olig2-Cre : Rosa26-YFP* at the level of rhombomere 5 (r5) at E12.5. Antibodies used are indicated. Sections were counterstained with Hoechst 33258 (Hst, blue).

Chapter 5 - Conclusion

5.1. Summary of results

The experimental strategy adopted in this Thesis involves the use of *Cre*-mediated recombination in transgenic mice to follow the cell-fates of precursors expressing *Nkx2.2* in the p3 domain of the spinal cord neuroepithelium. Although the initial expression of *Nkx2.2* is initially confined to the p3 domain, soon after E12.5 the domains of *Nkx2.2* and *Olig2* (which demarcates the pMN domain) switch from being mutually exclusive to overlapping (Zhou et al. 2001). In order to label cells emanating from the p3 domain and not from pMN, I have used a tamoxifen-inducible form of *Cre*-recombinase (*Cre-ER^{T2}*) which requires ligand (tamoxifen, TM) binding for activation. To insert the coding region of *Cre-ER^{T2}* into the *Nkx2.2* locus I used PAC vector and homologous recombination in bacteria. Mouse PAC clones that carry genomic DNA inserts containing *Nkx2.2* flanked by large genomic regions likely to include all the regulatory elements required for normal expression of *Nkx2.2* were identified. Suitable PAC inserts were then genetically engineered to ensure that *Cre-ER^{T2}* expression under the control of the *Nkx2.2* gene behaved in the same pattern as the endogenous gene. The resultant modified PAC was subsequently used for oocyte injections and generation of transgenic mice. Mice expressing *Cre-ER^{T2}* under the

© Sidney Harris
Sciencecartoonsplus.com

"THE NEANDERTHAL BRAIN WAS LARGER THAN OURS. OUR BRAINS ARE GETTING SMALLER — SO WE BETTER GET IN ALL THE THINKING WE CAN AS SOON AS POSSIBLE."

control of *Nkx2.2* (*Nkx2.2-Cre-ER^{T2}* mice) were then bred with reporter mouse strains containing an inactive reporter gene under the control of an ubiquitous promoter. The reporter gene was constitutively activated by *Cre*-mediated recombination upon TM administration, which allowed me to permanently label all the progenitor cells that express *Nkx2.2* and all their progeny once *Cre-ER^{T2}* was activated. TM administration was found to yield suitable levels of recombination when mature *Rosa26-YFP* reporter mice were used and TM was administered by gavage at the highest dose not conducive to significant levels of lethality.

Fate-mapping experiments using *Nkx2.2-Cre-ER^{T2} : Rosa26-YFP* mice enabled me to demonstrate that *Nkx2.2*-expressing p3 neuroepithelial cells of the spinal cord give rise to three distinct neuronal populations - *Sim1*-expressing V3 interneurons, pre-ganglionic motor neurons of the sympathetic nervous system (SPNs, visceral motor neurons of the thoracic spinal cord) and dorsally-located *Sim1*-expressing interneurons. *Nkx2.2*-expressing p3-progenitors also produce two spatially restricted subtypes of astrocytes (fibrous and protoplasmic), a small number of oligodendrocytes and ventrally-positioned ependymal cells. The majority of p3-derived glia (all astrocytes and a subset of p3-derived oligodendrocytes) migrate in a strictly radial manner and their final settling positions are confined to the most ventral regions of the spinal cord. Because of p3-derived glia settle within the region that their radial glia precursors originally project to, one can speculate that most p3-derived glia originate from p3-derived radial glia by direct trans-differentiation, as shown directly for oligodendrocytes that originate in the more dorsal *Dbx1*- or *Mxs3*- domains (Fogarty et al. 2005; Fogarty 2006; Richardson et al. 2006). Some scattered p3-derived oligodendrocytes were also found spread throughout the spinal cord. They cannot be derived directly from p3-derived radial glial, but could come from intermediate precursors that are derived initially from p3-derived radial glia and which proliferate and migrate over relatively long distances. It is known that ~80% of mature oligodendrocytes which populate the entire adult spinal cord arise from highly proliferative and migratory restricted progenitors – the so-called OLPs –that derive from the pMN domain (Richardson et al. 2006; Tripathi et al. 2011).

I found that *Cre-ER^{T2}* continues to be expressed (perdures) in SPNs and in p3-derived ventrally and dorsally-located *Sim1*-expressing interneurons after *Nkx2.2* is extinguished. One can be fairly confident that *Cre-ER^{T2}* behaves as a short-term p3 lineage tracer, because dorsally-located *Sim1 / CreER^{T2}*-expressing interneurons, as well as ventrally-located V3 INs, are lost in *Nkx2.2* null mice. Moreover, conditional loss of SHH signalling in *Nkx2.2*-expressing p3-precursors causes disruption to SPN production, and to that of *CreER^{T2}*-expressing cells at the same location, without affecting sMNs. I also found that SPNs come from progenitors with a history of both *Nkx2.2* and *Olig2* because I was able to label them in

Nkx2.2-Cre-ER^{T2} : Rosa26-YFP and *Olig2-Cre : Rosa26-YFP* cords. Since sMNs are known to derive from *Olig2*-expressing progenitors only, it implies that separate pools of progenitors produce SPNs and sMNs. Therefore, my results support a model in which motor neuron subtype specification already takes place in progenitor cells before they migrate away from the VZ. In the developing hindbrain, it is accepted that visceral and somatic MNs are derived from separate progenitor pools – the former from p3 progenitors and the latter from pMN ones. Additionally, I show that visceral MNs in the hindbrain originate from progenitors with a history of both *Nkx2.2* and *Olig2,* like their counterparts in thoracic spinal cord, whereas sMNs arise from progenitors that never express *Nkx2.2*. This is the same as I observed in the spinal cord, allowing me to propose that the same general program of MN specification is orchestrated all along the neuraxis.

5.2. Future developments/applications

The fact that visceral and somatic motor neurons develop from separate progenitor pools raises the possibility that the transcriptional programs underpinning their specification might differ substantially. It also establishes the idea that the mechanisms involved during visceral motor neuron development operating in the brainstem versus spinal cord could have more common features than we previously believed. The prospect of being able to find unique factors that specify visceral motor neuron development, distinct from those linked to somatic motor neuron development, would allow us, for example, to specifically produce visceral motor neurons *in vitro* for cell transplantation or even to regulate their development *in vivo*.

It is noteworthy that p3 progenitors generate both motor neurons and interneurons, two key elements of motor circuits. Moreover, different types of p3-derived neurons express some of the same neuronal markers during their development – for example, both dorsal and ventral p3-derived interneurons express *Sim1* during embryogenesis (Figure 3.16 and 3.17) and likewise SPNs and dorsally-located *Sim1*-expressing p3-derived INs can be marked with neurotransmitter nNOS in the postnatal cord (not shown). This raises the possibility that these different neuronal populations might interact with each other in the formation of a local sympathetic circuit. In preliminary experiments to visualise YFP immunolabelling in the transmission electron microscopy by diaminobenzidine histochemistry (Figure 5.1), I identified synapses on postnatal SPNs at which both pre- and post-synaptic structures were YFP-positive. These results suggest that different classes of p3-derived neurons might be electrically coupled. The idea that cells derived from the same progenitors have preferentially synapse with their sister cells already has a precedent (Yu et al. 2009). The

Nkx2.2-CreER^{T2} mice described in this Thesis are a valuable tool with which to study the neuronal circuitry of the spinal autonomic nervous system.
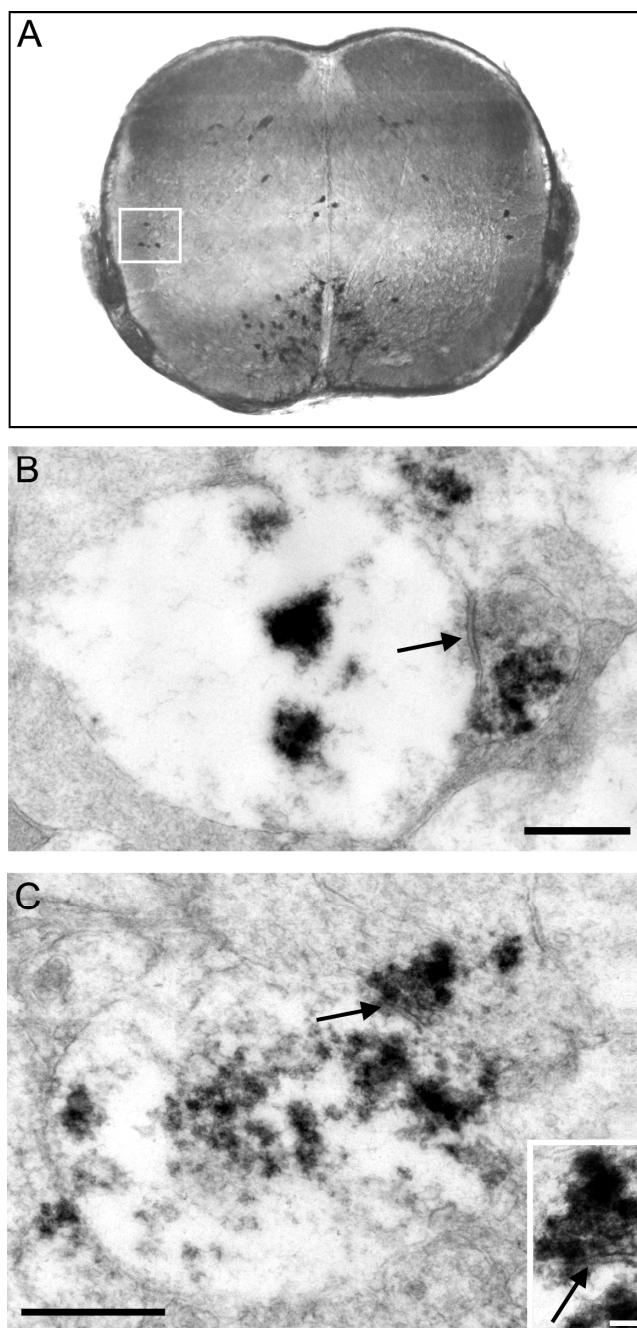
Figure 5.1 - Synaptic connectivity of p3-derived neurons might contribute to intra-spinal autonomic circuits. (please, see text for more details) Scale bars in B & C, 500nm, and in inset of C, 100nm.

Reference List

Agalliu, D., Takada, S., Agalliu, I., McMahon, A. P., and Jessell, T. M. 2009, "Motor neurons with axial muscle projections specified by Wnt4/5 signaling", *Neuron*, vol. 61, no. 5, pp. 708-720.

Agarwala, S. and Ragsdale, C. W. 2002, "A role for midbrain arcs in nucleogenesis", *Development*, vol. 129, no. 24, pp. 5779-5788.

Agarwala, S., Sanders, T. A., and Ragsdale, C. W. 2001, "Sonic hedgehog control of size and shape in midbrain pattern formation", *Science*, vol. 291, no. 5511, pp. 2147-2150.

Al-Mosawie, A., Wilson, J. M., and Brownstone, R. M. 2007, "Heterogeneity of V2-derived interneurons in the adult mouse spinal cord", *Eur.J.Neurosci.*, vol. 26, no. 11, pp. 3003-3015.

Andriezen, W. L. 1893, "The Neuroglia Elements in the Human Brain", *Br.Med.J*, vol. 2, no. 1700, pp. 227-230.

Anthony, T. E., Klein, C., Fishell, G., and Heintz, N. 2004, "Radial glia serve as neuronal progenitors in all regions of the central nervous system", *Neuron*, vol. 41, no. 6, pp. 881-890.

Arber, S., Han, B., Mendelsohn, M., Smith, M., Jessell, T. M., and Sockanathan, S. 1999, "Requirement for the homeobox gene Hb9 in the consolidation of motor neuron identity", *Neuron*, vol. 23, no. 4, pp. 659-674.

Awasaki, T., Lai, S. L., Ito, K., and Lee, T. 2008, "Organization and postembryonic development of glial cells in the adult central brain of Drosophila", *J Neurosci.*, vol. 28, no. 51, pp. 13742-13753.

Barnabe-Heider, F., Goritz, C., Sabelstrom, H., Takebayashi, H., Pfrieger, F. W., Meletis, K., and Frisen, J. 2010, "Origin of new glial cells in intact and injured adult spinal cord", *Cell Stem Cell*, vol. 7, no. 4, pp. 470-482.

Barres, B. A., Hart, I. K., Coles, H. S., Burne, J. F., Voyvodic, J. T., Richardson, W. D., and Raff, M. C. 1992a, "Cell death and control of cell survival in the oligodendrocyte lineage", *Cell*, vol. 70, no. 1, pp. 31-46.

Barres, B. A., Hart, I. K., Coles, H. S., Burne, J. F., Voyvodic, J. T., Richardson, W. D., and Raff, M. C. 1992b, "Cell death in the oligodendrocyte lineage", *J Neurobiol.*, vol. 23, no. 9, pp. 1221-1230.

Baumann, N. and Pham-Dinh, D. 2001, "Biology of oligodendrocyte and myelin in the mammalian central nervous system", *Physiol Rev.*, vol. 81, no. 2, pp. 871-927.

Bel-Vialar, S., Itasaki, N., and Krumlauf, R. 2002, "Initiating Hox gene expression: in the early chick neural tube differential sensitivity to FGF and RA signaling subdivides the HoxB genes in two distinct groups", *Development*, vol. 129, no. 22, pp. 5103-5115.

Bentivoglio, M. and Mazzarello, P. 1999, "The history of radial glia", *Brain Res.Bull.*, vol. 49, no. 5, pp. 305-315.

Bergles, D. E., Roberts, J. D., Somogyi, P., and Jahr, C. E. 2000, "Glutamatergic synapses on oligodendrocyte precursor cells in the hippocampus", *Nature*, vol. 405, no. 6783, pp. 187-191.

Bhat, R. V., Axt, K. J., Fosnaugh, J. S., Smith, K. J., Johnson, K. A., Hill, D. E., Kinzler, K. W., and Baraban, J. M. 1996, "Expression of the APC tumor suppressor protein in oligodendroglia", *Glia*, vol. 17, no. 2, pp. 169-174.

Briscoe, J. The gene regulatory logic for reading the Sonic Hedgehog gradient in the vertebrate neural tube. 27-1-2011. Venue: University College London, Host: Prof Lewis Wolpert. 27-1-2011.

Briscoe, J., Chen, Y., Jessell, T. M., and Struhl, G. 2001a, "A hedgehog-insensitive form of patched provides evidence for direct long-range morphogen activity of sonic hedgehog in the neural tube", *Mol.Cell*, vol. 7, no. 6, pp. 1279-1291.

Briscoe, J. and Ericson, J. 2001b, "Specification of neuronal fates in the ventral neural tube", *Curr.Opin.Neurobiol.*, vol. 11, no. 1, pp. 43-49.

Briscoe, J., Pierani, A., Jessell, T. M., and Ericson, J. 2000, "A homeodomain protein code specifies progenitor cell identity and neuronal fate in the ventral neural tube", *Cell*, vol. 101, no. 4, pp. 435-445.

Briscoe, J., Sussel, L., Serup, P., Hartigan-O'Connor, D., Jessell, T. M., Rubenstein, J. L., and Ericson, J. 1999, "Homeobox gene Nkx2.2 and specification of neuronal identity by graded Sonic hedgehog signalling", *Nature*, vol. 398, no. 6728, pp. 622-627.

Britto, J., Tannahill, D., and Keynes, R. 2002, "A critical role for sonic hedgehog signaling in the early expansion of the developing brain", *Nat.Neurosci.*, vol. 5, no. 2, pp. 103-110.

Brody, S. L., Yan, X. H., Wuerffel, M. K., Song, S. K., and Shapiro, S. D. 2000, "Ciliogenesis and left-right axis defects in forkhead factor HFH-4-null mice", *Am.J Respir.Cell Mol.Biol.*, vol. 23, no. 1, pp. 45-51.

Brown, A. G. 1981, "The spinocervical tract", *Prog.Neurobiol.*, vol. 17, no. 1-2, pp. 59-96.

Bruni, J. E. 1998, "Ependymal development, proliferation, and functions: a review", *Microsc.Res.Tech.*, vol. 41, no. 1, pp. 2-13.

Buchanan, C. M., Buchanan, N. L., Edgar, K. J., Little, J. L., Malcolm, M. O., Ruble, K. M., Wacher, V. J., and Wempe, M. F. 2007, "Pharmacokinetics of tamoxifen after intravenous and oral dosing of tamoxifen-hydroxybutenyl-beta-cyclodextrin formulations", *J.Pharm.Sci.*, vol. 96, no. 3, pp. 644-660.

Buchholz, F., Angrand, P. O., and Stewart, A. F. 1998, "Improved properties of FLP recombinase evolved by cycling mutagenesis", *Nat.Biotechnol.*, vol. 16, no. 7, pp. 657-662.

Buffo, A., Rite, I., Tripathi, P., Lepier, A., Colak, D., Horn, A. P., Mori, T., and Gotz, M. 2008, "Origin and progeny of reactive gliosis: A source of multipotent cells in the injured brain", *Proc.Natl.Acad Sci U.S.A*, vol. 105, no. 9, pp. 3581-3586.

Bukusoglu, C. and Krieger, N. R. 1996, "Estrogen-specific target site identified by progesterone-11 alpha-hemisuccinate-(2-[125I]-iodohistamine) in mouse brain membranes", *J.Steroid Biochem.Mol.Biol.*, vol. 58, no. 1, pp. 89-94.

Burne, J. F., Staple, J. K., and Raff, M. C. 1996, "Glial cells are increased proportionally in transgenic optic nerves with increased numbers of axons", *J Neurosci.*, vol. 16, no. 6, pp. 2064-2073.

Butt, A. M., Duncan, A., Hornby, M. F., Kirvell, S. L., Hunter, A., Levine, J. M., and Berry, M. 1999, "Cells expressing the NG2 antigen contact nodes of Ranvier in adult CNS white matter", *Glia*, vol. 26, no. 1, pp. 84-91.

Cabot, J. B. 1990, "Sympathetic Preganglionic Neurons: Cytoarchitecture, Ultrastructure, and Biophysical Properties," in *Central Regulation of Autonomic Functions*, First edn, A. D. Loewy & K. M. Spyer, eds., Oxford University Press, New York, pp. 44-67.

Cai, J., Qi, Y., Hu, X., Tan, M., Liu, Z., Zhang, J., Li, Q., Sander, M., and Qiu, M. 2005, "Generation of oligodendrocyte precursor cells from mouse dorsal spinal cord independent of Nkx6 regulation and Shh signaling", *Neuron*, vol. 45, no. 1, pp. 41-53.

Cai, J., Zhu, Q., Zheng, K., Li, H., Qi, Y., Cao, Q., and Qiu, M. 2010, "Co-localization of Nkx6.2 and Nkx2.2 homeodomain proteins in differentiated myelinating oligodendrocytes", *Glia*, vol. 58, no. 4, pp. 458-468.

Calver, A. R., Hall, A. C., Yu, W. P., Walsh, F. S., Heath, J. K., Betsholtz, C., and Richardson, W. D. 1998, "Oligodendrocyte population dynamics and the role of PDGF in vivo", *Neuron*, vol. 20, no. 5, pp. 869-882.

Cameron-Curry, P. and Le Douarin, N. M. 1995, "Oligodendrocyte precursors originate from both the dorsal and the ventral parts of the spinal cord", *Neuron*, vol. 15, no. 6, pp. 1299-1310.

Campbell, K. and Gotz, M. 2002, "Radial glia: multi-purpose cells for vertebrate brain development", *Trends Neurosci.*, vol. 25, no. 5, pp. 235-238.

Carlen, M., Meletis, K., Barnabe-Heider, F., and Frisen, J. 2006, "Genetic visualization of neurogenesis", *Exp.Cell Res.*, vol. 312, no. 15, pp. 2851-2859.

Carlen, M., Meletis, K., Goritz, C., Darsalia, V., Evergren, E., Tanigaki, K., Amendola, M., Barnabe-Heider, F., Yeung, M. S., Naldini, L., Honjo, T., Kokaia, Z., Shupliakov, O., Cassidy, R. M., Lindvall, O., and Frisen, J. 2009, "Forebrain ependymal cells are Notch-dependent and generate neuroblasts and astrocytes after stroke", *Nat.Neurosci.*, vol. 12, no. 3, pp. 259-267.

Caspary, T. and Anderson, K. V. 2003, "Patterning cell types in the dorsal spinal cord: what the mouse mutants say", *Nat.Rev.Neurosci.*, vol. 4, no. 4, pp. 289-297.

Chandrasekhar, A. 2004, "Turning heads: development of vertebrate branchiomotor neurons", *Dev.Dyn.*, vol. 229, no. 1, pp. 143-161.

Chen, M. H., Wilson, C. W., and Chuang, P. T. 2007, "SnapShot: hedgehog signaling pathway", *Cell*, vol. 130, no. 2, p. 386.

Chen, Y. and Struhl, G. 1996, "Dual roles for patched in sequestering and transducing Hedgehog", *Cell*, vol. 87, no. 3, pp. 553-563.

Cheng, L., Chen, C. L., Luo, P., Tan, M., Qiu, M., Johnson, R., and Ma, Q. 2003, "Lmx1b, Pet-1, and Nkx2.2 coordinately specify serotonergic neurotransmitter phenotype", *J.Neurosci.*, vol. 23, no. 31, pp. 9961-9967.

Chiang, C., Litingtung, Y., Lee, E., Young, K. E., Corden, J. L., Westphal, H., and Beachy, P. A. 1996, "Cyclopia and defective axial patterning in mice lacking Sonic hedgehog gene function", *Nature*, vol. 383, no. 6599, pp. 407-413.

Christopherson, K. S., Ullian, E. M., Stokes, C. C., Mullowney, C. E., Hell, J. W., Agah, A., Lawler, J., Mosher, D. F., Bornstein, P., and Barres, B. A. 2005, "Thrombospondins are astrocyte-secreted proteins that promote CNS synaptogenesis", *Cell*, vol. 120, no. 3, pp. 421-433.

Ciani, L. and Salinas, P. C. 2005, "WNTs in the vertebrate nervous system: from patterning to neuronal connectivity", *Nat.Rev.Neurosci.*, vol. 6, no. 5, pp. 351-362.

Cissell, M. A., Zhao, L., Sussel, L., Henderson, E., and Stein, R. 2003, "Transcription factor occupancy of the insulin gene in vivo. Evidence for direct regulation by Nkx2.2", *J.Biol.Chem.*, vol. 278, no. 2, pp. 751-756.

Clark, A. J., Bissinger, P., Bullock, D. W., Damak, S., Wallace, R., Whitelaw, C. B., and Yull, F. 1994, "Chromosomal position effects and the modulation of transgene expression", *Reprod.Fertil.Dev.*, vol. 6, no. 5, pp. 589-598.

Clarke, J. D. and Tickle, C. 1999, "Fate maps old and new", *Nat.Cell Biol.*, vol. 1, no. 4, p. E103-E109.

Conklin EG 1905, "Mosaic development in Ascidian eggs", *J.Exp.Zool.*, vol. 2, pp. 145-223.

Copeland, N. G., Jenkins, N. A., and Court DL 2001, "Recombineering: a powerful new tool for mouse functional genomics", *Nat.Rev.Genet.*, vol. 2, no. 10, pp. 769-779.

Craven, S. E., Lim, K. C., Ye, W., Engel, J. D., de, S. F., and Rosenthal, A. 2004, "Gata2 specifies serotonergic neurons downstream of sonic hedgehog", *Development*, vol. 131, no. 5, pp. 1165-1173.

Crone, S. A., Quinlan, K. A., Zagoraiou, L., Droho, S., Restrepo, C. E., Lundfald, L., Endo, T., Setlak, J., Jessell, T. M., Kiehn, O., and Sharma, K. 2008, "Genetic ablation of V2a ipsilateral interneurons disrupts left-right locomotor coordination in mammalian spinal cord", *Neuron*, vol. 60, no. 1, pp. 70-83.

Danielian, P. S., Muccino, D., Rowitch, D. H., Michael, S. K., and McMahon, A. P. 1998, "Modification of gene activity in mouse embryos in utero by a tamoxifen-inducible form of Cre recombinase", *Curr.Biol.*, vol. 8, no. 24, pp. 1323-1326.

Dasen, J. S., De, C. A., Wang, B., Tucker, P. W., and Jessell, T. M. 2008, "Hox repertoires for motor neuron diversity and connectivity gated by a single accessory factor, FoxP1", *Cell*, vol. 134, no. 2, pp. 304-316.

Dasen, J. S., Liu, J. P., and Jessell, T. M. 2003, "Motor neuron columnar fate imposed by sequential phases of Hox-c activity", *Nature*, vol. 425, no. 6961, pp. 926-933.

Debus, E., Weber, K., and Osborn, M. 1983, "Monoclonal antibodies specific for glial fibrillary acidic (GFA) protein and for each of the neurofilament triplet polypeptides", *Differentiation*, vol. 25, no. 2, pp. 193-203.

Del Barrio, M. G., Taveira-Marques, R., Muroyama, Y., Yuk, D. I., Li, S., Wines-Samuelson, M., Shen, J., Smith, H. K., Xiang, M., Rowitch, D., and Richardson, W. D. 2007, "A regulatory network involving Foxn4, Mash1 and delta-like 4/Notch1 generates V2a and V2b spinal interneurons from a common progenitor pool", *Development*.

Deneen, B., Ho, R., Lukaszewicz, A., Hochstim, C. J., Gronostajski, R. M., and Anderson, D. J. 2006, "The transcription factor NFIA controls the onset of gliogenesis in the developing spinal cord", *Neuron*, vol. 52, no. 6, pp. 953-968.

Deppe, U., Schierenberg, E., Cole, T., Krieg, C., Schmitt, D., Yoder, B., and von, E. G. 1978, "Cell lineages of the embryo of the nematode Caenorhabditis elegans", *Proc.Natl.Acad Sci U.S.A*, vol. 75, no. 1, pp. 376-380.

Dessaud, E., McMahon, A. P., and Briscoe, J. 2008, "Pattern formation in the vertebrate neural tube: a sonic hedgehog morphogen-regulated transcriptional network", *Development*, vol. 135, no. 15, pp. 2489-2503.

Dessaud, E., Ribes, V., Balaskas, N., Yang, L. L., Pierani, A., Kicheva, A., Novitch, B. G., Briscoe, J., and Sasai, N. 2010, "Dynamic assignment and maintenance of positional identity in the ventral neural tube by the morphogen sonic hedgehog", *PLoS.Biol.*, vol. 8, no. 6, p. e1000382.

Dessaud, E., Yang, L. L., Hill, K., Cox, B., Ulloa, F., Ribeiro, A., Mynett, A., Novitch, B. G., and Briscoe, J. 2007, "Interpretation of the sonic hedgehog morphogen gradient by a temporal adaptation mechanism", *Nature*, vol. 450, no. 7170, pp. 717-720.

Diez del, C. R., Breitkreuz, D. N., and Storey, K. G. 2002, "Onset of neuronal differentiation is regulated by paraxial mesoderm and requires attenuation of FGF signalling", *Development*, vol. 129, no. 7, pp. 1681-1691.

Diez del, C. R., Olivera-Martinez, I., Goriely, A., Gale, E., Maden, M., and Storey, K. 2003, "Opposing FGF and retinoid pathways control ventral neural pattern, neuronal differentiation, and segmentation during body axis extension", *Neuron*, vol. 40, no. 1, pp. 65-79.

Diez del, C. R. and Storey, K. G. 2004, "Opposing FGF and retinoid pathways: a signalling switch that controls differentiation and patterning onset in the extending vertebrate body axis", *Bioessays*, vol. 26, no. 8, pp. 857-869.

Doetsch, F., Caille, I., Lim, D. A., Garcia-Verdugo, J. M., and varez-Buylla, A. 1999, "Subventricular zone astrocytes are neural stem cells in the adult mammalian brain", *Cell*, vol. 97, no. 6, pp. 703-716.

Doherty, J., Logan, M. A., Tasdemir, O. E., and Freeman, M. R. 2009, "Ensheathing glia function as phagocytes in the adult Drosophila brain", *J Neurosci.*, vol. 29, no. 15, pp. 4768-4781.

Dower, W. J., Miller, J. F., and Ragsdale, C. W. 1988, "High efficiency transformation of E. coli by high voltage electroporation", *Nucleic Acids Res.*, vol. 16, no. 13, pp. 6127-6145.

Downing, S. J., Porter, D. G., and Lincoln, D. W. 1981, "Tamoxifen and the role of oestrogen in the timing of parturition in the rat", *J.Reprod.Fertil.*, vol. 62, no. 2, pp. 519-526.

Echelard, Y., Epstein, D. J., St-Jacques, B., Shen, L., Mohler, J., McMahon, J. A., and McMahon, A. P. 1993, "Sonic hedgehog, a member of a family of putative signaling molecules, is implicated in the regulation of CNS polarity", *Cell*, vol. 75, no. 7, pp. 1417-1430.

Eng, L. F., Vanderhaeghen, J. J., Bignami, A., and Gerstl, B. 1971, "An acidic protein isolated from fibrous astrocytes", *Brain Res.*, vol. 28, no. 2, pp. 351-354.

Ericson, J., Briscoe, J., Rashbass, P., van, H., V, and Jessell, T. M. 1997a, "Graded sonic hedgehog signaling and the specification of cell fate in the ventral neural tube", *Cold Spring Harb.Symp.Quant.Biol.*, vol. 62, pp. 451-466.

Ericson, J., Morton, S., Kawakami, A., Roelink, H., and Jessell, T. M. 1996, "Two critical periods of Sonic Hedgehog signaling required for the specification of motor neuron identity", *Cell*, vol. 87, no. 4, pp. 661-673.

Ericson, J., Rashbass, P., Schedl, A., Brenner-Morton, S., Kawakami, A., van, H., V, Jessell, T. M., and Briscoe, J. 1997b, "Pax6 controls progenitor cell identity and neuronal fate in response to graded Shh signaling", *Cell*, vol. 90, no. 1, pp. 169-180.

Erter, C. E., Wilm, T. P., Basler, N., Wright, C. V., and Solnica-Krezel, L. 2001, "Wnt8 is required in lateral mesendodermal precursors for neural posteriorization in vivo", *Development*, vol. 128, no. 18, pp. 3571-3583.

Fan, C. M., Kuwana, E., Bulfone, A., Fletcher, C. F., Copeland, N. G., Jenkins, N. A., Crews, S., Martinez, S., Puelles, L., Rubenstein, J. L., and Tessier-Lavigne, M. 1996, "Expression patterns of

two murine homologs of Drosophila single-minded suggest possible roles in embryonic patterning and in the pathogenesis of Down syndrome", *Mol.Cell Neurosci.*, vol. 7, no. 1, pp. 1-16.

Fancy, S. P., Zhao, C., and Franklin, R. J. 2004, "Increased expression of Nkx2.2 and Olig2 identifies reactive oligodendrocyte progenitor cells responding to demyelination in the adult CNS", *Mol.Cell Neurosci.*, vol. 27, no. 3, pp. 247-254.

Feil, R., Wagner, J., Metzger, D., and Chambon, P. 1997, "Regulation of Cre recombinase activity by mutated estrogen receptor ligand-binding domains", *Biochem.Biophys.Res.Commun.*, vol. 237, no. 3, pp. 752-757.

Fisher, A. L. and Caudy, M. 1998, "Groucho proteins: transcriptional corepressors for specific subsets of DNA-binding transcription factors in vertebrates and invertebrates", *Genes Dev.*, vol. 12, no. 13, pp. 1931-1940.

Fogarty, M. 2006, *Fate-mapping the mouse neural tube by Cre-loxP transgenesis,* PhD, The Wolfson Institute for Biomedical Research, University College London.

Fogarty, M., Richardson, W. D., and Kessaris, N. 2005, "A subset of oligodendrocytes generated from radial glia in the dorsal spinal cord", *Development*, vol. 132, no. 8, pp. 1951-1959.

Forni, P. E., Scuoppo, C., Imayoshi, I., Taulli, R., Dastru, W., Sala, V., Betz, U. A., Muzzi, P., Martinuzzi, D., Vercelli, A. E., Kageyama, R., and Ponzetto, C. 2006, "High levels of Cre expression in neuronal progenitors cause defects in brain development leading to microencephaly and hydrocephaly", *J.Neurosci.*, vol. 26, no. 37, pp. 9593-9602.

Frisen, J., Johansson, C. B., Torok, C., Risling, M., and Lendahl, U. 1995, "Rapid, widespread, and longlasting induction of nestin contributes to the generation of glial scar tissue after CNS injury", *J Cell Biol.*, vol. 131, no. 2, pp. 453-464.

Fruttiger, M., Karlsson, L., Hall, A. C., Abramsson, A., Calver, A. R., Bostrom, H., Willetts, K., Bertold, C. H., Heath, J. K., Betsholtz, C., and Richardson, W. D. 1999, "Defective oligodendrocyte development and severe hypomyelination in PDGF-A knockout mice", *Development*, vol. 126, no. 3, pp. 457-467.

Fu, H., Cai, J., Clevers, H., Fast, E., Gray, S., Greenberg, R., Jain, M. K., Ma, Q., Qiu, M., Rowitch, D. H., Taylor, C. M., and Stiles, C. D. 2009, "A genome-wide screen for spatially restricted expression patterns identifies transcription factors that regulate glial development", *J.Neurosci.*, vol. 29, no. 36, pp. 11399-11408.

Fu, H., Qi, Y., Tan, M., Cai, J., Hu, X., Liu, Z., Jensen, J., and Qiu, M. 2003, "Molecular mapping of the origin of postnatal spinal cord ependymal cells: evidence that adult ependymal cells are derived from Nkx6.1+ ventral neural progenitor cells", *J.Comp Neurol.*, vol. 456, no. 3, pp. 237-244.

Fu, H., Qi, Y., Tan, M., Cai, J., Takebayashi, H., Nakafuku, M., Richardson, W., and Qiu, M. 2002, "Dual origin of spinal oligodendrocyte progenitors and evidence for the cooperative role of Olig2 and Nkx2.2 in the control of oligodendrocyte differentiation", *Development*, vol. 129, no. 3, pp. 681-693.

Fu, H. and Qiu, M. 2001, "Migration and differentiation of Nkx-2.2+ oligodendrocyte progenitors in embryonic chicken retina", *Brain Res.Dev.Brain Res.*, vol. 129, no. 1, pp. 115-118.

Fuccillo, M., Rallu, M., McMahon, A. P., and Fishell, G. 2004, "Temporal requirement for hedgehog signaling in ventral telencephalic patterning", *Development*, vol. 131, no. 20, pp. 5031-5040.

Furr, B. J. and Jordan, V. C. 1984, "The pharmacology and clinical uses of tamoxifen", *Pharmacol.Ther.*, vol. 25, no. 2, pp. 127-205.

Geiman, E. J., Zhang, Y., Narayan, S., and Goulding, M. Anatomical characterization of V3 interneuron subpopulations in the neonatal mouse spinal cord. Society for Neuroscience [252.10 . V5]. 15-10-2006.

Genethliou, N., Panayiotou, E., Panayi, H., Orford, M., Mean, R., Lapathitis, G., and Malas, S. 2009, "Spatially distinct functions of PAX6 and NKX2.2 during gliogenesis in the ventral spinal cord", *Biochem.Biophys.Res.Commun.*

Gilbert, S. F. 2000, *Developmental Biology*, 9th edn, Sunderland (Massachusetts): Sinauer Associates Inc..

Glinka, A., Wu, W., Onichtchouk, D., Blumenstock, C., and Niehrs, C. 1997, "Head induction by simultaneous repression of Bmp and Wnt signalling in Xenopus", *Nature*, vol. 389, no. 6650, pp. 517-519.

Goldman, J. E. 2001, "Developmental Origins of Astrocytes," in *Glial Cell Development*, Second Edition edn, W. D. Richardson & R. K. Jessen, eds., Oxford University Press, Oxford, New York, pp. 55-74.

Gotoh, H., Ono, K., Takebayashi, H., Harada, H., Nakamura, H., and Ikenaka, K. 2011, "Genetically-defined lineage tracing of Nkx2.2-expressing cells in chick spinal cord", *Dev.Biol.*, vol. 349, no. 2, pp. 504-511.

Goulding, M. 2009, "Circuits controlling vertebrate locomotion: moving in a new direction", *Nat.Rev.Neurosci.*, vol. 10, no. 7, pp. 507-518.

Goulding, M., Lanuza, G., Sapir, T., and Narayan, S. 2002, "The formation of sensorimotor circuits", *Curr.Opin.Neurobiol.*, vol. 12, no. 5, pp. 508-515.

Gray, G. E. and Sanes, J. R. 1992, "Lineage of radial glia in the chicken optic tectum", *Development*, vol. 114, no. 1, pp. 271-283.

Gregg, C. and Weiss, S. 2003, "Generation of functional radial glial cells by embryonic and adult forebrain neural stem cells", *J Neurosci.*, vol. 23, no. 37, pp. 11587-11601.

Grove, E. A., Williams, B. P., Li, D. Q., Hajihosseini, M., Friedrich, A., and Price, J. 1993, "Multiple restricted lineages in the embryonic rat cerebral cortex", *Development*, vol. 117, no. 2, pp. 553-561.

Guillemot, F. 2007a, "Cell fate specification in the mammalian telencephalon", *Prog.Neurobiol.*

Guillemot, F. 2007b, "Spatial and temporal specification of neural fates by transcription factor codes", *Development*, vol. 134, no. 21, pp. 3771-3780.

Guthrie, S. 2007, "Patterning and axon guidance of cranial motor neurons", *Nat.Rev.Neurosci.*, vol. 8, no. 11, pp. 859-871.

Hall, A., Giese, N. A., and Richardson, W. D. 1996, "Spinal cord oligodendrocytes develop from ventrally derived progenitor cells that express PDGF alpha-receptors", *Development*, vol. 122, no. 12, pp. 4085-4094.

Hartfuss, E., Galli, R., Heins, N., and Gotz, M. 2001, "Characterization of CNS precursor subtypes and radial glia", *Dev.Biol.*, vol. 229, no. 1, pp. 15-30.

Harvey, R. P. 1996, "NK-2 homeobox genes and heart development", *Dev.Biol.*, vol. 178, no. 2, pp. 203-216.

Hashimoto, H., Itoh, M., Yamanaka, Y., Yamashita, S., Shimizu, T., Solnica-Krezel, L., Hibi, M., and Hirano, T. 2000, "Zebrafish Dkk1 functions in forebrain specification and axial mesendoderm formation", *Dev.Biol.*, vol. 217, no. 1, pp. 138-152.

Hayashi, S. and McMahon, A. P. 2002, "Efficient recombination in diverse tissues by a tamoxifen-inducible form of Cre: a tool for temporally regulated gene activation/inactivation in the mouse", *Dev.Biol.*, vol. 244, no. 2, pp. 305-318.

Hebert, J. M. 2005, "Unraveling the molecular pathways that regulate early telencephalon development", *Curr.Top.Dev.Biol.*, vol. 69, pp. 17-37.

Hebert, J. M. and Fishell, G. 2008, "The genetics of early telencephalon patterning: some assembly required", *Nat.Rev.Neurosci.*, vol. 9, no. 9, pp. 678-685.

Henrique, D., Adam, J., Myat, A., Chitnis, A., Lewis, J., and Ish-Horowicz, D. 1995, "Expression of a Delta homologue in prospective neurons in the chick", *Nature*, vol. 375, no. 6534, pp. 787-790.

Hernandez, R. E., Rikhof, H. A., Bachmann, R., and Moens, C. B. 2004, "vhnf1 integrates global RA patterning and local FGF signals to direct posterior hindbrain development in zebrafish", *Development*, vol. 131, no. 18, pp. 4511-4520.

Hessabi, B., Schmidt, I., and Walther, R. 2000, "The homeodomain of Nkx2.2 carries two cooperatively acting nuclear localization signals", *Biochem.Biophys.Res.Commun.*, vol. 270, no. 3, pp. 695-700.

Hewett, J. A. 2009, "Determinants of regional and local diversity within the astroglial lineage of the normal central nervous system", *J.Neurochem.*, vol. 110, no. 6, pp. 1717-1736.

Higashijima, S., Schaefer, M., and Fetcho, J. R. 2004, "Neurotransmitter properties of spinal interneurons in embryonic and larval zebrafish", *J.Comp Neurol.*, vol. 480, no. 1, pp. 19-37.

Hochstim, C., Deneen, B., Lukaszewicz, A., Zhou, Q., and Anderson, D. J. 2008, "Identification of positionally distinct astrocyte subtypes whose identities are specified by a homeodomain code", *Cell*, vol. 133, no. 3, pp. 510-522.

Holz, A., Kollmus, H., Ryge, J., Niederkofler, V., Dias, J., Ericson, J., Stoeckli, E. T., Kiehn, O., and Arnold, H. H. 2010, "The transcription factors Nkx2.2 and Nkx2.9 play a novel role in floor plate development and commissural axon guidance", *Development*.

Hosoya, T., Takizawa, K., Nitta, K., and Hotta, Y. 1995, "glial cells missing: a binary switch between neuronal and glial determination in Drosophila", *Cell*, vol. 82, no. 6, pp. 1025-1036.

Hynes, M., Ye, W., Wang, K., Stone, D., Murone, M., Sauvage, F., and Rosenthal, A. 2000, "The seven-transmembrane receptor smoothened cell-autonomously induces multiple ventral cell types", *Nat.Neurosci.*, vol. 3, no. 1, pp. 41-46.

Imayoshi, I., Ohtsuka, T., Metzger, D., Chambon, P., and Kageyama, R. 2006, "Temporal regulation of Cre recombinase activity in neural stem cells", *Genesis.*, vol. 44, no. 5, pp. 233-238.

Imura, T., Tane, K., Toyoda, N., and Fushiki, S. 2008, "Endothelial cell-derived bone morphogenetic proteins regulate glial differentiation of cortical progenitors", *Eur.J Neurosci.*, vol. 27, no. 7, pp. 1596-1606.

Indra, A. K., Warot, X., Brocard, J., Bornert, J. M., Xiao, J. H., Chambon, P., and Metzger, D. 1999, "Temporally-controlled site-specific mutagenesis in the basal layer of the epidermis: comparison of the recombinase activity of the tamoxifen-inducible Cre-ER(T) and Cre-ER(T2) recombinases", *Nucleic Acids Res.*, vol. 27, no. 22, pp. 4324-4327.

Ioannou, P. A., Amemiya, C. T., Garnes, J., Kroisel, P. M., Shizuya, H., Chen, C., Batzer, M. A., and de Jong, P. J. 1994, "A new bacteriophage P1-derived vector for the propagation of large human DNA fragments", *Nat.Genet.*, vol. 6, no. 1, pp. 84-89.

Itoh, M., Kim, C. H., Palardy, G., Oda, T., Jiang, Y. J., Maust, D., Yeo, S. Y., Lorick, K., Wright, G. J., riza-McNaughton, L., Weissman, A. M., Lewis, J., Chandrasekharappa, S. C., and Chitnis, A. B. 2003, "Mind bomb is a ubiquitin ligase that is essential for efficient activation of Notch signaling by Delta", *Dev.Cell*, vol. 4, no. 1, pp. 67-82.

Jacob, J. and Briscoe, J. 2003, "Gli proteins and the control of spinal-cord patterning", *EMBO Rep.*, vol. 4, no. 8, pp. 761-765.

Jeong, J. and McMahon, A. P. 2005, "Growth and pattern of the mammalian neural tube are governed by partially overlapping feedback activities of the hedgehog antagonists patched 1 and Hhip1", *Development*, vol. 132, no. 1, pp. 143-154.

Jeong, Y., El-Jaick, K., Roessler, E., Muenke, M., and Epstein, D. J. 2006, "A functional screen for sonic hedgehog regulatory elements across a 1 Mb interval identifies long-range ventral forebrain enhancers", *Development*, vol. 133, no. 4, pp. 761-772.

Jessell, T. M. 2000, "Neuronal specification in the spinal cord: inductive signals and transcriptional codes", *Nat.Rev.Genet.*, vol. 1, no. 1, pp. 20-29.

Jessen, R. K. and Richardson, W. D. 2001, *Glial cell development*, Second edition edn, Oxford University Press.

Johansson, C. B., Momma, S., Clarke, D. L., Risling, M., Lendahl, U., and Frisen, J. 1999, "Identification of a neural stem cell in the adult mammalian central nervous system", *Cell*, vol. 96, no. 1, pp. 25-34.

Jones, B. W., Fetter, R. D., Tear, G., and Goodman, C. S. 1995, "glial cells missing: a genetic switch that controls glial versus neuronal fate", *Cell*, vol. 82, no. 6, pp. 1013-1023.

Joshi, K., Lee, S., Lee, B., Lee, J. W., and Lee, S. K. 2009, "LMO4 controls the balance between excitatory and inhibitory spinal V2 interneurons", *Neuron*, vol. 61, no. 6, pp. 839-851.

Joshi, S., Levatte, M. A., Dekaban, G. A., and Weaver, L. C. 1995, "Identification of spinal interneurons antecedent to adrenal sympathetic preganglionic neurons using trans-synaptic transport of herpes simplex virus type 1", *Neuroscience*, vol. 65, no. 3, pp. 893-903.

Kang, S. H., Fukaya, M., Yang, J. K., Rothstein, J. D., and Bergles, D. E. 2010, "NG2+ CNS glial progenitors remain committed to the oligodendrocyte lineage in postnatal life and following neurodegeneration", *Neuron*, vol. 68, no. 4, pp. 668-681.

Kania, A. and Jessell, T. M. 2003, "Topographic motor projections in the limb imposed by LIM homeodomain protein regulation of ephrin-A:EphA interactions", *Neuron*, vol. 38, no. 4, pp. 581-596.

Kania, A., Johnson, R. L., and Jessell, T. M. 2000, "Coordinate roles for LIM homeobox genes in directing the dorsoventral trajectory of motor axons in the vertebrate limb", *Cell*, vol. 102, no. 2, pp. 161-173.

Karunaratne, A., Hargrave, M., Poh, A., and Yamada, T. 2002, "GATA proteins identify a novel ventral interneuron subclass in the developing chick spinal cord", *Dev.Biol.*, vol. 249, no. 1, pp. 30-43.

Kerszberg, M. and Wolpert, L. 2007, "Specifying positional information in the embryo: looking beyond morphogens", *Cell*, vol. 130, no. 2, pp. 205-209.

Kessaris, N., Fogarty, M., Iannarelli, P., Grist, M., Wegner, M., and Richardson, W. D. 2006, "Competing waves of oligodendrocytes in the forebrain and postnatal elimination of an embryonic lineage", *Nat.Neurosci.*, vol. 9, no. 2, pp. 173-179.

Kessaris, N., Pringle, N., and Richardson, W. D. 2001, "Ventral neurogenesis and the neuron-glial switch", *Neuron*, vol. 31, no. 5, pp. 677-680.

Kiecker, C. and Niehrs, C. 2001, "A morphogen gradient of Wnt/beta-catenin signalling regulates anteroposterior neural patterning in Xenopus", *Development*, vol. 128, no. 21, pp. 4189-4201.

Kimura, S., Hara, Y., Pineau, T., Fernandez-Salguero, P., Fox, C. H., Ward, J. M., and Gonzalez, F. J. 1996, "The T/ebp null mouse: thyroid-specific enhancer-binding protein is essential for the organogenesis of the thyroid, lung, ventral forebrain, and pituitary", *Genes Dev.*, vol. 10, no. 1, pp. 60-69.

Kitada, M. and Rowitch, D. H. 2006, "Transcription factor co-expression patterns indicate heterogeneity of oligodendroglial subpopulations in adult spinal cord", *Glia*.

Kohlerova, E. and Skarda, J. 2004, "Mouse bioassay to assess oestrogenic and anti-oestrogenic compounds: hydroxytamoxifen, diethylstilbestrol and genistein", *J.Vet.Med.A Physiol Pathol.Clin.Med.*, vol. 51, no. 5, pp. 209-217.

Krauss, S., Concordet, J. P., and Ingham, P. W. 1993, "A functionally conserved homolog of the Drosophila segment polarity gene hh is expressed in tissues with polarizing activity in zebrafish embryos", *Cell*, vol. 75, no. 7, pp. 1431-1444.

Kriegstein, A. and Alvarez-Buylla, A. 2009, "The Glial Nature of Embryonic and Adult Neural Stem Cells", *Annu.Rev.Neurosci.*, vol. 32, pp. 149-184.

Kuhlbrodt, K., Herbarth, B., Sock, E., Hermans-Borgmeyer, I., and Wegner, M. 1998, "Sox10, a novel transcriptional modulator in glial cells", *J.Neurosci.*, vol. 18, no. 1, pp. 237-250.

Kurrasch, D. M., Cheung, C. C., Lee, F. Y., Tran, P. V., Hata, K., and Ingraham, H. A. 2007, "The neonatal ventromedial hypothalamus transcriptome reveals novel markers with spatially distinct patterning", *J.Neurosci.*, vol. 27, no. 50, pp. 13624-13634.

Lamb, T. M. and Harland, R. M. 1995, "Fibroblast growth factor is a direct neural inducer, which combined with noggin generates anterior-posterior neural pattern", *Development*, vol. 121, no. 11, pp. 3627-3636.

Lanuza, G. M., Gosgnach, S., Pierani, A., Jessell, T. M., and Goulding, M. 2004, "Genetic identification of spinal interneurons that coordinate left-right locomotor activity necessary for walking movements", *Neuron*, vol. 42, no. 3, pp. 375-386.

Le Douarin, N. M. 1969, "[Details of the interphase nucleus in Japanese quail (Coturnix coturnix japonica)]", *Bull.Biol.Fr.Belg.*, vol. 103, no. 3, pp. 435-452.

Le Douarin, N. M. and Barq, G. 1969, "[Use of Japanese quail cells as "biological markers" in experimental embryology]", *C.R.Acad Sci Hebd.Seances Acad Sci D.*, vol. 269, no. 16, pp. 1543-1546.

Le Douarin, N. M., Renaud, D., Teillet, M. A., and Le Douarin, G. H. 1975, "Cholinergic differentiation of presumptive adrenergic neuroblasts in interspecific chimeras after heterotopic transplantations", *Proc.Natl.Acad Sci U.S.A*, vol. 72, no. 2, pp. 728-732.

Leber, S. M., Breedlove, S. M., and Sanes, J. R. 1990, "Lineage, arrangement, and death of clonally related motoneurons in chick spinal cord", *J.Neurosci.*, vol. 10, no. 7, pp. 2451-2462.

Lee, E. C., Yu, D., Martinez, d., V, Tessarollo, L., Swing, D. A., Court DL, Jenkins, N. A., and Copeland, N. G. 2001, "A highly efficient Escherichia coli-based chromosome engineering system adapted for recombinogenic targeting and subcloning of BAC DNA", *Genomics*, vol. 73, no. 1, pp. 56-65.

Lee, K. J., Dietrich, P., and Jessell, T. M. 2000, "Genetic ablation reveals that the roof plate is essential for dorsal interneuron specification", *Nature*, vol. 403, no. 6771, pp. 734-740.

Lee, S. K., Jurata, L. W., Funahashi, J., Ruiz, E. C., and Pfaff, S. L. 2004, "Analysis of embryonic motoneuron gene regulation: derepression of general activators function in concert with enhancer factors", *Development*, vol. 131, no. 14, pp. 3295-3306.

Lee, S. K., Lee, B., Ruiz, E. C., and Pfaff, S. L. 2005, "Olig2 and Ngn2 function in opposition to modulate gene expression in motor neuron progenitor cells", *Genes Dev.*, vol. 19, no. 2, pp. 282-294.

Lei, Q., Jeong, Y., Misra, K., Li, S., Zelman, A. K., Epstein, D. J., and Matise, M. P. 2006, "Wnt signaling inhibitors regulate the transcriptional response to morphogenetic shh-gli signaling in the neural tube", *Dev.Cell*, vol. 11, no. 3, pp. 325-337.

Lek, M., Dias, J. M., Marklund, U., Uhde, C. W., Kurdija, S., Lei, Q., Sussel, L., Rubenstein, J. L., Matise, M. P., Arnold, H. H., Jessell, T. M., and Ericson, J. 2010, "A homeodomain feedback circuit underlies step-function interpretation of a Shh morphogen gradient during ventral neural patterning", *Development*, vol. 137, no. 23, pp. 4051-4060.

Lendahl, U., Zimmerman, L. B., and McKay, R. D. 1990, "CNS stem cells express a new class of intermediate filament protein", *Cell*, vol. 60, no. 4, pp. 585-595.

Lewis, K. E. 2006, "How do genes regulate simple behaviours? Understanding how different neurons in the vertebrate spinal cord are genetically specified", *Philos.Trans.R.Soc.Lond B Biol.Sci.*, vol. 361, no. 1465, pp. 45-66.

Li, H., Paes de, F. J., Andrew, P., Nitarska, J., and Richardson, W. D. 2011, "Phosphorylation Regulates OLIG2 Cofactor Choice and the Motor Neuron-Oligodendrocyte Fate Switch", *Neuron*, vol. 69, no. 5, pp. 918-929.

Liem, K. F., Jr., Jessell, T. M., and Briscoe, J. 2000, "Regulation of the neural patterning activity of sonic hedgehog by secreted BMP inhibitors expressed by notochord and somites", *Development*, vol. 127, no. 22, pp. 4855-4866.

Liem, K. F., Jr., Tremml, G., and Jessell, T. M. 1997, "A role for the roof plate and its resident TGFbeta-related proteins in neuronal patterning in the dorsal spinal cord", *Cell*, vol. 91, no. 1, pp. 127-138.

Liem, K. F., Jr., Tremml, G., Roelink, H., and Jessell, T. M. 1995, "Dorsal differentiation of neural plate cells induced by BMP-mediated signals from epidermal ectoderm", *Cell*, vol. 82, no. 6, pp. 969-979.

Lim, L., Zhou, H., and Costa, R. H. 1997, "The winged helix transcription factor HFH-4 is expressed during choroid plexus epithelial development in the mouse embryo", *Proc.Natl.Acad Sci U.S.A*, vol. 94, no. 7, pp. 3094-3099.

Lin, S. C. and Bergles, D. E. 2004, "Synaptic signaling between GABAergic interneurons and oligodendrocyte precursor cells in the hippocampus", *Nat.Neurosci.*, vol. 7, no. 1, pp. 24-32.

Lin, S. C., Huck, J. H., Roberts, J. D., Macklin, W. B., Somogyi, P., and Bergles, D. E. 2005, "Climbing fiber innervation of NG2-expressing glia in the mammalian cerebellum", *Neuron*, vol. 46, no. 5, pp. 773-785.

Lints, T. J., Parsons, L. M., Hartley, L., Lyons, I., and Harvey, R. P. 1993, "Nkx-2.5: a novel murine homeobox gene expressed in early heart progenitor cells and their myogenic descendants", *Development*, vol. 119, no. 2, pp. 419-431.

Lipton, A., Vinijsanun, A., and Martin, L. 1984, "Acute inhibition of rat myometrial responses to oxytocin by tamoxifen stereoisomers and oestradiol", *J.Endocrinol.*, vol. 103, no. 3, pp. 383-388.

Litingtung, Y. and Chiang, C. 2000, "Specification of ventral neuron types is mediated by an antagonistic interaction between Shh and Gli3", *Nat.Neurosci.*, vol. 3, no. 10, pp. 979-985.

Liu, F., Massague, J., and Altaba, A. 1998, "Carboxy-terminally truncated Gli3 proteins associate with Smads", *Nat.Genet.*, vol. 20, no. 4, pp. 325-326.

Liu, J. P., Laufer, E., and Jessell, T. M. 2001, "Assigning the positional identity of spinal motor neurons: rostrocaudal patterning of Hox-c expression by FGFs, Gdf11, and retinoids", *Neuron*, vol. 32, no. 6, pp. 997-1012.

Liu, Y. and Rao, M. 2003, "Oligodendrocytes, GRPs and MNOPs", *Trends Neurosci.*, vol. 26, no. 8, pp. 410-412.

Liu, Z., Hu, X., Cai, J., Liu, B., Peng, X., Wegner, M., and Qiu, M. 2007, "Induction of oligodendrocyte differentiation by Olig2 and Sox10: evidence for reciprocal interactions and dosage-dependent mechanisms", *Dev.Biol.*, vol. 302, no. 2, pp. 683-693.

Livet, J., Weissman, T. A., Kang, H., Draft, R. W., Lu, J., Bennis, R. A., Sanes, J. R., and Lichtman, J. W. 2007, "Transgenic strategies for combinatorial expression of fluorescent proteins in the nervous system", *Nature*, vol. 450, no. 7166, pp. 56-62.

Lobjois, V., Benazeraf, B., Bertrand, N., Medevielle, F., and Pituello, F. 2004, "Specific regulation of cyclins D1 and D2 by FGF and Shh signaling coordinates cell cycle progression, patterning, and differentiation during early steps of spinal cord development", *Dev.Biol.*, vol. 273, no. 2, pp. 195-209.

Loewy, A. D. 1990, "Anatomy of the Autonomic Nervous System: An Overview," in *Central Regulation of Autonomic Functions*, A. D. Loewy & K. M. Spyer, eds., Oxford University Press, Inc., New York, pp. 3-16.

Long, F., Zhang, X. M., Karp, S., Yang, Y., and McMahon, A. P. 2001, "Genetic manipulation of hedgehog signaling in the endochondral skeleton reveals a direct role in the regulation of chondrocyte proliferation", *Development*, vol. 128, no. 24, pp. 5099-5108.

Lu, Q. R., Sun, T., Zhu, Z., Ma, N., Garcia, M., Stiles, C. D., and Rowitch, D. H. 2002, "Common developmental requirement for Olig function indicates a motor neuron/oligodendrocyte connection", *Cell*, vol. 109, no. 1, pp. 75-86.

Lu, Q. R., Yuk, D., Alberta, J. A., Zhu, Z., Pawlitzky, I., Chan, J., McMahon, A. P., Stiles, C. D., and Rowitch, D. H. 2000, "Sonic hedgehog--regulated oligodendrocyte lineage genes encoding bHLH proteins in the mammalian central nervous system", *Neuron*, vol. 25, no. 2, pp. 317-329.

Lumsden, A. and Krumlauf, R. 1996, "Patterning the vertebrate neuraxis", *Science*, vol. 274, no. 5290, pp. 1109-1115.

Lundfald, L., Restrepo, C. E., Butt, S. J., Peng, C. Y., Droho, S., Endo, T., Zeilhofer, H. U., Sharma, K., and Kiehn, O. 2007, "Phenotype of V2-derived interneurons and their relationship to the axon guidance molecule EphA4 in the developing mouse spinal cord", *Eur.J.Neurosci.*, vol. 26, no. 11, pp. 2989-3002.

Lupo, G., Harris, W. A., and Lewis, K. E. 2006, "Mechanisms of ventral patterning in the vertebrate nervous system", *Nat.Rev.Neurosci.*, vol. 7, no. 2, pp. 103-114.

Malatesta, P., Appolloni, I., and Calzolari, F. 2007, "Radial glia and neural stem cells", *Cell Tissue Res.*

Malatesta, P., Hack, M. A., Hartfuss, E., Kettenmann, H., Klinkert, W., Kirchhoff, F., and Gotz, M. 2003, "Neuronal or glial progeny: regional differences in radial glia fate", *Neuron*, vol. 37, no. 5, pp. 751-764.

Malatesta, P., Hartfuss, E., and Gotz, M. 2000, "Isolation of radial glial cells by fluorescent-activated cell sorting reveals a neuronal lineage", *Development*, vol. 127, no. 24, pp. 5253-5263.

Mansouri, A. and Gruss, P. 1998, "Pax3 and Pax7 are expressed in commissural neurons and restrict ventral neuronal identity in the spinal cord", *Mech.Dev.*, vol. 78, no. 1-2, pp. 171-178.

Mao, X., Fujiwara, Y., Chapdelaine, A., Yang, H., and Orkin, S. H. 2001, "Activation of EGFP expression by Cre-mediated excision in a new ROSA26 reporter mouse strain", *Blood*, vol. 97, no. 1, pp. 324-326.

Markham, J. A., Phelps, P. E., and Vaughn, J. E. 1991, "Development of rostrocaudal dendritic bundles in rat thoracic spinal cord: analysis of cholinergic sympathetic preganglionic neurons", *Brain Res.Dev.Brain Res.*, vol. 61, no. 2, pp. 229-236.

Marti, E., Bumcrot, D. A., Takada, R., and McMahon, A. P. 1995, "Requirement of 19K form of Sonic hedgehog for induction of distinct ventral cell types in CNS explants", *Nature*, vol. 375, no. 6529, pp. 322-325.

Martinez, S. 2001, "The isthmic organizer and brain regionalization", *Int.J Dev.Biol.*, vol. 45, no. 1, pp. 367-371.

Masahira, N., Takebayashi, H., Ono, K., Watanabe, K., Ding, L., Furusho, M., Ogawa, Y., Nabeshima, Y., varez-Buylla, A., Shimizu, K., and Ikenaka, K. 2006, "Olig2-positive progenitors in the embryonic spinal cord give rise not only to motoneurons and oligodendrocytes, but also to a subset of astrocytes and ependymal cells", *Dev.Biol.*, vol. 293, no. 2, pp. 358-369.

Mason, I. 2007, "Initiation to end point: the multiple roles of fibroblast growth factors in neural development", *Nat.Rev.Neurosci.*, vol. 8, no. 8, pp. 583-596.

Mathis, L., Bonnerot, C., Puelles, L., and Nicolas, J. F. 1997, "Retrospective clonal analysis of the cerebellum using genetic laacZ/lacZ mouse mosaics", *Development*, vol. 124, no. 20, pp. 4089-4104.

Matus, A. and Mughal, S. 1975, "Immunohistochemical localisation of S-100 protein in brain", *Nature*, vol. 258, no. 5537, pp. 746-748.

McCarthy, M., Turnbull, D. H., Walsh, C. A., and Fishell, G. 2001, "Telencephalic neural progenitors appear to be restricted to regional and glial fates before the onset of neurogenesis", *J.Neurosci.*, vol. 21, no. 17, pp. 6772-6781.

McConnell, S. K. 1988, "Fates of visual cortical neurons in the ferret after isochronic and heterochronic transplantation", *J Neurosci.*, vol. 8, no. 3, pp. 945-974.

McDonnell, D. P., Wijayaratne, A., Chang, C. Y., and Norris, J. D. 2002, "Elucidation of the molecular mechanism of action of selective estrogen receptor modulators", *Am.J.Cardiol.*, vol. 90, no. 1A, pp. 35F-43F.

McKenna, S. E., Simon, N. G., and Cologer-Clifford, A. 1992, "An assessment of agonist/antagonist effects of tamoxifen in the female mouse brain", *Horm.Behav.*, vol. 26, no. 4, pp. 536-544.

McMahon, A. P., Joyner, A. L., Bradley, A., and McMahon, J. A. 1992, "The midbrain-hindbrain phenotype of Wnt-1-/Wnt-1- mice results from stepwise deletion of engrailed-expressing cells by 9.5 days postcoitum", *Cell*, vol. 69, no. 4, pp. 581-595.

McMahon, J. A., Takada, S., Zimmerman, L. B., Fan, C. M., Harland, R. M., and McMahon, A. P. 1998, "Noggin-mediated antagonism of BMP signaling is required for growth and patterning of the neural tube and somite", *Genes Dev.*, vol. 12, no. 10, pp. 1438-1452.

Meletis, K., Barnabe-Heider, F., Carlen, M., Evergren, E., Tomilin, N., Shupliakov, O., and Frisen, J. 2008, "Spinal cord injury reveals multilineage differentiation of ependymal cells", *PLoS.Biol.*, vol. 6, no. 7, p. e182.

Merkle, F. T., Tramontin, A. D., Garcia-Verdugo, J. M., and varez-Buylla, A. 2004, "Radial glia give rise to adult neural stem cells in the subventricular zone", *Proc.Natl.Acad.Sci.U.S.A*, vol. 101, no. 50, pp. 17528-17532.

Meyer, N. P. and Roelink, H. 2003, "The amino-terminal region of Gli3 antagonizes the Shh response and acts in dorsoventral fate specification in the developing spinal cord", *Dev.Biol.*, vol. 257, no. 2, pp. 343-355.

Miles, G. B., Hartley, R., Todd, A. J., and Brownstone, R. M. 2007, "Spinal cholinergic interneurons regulate the excitability of motoneurons during locomotion", *Proc.Natl.Acad.Sci.U.S.A*, vol. 104, no. 7, pp. 2448-2453.

Miller, F. D. and Gauthier, A. S. 2007, "Timing is everything: making neurons versus glia in the developing cortex", *Neuron*, vol. 54, no. 3, pp. 357-369.

Miller, R. H. 2002, "Regulation of oligodendrocyte development in the vertebrate CNS", *Prog.Neurobiol.*, vol. 67, no. 6, pp. 451-467.

Miller, R. H., Payne, J., Milner, L., Zhang, H., and Orentas, D. M. 1997, "Spinal cord oligodendrocytes develop from a limited number of migratory highly proliferative precursors", *J.Neurosci.Res.*, vol. 50, no. 2, pp. 157-168.

Milligan, S. R. and Finn, C. A. 1997, "Minimal progesterone support required for the maintenance of pregnancy in mice", *Hum.Reprod.*, vol. 12, no. 3, pp. 602-607.

Mirzadeh, Z., Merkle, F. T., Soriano-Navarro, M., Garcia-Verdugo, J. M., and varez-Buylla, A. 2008, "Neural stem cells confer unique pinwheel architecture to the ventricular surface in neurogenic regions of the adult brain", *Cell Stem Cell*, vol. 3, no. 3, pp. 265-278.

Misson, J. P., Edwards, M. A., Yamamoto, M., and Caviness, V. S., Jr. 1988, "Mitotic cycling of radial glial cells of the fetal murine cerebral wall: a combined autoradiographic and immunohistochemical study", *Dev.Brain Res.*, vol. 38, no. 2, pp. 183-190.

Misson, J. P., Takahashi, T., and Caviness, V. S., Jr. 1991, "Ontogeny of radial and other astroglial cells in murine cerebral cortex", *Glia*, vol. 4, no. 2, pp. 138-148.

Miyata, T., Kawaguchi, A., Okano, H., and Ogawa, M. 2001, "Asymmetric inheritance of radial glial fibers by cortical neurons", *Neuron*, vol. 31, no. 5, pp. 727-741.

Miyata, T., Kawaguchi, A., Saito, K., Kawano, M., Muto, T., and Ogawa, M. 2004, "Asymmetric production of surface-dividing and non-surface-dividing cortical progenitor cells", *Development*, vol. 131, no. 13, pp. 3133-3145.

Mizuguchi, R., Sugimori, M., Takebayashi, H., Kosako, H., Nagao, M., Yoshida, S., Nabeshima, Y., Shimamura, K., and Nakafuku, M. 2001, "Combinatorial roles of olig2 and neurogenin2 in the coordinated induction of pan-neuronal and subtype-specific properties of motoneurons", *Neuron*, vol. 31, no. 5, pp. 757-771.

Molecular Probes (Invitrogen). Lipophilic Tracers - DiI, DiO, DiD, DiA, and DiR. 25-10-2007.

Moran-Rivard, L., Kagawa, T., Saueressig, H., Gross, M. K., Burrill, J., and Goulding, M. 2001, "Evx1 is a postmitotic determinant of v0 interneuron identity in the spinal cord", *Neuron*, vol. 29, no. 2, pp. 385-399.

Muhr, J., Andersson, E., Persson, M., Jessell, T. M., and Ericson, J. 2001, "Groucho-mediated transcriptional repression establishes progenitor cell pattern and neuronal fate in the ventral neural tube", *Cell*, vol. 104, no. 6, pp. 861-873.

Muldoon, T. G. 1987, "Prolactin mediation of estrogen-induced changes in mammary tissue estrogen and progesterone receptors", *Endocrinology*, vol. 121, no. 1, pp. 141-149.

Mullen, R. J., Buck, C. R., and Smith, A. M. 1992, "NeuN, a neuronal specific nuclear protein in vertebrates", *Development*, vol. 116, no. 1, pp. 201-211.

Mullenbach, R., Lagoda, P. J., and Welter, C. 1989, "An efficient salt-chloroform extraction of DNA from blood and tissues", *Trends Genet.*, vol. 5, no. 12, p. 391.

Munoz-Sanjuan, I. and Brivanlou, A. H. 2002, "Neural induction, the default model and embryonic stem cells", *Nat.Rev.Neurosci.*, vol. 3, no. 4, pp. 271-280.

Muroyama, Y., Fujiwara, Y., Orkin, S. H., and Rowitch, D. H. 2005, "Specification of astrocytes by bHLH protein SCL in a restricted region of the neural tube", *Nature*, vol. 438, no. 7066, pp. 360-363.

Nagy, A. 2000, "Cre recombinase: the universal reagent for genome tailoring", *Genesis.*, vol. 26, no. 2, pp. 99-109.

Nagy, A., Gertsentein M, Vintersten K, and Behringer, R. 2001, "Surgical Procedure: protocol 5 - Caesarean section and fostering," in *Manipulating the mouse embryo - a laboratory manual*, 3rd edn, pp. 272-273.

Nakashima, K., Takizawa, T., Ochiai, W., Yanagisawa, M., Hisatsune, T., Nakafuku, M., Miyazono, K., Kishimoto, T., Kageyama, R., and Taga, T. 2001, "BMP2-mediated alteration in the developmental pathway of fetal mouse brain cells from neurogenesis to astrocytogenesis", *Proc.Natl.Acad.Sci.U.S.A*, vol. 98, no. 10, pp. 5868-5873.

Nicolas, J. F., Mathis, L., Bonnerot, C., and Saurin, W. 1996, "Evidence in the mouse for self-renewing stem cells in the formation of a segmented longitudinal structure, the myotome", *Development*, vol. 122, no. 9, pp. 2933-2946.

Nieto, M., Schuurmans, C., Britz, O., and Guillemot, F. 2001, "Neural bHLH genes control the neuronal versus glial fate decision in cortical progenitors", *Neuron*, vol. 29, no. 2, pp. 401-413.

Nishi, Y., Ji, H., Wong, W. H., McMahon, A. P., and Vokes, S. A. 2009, "Modeling the spatio-temporal network that drives patterning in the vertebrate central nervous system", *Biochim.Biophys.Acta*, vol. 1789, no. 4, pp. 299-305.

Noctor, S. C., Martinez-Cerdeno, V., Ivic, L., and Kriegstein, A. R. 2004, "Cortical neurons arise in symmetric and asymmetric division zones and migrate through specific phases", *Nat.Neurosci.*, vol. 7, no. 2, pp. 136-144.

Noctor, S. C., Martinez-Cerdeno, V., and Kriegstein, A. R. 2008, "Distinct behaviors of neural stem and progenitor cells underlie cortical neurogenesis", *J.Comp Neurol.*, vol. 508, no. 1, pp. 28-44.

Nolte, C., Matyash, M., Pivneva, T., Schipke, C. G., Ohlemeyer, C., Hanisch, U. K., Kirchhoff, F., and Kettenmann, H. 2001, "GFAP promoter-controlled EGFP-expressing transgenic mice: a tool to visualize astrocytes and astrogliosis in living brain tissue", *Glia*, vol. 33, no. 1, pp. 72-86.

Nordstrom, U., Jessell, T. M., and Edlund, T. 2002, "Progressive induction of caudal neural character by graded Wnt signaling", *Nat.Neurosci.*, vol. 5, no. 6, pp. 525-532.

Novak, A., Guo, C., Yang, W., Nagy, A., and Lobe, C. G. 2000, "Z/EG, a double reporter mouse line that expresses enhanced green fluorescent protein upon Cre-mediated excision", *Genesis.*, vol. 28, no. 3-4, pp. 147-155.

Novitch, B. G., Chen, A. I., and Jessell, T. M. 2001, "Coordinate regulation of motor neuron subtype identity and pan-neuronal properties by the bHLH repressor Olig2", *Neuron*, vol. 31, no. 5, pp. 773-789.

Novitch, B. G., Wichterle, H., Jessell, T. M., and Sockanathan, S. 2003, "A requirement for retinoic acid-mediated transcriptional activation in ventral neural patterning and motor neuron specification", *Neuron*, vol. 40, no. 1, pp. 81-95.

Nowakowski, R. S. and Rakic, P. 1981, "The site of origin and route and rate of migration of neurons to the hippocampal region of the rhesus monkey", *J Comp Neurol.*, vol. 196, no. 1, pp. 129-154.

Nutt, S. L. and Busslinger, M. 1999, "Monoallelic expression of Pax5: a paradigm for the haploinsufficiency of mammalian Pax genes?", *Biol.Chem.*, vol. 380, no. 6, pp. 601-611.

Ong, W. Y. and Levine, J. M. 1999, "A light and electron microscopic study of NG2 chondroitin sulfate proteoglycan-positive oligodendrocyte precursor cells in the normal and kainate-lesioned rat hippocampus", *Neuroscience*, vol. 92, no. 1, pp. 83-95.

Orentas, D. M., Hayes, J. E., Dyer, K. L., and Miller, R. H. 1999, "Sonic hedgehog signaling is required during the appearance of spinal cord oligodendrocyte precursors", *Development*, vol. 126, no. 11, pp. 2419-2429.

Osumi, N., Hirota, A., Ohuchi, H., Nakafuku, M., Iimura, T., Kuratani, S., Fujiwara, M., Noji, S., and Eto, K. 1997, "Pax-6 is involved in the specification of hindbrain motor neuron subtype", *Development*, vol. 124, no. 15, pp. 2961-2972.

Pabst, O., Herbrand, H., and Arnold, H. H. 1998, "Nkx2-9 is a novel homeobox transcription factor which demarcates ventral domains in the developing mouse CNS", *Mech.Dev.*, vol. 73, no. 1, pp. 85-93.

Pabst, O., Rummelies, J., Winter, B., and Arnold, H. H. 2003, "Targeted disruption of the homeobox gene Nkx2.9 reveals a role in development of the spinal accessory nerve", *Development*, vol. 130, no. 6, pp. 1193-1202.

Panayi, H., Panayiotou, E., Orford, M., Genethliou, N., Mean, R., Lapathitis, G., Li, S., Xiang, M., Kessaris, N., Richardson, W. D., and Malas, S. 2010, "Sox1 is required for the specification of a novel p2-derived interneuron subtype in the mouse ventral spinal cord", *J Neurosci.*, vol. 30, no. 37, pp. 12274-12280.

Park, H. C. and Appel, B. 2003, "Delta-Notch signaling regulates oligodendrocyte specification", *Development*, vol. 130, no. 16, pp. 3747-3755.

Parnell, S. E., Dehart, D. B., Wills, T. A., Chen, S. Y., Hodge, C. W., Besheer, J., Waage-Baudet, H. G., Charness, M. E., and Sulik, K. K. 2006, "Maternal oral intake mouse model for fetal alcohol spectrum disorders: ocular defects as a measure of effect", *Alcohol Clin.Exp.Res.*, vol. 30, no. 10, pp. 1791-1798.

Patten, I. and Placzek, M. 2002, "Opponent activities of Shh and BMP signaling during floor plate induction in vivo", *Curr.Biol.*, vol. 12, no. 1, pp. 47-52.

Pattyn, A., Hirsch, M., Goridis, C., and Brunet, J. F. 2000, "Control of hindbrain motor neuron differentiation by the homeobox gene Phox2b", *Development*, vol. 127, no. 7, pp. 1349-1358.

Pattyn, A., Vallstedt, A., Dias, J. M., Samad, O. A., Krumlauf, R., Rijli, F. M., Brunet, J. F., and Ericson, J. 2003a, "Coordinated temporal and spatial control of motor neuron and serotonergic neuron generation from a common pool of CNS progenitors", *Genes Dev.*, vol. 17, no. 6, pp. 729-737.

Pattyn, A., Vallstedt, A., Dias, J. M., Sander, M., and Ericson, J. 2003b, "Complementary roles for Nkx6 and Nkx2 class proteins in the establishment of motoneuron identity in the hindbrain", *Development*, vol. 130, no. 17, pp. 4149-4159.

Peng, C. Y., Yajima, H., Burns, C. E., Zon, L. I., Sisodia, S. S., Pfaff, S. L., and Sharma, K. 2007, "Notch and MAML signaling drives Scl-dependent interneuron diversity in the spinal cord", *Neuron*, vol. 53, no. 6, pp. 813-827.

Pfaff, S. L., Mendelsohn, M., Stewart, C. L., Edlund, T., and Jessell, T. M. 1996, "Requirement for LIM homeobox gene Isl1 in motor neuron generation reveals a motor neuron-dependent step in interneuron differentiation", *Cell*, vol. 84, no. 2, pp. 309-320.

Picard, D. 1994, "Regulation of protein function through expression of chimaeric proteins", *Curr.Opin.Biotechnol.*, vol. 5, no. 5, pp. 511-515.

Pierani, A., Brenner-Morton, S., Chiang, C., and Jessell, T. M. 1999, "A sonic hedgehog-independent, retinoid-activated pathway of neurogenesis in the ventral spinal cord", *Cell*, vol. 97, no. 7, pp. 903-915.

Pierani, A., Moran-Rivard, L., Sunshine, M. J., Littman, D. R., Goulding, M., and Jessell, T. M. 2001, "Control of interneuron fate in the developing spinal cord by the progenitor homeodomain protein Dbx1", *Neuron*, vol. 29, no. 2, pp. 367-384.

Pierfelice, T., Alberi, L., and Gaiano, N. 2011, "Notch in the vertebrate nervous system: an old dog with new tricks", *Neuron*, vol. 69, no. 5, pp. 840-855.

Placzek, M. and Briscoe, J. 2005, "The floor plate: multiple cells, multiple signals", *Nat.Rev.Neurosci.*, vol. 6, no. 3, pp. 230-240.

Pompolo, S. and Harley, V. R. 2001, "Localisation of the SRY-related HMG box protein, SOX9, in rodent brain", *Brain Res.*, vol. 906, no. 1-2, pp. 143-148.

Poncet, C., Soula, C., Trousse, F., Kan, P., Hirsinger, E., Pourquie, O., Duprat, A. M., and Cochard, P. 1996, "Induction of oligodendrocyte progenitors in the trunk neural tube by ventralizing signals: effects of notochord and floor plate grafts, and of sonic hedgehog", *Mech.Dev.*, vol. 60, no. 1, pp. 13-32.

Pownall, M. E., Tucker, A. S., Slack, J. M., and Isaacs, H. V. 1996, "eFGF, Xcad3 and Hox genes form a molecular pathway that establishes the anteroposterior axis in Xenopus", *Development*, vol. 122, no. 12, pp. 3881-3892.

Price, J., Turner, D., and Cepko, C. 1987, "Lineage analysis in the vertebrate nervous system by retrovirus-mediated gene transfer", *Proc.Natl.Acad.Sci.U.S.A*, vol. 84, no. 1, pp. 156-160.

Price, M., Lazzaro, D., Pohl, T., Mattei, M. G., Ruther, U., Olivo, J. C., Duboule, D., and Di, L. R. 1992, "Regional expression of the homeobox gene Nkx-2.2 in the developing mammalian forebrain", *Neuron*, vol. 8, no. 2, pp. 241-255.

Pringle, N. P., Guthrie, S., Lumsden, A., and Richardson, W. D. 1998, "Dorsal spinal cord neuroepithelium generates astrocytes but not oligodendrocytes", *Neuron*, vol. 20, no. 5, pp. 883-893.

Pringle, N. P., Mudhar, H. S., Collarini, E. J., and Richardson, W. D. 1992, "PDGF receptors in the rat CNS: during late neurogenesis, PDGF alpha-receptor expression appears to be restricted to glial cells of the oligodendrocyte lineage", *Development*, vol. 115, no. 2, pp. 535-551.

Pringle, N. P. and Richardson, W. D. 1993, "A singularity of PDGF alpha-receptor expression in the dorsoventral axis of the neural tube may define the origin of the oligodendrocyte lineage", *Development*, vol. 117, no. 2, pp. 525-533.

Pringle, N. P., Yu, W. P., Guthrie, S., Roelink, H., Lumsden, A., Peterson, A. C., and Richardson, W. D. 1996, "Determination of neuroepithelial cell fate: induction of the oligodendrocyte lineage by ventral midline cells and sonic hedgehog", *Dev.Biol.*, vol. 177, no. 1, pp. 30-42.

Psachoulia, K., Jamen, F., Young, K. M., and Richardson, W. D. 2009, "Cell cycle dynamics of NG2 cells in the postnatal and ageing brain", *Neuron Glia Biol.*, vol. 5, no. 3-4, pp. 57-67.

Qi, Y., Cai, J., Wu, Y., Wu, R., Lee, J., Fu, H., Rao, M., Sussel, L., Rubenstein, J., and Qiu, M. 2001, "Control of oligodendrocyte differentiation by the Nkx2.2 homeodomain transcription factor", *Development*, vol. 128, no. 14, pp. 2723-2733.

Qian, X., Shen, Q., Goderie, S. K., He, W., Capela, A., Davis, A. A., and Temple, S. 2000, "Timing of CNS cell generation: a programmed sequence of neuron and glial cell production from isolated murine cortical stem cells", *Neuron*, vol. 28, no. 1, pp. 69-80.

Rakic, P. 1995, "A small step for the cell, a giant leap for mankind: a hypothesis of neocortical expansion during evolution", *Trends Neurosci.*, vol. 18, no. 9, pp. 383-388.

Rakic, P. 2003, "Elusive radial glial cells: historical and evolutionary perspective", *Glia*, vol. 43, no. 1, pp. 19-32.

Rao, M. S., Noble, M., and Mayer-Proschel, M. 1998, "A tripotential glial precursor cell is present in the developing spinal cord", *Proc.Natl.Acad Sci U.S.A*, vol. 95, no. 7, pp. 3996-4001.

Reichenbach, A., Derouiche, A., and Kirchhoff, F. 2010, "Morphology and dynamics of perisynaptic glia", *Brain Res.Rev.*, vol. 63, no. 1-2, pp. 11-25.

Reuss, M. H. and Reuss, S. 2001, "Nitric oxide synthase neurons in the rodent spinal cord: distribution, relation to Substance P fibers, and effects of dorsal rhizotomy", *J.Chem.Neuroanat.*, vol. 21, no. 2, pp. 181-196.

Ribes, V. The temporal dynamics of Sonic Hedgehog signaling and pattern formation in the ventral spinal cord. 19-5-2010. Venue: University College London, Host: Glenda Young.

Ribes, V., Balaskas, N., Sasai, N., Cruz, C., Dessaud, E., Cayuso, J., Tozer, S., Yang, L. L., Novitch, B., Marti, E., and Briscoe, J. 2010, "Distinct Sonic Hedgehog signaling dynamics specify floor plate and ventral neuronal progenitors in the vertebrate neural tube", *Genes Dev.*, vol. 24, no. 11, pp. 1186-1200.

Ribes, V. and Briscoe, J. 2009, "Establishing and Interpreting Graded Sonic Hedgehog Signaling during Vertebrate Neural Tube Patterning: The Role of Negative Feedback", *Cold Spring Harb.Perspect.Biol.*, vol. 1, no. 2, p. a002014.

Richardson, W. D., Kessaris, N., and Pringle, N. 2006, "Oligodendrocyte wars", *Nat.Rev.Neurosci.*, vol. 7, no. 1, pp. 11-18.

Richardson, W. D., Pringle, N. P., Yu, W. P., and Hall, A. C. 1997, "Origins of spinal cord oligodendrocytes: possible developmental and evolutionary relationships with motor neurons", *Dev.Neurosci.*, vol. 19, no. 1, pp. 58-68.

Richardson, W. D., Smith, H. K., Sun, T., Pringle, N. P., Hall, A., and Woodruff, R. 2000, "Oligodendrocyte lineage and the motor neuron connection", *Glia*, vol. 29, no. 2, pp. 136-142.

Richardson, W. D., Young, K. M., Tripathi, R. B., and McKenzie, I. 2011, "NG2-glia as Multipotent Neural Stem Cells: Fact or Fantasy?", *Neuron*, vol. 70, no. 4, pp. 661-673.

Rivers, L. E., Young, K. M., Rizzi, M., Jamen, F., Psachoulia, K., Wade, A., Kessaris, N., and Richardson, W. D. 2008, "PDGFRA/NG2 glia generate myelinating oligodendrocytes and piriform projection neurons in adult mice", *Nat.Neurosci.*, vol. 11, no. 12, pp. 1392-1401.

Robinson, S. P., Langan-Fahey, S. M., Johnson, D. A., and Jordan, V. C. 1991, "Metabolites, pharmacodynamics, and pharmacokinetics of tamoxifen in rats and mice compared to the breast cancer patient", *Drug Metab Dispos.*, vol. 19, no. 1, pp. 36-43.

Roelink, H., Porter, J. A., Chiang, C., Tanabe, Y., Chang, D. T., Beachy, P. A., and Jessell, T. M. 1995, "Floor plate and motor neuron induction by different concentrations of the amino-terminal cleavage product of sonic hedgehog autoproteolysis", *Cell*, vol. 81, no. 3, pp. 445-455.

Ross, S. E., Greenberg, M. E., and Stiles, C. D. 2003, "Basic helix-loop-helix factors in cortical development", *Neuron*, vol. 39, no. 1, pp. 13-25.

Rousso, D. L., Gaber, Z. B., Wellik, D., Morrisey, E. E., and Novitch, B. G. 2008, "Coordinated actions of the forkhead protein Foxp1 and Hox proteins in the columnar organization of spinal motor neurons", *Neuron*, vol. 59, no. 2, pp. 226-240.

Rowitch, D. H. 2004, "Glial specification in the vertebrate neural tube", *Nat.Rev.Neurosci.*, vol. 5, no. 5, pp. 409-419.

Rudnick, A., Ling, T. Y., Odagiri, H., Rutter, W. J., and German, M. S. 1994, "Pancreatic beta cells express a diverse set of homeobox genes", *Proc.Natl.Acad.Sci.U.S.A*, vol. 91, no. 25, pp. 12203-12207.

Sadek, S. and Bell, S. C. 1996, "The effects of the antihormones RU486 and tamoxifen on fetoplacental development and placental bed vascularisation in the rat: a model for intrauterine fetal growth retardation", *Br.J.Obstet.Gynaecol.*, vol. 103, no. 7, pp. 630-641.

Sairam, M. R., Danilovich, N., and Lussier-Cacan, S. 2002, "The FORKO mouse as a genetic model for exploring estrogen replacement therapy", *J.Reprod.Med.*, vol. 47, no. 5, pp. 412-418.

Sambrook, J. and Russell, D. 2001, *Molecular Cloning: a laboratory manual*, Third edn, Cold Spring Harbor Laboratory Press.

Sander, K. and Faessler, P. E. 2001, "Introducing the Spemann-Mangold organizer: experiments and insights that generated a key concept in developmental biology", *Int.J Dev.Biol.*, vol. 45, no. 1, pp. 1-11.

Sander, M., Paydar, S., Ericson, J., Briscoe, J., Berber, E., German, M., Jessell, T. M., and Rubenstein, J. L. 2000, "Ventral neural patterning by Nkx homeobox genes: Nkx6.1 controls somatic motor neuron and ventral interneuron fates", *Genes Dev.*, vol. 14, no. 17, pp. 2134-2139.

Sapir, T., Geiman, E. J., Wang, Z., Velasquez, T., Mitsui, S., Yoshihara, Y., Frank, E., Alvarez, F. J., and Goulding, M. 2004, "Pax6 and engrailed 1 regulate two distinct aspects of renshaw cell development", *J.Neurosci.*, vol. 24, no. 5, pp. 1255-1264.

Sari, Y. and Zhou, F. C. 2004, "Prenatal alcohol exposure causes long-term serotonin neuron deficit in mice", *Alcohol Clin.Exp.Res.*, vol. 28, no. 6, pp. 941-948.

Saueressig, H., Burrill, J., and Goulding, M. 1999, "Engrailed-1 and netrin-1 regulate axon pathfinding by association interneurons that project to motor neurons", *Development*, vol. 126, no. 19, pp. 4201-4212.

Scardigli, R., Schuurmans, C., Gradwohl, G., and Guillemot, F. 2001, "Crossregulation between Neurogenin2 and pathways specifying neuronal identity in the spinal cord", *Neuron*, vol. 31, no. 2, pp. 203-217.

Schmechel, D. E. and Rakic, P. 1979, "A Golgi study of radial glial cells in developing monkey telencephalon: morphogenesis and transformation into astrocytes", *Anat.Embryol.(Berl)*, vol. 156, no. 2, pp. 115-152.

Schmidt, E. E., Taylor, D. S., Prigge, J. R., Barnett, S., and Capecchi, M. R. 2000, "Illegitimate Cre-dependent chromosome rearrangements in transgenic mouse spermatids", *Proc.Natl.Acad.Sci.U.S.A*, vol. 97, no. 25, pp. 13702-13707.

Schonhoff, S. E., Giel-Moloney, M., and Leiter, A. B. 2004, "Neurogenin 3-expressing progenitor cells in the gastrointestinal tract differentiate into both endocrine and non-endocrine cell types", *Dev.Biol.*, vol. 270, no. 2, pp. 443-454.

Sharma, K., Leonard, A. E., Lettieri, K., and Pfaff, S. L. 2000, "Genetic and epigenetic mechanisms contribute to motor neuron pathfinding", *Nature*, vol. 406, no. 6795, pp. 515-519.

Sharma, K., Sheng, H. Z., Lettieri, K., Li, H., Karavanov, A., Potter, S., Westphal, H., and Pfaff, S. L. 1998, "LIM homeodomain factors Lhx3 and Lhx4 assign subtype identities for motor neurons", *Cell*, vol. 95, no. 6, pp. 817-828.

Shimamura, K., Hartigan, D. J., Martinez, S., Puelles, L., and Rubenstein, J. L. 1995, "Longitudinal organization of the anterior neural plate and neural tube", *Development*, vol. 121, no. 12, pp. 3923-3933.

Small, E. M., Vokes, S. A., Garriock, R. J., Li, D., and Krieg, P. A. 2000, "Developmental expression of the Xenopus Nkx2-1 and Nkx2-4 genes", *Mech.Dev.*, vol. 96, no. 2, pp. 259-262.

Smith, E., Hargrave, M., Yamada, T., Begley, C. G., and Little, M. H. 2002, "Coexpression of SCL and GATA3 in the V2 interneurons of the developing mouse spinal cord", *Dev.Dyn.*, vol. 224, no. 2, pp. 231-237.

Sockanathan, S. and Jessell, T. M. 1998, "Motor neuron-derived retinoid signaling specifies the subtype identity of spinal motor neurons", *Cell*, vol. 94, no. 4, pp. 503-514.

Sockanathan, S., Perlmann, T., and Jessell, T. M. 2003, "Retinoid receptor signaling in postmitotic motor neurons regulates rostrocaudal positional identity and axonal projection pattern", *Neuron*, vol. 40, no. 1, pp. 97-111.

Sommer, L., Ma, Q., and Anderson, D. J. 1996, "neurogenins, a novel family of atonal-related bHLH transcription factors, are putative mammalian neuronal determination genes that reveal progenitor cell heterogeneity in the developing CNS and PNS", *Mol.Cell Neurosci.*, vol. 8, no. 4, pp. 221-241.

Song, M. R., Shirasaki, R., Cai, C. L., Ruiz, E. C., Evans, S. M., Lee, S. K., and Pfaff, S. L. 2006, "T-Box transcription factor Tbx20 regulates a genetic program for cranial motor neuron cell body migration", *Development*, vol. 133, no. 24, pp. 4945-4955.

Soriano, P. 1999, "Generalized lacZ expression with the ROSA26 Cre reporter strain", *Nat.Genet.*, vol. 21, no. 1, pp. 70-71.

Soula, C., Danesin, C., Kan, P., Grob, M., Poncet, C., and Cochard, P. 2001, "Distinct sites of origin of oligodendrocytes and somatic motoneurons in the chick spinal cord: oligodendrocytes arise from Nkx2.2-expressing progenitors by a Shh-dependent mechanism", *Development*, vol. 128, no. 8, pp. 1369-1379.

Sousa, V. H. and Fishell, G. 2010, "Sonic hedgehog functions through dynamic changes in temporal competence in the developing forebrain", *Curr.Opin.Genet.Dev.*

Spassky, N., Goujet-Zalc, C., Parmantier, E., Olivier, C., Martinez, S., Ivanova, A., Ikenaka, K., Macklin, W., Cerruti, I., Zalc, B., and Thomas, J. L. 1998, "Multiple restricted origin of oligodendrocytes", *J.Neurosci.*, vol. 18, no. 20, pp. 8331-8343.

Spassky, N., Merkle, F. T., Flames, N., Tramontin, A. D., Garcia-Verdugo, J. M., and varez-Buylla, A. 2005, "Adult ependymal cells are postmitotic and are derived from radial glial cells during embryogenesis", *J.Neurosci.*, vol. 25, no. 1, pp. 10-18.

Spassky, N., Olivier, C., Perez-Villegas, E., Goujet-Zalc, C., Martinez, S., Thomas, J., and Zalc, B. 2000, "Single or multiple oligodendroglial lineages: a controversy", *Glia*, vol. 29, no. 2, pp. 143-148.

Spemann, H. and Mangold, H. 1924, "Über induktion von Embryonalagen durch Implantation Artfremder Organisatoren", *Roux' Arch.Entw.Mech.*, vol. 100, pp. 599-638.

Srinivas, S., Watanabe, T., Lin, C. S., William, C. M., Tanabe, Y., Jessell, T. M., and Costantini, F. 2001, "Cre reporter strains produced by targeted insertion of EYFP and ECFP into the ROSA26 locus", *BMC.Dev.Biol.*, vol. 1, p. 4.

Stamataki, D., Ulloa, F., Tsoni, S. V., Mynett, A., and Briscoe, J. 2005, "A gradient of Gli activity mediates graded Sonic Hedgehog signaling in the neural tube", *Genes Dev.*, vol. 19, no. 5, pp. 626-641.

Stern, C. D. 2006, "Neural induction: 10 years on since the 'default model'", *Curr.Opin.Cell Biol.*, vol. 18, no. 6, pp. 692-697.

Stolt, C. C., Lommes, P., Sock, E., Chaboissier, M. C., Schedl, A., and Wegner, M. 2003, "The Sox9 transcription factor determines glial fate choice in the developing spinal cord", *Genes Dev.*, vol. 17, no. 13, pp. 1677-1689.

Strahle, U., Lam, C. S., Ertzer, R., and Rastegar, S. 2004, "Vertebrate floor-plate specification: variations on common themes", *Trends Genet.*, vol. 20, no. 3, pp. 155-162.

Streit, A., Berliner, A. J., Papanayotou, C., Sirulnik, A., and Stern, C. D. 2000, "Initiation of neural induction by FGF signalling before gastrulation", *Nature*, vol. 406, no. 6791, pp. 74-78.

Sugimori, M., Nagao, M., Bertrand, N., Parras, C. M., Guillemot, F., and Nakafuku, M. 2007, "Combinatorial actions of patterning and HLH transcription factors in the spatiotemporal control of neurogenesis and gliogenesis in the developing spinal cord", *Development*.

Sugimori, M., Nagao, M., Parras, C. M., Nakatani, H., Lebel, M., Guillemot, F., and Nakafuku, M. 2008, "Ascl1 is required for oligodendrocyte development in the spinal cord", *Development*.

Sun, T., Dong, H., Wu, L., Kane, M., Rowitch, D. H., and Stiles, C. D. 2003, "Cross-repressive interaction of the Olig2 and Nkx2.2 transcription factors in developing neural tube associated with formation of a specific physical complex", *J.Neurosci.*, vol. 23, no. 29, pp. 9547-9556.

Sun, T., Echelard, Y., Lu, R., Yuk, D. I., Kaing, S., Stiles, C. D., and Rowitch, D. H. 2001a, "Olig bHLH proteins interact with homeodomain proteins to regulate cell fate acquisition in progenitors of the ventral neural tube", *Curr.Biol.*, vol. 11, no. 18, pp. 1413-1420.

Sun, T., Pringle, N. P., Hardy, A. P., Richardson, W. D., and Smith, H. K. 1998, "Pax6 influences the time and site of origin of glial precursors in the ventral neural tube", *Mol.Cell Neurosci.*, vol. 12, no. 4-5, pp. 228-239.

Sun, Y., Nadal-Vicens, M., Misono, S., Lin, M. Z., Zubiaga, A., Hua, X., Fan, G., and Greenberg, M. E. 2001b, "Neurogenin promotes neurogenesis and inhibits glial differentiation by independent mechanisms", *Cell*, vol. 104, no. 3, pp. 365-376.

Sussel, L., Kalamaras, J., Hartigan-O'Connor, D. J., Meneses, J. J., Pedersen, R. A., Rubenstein, J. L., and German, M. S. 1998, "Mice lacking the homeodomain transcription factor Nkx2.2 have diabetes due to arrested differentiation of pancreatic beta cells", *Development*, vol. 125, no. 12, pp. 2213-2221.

Takebayashi, H., Nabeshima, Y., Yoshida, S., Chisaka, O., Ikenaka, K., and Nabeshima, Y. 2002, "The basic helix-loop-helix factor olig2 is essential for the development of motoneuron and oligodendrocyte lineages", *Curr.Biol.*, vol. 12, no. 13, pp. 1157-1163.

Takebayashi, H., Yoshida, S., Sugimori, M., Kosako, H., Kominami, R., Nakafuku, M., and Nabeshima, Y. 2000, "Dynamic expression of basic helix-loop-helix Olig family members: implication of Olig2 in neuron and oligodendrocyte differentiation and identification of a new member, Olig3", *Mech.Dev.*, vol. 99, no. 1-2, pp. 143-148.

Tanabe, Y., William, C., and Jessell, T. M. 1998, "Specification of motor neuron identity by the MNR2 homeodomain protein", *Cell*, vol. 95, no. 1, pp. 67-80.

Taveira-Marques, R. 2010, *Fate-mapping neural stem cell sub-populations in the mouse ventral neural tube by Cre-lox transgenesis,* PhD, University College London.

Taveira-Marques, R., Tsai, H.-H., Holz, A., Arnold, H. H., Rowitch, D. H., Kessaris, N., and Richardson, W. D. 2010, "Separate neuroepithelial precursors for visceral (sympathetic) and somatic motor neurons in the embryonic spinal cord", *In preparation.*

Taylor, M. D., Poppleton, H., Fuller, C., Su, X., Liu, Y., Jensen, P., Magdaleno, S., Dalton, J., Calabrese, C., Board, J., Macdonald, T., Rutka, J., Guha, A., Gajjar, A., Curran, T., and Gilbertson, R. J. 2005, "Radial glia cells are candidate stem cells of ependymoma", *Cancer Cell*, vol. 8, no. 4, pp. 323-335.

Thaler, J. P., Koo, S. J., Kania, A., Lettieri, K., Andrews, S., Cox, C., Jessell, T. M., and Pfaff, S. L. 2004, "A postmitotic role for Isl-class LIM homeodomain proteins in the assignment of visceral spinal motor neuron identity", *Neuron*, vol. 41, no. 3, pp. 337-350.

Theiler, K. 1972, *The mouse house - development and normal stages from fertilization to 4 weeks of age* Berlin Heidelberg, New York.

Timmer, J. R., Wang, C., and Niswander, L. 2002, "BMP signaling patterns the dorsal and intermediate neural tube via regulation of homeobox and helix-loop-helix transcription factors", *Development*, vol. 129, no. 10, pp. 2459-2472.

Tripathi, R. B., Clarke, L. E., Burzomato, V., Kessaris, N., Anderson, P. N., Attwell, D., and Richardson, W. D. 2011, "Dorsally and ventrally derived oligodendrocytes have similar electrical properties but myelinate preferred tracts", *J Neurosci.*, vol. 31, no. 18, pp. 6809-6819.

Tsuchida, T., Ensini, M., Morton, S. B., Baldassare, M., Edlund, T., Jessell, T. M., and Pfaff, S. L. 1994, "Topographic organization of embryonic motor neurons defined by expression of LIM homeobox genes", *Cell*, vol. 79, no. 6, pp. 957-970.

Turing A.M. 1952, "The Chemical Basis of Morphogenesis", *Philos.Trans.R.Soc.Lond B Biol.Sci.*, vol. 237, no. 641, pp. 37-72.

Turner, D. L. and Cepko, C. L. 1987, "A common progenitor for neurons and glia persists in rat retina late in development", *Nature*, vol. 328, no. 6126, pp. 131-136.

Ulloa, F. and Marti, E. 2010, "Wnt won the war: antagonistic role of Wnt over Shh controls dorso-ventral patterning of the vertebrate neural tube", *Dev.Dyn.*, vol. 239, no. 1, pp. 69-76.

Vallstedt, A., Klos, J. M., and Ericson, J. 2005, "Multiple dorsoventral origins of oligodendrocyte generation in the spinal cord and hindbrain", *Neuron*, vol. 45, no. 1, pp. 55-67.

Vallstedt, A., Muhr, J., Pattyn, A., Pierani, A., Mendelsohn, M., Sander, M., Jessell, T. M., and Ericson, J. 2001, "Different levels of repressor activity assign redundant and specific roles to Nkx6 genes in motor neuron and interneuron specification", *Neuron*, vol. 31, no. 5, pp. 743-755.

van Heyningen, P., Calver, A. R., and Richardson, W. D. 2001, "Control of progenitor cell number by mitogen supply and demand", *Curr.Biol.*, vol. 11, no. 4, pp. 232-241.

Vincent, J. P. and Briscoe, J. 2001, "Morphogens", *Curr.Biol.*, vol. 11, no. 21, p. R851-R854.

Vogt W 1929, "Gestaltungsanalyse am Amphibienkeim mit ortlicher Vitalfarbung. II. Teil Gastrulation und Mesodermbildung bie Urodelen und Anuren", *Wilhelm Roux Arch.Entwicklungsmech.Org.*, vol. 120, pp. 384-706.

Voigt, T. 1989, "Development of glial cells in the cerebral wall of ferrets: direct tracing of their transformation from radial glia into astrocytes", *J.Comp Neurol.*, vol. 289, no. 1, pp. 74-88.

Vokes, S. A., Ji, H., McCuine, S., Tenzen, T., Giles, S., Zhong, S., Longabaugh, W. J., Davidson, E. H., Wong, W. H., and McMahon, A. P. 2007, "Genomic characterization of Gli-activator targets in sonic hedgehog-mediated neural patterning", *Development*.

Vokes, S. A., Ji, H., Wong, W. H., and McMahon, A. P. 2008, "A genome-scale analysis of the cis-regulatory circuitry underlying sonic hedgehog-mediated patterning of the mammalian limb", *Genes Dev.*, vol. 22, no. 19, pp. 2651-2663.

Vue, T. Y., Aaker, J., Taniguchi, A., Kazemzadeh, C., Skidmore, J. M., Martin, D. M., Martin, J. F., Treier, M., and Nakagawa, Y. 2007, "Characterization of progenitor domains in the developing mouse thalamus", *J.Comp Neurol.*, vol. 505, no. 1, pp. 73-91.

Wade, G. N. and Heller, H. W. 1993, "Tamoxifen mimics the effects of estradiol on food intake, body weight, and body composition in rats", *Am.J.Physiol*, vol. 264, no. 6 Pt 2, p. R1219-R1223.

Wang, J., Elghazi, L., Parker, S. E., Kizilocak, H., Asano, M., Sussel, L., and Sosa-Pineda, B. 2004, "The concerted activities of Pax4 and Nkx2.2 are essential to initiate pancreatic beta-cell differentiation", *Dev.Biol.*, vol. 266, no. 1, pp. 178-189.

Watada, H., Mirmira, R. G., Kalamaras, J., and German, M. S. 2000, "Intramolecular control of transcriptional activity by the NK2-specific domain in NK-2 homeodomain proteins", *Proc.Natl.Acad.Sci.U.S.A*, vol. 97, no. 17, pp. 9443-9448.

Watanabe, M., Hadzic, T., and Nishiyama, A. 2004, "Transient upregulation of Nkx2.2 expression in oligodendrocyte lineage cells during remyelination", *Glia*, vol. 46, no. 3, pp. 311-322.

Wegner, M. and Stolt, C. C. 2005, "From stem cells to neurons and glia: a Soxist's view of neural development", *Trends Neurosci.*, vol. 28, no. 11, pp. 583-588.

Wei, Q., Miskimins, W. K., and Miskimins, R. 2005, "Stage-specific expression of myelin basic protein in oligodendrocytes involves Nkx2.2-mediated repression that is relieved by the Sp1 transcription factor", *J.Biol.Chem.*, vol. 280, no. 16, pp. 16284-16294.

Wetts, R. and Vaughn, J. E. 1994, "Choline acetyltransferase and NADPH diaphorase are co-expressed in rat spinal cord neurons", *Neuroscience*, vol. 63, no. 4, pp. 1117-1124.

Wijgerde, M., McMahon, J. A., Rule, M., and McMahon, A. P. 2002, "A direct requirement for Hedgehog signaling for normal specification of all ventral progenitor domains in the presumptive mammalian spinal cord", *Genes Dev.*, vol. 16, no. 22, pp. 2849-2864.

Wilson, J. M., Hartley, R., Maxwell, D. J., Todd, A. J., Lieberam, I., Kaltschmidt, J. A., Yoshida, Y., Jessell, T. M., and Brownstone, R. M. 2005, "Conditional rhythmicity of ventral spinal interneurons defined by expression of the Hb9 homeodomain protein", *J.Neurosci.*, vol. 25, no. 24, pp. 5710-5719.

Wolpert, L. 1969, "Positional information and the spatial pattern of cellular differentiation", *J Theor.Biol.*, vol. 25, no. 1, pp. 1-47.

Wolpert, L., Jessell, T. M., Lawrence P., Meyerowitz E., Robertson E., and Smith J. 2006, *Principles of Development*, Third Edition edn, Oxford University Press, New York.

Woodruff, R. H., Tekki-Kessaris, N., Stiles, C. D., Rowitch, D. H., and Richardson, W. D. 2001, "Oligodendrocyte development in the spinal cord and telencephalon: common themes and new perspectives", *Int.J.Dev.Neurosci.*, vol. 19, no. 4, pp. 379-385.

Wu, Y., Niwa, K., Onogi, K., Tang, L., Mori, H., and Tamaya, T. 2007, "Effects of selective estrogen receptor modulators and genistein on the expression of ERalpha/beta and COX-1/2 in ovarectomized mouse uteri", *Eur.J.Gynaecol.Oncol.*, vol. 28, no. 2, pp. 89-94.

Xu, Q., Guo, L., Moore, H., Waclaw, R. R., Campbell, K., and Anderson, S. A. 2010, "Sonic hedgehog signaling confers ventral telencephalic progenitors with distinct cortical interneuron fates", *Neuron*, vol. 65, no. 3, pp. 328-340.

Xu, X., Cai, J., Fu, H., Wu, R., Qi, Y., Modderman, G., Liu, R., and Qiu, M. 2000, "Selective expression of Nkx-2.2 transcription factor in chicken oligodendrocyte progenitors and implications for the embryonic origin of oligodendrocytes", *Mol.Cell Neurosci.*, vol. 16, no. 6, pp. 740-753.

Yang, X. W., Model, P., and Heintz, N. 1997, "Homologous recombination based modification in Escherichia coli and germline transmission in transgenic mice of a bacterial artificial chromosome", *Nat.Biotechnol.*, vol. 15, no. 9, pp. 859-865.

Yelin, R., Kot, H., Yelin, D., and Fainsod, A. 2007, "Early molecular effects of ethanol during vertebrate embryogenesis", *Differentiation*, vol. 75, no. 5, pp. 393-403.

Yelin, R., Schyr, R. B., Kot, H., Zins, S., Frumkin, A., Pillemer, G., and Fainsod, A. 2005, "Ethanol exposure affects gene expression in the embryonic organizer and reduces retinoic acid levels", *Dev.Biol.*, vol. 279, no. 1, pp. 193-204.

Young, K. M., Mitsumori, T., Pringle, N., Grist, M., Kessaris, N., and Richardson, W. D. 2010, "An Fgfr3-iCreER(T2) transgenic mouse line for studies of neural stem cells and astrocytes", *Glia*, vol. 58, no. 8, pp. 943-953.

Yu, D., Ellis, H. M., Lee, E. C., Jenkins, N. A., Copeland, N. G., and Court DL 2000, "An efficient recombination system for chromosome engineering in Escherichia coli", *Proc.Natl.Acad.Sci.U.S.A*, vol. 97, no. 11, pp. 5978-5983.

Yu, Y. C., Bultje, R. S., Wang, X., and Shi, S. H. 2009, "Specific synapses develop preferentially among sister excitatory neurons in the neocortex", *Nature*.

Zhang, R. L., Zhang, Z. G., Wang, Y., LeTourneau, Y., Liu, X. S., Zhang, X., Gregg, S. R., Wang, L., and Chopp, M. 2007, "Stroke induces ependymal cell transformation into radial glia in the

subventricular zone of the adult rodent brain", *J Cereb.Blood Flow Metab*, vol. 27, no. 6, pp. 1201-1212.

Zhang, X. M., Ramalho-Santos, M., and McMahon, A. P. 2001, "Smoothened mutants reveal redundant roles for Shh and Ihh signaling including regulation of L/R asymmetry by the mouse node", *Cell*, vol. 105, no. 6, pp. 781-792.

Zhang, Y. and Barres, B. A. 2010, "Astrocyte heterogeneity: an underappreciated topic in neurobiology", *Curr.Opin.Neurobiol*.

Zhang, Y., Narayan, S., Geiman, E., Lanuza, G. M., Velasquez, T., Shanks, B., Akay, T., Dyck, J., Pearson, K., Gosgnach, S., Fan, C. M., and Goulding, M. 2008, "V3 spinal neurons establish a robust and balanced locomotor rhythm during walking", *Neuron*, vol. 60, no. 1, pp. 84-96.

Zhou, F. C., Sari, Y., Powrozek, T., Goodlett, C. R., and Li, T. K. 2003, "Moderate alcohol exposure compromises neural tube midline development in prenatal brain", *Brain Res.Dev.Brain Res.*, vol. 144, no. 1, pp. 43-55.

Zhou, Q. and Anderson, D. J. 2002, "The bHLH transcription factors OLIG2 and OLIG1 couple neuronal and glial subtype specification", *Cell*, vol. 109, no. 1, pp. 61-73.

Zhou, Q., Choi, G., and Anderson, D. J. 2001, "The bHLH transcription factor Olig2 promotes oligodendrocyte differentiation in collaboration with Nkx2.2", *Neuron*, vol. 31, no. 5, pp. 791-807.

Zhou, Q., Wang, S., and Anderson, D. J. 2000, "Identification of a novel family of oligodendrocyte lineage-specific basic helix-loop-helix transcription factors", *Neuron*, vol. 25, no. 2, pp. 331-343.